

# Ecosystem Status Report 2022

## EASTERN BERING SEA



*Edited by:*

Elizabeth Siddon

Auke Bay Laboratories, Alaska Fisheries Science Center, NOAA Fisheries

*With contributions from:*

Anna Abelman, Grant Adams, Opik Ahkinga, Don Anderson, Alex Andrews, Kerim Aydin, Steve Barbeaux, Cheryl Barnes, Lewis Barnett, Jenna Barrett, Sonia Batten, Shaun W. Bell, Nick Bond, Emily Bowers, Caroline Brown, Thaddaeus Buser, Matt Callahan, Louisa Castrodale, Patricia Chambers, Patrick Charapata, Wei Cheng, Daniel Cooper, Bryan Cormack, Jessica Cross, Deana Crouser, Curry J. Cunningham, Seth Danielson, Alison Deary, Andrew Dimond, Lauren Divine, Sherri Dressel, Kathleen Easley, Anne Marie Eich, Lisa Eisner, Jack Erickson, Evangeline Fachon, Ed Farley, Thomas Farrugia, Sarah Gaichas, Jeanette C. Gann, Sabrina Garcia, Jordan Head, Ron Heintz, Hanna Hellen, Tyler Hennon, Albert Hermann, Kirstin K. Holsman, Kathrine Howard, Tom Hurst, Jim Ianello, Phil Joy, Kelly Kearney, Esther Kennedy, Mandy Keogh, David Kimmel, Jesse Lamb, Geoffrey M. Lang, Ben Laurel, Elizabeth Lee, Kathi Lefebvre, Emily Lemagie, Aaron Lestenkof, W. Christopher Long, Sara Miller, Calvin W. Mordy, Franz Mueter, James Murphy, Jens M. Nielsen, Cecilia O'Leary, Ivonne Ortiz, Clare Ostle, Jim Overland, Veronica Padula, Emma Pate, Noel Pelland, Robert Pickart, Darren Pilcher, Cody Pinger, Steven Porter, Bianca Prohaska, Patrick Ressler, Sarah Rheinsmith, Jon Richar, Sean Rohan, Natalie Rouse, Kate Savage, Terese Schomogyi, Gay Sheffield, Kalei Shotwell, Elizabeth Siddon, Scott Smeltz, Joseph Spaeder, Adam Spear, Ingrid Spies, Phyllis Stabeno, Wesley Strasburger, Robert Suryan, Rick Thoman, Cathy Tide, Rod Towell, Stacy Vega, Vanessa von Biela, Muyin Wang, Jordan Watson, George A. Whitehouse, Kevin Whitworth, Megan Williams, Ellen Yasumiishi, Stephani Zador, and Molly Zaleski

*Reviewed by:*  
The Bering Sea and Aleutian Islands Groundfish Plan Team  
November 18, 2022  
North Pacific Fishery Management Council  
1007 West 3<sup>rd</sup> Ave., Suite 400  
Anchorage, AK 99501

Support for the assembly and editing of this document was provided jointly by NOAA Fisheries and the NOAA Integrated Ecosystem Assessment (IEA) program.  
This document is NOAA IEA program contribution #2022\_2.

The recommended citation for this document is as follows:  
Siddon, E. 2022. Ecosystem Status Report 2022: Eastern Bering Sea, Stock Assessment and Fishery Evaluation Report, North Pacific Fishery Management Council, 1007 West 3<sup>rd</sup> Ave., Suite 400, Anchorage, Alaska 99501.

QR code for NOAA Alaska Fisheries Science Center's Ecosystem Status Reports webpage:



# 2022 Contributing Partners



# Purpose of the Ecosystem Status Reports

This document is intended to provide the North Pacific Fishery Management Council, including its Scientific and Statistical Committee (SSC) and Advisory Panel (AP), with information on ecosystem status and trends. This information provides context for the SSC's acceptable biological catch (ABC) and overfishing limit (OFL) recommendations, as well as for the Council's final total allowable catch (TAC) determination for groundfish and crab. It follows the same annual schedule and review process as groundfish stock assessments, and is made available to the Council at the annual December meeting when Alaska's federal groundfish harvest recommendations are finalized.

Ecosystem Status Reports (ESRs) include assessments based on ecosystem indicators that reflect the current status and trends of ecosystem components, which range from physical oceanography to biology and human dimensions. Many indicators are based on data collected from NOAA's Alaska Fishery Science Center surveys. All are developed by, and include contributions from, scientists and fishery managers at NOAA, other U.S. federal and state agencies, academic institutions, tribes, nonprofits, and other sources. The ecosystem information in this report will be integrated into the annual harvest recommendations through inclusion in stock assessment-specific risk tables (Dorn and Zador, 2020), presentations to the Groundfish and Crab plan teams in annual September and November meetings, presentations to the Council in their annual October and December meetings, and submission of the final report to the Council in December (see Figure 1).

The SSC is the primary audience for this report, as the final ABCs are determined by the SSC, based on biological and environmental scientific information through the stock assessment and Tier process<sup>1,2</sup>. TACs may be set lower than the ABCs due to biological and socioeconomic information. Thus, the ESRs are also presented to the AP and Council to provide ecosystem context to inform TAC and as well as other Council decisions. Additional background can be found in the Appendix (p. 214).

---

<sup>1</sup><https://www.npfmc.org/wp-content/PDFdocuments/fmp/GOA/GOAfmf.pdf>

<sup>2</sup><https://www.npfmc.org/wp-content/PDFdocuments/fmp/BSAI/BSAIfmf.pdf>

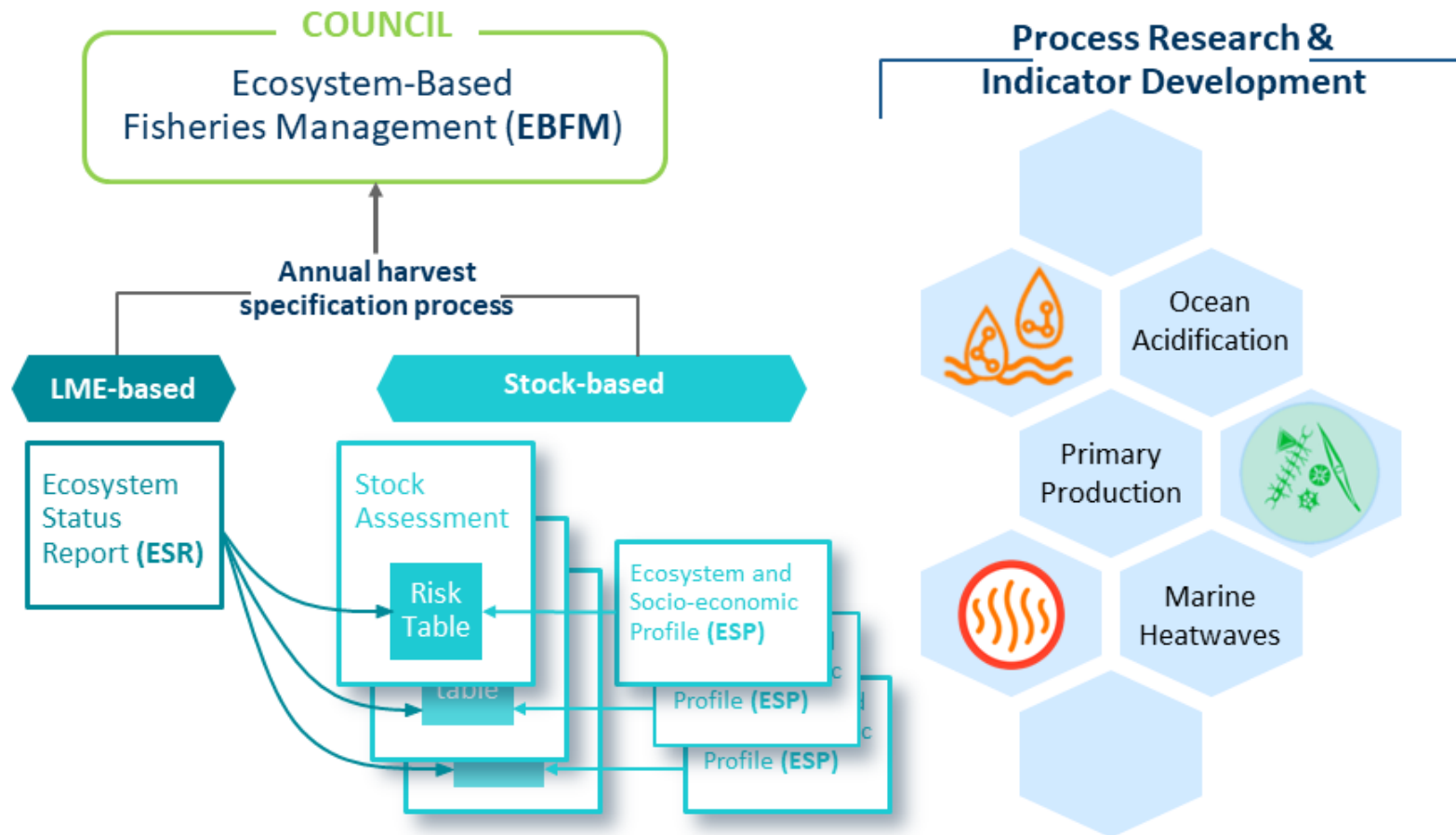


Figure 1: Ecosystem information mapping to support Ecosystem-Based Fisheries Management through Alaska’s annual harvest specification process. The ‘honeycomb’ on the right shows examples of ecosystem indicators that are provided to Ecosystem Status Reports (ESRs) at the Large Marine Ecosystem (LME) scale and/or to Ecosystem and Socioeconomic Profiles (ESPs) at the species-based level.

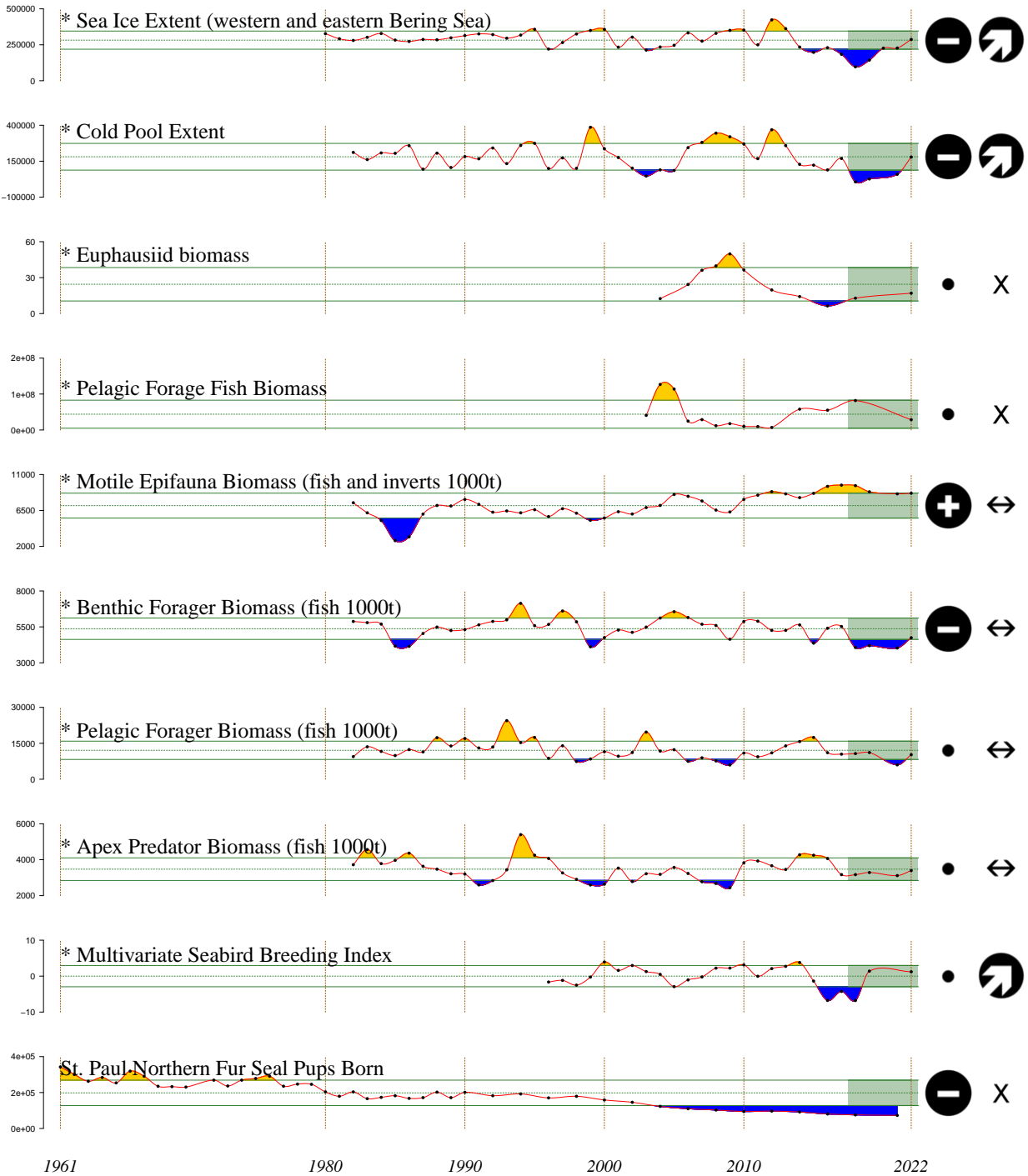
# Eastern Bering Sea 2022 Report Card

For more information on individual Report Card indicators, please see ‘Description of the Report Card indicators’ (p. 224). For more information on the methods for plotting the Report Card indicators, please see ‘Methods Description for the Report Card Indicators’ (p. 227).

\* indicates Report Card information updated with 2022 data.

- \* The mean **sea-ice extent** across the Bering Sea (ice year is defined as 1 August to 31 July; western and eastern) exhibited no long-term trend (1980–2022), although a **steep decline in ice extent** was observed from 2012 (highest extent on record) to 2018 (lowest extent on record). Sea-ice extent increased from 2018 to present, with the 2021–2022 daily mean extent of 287,315 km<sup>2</sup> being **at the long-term mean**. Seasonal sea-ice extent has implications, for example, to the cold pool, spring bloom strength and timing, and bottom-up productivity.
- \* The areal **extent of the cold pool** in the eastern Bering Sea (EBS), as measured during the bottom trawl survey (Jun-Aug; including strata 82 and 90; 1982–2022), has increased since 2018. The 2022 extent (178,625 km<sup>2</sup>) was near the time series average (181,018 km<sup>2</sup>). The cold pool extent in 2022 represents a major change from the three prior survey years (2018, 2019, 2021).
- \* An acoustic estimate of euphausiid density was **below average** in 2022 (2004–2022), but remained **greater than the lowest** point in the time series that occurred in 2016.
- \* The biomass of **pelagic forage fish** (i.e., age-0 pollock, age-0 Pacific cod, herring, capelin, and all species of juvenile salmonids) sampled by surface trawl in late-summer (Aug-Sep; 2003–2022) peaked in 2004 and 2005, was below the time series average from 2006–2012, was above average in 2014, 2016, and 2018, but **dropped to just below the long-term mean in 2022**. The trends are dominated by age-0 pollock and juvenile sockeye salmon, largely by age-0 pollock in surface waters during warm years. The biomass in 2022 was largely driven by higher juvenile sockeye salmon and lower age-0 pollock.
- \* The biomass of **motile epifauna** measured during the standard EBS bottom trawl survey (Jun-Aug; 1982–2022) peaked in 2017 and remained **above their long-term mean in 2022**. Trends in motile epifauna biomass **indicate benthic productivity**, although individual species and/or taxa may reflect varying time scales of productivity. Collectively, brittle stars, sea stars, and other echinoderms account for more than 50% of the biomass in this guild and the current (2016–2022) mean biomass indices for all three of these functional groups are well above their long-term means. The current mean biomass indices for king crabs, tanner crab, and snow crab are all below their long-term means.

- \* The biomass of **benthic foragers** measured during the standard EBS bottom trawl survey (Jun-Aug; 1982–2022) increased 18% from 2021 to 2022, but **remained below the time series mean**. Trends in benthic forager biomass are variable over the time series and **indirectly indicate availability of infauna** (i.e., prey of these species). There were increases in biomass for the four most dominant species in this guild – yellowfin sole, northern rock sole, flathead sole, and Alaska plaice – though all but flathead sole remain below their long-term mean (1982–2022).
- \* The biomass of **pelagic foragers** measured during the standard EBS bottom trawl survey (Jun-Aug; 1982–2022) **increased sharply from 2021 to 2022, up more than 70%**. The biomass of the pelagic forager guild was generally stable from 2016 to 2019, but dropped to its second lowest value over the time series (1982–2022) in 2021. The trend in the pelagic forager guild is largely driven by walleye pollock which, on average, account for more than 67% of the biomass in this guild. In 2022, the survey index for **pollock increased 50% from 2021**. Among species of secondary importance, **Pacific herring were up more than 200% from 2021**, well above their long-term mean.
- \* The biomass of **apex predators** measured during the standard EBS bottom trawl survey (Jun-Aug; 1982–2022) in 2022 was up from 2021 and **nearly equal to their long-term mean**. Trends in apex predator biomass reflect relative **predation pressure on zooplankton and juvenile fishes**. The trend in the apex predator guild is largely driven by Pacific cod and Arrowtooth flounder, both of which have increased from 2021.
- \* The **multivariate seabird breeding index** indicated that, on the whole, seabirds bred earlier and had better reproductive success in 2022 compared to years with very poor success from 2016–2018. Comparisons with the most recent two years are not possible because colonies were not monitored due to the COVID-19 pandemic. Reproductive success and/or early breeding are assumed to be mediated through food supply, therefore above-average values indicate better than average recruitment of year classes that seabirds feed on (e.g., age-0 pollock), or better than average supply of forage fish that commercially fished species feed on (e.g., capelin eaten by both seabirds and Pacific cod).
- **Northern fur seal pup production** at St. Paul Island in 2021 continued a declining trend since 1998 that may be partially attributed to low pup growth rates.



2018–2022 Mean

⊕ 1 s.d. above mean

⊖ 1 s.d. below mean

• within 1 s.d. of mean

2018–2022 Trend

↻ increase by 1 s.d. over time window

↺ decrease by 1 s.d. over time window

↔ change <1 s.d. over window

Figure 2: 2022 Eastern Bering Sea report card; see text for indicator descriptions.

\* indicates time series updated with 2022 data.

# Ecosystem Assessment

Elizabeth Siddon

Auke Bay Laboratories, Alaska Fisheries Science Center, NOAA Fisheries

Contact: elizabeth.h.siddon@noaa.gov

**Last updated: November 2022**

During 2022, operational impacts due to COVID-19 had a negligible effect on information used in this report, due in large-part to effective mitigation strategies put in place to protect the health and safety of field research personnel and communities. The Alaska Fisheries Science Center’s Ecosystem Status Reports are informed by the continuation of survey- and lab-based data streams, as well as information contributed through new and existing partnerships.

## The Recent Warm Stanza

Beginning in approximately 2014, the eastern Bering Sea (EBS) entered a warm phase of unprecedented duration (e.g., Figures 15 and 20). The impact of this sustained warming can be seen in a variety of ecosystem indicators, as described below. Ecosystem response can be immediate (i.e., occurs in the same year as the perturbation), can be lagged (i.e., seen in a subsequent year from the perturbation), or can be cumulative (i.e., carry-over impacts that have positive or negative feedback loops). The past year (fall 2021 through summer 2022) has seen a relaxation to more average thermal conditions. With “reasonably normal conditions” (p. 64) forecast into 2023, and a potential bookend to the recent prolonged warm phase, the ecosystem response and impacts to managed groundfish and crab stocks are assessed below.

### **Physical environment responses to the recent warm stanza:**

Immediate ecosystem responses to warming can be seen in surface and bottom temperatures from the NOAA-AFSC bottom trawl survey (Figure 27), which were above their long-term means beginning in 2014 and largely remained above average through 2022 (bottom temperatures were at the long-term mean in 2017 and 2022). The spatial extent of the cold pool (<2°C bottom water; Figures 35 and 36) is a direct reflection of sea-ice extent over the eastern Bering Sea shelf the preceding winter. The cold pool extent dropped below the time series average beginning in 2014; years 2018, 2019, and 2021 (no survey in 2020) were the lowest cold pool extents in the time series (see the 2022 Report Card, Figure 2).

Cumulative ecosystem responses are best exemplified through sea-ice dynamics. Throughout the recent warm stanza, residual warmth in the system resulted in delayed sea-ice formation (Figure 29). Delayed freeze-up led to shortened ice seasons that in turn had impacts on ice thickness (Figure 33), ice algae, and thermal modulation of the ecosystem. Thinner sea ice resulted in earlier ice retreat, as it was more susceptible to being eroded by storms, further truncating the ice season (Figure 31) and perpetuating the residual warmth into the following year (i.e., carry-over impacts). The additive effects of residual warmth in the system and loss of sea ice resulted in an increased rate of warming in the northern Bering Sea (see p. 27, Figure 5).

The loss of sea ice over time may also have contributed to an observed increase in salinity at the Pribilof Islands. Community-led monitoring of temperature and salinity on St. Paul Island shows an increasing trend in salinity that corresponds to the recent warm phase (Figure 24). In the Bering Sea, ice growth occurs in the north, which extrudes salts and results in localized increases in salinity. The sea ice is advected south, largely due to winds, and melting occurs at the ice edge, resulting in decreased salinity (i.e., sea ice “conveyor belt”; Pease (1980)). Changes in the salinity structure of the water column can impact the vertical stratification and, ultimately, vertical mixing of primary and secondary productivity. If production is mixed deeper in the water column, for example, a vertical mismatch of prey for surface-foraging seabirds or forage fish may occur. It is worth noting that the salinity observations indicate decreased salinity in 2022, potentially due to sea-ice extent reaching the Pribilof Islands during winter 2021/2022.

### **Biological responses to the recent warm stanza:**

Structural epifauna, such as sea anemones and sponges, provide habitat to benthic-associated organisms and fishes, including rockfishes. Declines in structural epifauna have been observed, both in the NOAA AFSC bottom trawl survey (see p. 66) and as non-target catch reported from groundfish fisheries in the Eastern Bering Sea (EBS (see p. 177), since approximately 2013. While the causes of these declines are not fully understood at this time, the resulting trends may indicate that there are system-wide changes in benthic versus pelagic energy flow (Grebmeier et al., 2006). Satellite measures of chlorophyll-a, an estimate of phytoplankton biomass in the surface level and an indicator of primary production available to the food web, along the shelf break were low in 2022, continuing a decreasing trend since 2014 (see off-shelf region in Figure 40) suggesting potential limitations at the base of the food web.

Zooplankton form the prey base for pelagic stages of groundfish and crab, including important forage fish and age-0 pollock. In spring, small copepods form the prey base for earlier life stages of pollock; by late-summer, age-0 pollock overwinter survival and recruitment success is correlated with the abundance of large, lipid-rich copepods (Eisner et al., 2020) and/or euphausiids (Andrews III et al., 2019). During the recent warm stanza, spring zooplankton surveys documented a distinct increase in small copepods alongside a decrease in large copepods (Figure 48). Late-summer zooplankton surveys over the southern shelf noted no long-term trend in the abundance of small copepods, but a shift to markedly lower abundances of large copepods during the recent warm stanza (Figure 51). These observations suggest that prey conditions in spring have been favorable for early life stages of pollock, but that the availability of large, lipid-rich copepods in fall was low and may have limited age-0 overwinter survival (Heintz et al., 2013).

Concomitantly, increases in forage fish have been observed in biennial surface trawl surveys during this warm stanza (e.g., 2014, 2016, 2018) compared to lower abundances during the preceding cooler stanza (~2009–2013) (Figures 60, 61, and 66). The combined forage fish index includes age-0 pollock, age-0 Pacific cod, capelin, herring, and juvenile chum, Chinook, coho, pink, and sockeye salmon biomass. The trends in this index are driven by age-0 pollock, particularly during warm years, as age-0 pollock occur closer to the surface during warmer years (Spear and Andrews III, 2021). This trend suggests that the summer foraging conditions were more robust during the recent warm stanza, especially for surface-feeding organisms like piscivorous seabirds.

Bristol Bay adult sockeye salmon returns showed a large increase during the recent warm stanza, with inshore run sizes in 2015–2022 that all exceeded 50 million salmon. The 2022 Bristol Bay sockeye salmon inshore run estimate is the largest on record since 1963 (see p. 109; Figure 70). These large run sizes indicate favorable ocean conditions for juveniles at entry since the summer of 2012–2013 and winters 2012/2013 and 2013/2014. In contrast, declines in NBS juvenile Chinook salmon have been observed since ~2013 (Figure 67) and adult salmon runs (e.g., Chinook, chum, and coho) throughout the Arctic-Yukon-Kuskokwim region have experienced unprecedented failures in recent years (see Liller (2021) for 2021 Noteworthy and p. 24 for 2022 Noteworthy). These contrasting trends highlight different responses to changing ocean conditions; the dynamic life histories within salmon species are impacted by a myriad of freshwater and marine habitat conditions.

Adult groundfish condition provides indication of prey availability, growth, general health, and habitat condition (Blackwell et al., 2000; Froese, 2006). Below-average condition has been observed in adult pollock since 2015 (except 2019) while juvenile pollock (100–250mm) have experienced above-average condition since 2014 (except 2015) (Figure 75). The 2018 year class of pollock in the EBS is well above-average (Ianelli et al., 2022), likely due to a combination of factors. For example, several indicators of bottom-up drivers of recruitment success support the hypothesis of increased overwinter survival to age-1 in 2019. Specifically, age-0 pollock experienced relatively cool summer sea surface temperatures in 2018 that were followed by warmer spring conditions for age-1 fish in 2019 (see p. 133). Diet composition of age-0 pollock in 2018 revealed a large proportion of euphausiids (Andrews III et al., 2019), supporting the hypothesis that increased euphausiid abundances during warm years may compensate for lower large copepod abundances (Duffy-Anderson et al., 2017). Additionally, the CEATTLE model (see p. 128) has shown continued declines in predation mortality on age-1 pollock due to declines in total predator biomass (i.e., reduced predation and mortality 2019–2021). A reduction in predator biomass is combined with a likely reduction in the spatial overlap between juvenile and adult pollock (Mueter and Litzow, 2008). The reduction in cold pool extent, and subsequent expansion of the adult pollock distribution into the NBS, further released predation pressure on the 2018 year class.

Species guilds derived from samples collected during the standard (southern Bering Sea) bottom trawl survey are grouped by functional roles within the ecosystem, and trends inform dynamics across these roles (e.g., predation pressure, prey availability) (Report Card, Figure 2). While functional guilds provide ecologically relevant information, species-specific trends within a guild may be “masked”, such as in the motile epifauna guild. Trends in motile epifauna indicate benthic productivity, and this guild has increased since 2014 and remains above the long-term mean. However, within the guild, the biomass of brittle stars, sea stars, and other echinoderms are well above their long-term means while the biomass for king crabs, tanner crab, and snow crab are all below their long-term means (see also p. 140). Comparing species-specific trends within the broader guild trend can inform niche partitioning within the ecosystem. The pelagic foragers guild, predominantly driven by pollock, decreased from above the long-term mean to below the long-term mean between 2015 and 2021, reflecting the decline in pollock biomass through 2021. This trend reversed in 2022 due to the strong recruitment of the 2018 year class of pollock. The apex predator guild declined from above the long-term mean to within  $\pm 1$  standard deviation of the mean between 2014 and 2022. Trends in this guild are largely driven by Pacific cod and Arrowtooth flounder; however, trends should be interpreted with caution as individual stock dynamics continue to shift and fluctuate between the southern and northern shelves (e.g., EBS Pacific cod; Barbeaux et al. (2022)).

### **Summary:**

The recent warm stanza in the eastern Bering Sea has resulted in protracted ecosystem conditions as well as pulse perturbations. The warm stanza was unprecedented in terms of magnitude and duration (Figure 15), but also contained a pulse event of near-absence of sea ice (and subsequent absence of cold pool over the southern Bering Sea shelf) in the winters of 2017/2018 and 2018/2019. The ecosystem indicators contained in this Ecosystem Status Report provide evidence of various ecosystem responses, both immediate and cumulative, that have direct and indirect implications on groundfish and crab stocks in the eastern Bering Sea. Overall, shifts in the distribution of groundfish and crab stocks in response to changes in sea ice and cold pool extent have been documented (see p. 155, Thorson et al. (2019)). There are several examples of stocks that are “winners” and “losers” (Stabeno et al., 2012) in the EBS ecosystem, although the exact mechanisms may not be fully understood at this time. Stocks experiencing increased survival for recent year classes include the 2018 year class of pollock, the 2014–2019 year classes of sablefish (with juvenile sablefish increasing in the EBS; Goethel et al. (2022)), the 2017 year class of Togiak herring (see p. 102), and the last 8 years of Bristol Bay sockeye salmon returns (year classes precede returns by 3-5 years; see p. 109). Conversely, stocks experiencing reduced survival and stock declines include several crab stocks (notably snow crab and Bristol Bay red king crab; Figure 92) and multiple Western Alaska Chinook, chum, and coho salmon runs. With cooler conditions predicted into 2023 (i.e., sea-ice extent and bottom temperatures near historical averages, see p. 64) (Figure 37), the ecological responses to this recent prolonged warm phase will continue to come into sharper focus.

## Current Conditions: 2022

### Oceanographic conditions:

Observations over the last year (September 2021–August 2022) indicate that the extended warm phase experienced by the EBS has ended, with a variety of metrics showing the relaxation to average thermal conditions. The combined states of three climate indices (positive North Pacific Index and Arctic Oscillation, and continued La Niña; see p. 33 and Figure 7) meant a return to more average sea surface temperature conditions for the EBS shelf. During this past year, marine heatwaves have been infrequent and brief compared to recent years (Figure 19). Rapid sea-ice growth in November 2021 resulted in above-average early ice extent (highest since 2012; Figure 29) that was followed by dramatic ice loss in April due to thin ice (Figure 33) that retreated quickly (Figure 31) with relatively warm air temperatures. The area of the 2022 cold pool (<2°C bottom water) expanded and was near the time series average, representing a major change from the three prior survey years (2018, 2019, 2021) (Figure 2).

Ocean acidification (OA) research shows an expansion of bottom water conditions ( $\Omega_{\text{arag}}$  and pH; Figure 108) that have been experimentally shown to negatively impact pteropods and red king crab. In 2022, relatively lower pH was predicted for most of the outer and middle shelves and near Bering Strait. However, at this time, there is no evidence that OA can be linked to recent declines in surveyed snow crab and red king crab populations (see p. 164).

Lastly, a localized pulse disturbance event heavily impacted the western Alaska region when Typhoon Merbok hit on September 17, 2022. The storm’s timing (i.e., early in the fall for a storm of this strength) and intensity were fueled by warm ocean waters from the north-central Pacific to the northern Bering Sea (developing warmth can be seen in Figure 16d). Immediate impacts of the storm included damage to infrastructure (e.g., seawalls) and disruption of the fall subsistence harvest season<sup>3</sup>. Longer-term impacts due to storm surges and coastal and river flooding are not yet known, but may include disturbance of HAB cyst beds or salmon eggs. We anticipate these longer-term impacts to be identified over time.

### Biological conditions:

Overall productivity within the EBS ecosystem shows immediate (e.g., primary production) and potentially lagged (e.g., higher trophic level) responses to the return to more average thermal conditions in 2022. Primary production, as measured by chlorophyll-a concentration, varied spatially over the shelf in 2022 and estimates of the spring bloom peak timing suggest that 2022 was similar to the long-term average (see p. 68). The direct mechanisms linking primary production to groundfish and crab stock dynamics are not fully understood, though continued research into the relationship between eddies, chlorophyll-a blooms, and spatial hotspots is on-going and future contributions to this Ecosystem Status Report are anticipated. The 2022 coccolithophore bloom index for both the south inner and middle shelf was among the highest ever observed (p. 73). The milky aquamarine color of the water during a bloom can reduce the foraging success for visual predators, such as seabirds, though monitored seabird species at the Pribilof Islands had an exceptional year in terms of reproductive success (except thick-billed murres) (Figures 93 and 94) suggesting that their foraging conditions were not limited by the coccolithophore bloom.

Zooplankton community composition was observed on three surveys in the Bering Sea during 2022: (1) spring along the 70-m isobath, (2) late summer over the southern shelf, and (3) late summer over the northeastern shelf (see p. 79). During spring 2022, the zooplankton composition appeared similar to previous warm years (i.e., relatively lower abundance of large copepods, higher abundance of small copepods). By late summer over the southern shelf, both large and small copepods were in low abundance; this decrease in available prey base over the southern shelf may have been mitigated by an increased abundance of euphausiids sampled during the same survey. Euphausiids were also sampled in higher abundances over the northeastern shelf, suggesting widespread abundance over the Bering Sea shelf.

---

<sup>3</sup><https://theconversation.com/typhoon-merbok-fueled-by-unusually-warm-pacific-ocean-pounded-alaskas-vulnerable-coastal-communities-at-a-critical-time-190898>

Forage fish represent a critical trophic linkage in the ecosystem and are prey for larger fish, seabirds, and marine mammals. An aggregate forage fish index derived from surface trawl surveys in the southern and northern Bering Sea indicates lower availability of forage in surface waters, especially in the northern Bering Sea during 2022 (Figure 60). Patterns in seabird reproductive success track patterns in prey availability, with planktivorous seabirds doing well at the Pribilof Islands and on St. Lawrence Island. While piscivorous seabirds did well at the Pribilof Islands, reproductive failures were observed for piscivorous seabirds on St. Lawrence Island (see p. 142), in line with the low forage fish availability suggested by the aggregate index.

Adult fish condition reflects prey availability and growth potential, both impacted by climate-driven changes in metabolic demand (higher in warmer conditions) and trophic interactions (changes in prey quality and quantity). Through 2021, bioenergetic work indicates declining conditions for groundfish during the recent warm stanza (see p. 123) that is reflected in groundfish condition (Figure 75). The cooler sea surface temperatures and bottom temperatures that began in 2021 (though still above average), and the relaxation to average thermal conditions in 2022, would be expected to coincide with better groundfish condition. In fact, groundfish condition improved from 2021 to 2022 for all monitored species over the southern shelf, except adult pollock that remained comparable to 2021 (Figure 75), while groundfish condition trends were more variable for monitored species over the northern shelf (Figure 78).

The groundfish community shifted northward during the recent warm stanza and remained near its northern maximum through 2019 before shifting south again in 2021 as conditions cooled (see p. 155). The mean latitude did not change between 2021 and 2022, but the groundfish community on average shifted into slightly deeper waters (Figure 101). The bottom trawl survey catch-per-unit-effort (CPUE; kg/ha) between the southern and northern shelves (Figure 98) also demonstrates a northward shift in the groundfish community. The drop in CPUE in the northern Bering Sea between 2019 and 2021 reflected large decreases in all of the dominant species (Figure 99) that had moved northward with the lack of cold pool in 2018/2019. The drop in CPUE in the NBS may indicate migration out of the survey area or that the carrying capacity of the system was exceeded during the exceptionally warm years.

The salmon run failures in the Arctic-Yukon-Kuskokwim Region (see Liller (2021)) continued in 2022, negatively impacting the human communities of the region. In response to the Scientific and Statistical Committee's request (see p. 217), and in collaboration with tribal, state, federal, and NGO partners, the factors affecting the 2022 Western Alaska Chinook salmon runs and subsistence harvest are explored in a Noteworthy topic (see p. 24).

# Contents

- Eastern Bering Sea 2022 Contributing Partners** **3**
  
- Purpose of the Ecosystem Status Reports** **4**
  
- Eastern Bering Sea 2022 Report Card** **6**
  
- Ecosystem Assessment** **9**
  - The Recent Warm Stanza . . . . . 9
  - Current Conditions: 2022 . . . . . 12
  
- Ecosystem Indicators** **24**
  - Noteworthy Topics . . . . . 24
    - †\*Factors Affecting 2022 Western Alaska Chinook Salmon Runs & Subsistence Harvest . . . . . 24
    - †\*High Resolution Climate Change Projections for the Eastern Bering Sea . . . . . 27
  - Ecosystem Status Indicators . . . . . 31
    - Physical Environment Synthesis . . . . . 31
      - \*Climate Overview . . . . . 33
      - \*Regional Highlights . . . . . 34
      - \*Winds and Surface Transport . . . . . 36
      - \*Sea Surface Temperature (SST) and Bottom Temperature . . . . . 45
      - \*Sea Ice . . . . . 56
      - \*Cold Pool . . . . . 60
      - \*Seasonal Projections from the National Multi-Model Ensemble (NMME) . . . . . 64
    - Habitat . . . . . 66
      - \*Structural Epifauna - Eastern Bering Sea Shelf . . . . . 66
    - Primary Production . . . . . 68

*Spring Satellite Chlorophyll-a Concentrations in the Eastern Bering Sea . . . . .	68
*Coccolithophores in the Bering Sea . . . . .	73
Zooplankton . . . . .	76
Continuous Plankton Recorder Data from the Eastern Bering Sea . . . . .	76
*Current and Historical Trends for Zooplankton in the Bering Sea . . . . .	79
*Eastern Bering Sea Euphausiids ('Krill') . . . . .	91
Jellyfish . . . . .	94
†*Trends in the Biomass of Jellyfish in the Southeastern and Northeastern Bering Sea During the Late-Summer Surface Trawl Survey, 2003–2022 . . . . .	94
*Jellyfishes - Eastern Bering Sea Shelf . . . . .	95
Ichthyoplankton . . . . .	97
Forage Fish . . . . .	97
†*Trends in the Biomass of Forage Fish Species in the Southeastern and Northeastern Bering Sea During the Late-Summer Surface Trawl Survey, 2003–2022 . . . . .	97
†*Trends in the Biomass of Age-0 Walleye Pollock in the Southeastern and Northeast- ern Bering Sea During the Late-Summer Surface Trawl Survey, 2003–2022 . . . . .	97
Herring . . . . .	100
†*Trends in the Biomass of Pacific Herring and Capelin in the Southeastern and North- eastern Bering Sea During the Late-Summer Surface Trawl Survey, 2003–2022	100
*Togiak Herring Population Trends . . . . .	102
Salmon . . . . .	105
†*Trends in the Abundance of Juvenile Sockeye Salmon in the Southeastern and North- eastern Bering Sea During the Late-Summer Surface Trawl Survey, 2003–2022	105
†*Northern Bering Sea Juvenile Salmon Abundance Indices . . . . .	106
*Temporal Trend in the Annual Inshore Run Size of Bristol Bay Sockeye Salmon ( <i>Oncorhynchus nerka</i> ) . . . . .	109
*Trends in Alaska Commercial Salmon Catch – Bering Sea . . . . .	111
Groundfish . . . . .	114
*Eastern and Northern Bering Sea Groundfish Condition . . . . .	114
*Patterns in Foraging and Energetics of Walleye Pollock, Pacific Cod, Arrowtooth Flounder, and Pacific Halibut . . . . .	123
*Multispecies Model Estimates of Time-varying Natural Mortality . . . . .	128
Groundfish Recruitment Predictions . . . . .	133
*Temperature Change Index and the Recruitment of Bering Sea Pollock . . . . .	133

*Large Copepod Abundance (Sample-Based and Modeled) as an Indicator of Pollock Recruitment to Age-3 in the Southeastern Bering Sea . . . . .	135
Benthic Communities and Non-target Fish Species . . . . .	138
*Miscellaneous Species - Eastern Bering Sea Shelf . . . . .	138
*Eastern Bering Sea Commercial Crab Stock Biomass Indices . . . . .	140
Seabirds . . . . .	142
*Integrated Seabird Information . . . . .	142
Marine Mammals . . . . .	149
*Marine Mammal Stranding Network: Eastern Bering Sea . . . . .	149
Ecosystem or Community Indicators . . . . .	152
*Aggregated Catch-Per-Unit-Effort of Fish and Invertebrates in Bottom Trawl Surveys on the Eastern and Northern Bering Sea Shelf, 1982–2022 . . . . .	152
*Spatial Distribution of Groundfish Stocks in the Eastern Bering Sea . . . . .	153
*Mean Lifespan of the Fish Community . . . . .	156
*Mean Length of the Fish Community . . . . .	159
*Stability of Groundfish Biomass . . . . .	162
Emerging Stressors . . . . .	164
*Ocean Acidification . . . . .	164
*Harmful Algal Blooms . . . . .	167
*ECO HAB: Harmful Algal Bloom (HAB) Toxins in Arctic Food Webs . . . . .	170
Discards and Non-Target Catch . . . . .	174
*Time Trends in Groundfish Discards . . . . .	174
Time Trends in Non-Target Species Catch . . . . .	177
Seabird Bycatch Estimates in the Eastern Bering Sea, 2012–2021 . . . . .	180
Maintaining and Restoring Fish Habitats . . . . .	186
Fishing Effects to Essential Fish Habitat . . . . .	186
Habitat Conservation Area Maps . . . . .	186
Sustainability . . . . .	187
*Fish Stock Sustainability Index – Bering Sea and Aleutian Islands . . . . .	187
Total Annual Surplus Production and Overall Exploitation Rates of Commercial Ground- fish Stocks in the Bering Sea / Aleutian Islands Management Area . . . . .	191

**References**

**194**

<b>Appendix</b>	<b>209</b>
†*High resolution climate change projections for the Eastern Bering Sea . . . . .	209
History of the ESRs . . . . .	214
*Responses to SSC comments from December 2021 and October 2022 . . . . .	217
*Description of the Report Card Indicators . . . . .	224
Methods Description for the Report Card Plots . . . . .	227

† indicates new Ecosystem Status Indicator contribution

\* indicates Ecosystem Status Indicator contribution updated with 2022 data

# List of Tables

1	Reported stranded NMFS marine mammal species for the last five years. . . . .	151
2	Estimated seabird bycatch in southeastern Bering Sea groundfish and halibut fisheries. . . . .	181
3	Estimated seabird bycatch in northern Bering Sea groundfish and halibut fisheries. . . . .	182
4	Summary of status for the 21 FSSI stocks in the BSAI, updated through June 2022. . . . .	188
5	BSAI FSSI stocks under NPFMC jurisdiction updated through June 2022. . . . .	190
6	Species included in annual surplus production in BSAI management area. . . . .	191
7	Composition of foraging guilds in the eastern Bering Sea. . . . .	225

# List of Figures

1	Ecosystem information mapping to support Ecosystem-Based Fisheries Management in Alaska.	5
2	2022 Eastern Bering Sea Report Card.	8
3	Factors affecting 2022 Western Alaska Chinook salmon runs and subsistence harvest.	26
4	Summer surface and bottom temperatures for the SEBS under high and low mitigation scenarios.	27
5	Summer surface and bottom temperatures for the NEBS under high and low mitigation scenarios.	29
6	Summer bottom and surface temperatures as a function of CMIP6 Global Warming Levels.	30
7	Time series of the NINO3.4, PDO, NPI, NPGO, and AO indices for 2011–2022.	34
8	Mean and anomaly plots of SLP.	37
9	Mean sea level pressure for spring and summer 2022.	38
10	Winter average north-south wind speed in the Bering Sea, 1949–2022.	39
11	Average 10m wind anomalies during February and March 2022.	40
12	Correlation between February wind and the rate of Bering Sea sea-ice advance/retreat.	41
13	Map showing along-shelf and cross-shelf wind components in the Bering Sea.	42
14	Seasonal cycle of along-shelf and cross-shelf wind components in the Bering Sea.	43
15	St. Paul air temperature anomalies.	44
16	SST anomalies for autumn, winter, spring, and summer.	46
17	Air temperature anomaly at 925 mb for summer 2022.	47
18	Time series trend of SST for the northern and southeastern Bering Sea shelves.	48
19	Marine heatwaves in the northern and southeastern Bering Sea since September 2019.	48
20	Cumulative annual sea surface temperature anomalies.	49
21	Seasonal mean SSTs, apportioned by season.	49
22	Map of the eastern Bering Sea.	50
23	Mean SST and bottom temperature for the northern and southeastern shelf domains.	51
24	Observations of temperature, salinity, and density from St. Paul Island.	53

25	Monthly averages for temperature, salinity, and density from St. Paul Island. . . . .	53
26	Monthly average chlorophyll concentrations at St. Paul Island. . . . .	54
27	Average summer surface and bottom temperatures on the EBS shelf. . . . .	55
28	Maps of bottom temperatures from EBS and NBS bottom trawl surveys. . . . .	55
29	Early season sea-ice extent in the Bering Sea, 1979–2021. . . . .	56
30	Mean sea-ice extent in the Bering Sea from 1979/1980–2021/2022. . . . .	57
31	Daily ice extent in the Bering Sea. . . . .	57
32	Map of five areas within which ice thickness was calculated. . . . .	58
33	Sea-ice thickness in the Bering Sea. . . . .	59
34	Sea-ice thickness between St. Matthew Island and St. Paul Island. . . . .	60
35	Bering 10K ROMS hindcast of cold pool extent, 2003–2022. . . . .	61
36	Cold pool extent, as measured from the EBS bottom trawl survey. . . . .	62
37	Predicted SST anomalies ( $^{\circ}\text{C}$ ) from the NMME model for the 2022–2023 season. . . . .	65
38	Relative CPUE for benthic epifauna during May–August from 1982–2022. . . . .	67
39	Map of regions used for satellite chl-a analyses. . . . .	69
40	Average spring chl-a concentrations in the eastern Bering Sea. . . . .	70
41	Heatmap of 8-day average chl-a concentrations in the eastern Bering Sea. . . . .	71
42	Peak spring bloom timing in the southeastern Bering Sea and at mooring M2. . . . .	72
43	Maps illustrating the location and extent of coccolithophore blooms in September. . . . .	74
44	Coccolithophore index for the southeastern Bering Sea shelf. . . . .	75
45	Location of Continuous Plankton Recorder data. . . . .	77
46	Annual anomalies of lower trophic levels for the eastern Bering Sea. . . . .	78
47	Maps of zooplankton abundance during the spring 2022 70m isobath survey. . . . .	80
48	Time series of zooplankton abundance during the spring 2022 70m isobath survey. . . . .	81
49	Lipid content for zooplankton during the spring 2022 70m isobath survey. . . . .	82
50	Maps of zooplankton abundance during the late-summer 2022 BASIS survey. . . . .	83
51	Time series of zooplankton abundance during the late-summer 2022 BASIS survey. . . . .	84
52	Lipid content for zooplankton during the late-summer 2022 BASIS survey. . . . .	85
53	Maps of zooplankton abundance during the late-summer 2022 NBS survey. . . . .	87
54	Time series of zooplankton abundance during the late-summer 2022 NBS survey. . . . .	88
55	Lipid content for zooplankton during the late-summer 2022 NBS survey. . . . .	89
56	Estimated euphausiid density in the 2022 EBS summer acoustic-trawl survey. . . . .	91

57	Average euphausiid abundance from NOAA-AFSC EBS summer acoustic-trawl surveys. . . .	92
58	Biomass of jellyfish in surface waters during late summer, 2003–2022. . . . .	95
59	Relative CPUE for jellyfish during May–August from 1982–2022. . . . .	96
60	Biomass of forage fish in surface waters during late summer, 2003–2022. . . . .	98
61	Biomass of age-0 Walleye pollock in surface waters during late summer, 2003–2022. . . . .	99
62	Biomass of Pacific herring in surface waters during late summer, 2003–2022. . . . .	100
63	Biomass of capelin in surface waters during late summer, 2003–2022. . . . .	101
64	Estimated biomass (tons) of Togiak herring. . . . .	102
65	Model estimates of age-4 recruit strength for Togiak herring. . . . .	103
66	Abundance of juvenile sockeye salmon in surface waters during late summer, 2003–2022. . . .	105
67	Juvenile Chinook salmon abundance estimates in the NBS, 2003–2022. . . . .	107
68	Juvenile chum salmon abundance index for the Upper Yukon River (fall) stock group, 2003–2022.	107
69	Juvenile pink salmon relative index for the NBS, 2003–2022. . . . .	108
70	Annual Bristol Bay sockeye salmon inshore run size 1963–2022. . . . .	110
71	Annual Bristol Bay sockeye salmon inshore run size 1963–2022 by fishing district. . . . .	110
72	Alaska statewide commercial salmon catches. . . . .	112
73	Commercial salmon catches in the eastern Bering Sea. . . . .	112
74	Bottom trawl survey strata and station locations in the EBS and NBS. . . . .	114
75	Condition of groundfish collected during the EBS bottom trawl survey: 1999–2022. . . . .	117
76	Time series of groundfish condition anomalies for the EBS. . . . .	118
77	Length-weight residual condition versus VAST relative condition for the EBS. . . . .	119
78	Condition of groundfish collected during the NBS bottom trawl survey: 2010, 2017–2022. . .	120
79	Length-weight residual condition versus VAST relative condition for the NBS. . . . .	121
80	Average thermal experience of groundfish in the SEBS. . . . .	124
81	Bioenergetic diet indices for groundfish in the SEBS. . . . .	126
82	Bioenergetic (potential) scope for growth for fish in recent years. . . . .	127
83	Total mortality for age-1 pollock, P. cod, and Arrowtooth. . . . .	129
84	Estimates of prey biomass consumed by predators in the CEATTLE model. . . . .	130
85	Predation mortality for age-1 pollock from pollock, P. cod, and Arrowtooth. . . . .	131
86	Annual ration for adult predators: pollock, P. cod, and Arrowtooth. . . . .	132
87	Temperature Change index values for the 1950 to 2021. . . . .	133
88	Temperature change index of conditions experienced by the 1960–2021 year classes. . . . .	134

89	Relationship between estimated abundance of large copepods and age-3 pollock. . . . .	136
90	Abundance of age-3 pollock estimated from large copepod abundance estimates. . . . .	137
91	Relative CPUE for miscellaneous fish species during May–August from 1982–2022. . . . .	139
92	Biomass for commercial crab stocks caught on the bottom trawl survey, 1998–2022. . . . .	141
93	Reproductive success of seabirds at St. George and St. Paul Islands, 1996–2022. . . . .	144
94	2022 Seabird Report Card. . . . .	145
95	Beached bird relative abundance for the eastern Bering Sea. . . . .	147
96	Map of seabird carcass reports for Alaska, May–September 2022. . . . .	148
97	CPUE for fish and invertebrates from bottom trawl surveys in the EBS and NBS. . . . .	153
98	CPUE of fish and invertebrates sampled during bottom trawl surveys between 2010 and 2022. . . . .	154
99	Changes in mean CPUE of 41 major taxa in the northern Bering Sea. . . . .	154
100	Shifts in latitude and depth distribution of groundfish in the eastern Bering Sea. . . . .	156
101	Average displacement of 39 taxa on the eastern Bering Sea shelf. . . . .	157
102	Latitudinal trends in density for all fish and invertebrate taxa. . . . .	157
103	Mean lifespan of the eastern Bering Sea demersal fish community. . . . .	159
104	Mean length of the groundfish community, 1982–2022. . . . .	160
105	Stability of the groundfish biomass in the eastern Bering Sea. . . . .	163
106	Maps of Jul-Sep bottom water pH. . . . .	165
107	Time series of Jul-Sep pH and $\Omega_{\text{arag}}$ undersaturation indices as percent of EBS shelf. . . . .	166
108	Timeseries of annualized Jul-Sep average bottom water $\Omega_{\text{arag}}$ and pH. . . . .	166
109	Map of 2022 HABs sampling areas and partners by the AHAB Network. . . . .	168
110	Algal toxins detected in stranded and harvested marine mammals in Alaska. . . . .	170
111	<i>Alexandrium</i> densities and Paralytic shellfish toxins sampled in August 2022. . . . .	172
112	Total biomass and percent of total catch biomass of FMP groundfish discards. . . . .	174
113	Total biomass of FMP groundfish discarded in the EBS by sector and week, 2017–2022. . . . .	176
114	Total catch of non-target species in EBS groundfish fisheries (2011–2021). . . . .	179
115	Estimated seabird bycatch by region, 2012–2021. . . . .	183
116	Spatial distribution of observed seabird bycatch from 2016–2021. . . . .	184
117	Estimated albatross bycatch by region, 2012–2021. . . . .	185
118	The trend in overall Alaska FSSI from 2006 through 2022. . . . .	188
119	The trend in BSAI FSSI from 2006 through 2022. . . . .	189
120	Total ASP across major groundfish stocks in the BSAI. . . . .	192

121	Contributions of each stock to mean annual surplus production . . . . .	192
122	Total ASP across the major commercial stocks, <i>excluding Walleye pollock</i> . . . . .	193
123	SEBS bottom water temperature (°C) projected under two climate scenarios. . . . .	210
124	NEBS bottom water temperature (°C) projected under two climate scenarios. . . . .	213
125	The IEA (integrated ecosystem assessment) process. . . . .	216
126	NOAA Alaska Fisheries Science Center’s human dimensions indicators mapping. . . . .	219

# Ecosystem Indicators

## Noteworthy Topics

Here we present items that are new or noteworthy and of potential interest to fisheries managers.

### Factors Affecting 2022 Western Alaska Chinook Salmon Runs & Subsistence Harvest

Western Alaska Chinook salmon runs have concurrently declined to low abundance levels for over a decade (ADFG, 2013; Schindler et al., 2013; KRITFC, 2022; Liller, 2021)<sup>4</sup>. Salmon are integral to the Western Alaska ecosystem, bridging marine and freshwater habitats, filling both prey and predator niches, and supporting vital subsistence harvests (Courtney et al., 2019; KRITFC, 2022). Figure 3 highlights the factors that contributed to the 2022 run sizes of Chinook salmon across Western Alaska as evidenced by Western science, Indigenous Knowledge, and community observations from the Kuskokwim and Yukon rivers.

Cumulative ecosystem factors since 2016 impacted the spawning adults, to the marine-stage juveniles, and ultimately the returning adults in 2022. For the parent spawners in 2016 and 2017, marine heatwave conditions (p. 31), smaller and younger size at maturity (Lewis et al., 2015; Oke et al., 2020), and warm river temperatures during the adult spawning migration likely contributed to reduced reproductive success (von Biela et al. (2020), Howard & von Biela (in review)). Low summer water levels and warm river conditions had the potential to impact eggs (2016–2017), and freshwater conditions could continue to influence fry and smolt growth and survival (2017–2018), but those relationships vary in different places depending on the absolute values of temperature, flow, and water level and are not fully understood across different tributaries.

Marine juveniles experienced heatwave conditions again in the eastern Bering Sea in 2019 when low zooplankton productivity (p. 79) contributed to empty stomachs and decreased fish condition (Murphy et al., 2021). In 2019 and 2020 combined, approximately 28,300 immature Chinook salmon from Western Alaska (Yukon and Coastal Western Alaska regions) were caught as bycatch<sup>5</sup>). The estimated impact rate of bycatch to combined Western Alaska Chinook salmon stocks averaged 1.9% for the 2011–2021 runs (see Table 9 here<sup>6</sup>) or annual estimates of 6,331–10,614 fewer spawners to Western Alaska (see Table 7 here<sup>6</sup>). The impact rate for the 2022 run is not yet available, but is expected to be higher based on low run sizes in 2022 (i.e., impact rate is inversely related to run size).

---

<sup>4</sup>[https://static1.squarespace.com/static/5afdc3d5e74940913f78773d/t/6359792089ec3e15693c80dd/1666808118921/Salmon+Sit+Report+2022\\_10-03-22\\_FINAL.pdf](https://static1.squarespace.com/static/5afdc3d5e74940913f78773d/t/6359792089ec3e15693c80dd/1666808118921/Salmon+Sit+Report+2022_10-03-22_FINAL.pdf)

<sup>5</sup><https://meetings.npfmc.org/CommentReview/DownloadFile?p=38f9b0d4-52be-4718-8dc7-d837d1be531c.pdf&fileName=D1b%20Bering%20Sea%20Chinook%20Genetics%202020.pdf>

<sup>6</sup><https://meetings.npfmc.org/CommentReview/DownloadFile?p=c16a58bc-e94e-4fd3-a23f-08909946bf20.pdf&fileName=D1c%20Chinook%20Salmon%20AEQ.pdf>

Marine temperatures largely relaxed to average conditions over the past year (Figure 23), which may have a positive effect on 2022 spawning success. However, amounts necessary for subsistence use of Chinook salmon in Kuskokwim and Yukon communities have not been met since 2010 and were not met again in 2022. Food security impacts associated with Chinook salmon declines in Western Alaska have been compounded by declines regionally in other salmon species, such as coho and chum salmon (KRITFC, 2022).

*Contributed by*

*Kevin Whitworth and Terese Schomogyi - Kuskokwim River Inter-Tribal Fish Commission*

*Joseph Spaeder - Bering Sea Fishermen's Association Research Coordinator*

*Kathrine Howard - Alaska Department of Fish & Game*

*Vanessa von Biela - U.S. Geological Survey, Alaska Science Center*

*Megan Williams and Patricia Chambers - Ocean Conservancy*

*Elizabeth Siddon - NOAA Fisheries, Alaska Fisheries Science Center*



# High Resolution Climate Change Projections for the Eastern Bering Sea

“Carbon mitigation” includes national and global policies and technologies to reduce greenhouse gas emissions and increase atmospheric carbon recapture in order to reduce global warming and climate change. In the absence of immediate implementation of widespread carbon mitigation measures, significant warming of sea surface and bottom water temperatures (SST and BT, respectively) are projected to occur across the Bering Sea over the next century, driving average water temperatures at the end of the century to be as warm or warmer than those observed during recent marine heatwaves. Specifically, under a low carbon mitigation scenario (‘ssp585’) modeled bottom temperatures consistently exceed average historical (1980–2013) ranges by 2040–2060. In contrast, in scenarios with immediate implementation of high carbon mitigation actions, warming is projected to be much more gradual over the next century and by 2080–2100 only moderately warmer than present day. In essence, scenarios that include immediate and large-scale implementation of carbon mitigation measures predict a future Bering Sea that is slightly warmer but relatively similar to contemporary conditions, while scenarios with delayed or minimal implementation project warming that drives the modeled Bering Sea system to conditions well beyond those observed to date (Figures 4 and 5).

## SEBS Climate projections

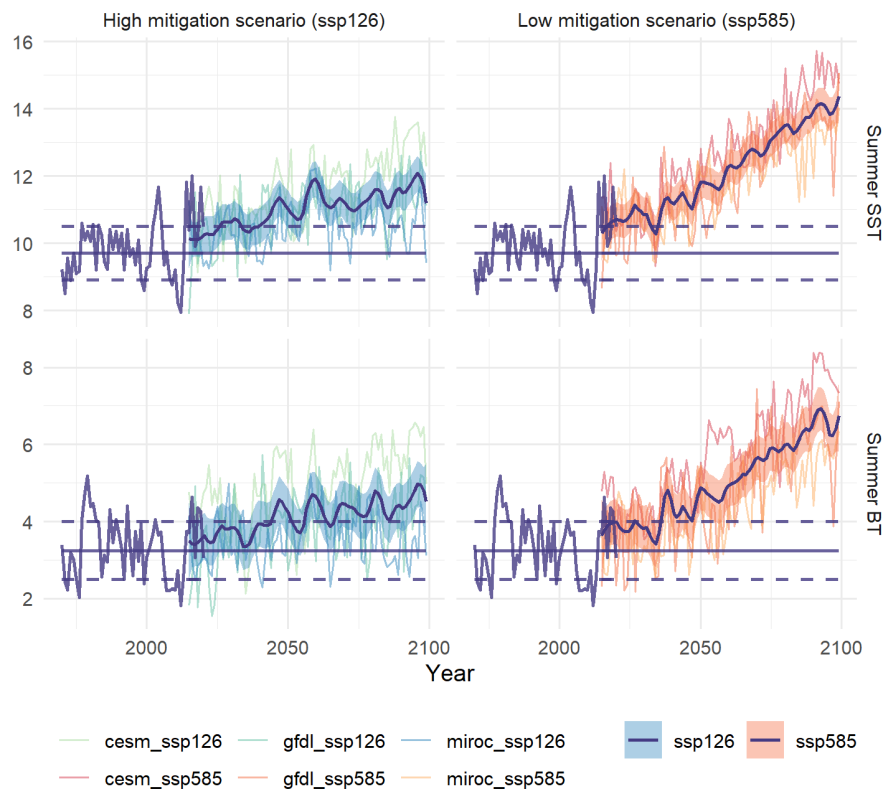


Figure 4: Bias-corrected summer sea surface temperature (top row) and bottom temperature (bottom row) for the southern Bering Sea (SEBS) from the hindcast (dark blue line) and projections under high (ssp126, left column; cool colors) and low (ssp585, right column, warm colors) mitigation scenarios. A ten year running mean is shown in the dark line and shading indicates the standard error of mean values; individual Earth System Models are shown as individual lines. Average modeled temperatures from the reference period (1980–2013) of the hindcast are shown as the horizontal blue line; dashed lines represent  $\pm 1$  standard deviation of the mean. Note different scales between rows.

Projected warming differs slightly across seasons as well as mitigation scenarios. Warming is generally larger across all regions and seasons under low carbon mitigation scenarios. However, in the northeastern Bering Sea (NEBS) there are large differences in winter bottom water warming between low and high carbon mitigation scenarios. We examined three contrasting earth systems models to evaluate the spread and characterize the agreement in projections (see methods in Hermann et al. (2021) for more detail). Under high mitigation scenarios, two of the three models projected continuation of cold winter conditions, indicating the potential for sea ice and cold bottom water temperatures to be preserved to some extent over the next century in these scenarios.

Global Warming Levels (GWLs) are an index used internationally by policy makers to standardize discussions around future climate change impacts. GWL indices represent average warming across the entire globe (all seasons and regions) in degrees Celsius relative to pre-industrial average global temperatures from the years 1850–1900. Present day GWL is around +1.1°C, meaning that on average the earth’s atmosphere near the surface is 1.1°C warmer than it was during the pre-industrial era at the end of the last century. This warming is unprecedented in the last 2000 years, and temperatures in the most recent decade (2011–2020) are warmer than any period in the last 125,000 years (IPCC, 2021). Based on multiple lines of evidence, the IPCC and other experts have identified critical GWLs of +1.5 and +2°C, beyond which climate change impacts and risks across sectors and nations rapidly increase, and the feasibility and effectiveness of adaptation actions become highly uncertain (IPCC, 2022). Of note, GWLs of +1.5 and +2°C represent the target and limit respectively of the Paris Agreement, a legally binding international treaty on climate change (i.e., UNFCCC Paris Agreement and Nationally Determined Contributions (NDCs)<sup>7</sup>).

While the earth as a whole has warmed approximately 1.1°C, warming to date has not been even across regions and the Arctic has warmed roughly +2 to +3°C to date. To understand what GWLs mean for the Bering Sea marine ecosystem, we used high resolution model projections to translate GWL indices into regional changes in SST and BT. A GWL of +1.5°C (over the pre-industrial average, or roughly +0.4°C global warming relative to present day) is projected to result in eastern Bering Sea SSTs and BTs that are similar to present day conditions (Figure 6). However, at GWL of +3 and +4°C (or +1.9 to +2.9°C global warming relative to present day), significant warming is projected to push water temperatures well beyond those observed to date, even during recent marine heatwaves. Ongoing work as part of the Alaska Climate Integrated Modeling (ACLIM) project<sup>8</sup> and numerous climate change studies find evidence of increasing risk for Bering sea ecosystems, fisheries, subsistence resources, and coastal communities associated with higher warming rates (IPCC, 2022). Differences in trends between low and high carbon mitigation scenarios demonstrate the scope for warming of the Bering Sea to be ameliorated through carbon mitigation. Importantly, there is high potential to limit summer bottom temperature warming to less than ~3°C (over 1980–2013 averages), provided sufficient global cooperation results in necessary reductions in carbon emissions.

For more details on these high resolution climate change projections for the eastern Bering Sea, please see p. 209.

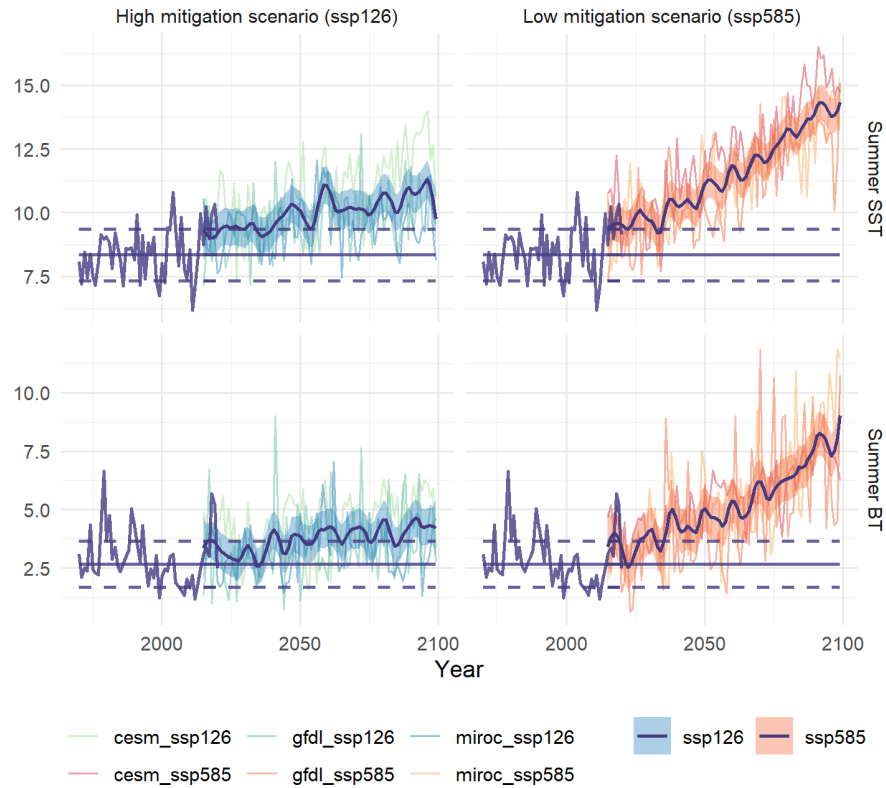
*Kirstin K. Holsman - NOAA Fisheries, Alaska Fisheries Science Center*  
*Albert Hermann and Wei Cheng - Cooperative Institute for Climate, Ocean and Ecosystem Studies,*  
*University of Washington, Seattle, WA*  
*and Pacific Marine Environmental Laboratory, Seattle, WA*  
*Kelly Kearney and Darren Pilcher - Cooperative Institute for Climate, Ocean and Ecosystem Studies,*  
*University of Washington, Seattle, WA*  
*Kerim Aydin - NOAA Fisheries, Alaska Fisheries Science Center*  
*Ivonne Ortiz - Cooperative Institute for Climate, Ocean and Ecosystem Studies,*  
*University of Washington, Seattle, WA*

---

<sup>7</sup><https://unfccc.int/ndc-synthesis-report-2022>

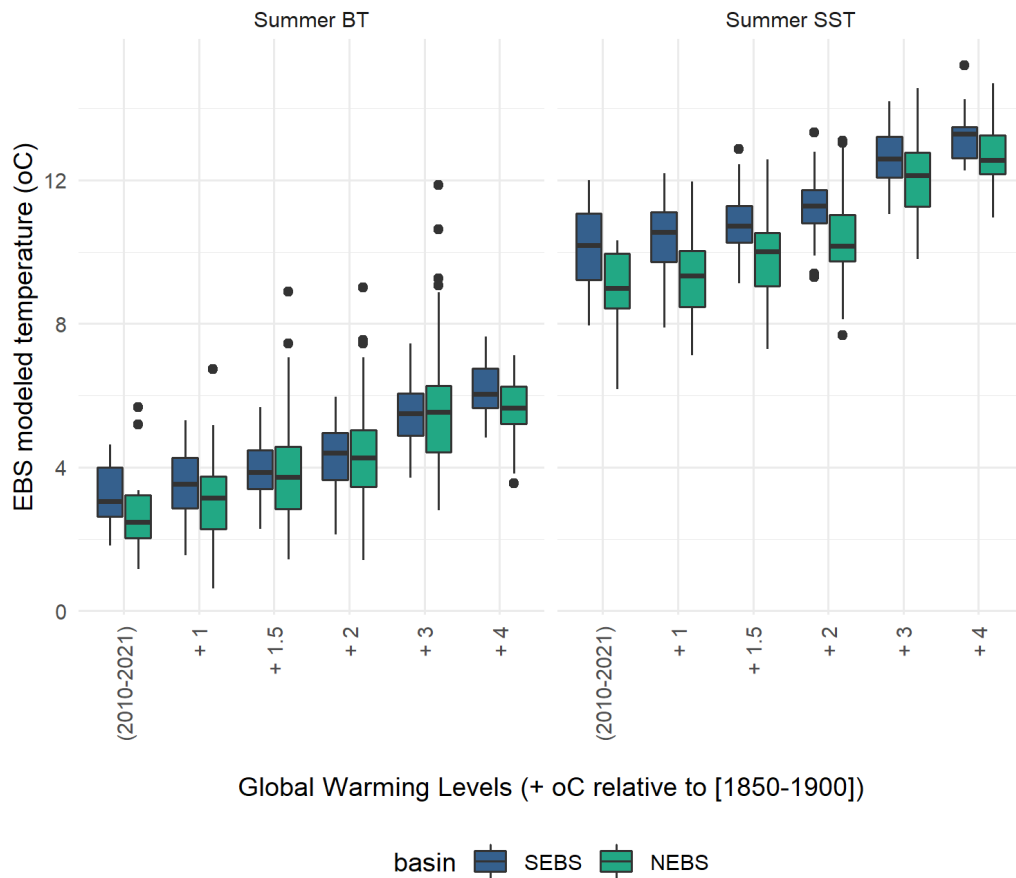
<sup>8</sup><https://www.fisheries.noaa.gov/alaska/ecosystems/alaska-climate-integrated-modeling-project>

## NEBS Climate projections



Operational hindcasts: AK IEA | Projections: ACLIM2 | Model: Bering10K 30-layer

Figure 5: Bias-corrected summer sea surface temperature (top row) and bottom temperature (bottom row) for the northern Bering Sea (NEBS) from the hindcast (dark blue line) and projections under high (ssp126, left column; cool colors) and low (ssp585, right column, warm colors) mitigation scenarios. A ten year running mean is shown in the dark line and shading indicates the standard error of mean values; individual Earth System Models are shown as individual lines. Average modeled temperatures from the reference period (1980–2013) of the hindcast are show as the horizontal blue line; dashed lines represent  $\pm 1$  standard deviation of the mean. Note different scales between rows.



Operational hindcasts: AK IEA | Projections: ACLIM2 | Model: Bering10K 30-layer

Figure 6: Southern and Northern Bering Sea (‘SEBS’ and ‘NEBS’, respectively) modeled summer bottom and sea surface temperatures (‘BT’ and ‘SST’, respectively) as a function of CMIP6 Global Warming Levels (mean global increase in temperature relative to pre-industrial temperatures (1850–1900)). Recent hindcast ranges are reported (‘2010–2021’) as well as bias corrected projections from the Bering10K model for each GWL (+1 to +4°C GWL). Boxplots represent the 25<sup>th</sup> and 75<sup>th</sup> percentile (i.e., the interquartile range) with the horizontal line representing the median temperature, and the error bars representing the min or max (IQR ± IQR\*1.5). Outliers are represented by points (e.g., marine heatwave years if above the boxplot). For more information on interpretation of boxplots see <https://r-graph-gallery.com/boxplot.html>.

# Ecosystem Status Indicators

Indicators presented in this section are intended to provide detailed information and updates on the status and trends of ecosystem components. Older contributions that have not been updated are excluded from this edition of the report. Please see archived versions available at: <http://access.afsc.noaa.gov/reem/ecoweb/index.php>

## Physical Environment Synthesis

*This synthesis section provides an overview of physical oceanographic variables and contains contributions from (in alphabetical order):*

**Lewis Barnett** - NOAA Fisheries, Alaska Fisheries Science Center, Resource Assessment and Conservation Engineering Division

**Nick Bond** - University of Washington, Cooperative Institute for Climate, Ocean, and Ecosystem Studies [CICOES]

**Matt Callahan** - Pacific States Marine Fisheries Commission

**Seth Danielson** - University of Alaska Fairbanks, College of Fisheries and Ocean Sciences

**Lauren Divine** - Ecosystem Conservation Office at Aleut Community of St. Paul Island

**Tyler Hennon** - University of Alaska Fairbanks, College of Fisheries and Ocean Sciences

**Kelly Kearney** - University of Washington, CICOES and NOAA Fisheries, Alaska Fisheries Science Center

**Emily Lemagie** - NOAA Pacific Marine Environmental Lab [PMEL]

**Aaron Lestenkof** - Ecosystem Conservation Office at Aleut Community of St. Paul Island

**Jim Overland** - NOAA PMEL

**Noel Pelland** - University of Washington, CICOES

**Sean Rohan** - NOAA Fisheries, Alaska Fisheries Science Center, Resource Assessment and Conservation Engineering Division

**Rick Thoman** - University of Alaska Fairbanks, International Arctic Research Center, Alaska Center for Climate Assessment and Policy

**Muyin Wang** - University of Washington, CICOES and NOAA PMEL

*Synthesis compiled by Tyler Hennon  
University of Alaska Fairbanks  
College of Fisheries and Ocean Sciences*

**Last updated: October 2022**

## Introduction

In this section, we provide an overview of the physical oceanographic conditions impacting the eastern Bering Sea (EBS), describe conditions observed from fall 2021 through summer 2022, and place 2022 in the context of recent years. The physical environment impacts ecosystem dynamics and productivity important to fisheries and their management. We merge across information sources, from broad-scale to local-scale, as follows:

## Outline

1. Climate Overview
2. Regional Highlights
3. Winds and Surface Transport
4. Sea Surface Temperature (SST) and Bottom Temperature
5. Sea Ice
6. Cold Pool
7. Seasonal Projections of SST from the National Multi-Model Ensemble (NMME)

## Executive Statement

Observations over the last year (September 2021–August 2022) show that the extended warm phase experienced by the EBS has ended. Across a variety of metrics, the past year has seen the relaxation to more average thermal conditions. Sea surface air temperatures were average, or even slightly below average over the EBS for much of the year, and, correspondingly, satellite-based observations of sea surface temperature (SST) were within one standard deviation of the long-term mean (e.g., Figures 16 and 23). Bottom temperatures also returned to near the long-term average, and consequently the cold pool ( $<2^{\circ}\text{C}$  bottom water) expanded to an average areal extent after several years of a significantly reduced footprint (Figures 36 and 35). For much of the year, ice extent was at or above average, though spring ice melt in 2022 occurred faster and earlier than average beginning in mid-April (Figure 31). Despite greater ice extent compared to last year, ice thickness in the 3<sup>rd</sup> week of March was generally lower than in the 2020–2021 winter (though near the 10-year average) (Figures 33 and 34). For projections into the next year, estimates from the National Multi-Model Ensemble (NMME) show that SST over the EBS is expected to be within  $\sim 0.5^{\circ}\text{C}$  of average through March 2023, suggesting at least a short-term persistence of average thermal conditions (Figure 37).

## Synthesis Summary

The extended warm phase experienced by the EBS and much of the north Pacific since  $\sim 2014$  largely relaxed to more average conditions over the prior year (September 2021–August 2022). The  $>100$  year record of sea level air temperature at St. Paul Island, which documented the extended warm phase, shows that average air temperature over the last year is close to the long-term average (Figure 15). Unlike in 2018 and 2019, where strong and anomalous southerly winds coincided with a strong and persistent marine heat wave (MHW) (Figure 18), wind patterns over the shelf have been much closer to average over the past year (Figures 10 and 14).

The return to average sea surface temperatures (SST) over the whole of the Bering Sea is also corroborated by satellite observations (NOAA’s Coral Reef Watch Program and Extended SST V5), which show that, over much of the past year, SST was within  $\sim 0.5^{\circ}\text{C}$  of average, except from December 2021 to February 2022, where SST over large portions of the Bering shelf was  $0.5$ – $1.5^{\circ}\text{C}$  below average (Figure 23, top 2 rows). Marine heatwaves (MHWs) were still present in satellite-based observations of SST over the prior year; however, they were relatively weak and short-lived compared to the MHWs documented in the recent warm stanza (Figure 19).

A Bering 10K Regional Ocean Modeling System (ROMS) hindcast simulation suggests that bottom temperatures in the northern Bering Sea (NBS) over the past year were well within the historical (1971–2022)

average. ROMS bottom temperature estimates in the southeastern Bering Sea (SEBS), in contrast to recent years, exhibited periods that were significantly cooler than average. In the outer shelf domain, bottom temperature was consistently  $\sim 1^\circ\text{C}$  cooler than average, while in the middle and inner domains, bottom temperature was approximately  $1\text{--}2^\circ\text{C}$  cooler than average in winter (Dec-Mar), and near average conditions the rest of the year (Figure 23, bottom 2 rows).

Bering Sea sea-ice extent was generally higher than average throughout much of the 2021–2022 winter, reaching peaks of about  $800,000\text{ km}^2$  ( $\sim 100,000\text{ km}^2$  higher than average). Sea ice advanced rapidly in November, and ice extent generally remained above historical averages until an abrupt, and earlier than average, spring-time retreat beginning in mid-April (Figure 31). There was significant variability in February and March, where sea-ice extent co-varied with prevailing wind patterns (Figure 12), advancing with northerly winds and retreating with southerly winds (Figure 11).

Sea-ice thickness is evaluated at the 3<sup>rd</sup> week of March, which is generally when extent is at its greatest. During this period, sea-ice thickness was approximately average across all the regions of evaluation, though there is considerable variability, such as below-average ice thickness in Norton Sound and above-average ice thickness between St. Matthew Island and St. Paul Island. However, somewhat unexpectedly, the sea-ice thickness was almost universally lower than the previous winter (2020–2021) (Figures 33 and 34).

The cool-to-average winter temperatures throughout the water column of the EBS were favorable to cold pool formation. The bottom trawl survey documented a cold pool (bottom temperature  $< 2^\circ\text{C}$ ) extent of  $\sim 178,625\text{ km}^2$ . This is very near the 30-year average (1982–2022) of  $181,018\text{ km}^2$ , and a sharp increase from the 2018–2021, a period with the smallest cold pools on record. The extents of the  $\leq -1^\circ\text{C}$  ( $12,075\text{ km}^2$ ),  $\leq 0^\circ\text{C}$  ( $45,000\text{ km}^2$ ), and  $\leq 1^\circ\text{C}$  ( $107,300\text{ km}^2$ ) isotherms were also much larger than during the three prior surveys and near their time-series averages (Figure 36).

The National Multi-Model Ensemble (NMME) of coupled atmosphere-ocean climate models predicts that sea surface temperature will be within  $0.25^\circ\text{C}$  of the long-term average this coming winter (Oct-Mar), although much of the Pacific south of the Aleutian Islands and western Bering Sea are expected to be warmer than average by  $\sim 0.5\text{--}1.5^\circ\text{C}$ . If this prediction holds, we may expect the EBS sea-ice extent and bottom temperatures (especially in the shallower regions) to be near historical averages (Figure 37).

## 1. Climate Overview

Contributed by Nick Bond, *nicholas.bond@noaa.gov*

Climate indices provide a means of characterizing the state of the North Pacific atmosphere-ocean system. Five commonly used indices are presented here: the NINO3.4 index for the state of the El Niño/Southern Oscillation (ENSO) phenomenon, the PDO index (the leading mode of North Pacific SST variability), the North Pacific Index (NPI), the North Pacific Gyre Oscillation (NPGO) and the Arctic Oscillation (AO). The time series of these indices, with the application of three-month running means, from 2012 into spring/summer 2022 are plotted in Figure 7. Two indices, the NPI and the AO, best represent conditions impacting the EBS shelf and are described in more detail below.

The state of the Aleutian low can be encapsulated by the NPI, with negative (positive) values signifying relatively low (high) SLP. The NPI was positive from autumn 2021 into the following winter, with particularly high values from November 2021 through January 2022. A brief reversal occurred in February 2022, with the return of weakly positive values during the spring and early summer of 2022. The NPI has been positive during 5 of the last 6 winters, with the exception being the winter of 2018–2019. The systematically positive state of the NPI, i.e., weak Aleutian low, is consistent with the overall decline in the PDO during the interval.

The AO represents a measure of the strength of the polar vortex, with positive values signifying anomalously low pressure over the Arctic and high pressure over the North Pacific at a latitude of roughly  $45^\circ\text{N}$ . The AO has been mostly positive since the spring of 2021, with the exception of the autumn of 2021. A positive state of the AO during winter, as occurred during 2021–2022, is generally associated with arctic air being

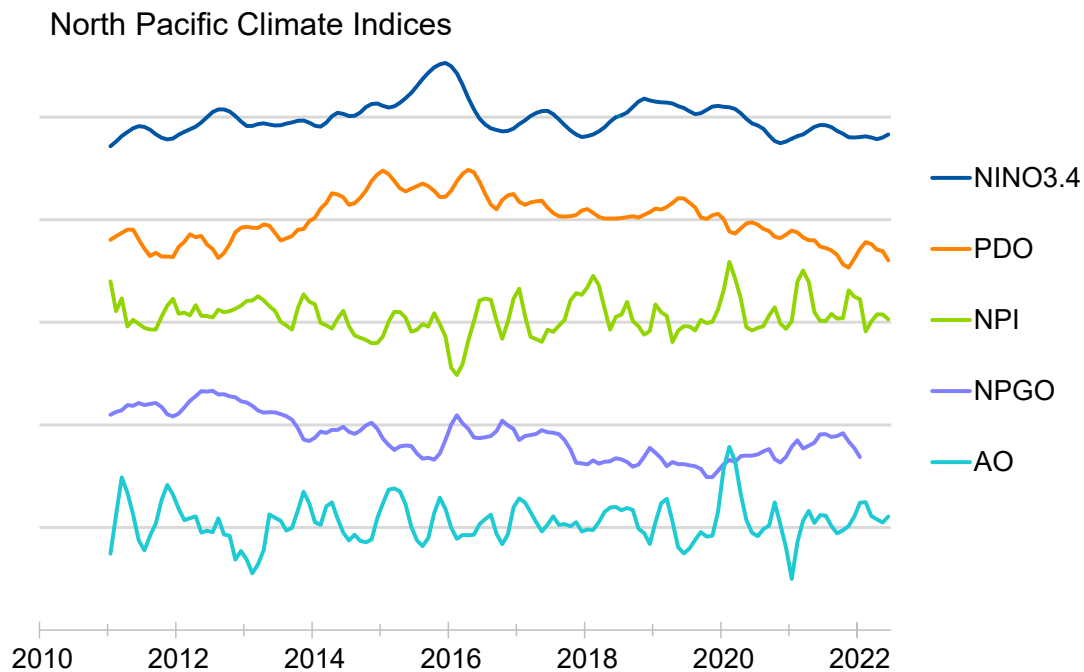


Figure 7: Time series of the NINO3.4, PDO, NPI, NPGO, and AO indices (ordered from top to bottom) for 2011–2022. Each time series represents monthly values that are normalized using a climatology based on the years of 1991–2020, and then smoothed with the application of three-month running means. The distance between the horizontal grid lines represents 5 standard deviations. More information on these indices is available from NOAA’s Physical Sciences Laboratory at <https://psl.noaa.gov/data/climateindices/>.

retained in the higher latitudes of the Northern Hemisphere, often leading to relatively cold weather for Alaska. That was not the case during the winter of 2021–2022, when the regional atmospheric circulation resulted in near-average temperatures for Alaska.

## 2. Regional Highlights

Contributed by Nick Bond, [nicholas.bond@noaa.gov](mailto:nicholas.bond@noaa.gov)

### Summary

A variety of sea level pressure (SLP) distributions relative to their seasonal norms occurred in the North Pacific atmosphere-ocean climate system during autumn 2021 through summer 2022. Lower than average SLP in the Gulf of Alaska (GOA) during autumn 2021 was accompanied by northwesterly wind anomalies and cooling on the SEBS shelf; a transition to strongly positive SLP anomalies south of the GOA during the winter of 2021–2022 resulted in a reversal in the wind anomalies for much of the North Pacific.

Mostly positive SLP anomalies prevailed in the middle latitudes of the North Pacific accompanied by positive sea surface temperature (SST) anomalies. The presence of relatively cool to near-average SSTs in Alaskan waters from late 2021 into 2022 part follows a multi-year interval of mostly above-average temperatures. It is unclear the extent to which the atmospheric circulation of the North Pacific was impacted by external factors, but the period of interest did include the co-occurrence of moderate La Niña conditions in the tropical Pacific. The PDO was negative in large part due to long-standing positive SST anomalies in the western and central North Pacific.

The climate models used for seasonal weather predictions indicate that La Niña is more likely than not to persist through the remainder of 2022. These models as a group indicate SST distributions in early 2023 that include colder than average temperatures for the GOA, near-average temperatures for the EBS and eastern Aleutian Islands, and warmer than average temperatures for the western Aleutians. A winter resembling the climatological mean is anticipated for the SEBS shelf, with sea ice expected to extend south to at least 60°N.

#### *Alaska Peninsula*

The coastal waters in the vicinity of the Alaska Peninsula were cooler than average, based on the period of 1991–2020, during the winter and spring of 2022, especially on the north side over the SEBS shelf. The cool waters are consistent with the cold air temperatures that occurred from November 2021 into February 2022, with the exception of a brief period of record-setting warm temperatures in late December 2021. Overall, the spring and summer air temperatures in 2022 were near seasonal norms.

#### *Aleutian Islands*

The near-surface waters of the Aleutian Islands were generally warmer than average, especially during winter 2021–2022 and summer 2022 in the western portion of the chain. These warm waters were accompanied by relatively shallow upper mixed layer depths in 2022. The mean wind anomalies during the winter of 2021–2022 included a component from the east, which is associated with enhanced northward flow through Unimak Pass (Stabeno and Hunt, 2002).

#### *Eastern Bering Sea*

The EBS shelf experienced an early start to its seasonal cooling during the autumn of 2021, relative to recent years. The rate of cooling, and the growth of ice then slowed, with resulting overall SST and ice cover extent that were near their averages for the last 30–40 years. The spring of 2022 featured relatively warm air temperatures in this region, and this weather pattern resulted in a relatively rapid retreat of sea ice. Upper ocean temperatures over the SEBS shelf were cooler during the summer of 2022 than the previous summer. More detail on the sea ice and ocean temperatures in this region is included below.

#### *Bering Sea Deep Basin*

Warm air and upper ocean temperature anomalies prevailed in the western, deep portion of the Bering Sea during the winter and spring of 2022. The winter was also relatively stormy. Despite the enhanced wind mixing, the heat fluxes at the air-sea interface appear to have been weaker than average, and upper mixed layer depths were less than average in spring 2022, according to the Global Ocean Data Assimilation System (GODAS). This was especially the case in the southern portion of the Bering Sea basin. The waters in the western portion of this region off the east coast of the Kamchatka Peninsula remained warmer than average through the summer of 2022.

#### *Arctic*

The Arctic region of northern Alaska during the period of fall 2021 through summer 2022 experienced somewhat greater sea-ice cover than during recent past years. In particular, there was a much more rapid advance of sea ice southward through the Chukchi Sea and then Bering Strait late in 2021 as compared with 2019 and 2020. On the other hand, the period of May through July included a relatively rapid retreat in the ice in association with strong winds from the south; by late summer 2022 the ice edge was considerably farther north than usual in the Chukchi Sea, and to a lesser extent in the Beaufort Sea. For the Arctic as a whole, the total area of sea-ice cover was quite low in early summer, but the decline through the remainder of summer was not as steep as in 2020, and the minimum area at the end of summer is apt to be significantly greater than the record low ice year of 2012.

### 3. Winds and Surface Transport

#### *Sea Level Pressure Anomalies*

Contributed by Nick Bond, [nicholas.bond@noaa.gov](mailto:nicholas.bond@noaa.gov), and Jim Overland, [james.e.overland@noaa.gov](mailto:james.e.overland@noaa.gov)

The state of the North Pacific climate from autumn 2021 through summer 2022 is summarized in terms of seasonal mean sea level pressure (SLP) anomaly maps. The SLP anomalies are relative to mean conditions over the period of 1991–2020. The SLP data are from the NCEP/NCAR Reanalysis project and are available from NOAA’s Physical Sciences Laboratory (PSL)<sup>9</sup>.

The autumn (Sep–Nov) of 2021 (Figure 8a and b) included prominent negative SLP anomalies in the north-eastern Gulf of Alaska (GOA), and weaker positive anomalies in an arc from the Sea of Okhotsk and western Bering Sea through the central North Pacific to the waters offshore of California. This SLP distribution resulted in anomalous winds from the northwest for the southeast Bering Sea shelf.

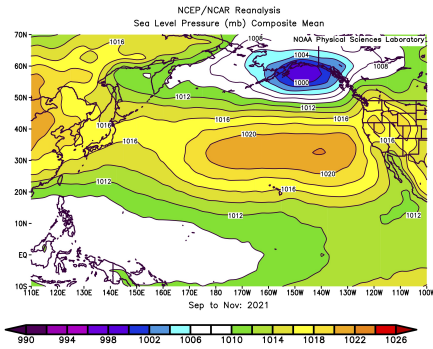
The SLP anomaly pattern for the winter (Dec–Feb) of 2021–2022 (Figure 8c and d) featured a large region of strongly positive SLP anomalies in the northeast Pacific centered south of the GOA, and much weaker negative SLP anomalies extending from the Sea of Okhotsk to the Hawaiian Islands. The accompanying wind anomalies included suppressed westerlies across the central and eastern North Pacific between roughly 25°N and 45°N. Enhanced westerlies were present across the eastern North Pacific farther north, implying anomalous equatorward Ekman transports in the upper ocean mixed layer.

Much weaker SLP anomalies were present in the NE Pacific during the spring (Mar–May) of 2022 (Figure 8e and f). Higher than average SLP occurred between roughly 25°N and 45°N across the basin with weak negative SLP anomalies in the GOA. The latter, in combination with relatively high SLP in the northwestern Bering Sea, resulted in anomalous winds from the north of about 2 ms<sup>-1</sup> for the SEBS shelf. Mean SLP over the Bering Sea shows the position of the jet stream (along the contours) to the south with the Aleutian Low Pressure System centered south of the Aleutian chain (Figure 9a). This pattern is reflective of more ‘typical’ conditions over the SEBS shelf, however the NBS and Arctic experienced warm conditions similar to the recent past.

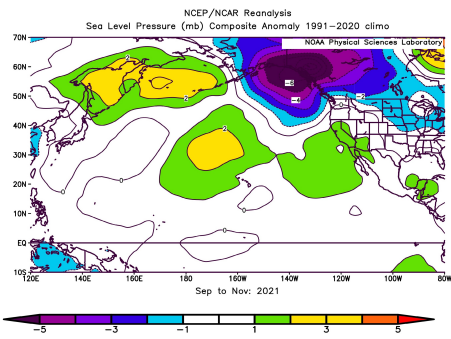
The summer (Jun–Aug) of 2022 included mostly negative SLP anomalies in the mid-latitude North Pacific, with the exception of a region of positive anomalies located south of the Alaska Peninsula (Figure 8g and h). The winds during this period included anomalies of about 1.5 to 2.5 ms<sup>-1</sup> from the northwest in the western Aleutian Island region; generally weak wind anomalies prevailed in the EBS. The high-pressure center in the Chukchi Sea in spring was replaced by two low pressure centers in the summer, both located over land. The jet stream “disappeared” and the pressure gradient was significantly reduced over the entire Bering Sea (Figure 9b).

---

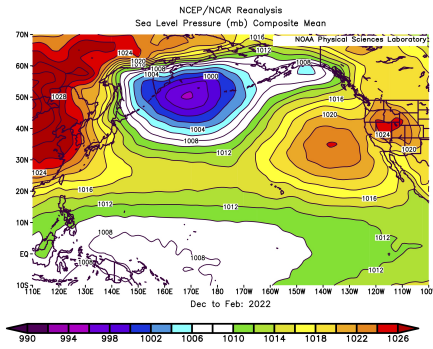
<sup>9</sup><https://www.psl.noaa.gov/cgi-bin/data/composites/printpage.pl>.



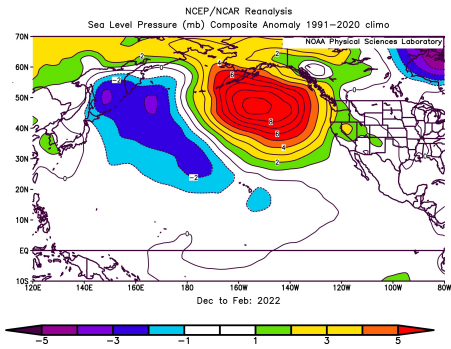
(a) Autumn Mean



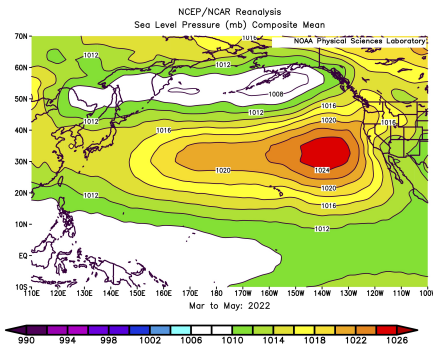
(b) Autumn Anomaly



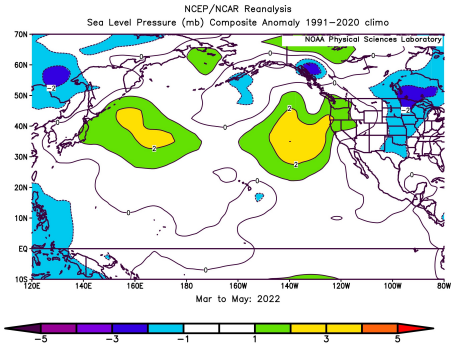
(c) Winter Mean



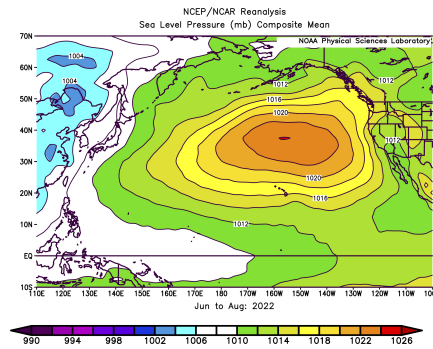
(d) Winter Anomaly



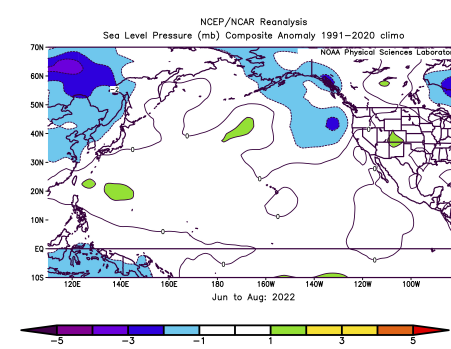
(e) Spring Mean



(f) Spring Anomaly

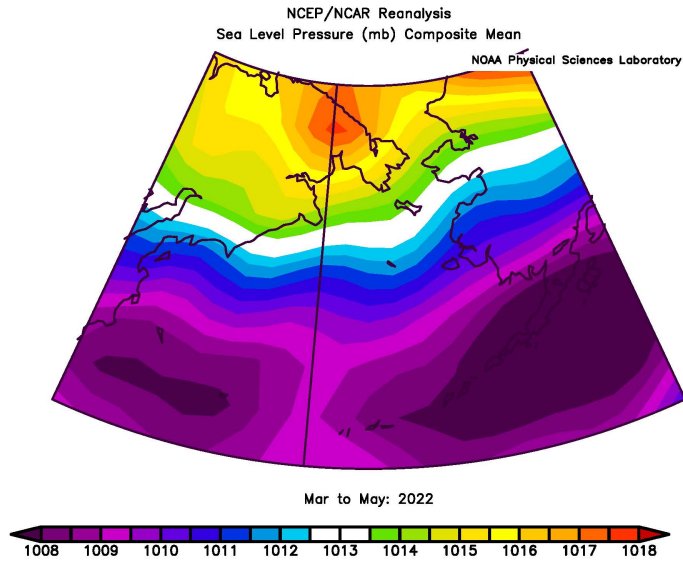


(g) Summer Mean

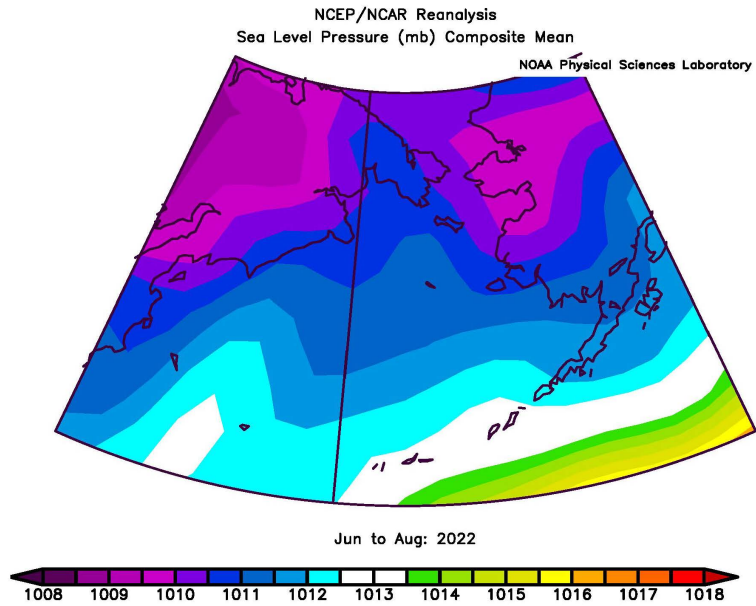


(h) Summer Anomaly

Figure 8: Sea level pressure mean (left column) and anomaly (right column) for autumn (Sept-Nov 2021; a and b), winter (Dec 2021-Feb 2022; c and d), spring (Mar-May 2022; e and f), and summer (Jun-Aug 2022; g and h). The SLP data are from the NCEP/NCAR Reanalysis project and are available by NOAA's Physical Sciences Laboratory (PSL)<sup>10</sup>.



(a) Spring



(b) Summer

Figure 9: Mean sea level pressure averaged for (a) spring (Mar-May) and (b) summer (Jun-Aug) 2022.

### Winter Wind Speed and Direction

Contributed by Rick Thoman, [rthoman@alaska.edu](mailto:rthoman@alaska.edu)

The average winter (Nov-Mar) wind speed can be used to categorize years as having prevailing north winds or south winds. No long-term trend is exhibited, although winters ending in 2018 and 2019 were among 5 years with the strongest south winds, which contributed to low sea-ice extent in those years. Red dots denote five years with strongest south winds, blue dots the five strongest north winds. For winter 2021–2022, the north-south component of the low level wind was only slightly stronger (more northerly) than the time series average, but this was the first winter since 2016–2017 with excess northerly winds (Figure 10).

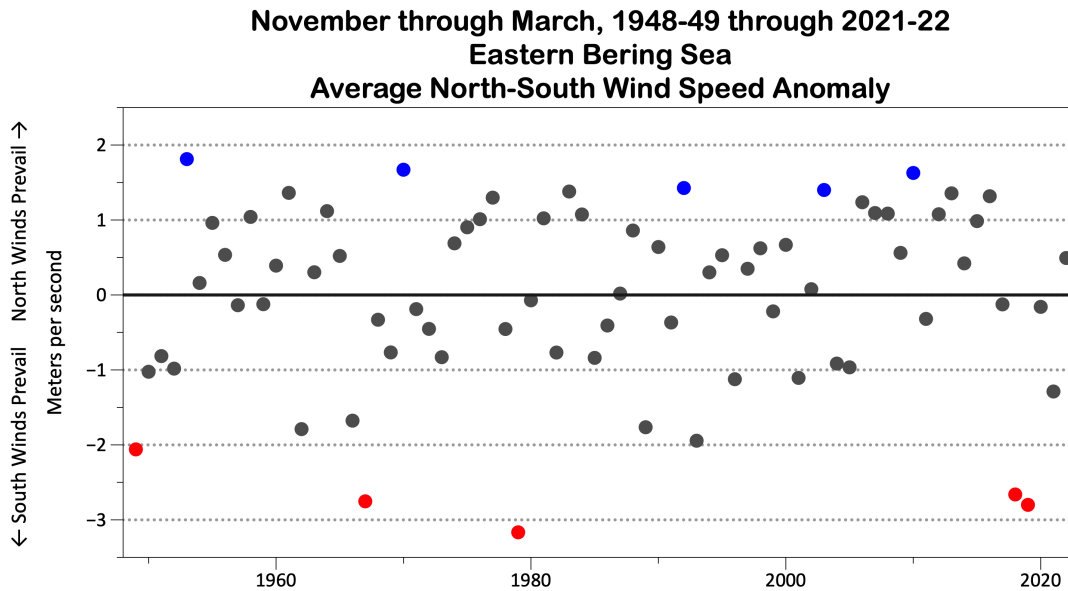


Figure 10: Winter (Nov-Mar) average north-south wind speed anomaly in the Bering Sea, 1949–2022. Red dots denote five years with strongest south winds, blue dots the five strongest north winds. **Note:** the north-south (meridional) component of the wind is plotted inversely to meteorological convention, with south to north as negative values and north to south as positive values. Source: NCEP/NCAR reanalysis.

### Spatial Variability of Prevailing Winds in Late-Winter and Early-Spring

Contributed by Tyler Hennon, [tdhennon@alaska.edu](mailto:tdhennon@alaska.edu)

The NCAR/NCEP 10m wind reanalysis (2000 to present) was used to examine the variability of the prevailing wind anomalies over the Bering Sea. In February of 2018 and 2019, strong and anomalous southerly winds likely were a major factor in the very low sea-ice extent observed during those years. In late winter and early spring of 2022, substantial variability in wind anomalies appear to correlate with shifts in ice extent over the Bering Sea shelf (Figure 11, a-c and Figure 31). Southerly winds in the second half of February coincided with a sudden retreat in sea ice, while northerly winds several weeks later coincided with a substantial rebound in sea-ice extent.

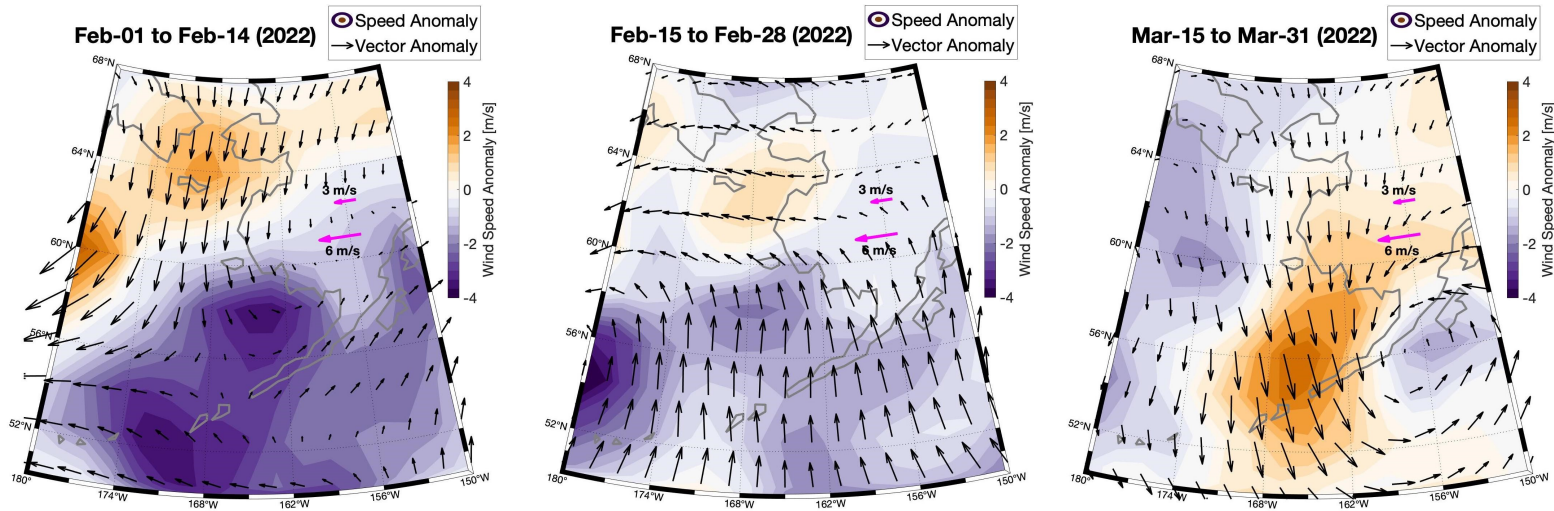


Figure 11: Average 10m wind anomaly vectors (black arrows) and anomalies in wind speed (color maps) during three 2-week periods between February 1<sup>st</sup> and March 31<sup>st</sup> 2022 (a-c). Anomaly is defined as the residual from the average annual signal. Magenta arrows indicate vector scale. *Nota bena*: wind speed and the length of velocity vectors do not have a 1:1 relationship. For example, strong winds that oscillate between northerly and southerly will have high speed but short velocity vectors (velocities average near zero), whereas strong steady winds will have both a high speed and a long velocity vector.

Examination of longer records of Bering Sea sea-ice extent and meridional winds reveals similar trends across many years. Meridional wind anomalies averaged across the Bering Sea ( $V'$ ) and anomalies in the rate of sea-ice advance/retreat  $(dA_{ice}/dt)'$  were significantly correlated ( $r=-0.58$ ,  $p<0.01$ ) when aggregating data from all Februarys since 2000 (Figure 12). Anomalies  $V'$  and  $(dA_{ice}/dt)'$  are defined as the residual to the average annual cycle. When winds are anomalously southerly, sea-ice extent diminishes faster than average, whereas if there are anomalous northerly winds, sea-ice extent advances. The correlation between  $V'$  and  $(dA_{ice}/dt)'$  is also significant ( $p<0.05$ ) for March, though slightly less strongly correlated ( $r=-0.37$ ). There is no significant relationship in January or beyond March, though this may be due to other drivers (e.g., local radiative forces) dominating changes in ice extent and washing out the signal from the winds.

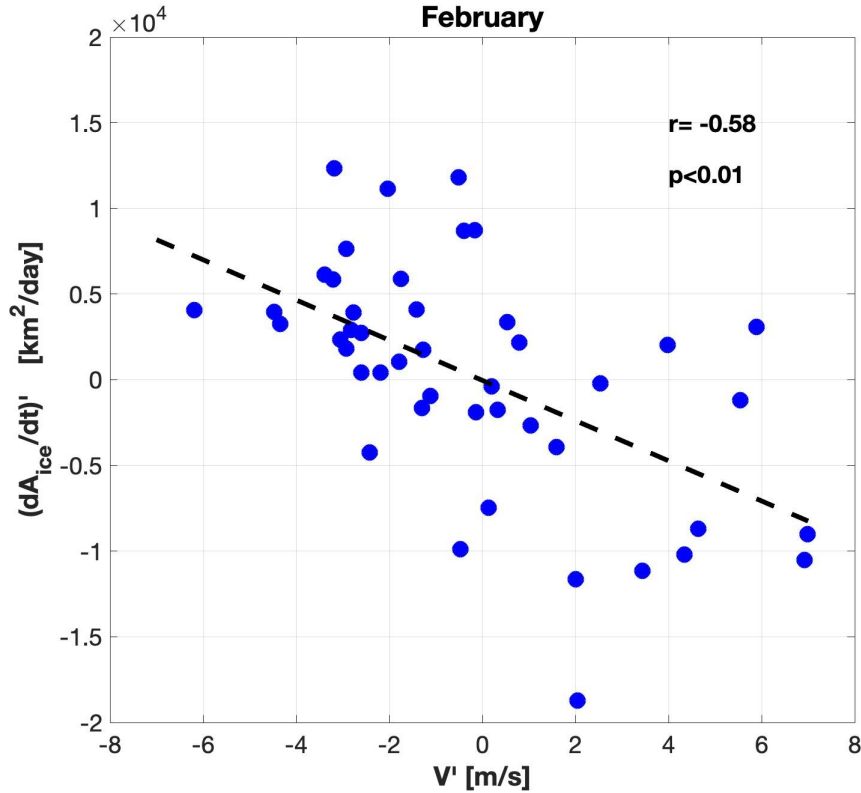


Figure 12: Dots show relationship between the anomaly of Bering Sea meridional winds ( $V'$ ) and the anomaly of the rate of Bering Sea areal sea-ice advance/retreat ( $[dA_{ice}/dt]'$ ) for the month of February (all years since 2000). Positive  $V'$  indicates anomalously southerly winds, and positive  $[dA_{ice}/dt]'$  indicates faster gain in sea-ice coverage than average (while negative is faster retreat than average). Each dot represents an average of two weeks of data (within February) over the period of 2000–2022. Black dashed line shows the best-fit linear regression.

The exact mechanisms driving the relationship between winds and sea-ice extent are not immediately obvious, though it could be a combination of: 1) stress of the winds physically transporting sea ice north or south (thereby altering the edge of sea-ice extent) and 2) the thermal content of the winds, where warm southerly winds may act to melt ice, and cold northerly winds could cause ice formation. A more detailed analysis (e.g., analysis of surface heat fluxes) is needed to establish the relative importance of each of these processes.

### *Winds at the Bering Sea Shelf Break*

Contributed by Tyler Hennon, [tdhennon@alaska.edu](mailto:tdhennon@alaska.edu)

NCEP/NCAR wind reanalysis was used to examine the along- and cross-slope wind components along the Bering Sea shelf break. Four-times daily wind data dating back to January 2000 were interpolated to a transect approximating the shelf break (Figure 13), and the zonal and meridional components were rotated into along- and cross-shelf components. These components of wind were then averaged across the whole transect for each month dating back to 2000.

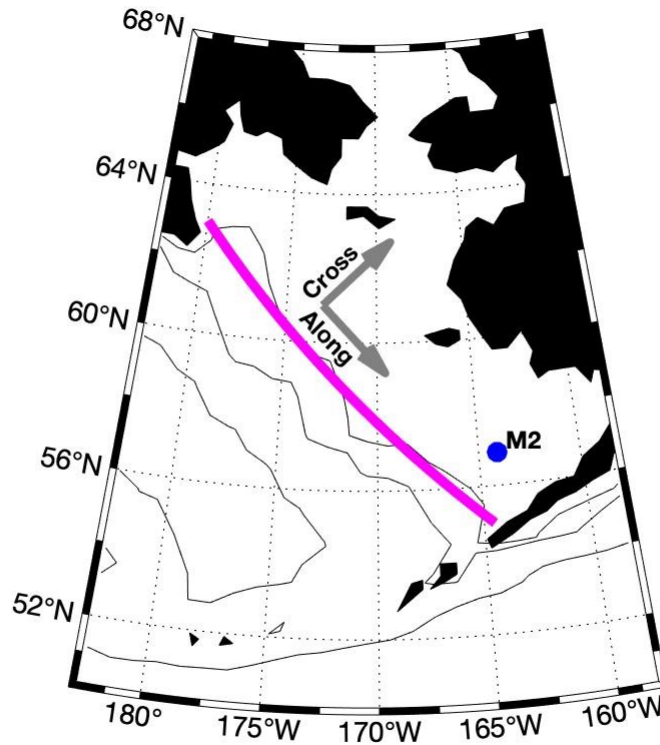


Figure 13: The magenta line shows the line chosen to evaluate along-shelf and cross-shelf wind components in the Bering Sea. Annotation arrows show the direction used to define positive cross and along shelf components of wind. Contours show isobaths at 100m, 500m, and 3500m. The blue dot shows the location of the M2 mooring.

The average annual cycle (2000 to 2021) was stronger for the cross-shelf component than along-shelf, and wind speeds were generally higher for the cross-shelf component as well (Figure 14). Generally, the Ekman transport associated with cross-shelf winds will be parallel to the shelf break, and could either inhibit or enhance near surface transport associated with the current along the shelf break. Winds oriented along the shelf break will either favor on- or off-shelf transport. Measurements taken at the M2 mooring show that the Ekman layer is not deeper than 30-40 meters from May–October. This suggests the cross-shelf transport driven by winds is unlikely to drive upwelling or downwelling at the shelf break, as the water is substantially deeper there. However, the Ekman transport associated with surface wind stress may still be informative for understanding the dispersal of fish larvae and other zooplankton in the upper ocean. In 2022, the seasonality of cross-shelf winds was generally consistent with the long-term mean, though the magnitude was generally higher. In both 2021 and 2022, the direction of along-shelf winds were variable from month to month, though the magnitude was again higher than the long-term mean.

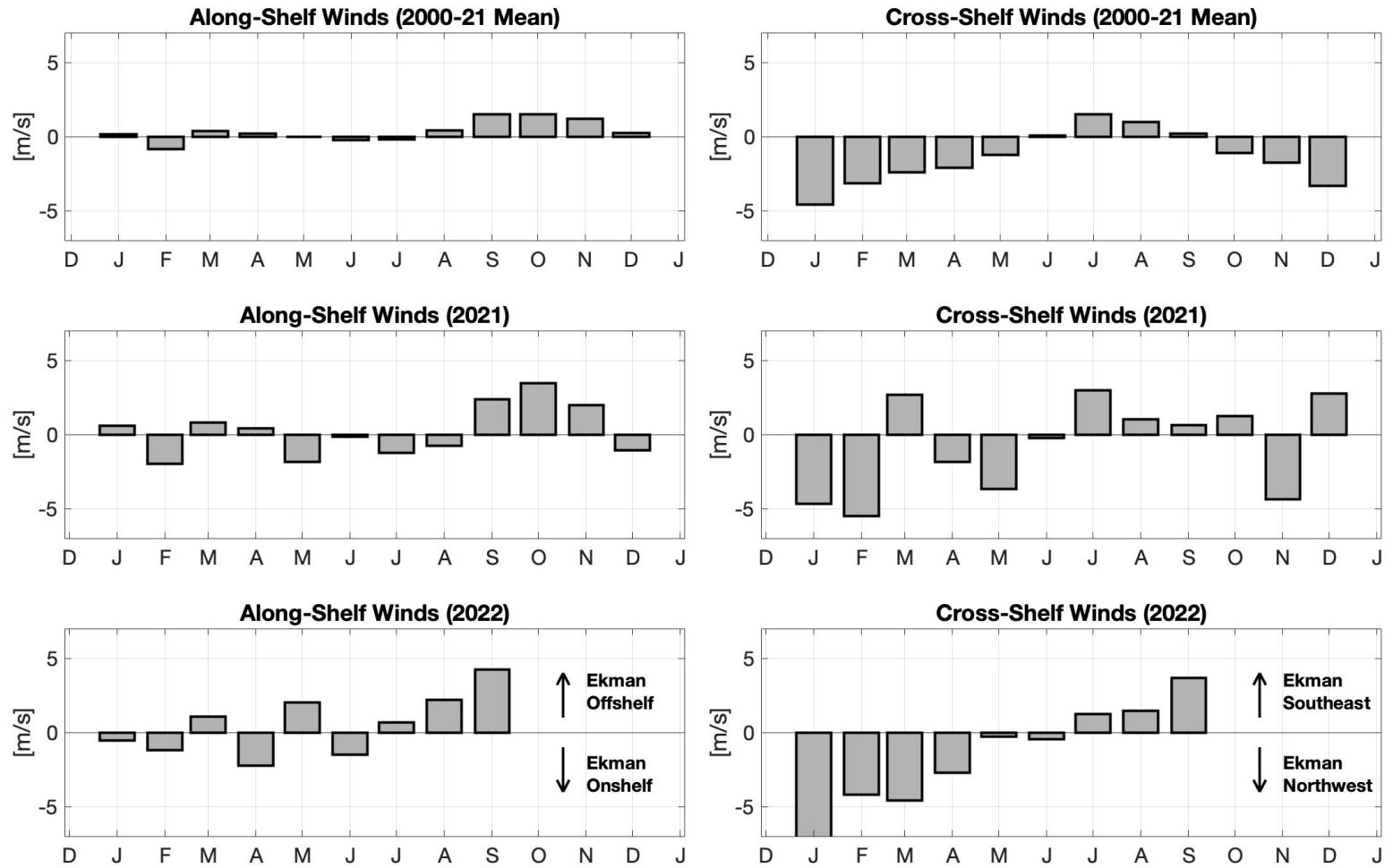


Figure 14: Along-shelf (left set of panels) and cross-shelf (right set of panels) wind components averaged along the magenta line in 13. Top panels show the monthly averages across the period of record. Middle panels show the monthly averages for 2021, and bottom panels show the monthly average for 2022. Positive along-shelf winds are defined as blowing to the southeast, and positive cross-shelf winds are defined as blowing to the northeast.

### St. Paul Air Temperature Anomalies

Contributed by Jim Overland, [james.e.overland@noaa.gov](mailto:james.e.overland@noaa.gov), and Muyin Wang, [muyin.wang@noaa.gov](mailto:muyin.wang@noaa.gov)

Monthly surface air temperature anomalies at St. Paul Island (WMO ID 25713) are shown in Figure 15. The anomaly is computed relative to the 1981–2010 period mean. Data are obtained from [https://data.giss.nasa.gov/gistemp/station\\_data\\_v4\\_globe](https://data.giss.nasa.gov/gistemp/station_data_v4_globe).

A linear trend in air temperature of  $0.46^{\circ}\text{C}/\text{decade}$  has been observed since 1980. This linear trend in 2022 is reduced compared to 2021 ( $0.51^{\circ}\text{C}/\text{decade}$ ) due to the recent negative anomalies observed (Jan, May, Jul, and Aug 2022). The largest positive anomaly observed in recent years was February 2018 ( $5.77^{\circ}\text{C}$ ). The last decade (2013–2022) was dominated by the warm anomalies. From 1980 through September 2022, there were only 12 months where below-average temperatures were observed (negative anomalies) relative to 1981–2010 period mean.

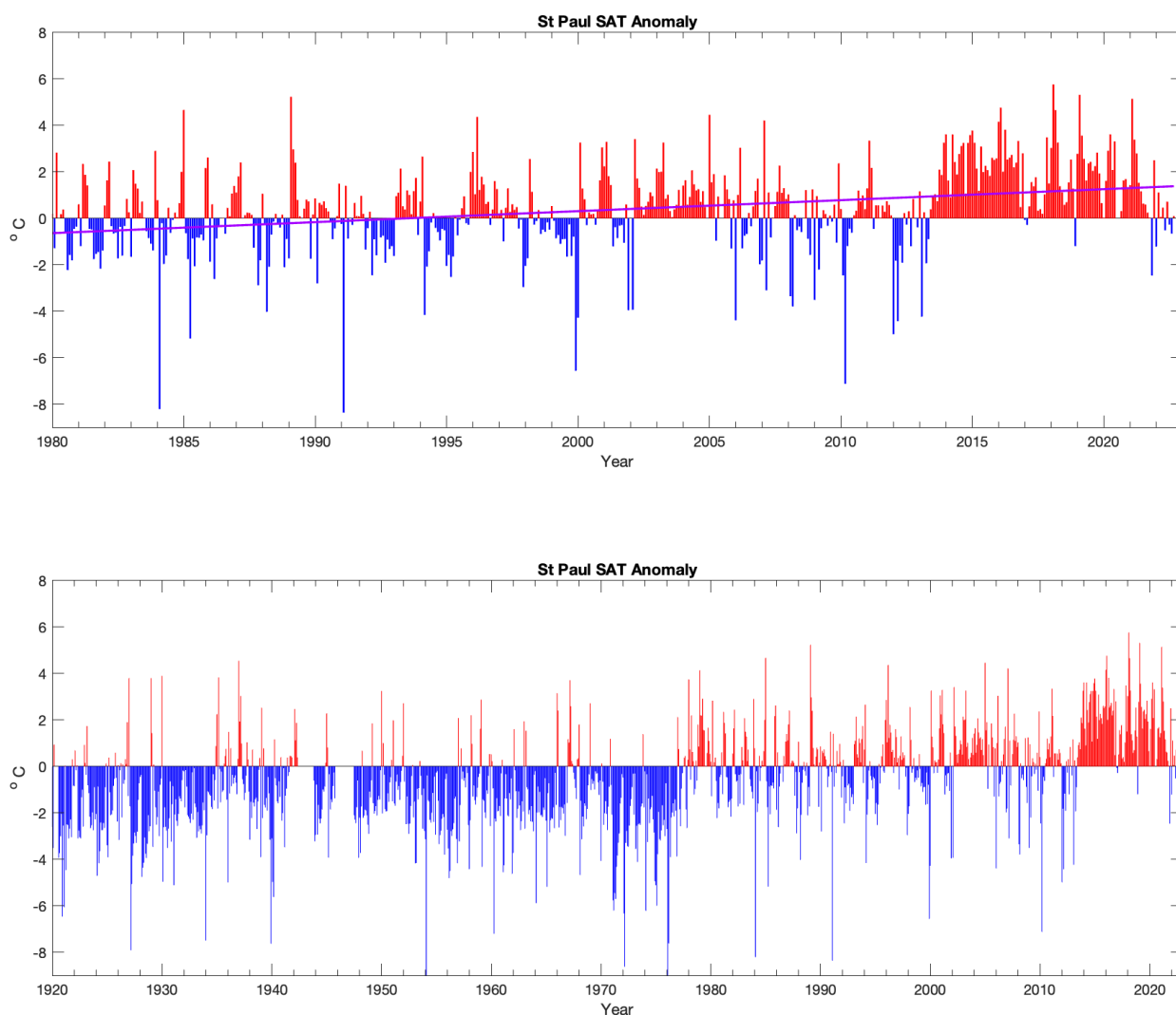


Figure 15: St. Paul air temperature anomalies updated to September 2022.

## 4. Sea Surface Temperature (SST) and Bottom Temperature

### *North Pacific Sea Surface Temperature (SST) Anomalies*

Contributed by Nick Bond, [nicholas.bond@noaa.gov](mailto:nicholas.bond@noaa.gov), and Jim Overland, [james.e.overland@noaa.gov](mailto:james.e.overland@noaa.gov)

The state of the North Pacific climate from autumn 2021 through summer 2022 is summarized in terms of seasonal sea surface temperature (SST) anomaly maps. The SST anomalies are relative to mean conditions over the period of 1991–2020. The SST data are from NOAA’s Extended SST V5 (ERSST) analysis and are available from NOAA’s Physical Sciences Laboratory (PSL)<sup>11</sup>.

The SST anomaly pattern during autumn (Sep–Nov) of 2021 (Figure 16a) included cooler than average SSTs for the GOA and the sub-tropical North Pacific from the Hawaiian Islands to California; warm water with peak anomalies exceeding 2°C was present in the central North Pacific between about 25°N and 45°N. The central and eastern tropical Pacific was cooler than average in association with weak-moderate La Niña conditions.

The overall distribution of SST anomalies persisted through the winter (Dec–Feb) of 2021–2022 (Figure 16b). This period featured development of quite cold SSTs in the SEBS shelf, with temperatures on the inner shelf more than 2°C colder than average. La Niña remained present, with the most prominent anomalies occurring in the eastern tropical Pacific.

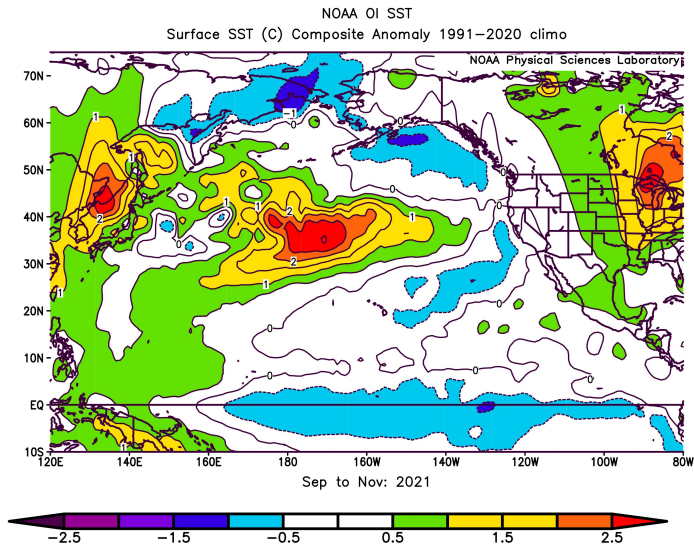
The large-scale SST anomaly pattern for the North Pacific was more or less static through spring (Mar–May) of 2022 (Figure 16c). There were several changes since the previous season including intensification of the warm anomaly in the waters north of the Hawaiian Islands, a decline in the magnitude of the negative anomaly on the SEBS shelf, and essentially elimination of the cold water in the GOA. La Niña continued in the tropical Pacific.

The summer (Jun–Aug) of 2022 brought modest warming of the waters offshore of western North America from Northern California to the Bering Sea (Figure 16d). This warming can be attributed in part to the aforementioned downwelling favorable winds along the coast of the Pacific Northwest and relatively warm weather/air temperatures in coastal Alaska. The tropical Pacific remained cooler than average, with the most prominent anomalies near the dateline.

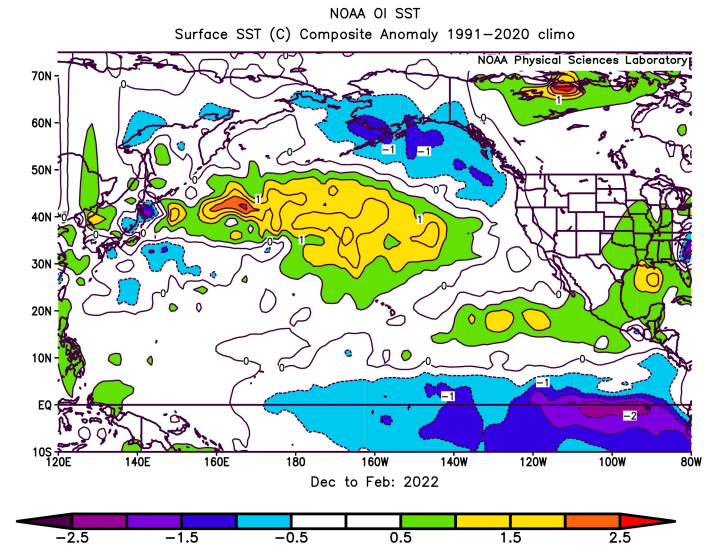
As the jet stream weakened in summer, the temperature gradients reduced for most of the Bering Sea, especially in the EBS (Figure 17). Positive temperature anomalies in western Bering and Russian side were replaced by negative anomalies (cold) in that region.

---

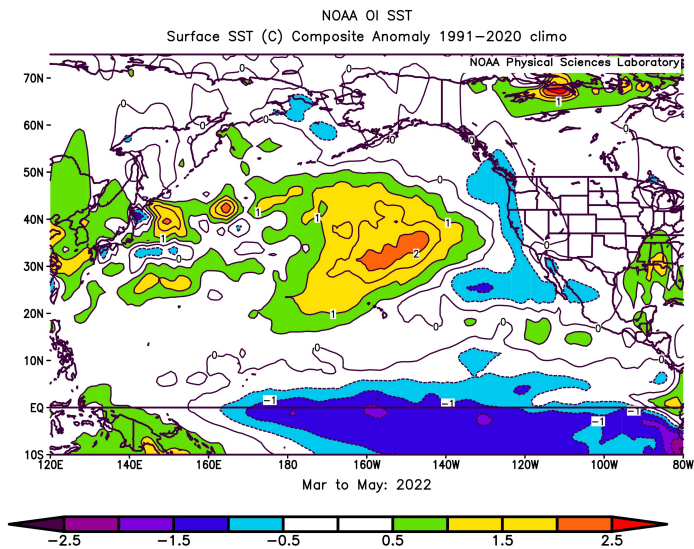
<sup>11</sup><https://www.psl.noaa.gov/cgi-bin/data/composites/printpage.pl>.



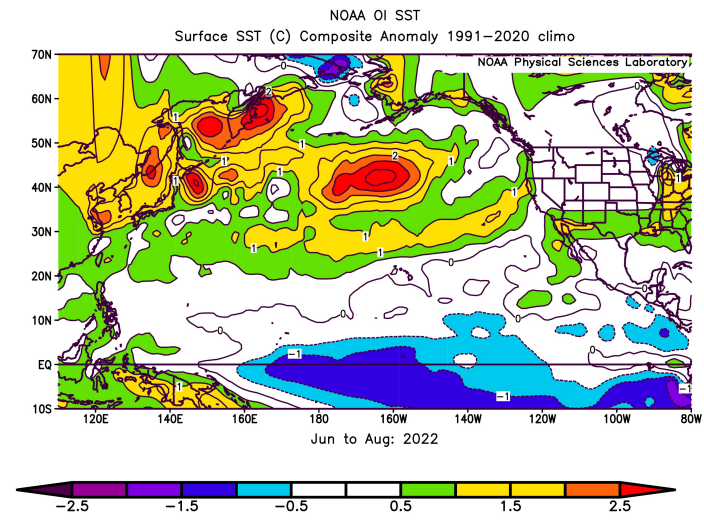
(a) Autumn



(b) Winter



(c) Spring



(d) Summer

Figure 16: Sea surface temperature anomalies for (a) autumn (Sept-Nov 2021), (b) winter (Dec 2021-Feb 2022), (c) spring (Mar-May 2022), and (d) summer (Jun-Aug 2022).

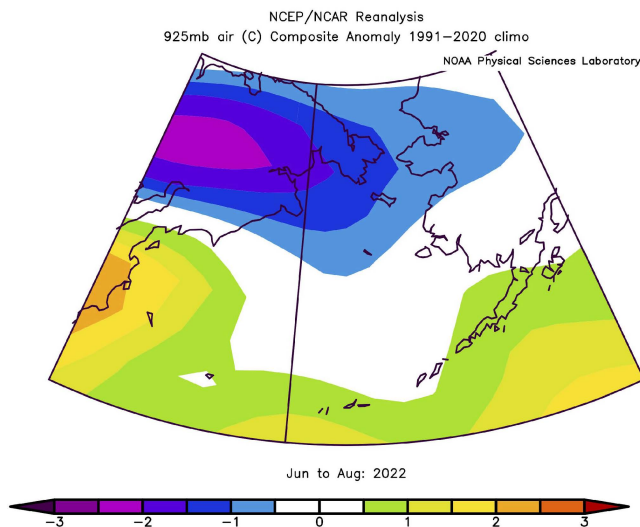


Figure 17: Air temperature anomaly at 925 mb for summer (Jun-Aug) 2022.

### *Bering Sea SST Anomalies*

Contributed by Emily Lemagie, [emily.lemagie@noaa.gov](mailto:emily.lemagie@noaa.gov), and Matt Callahan, [matt.callahan@noaa.gov](mailto:matt.callahan@noaa.gov). Satellite SST data (source: NOAA Coral Reef Watch Program) were accessed via the Alaska Fisheries Information Network (AKFIN). Daily data were averaged within the southeastern (south of 60°N) and northern (60°–65.75°N) Bering Sea shelf (10–200m depth). Detailed methods are available online<sup>12</sup>.

Trend analysis removed seasonal variability from the SST time series (Edullantes, 2019) to illustrate better the long-term trends in the SST data (Figure 18). Trends are compared to the mean ( $\pm 1$  standard deviation [SD]) from a 30-yr baseline (1985–2014) and demonstrate that both the NBS and SEBS cooled relative to the recent persistent warm stanza. In the most recent data, the trend dropped within 1 SD of the mean for the first time since the mid-2010s. *Note:* The time series trend analysis requires truncation of the ends of the time series (due to differencing) so the trend line extends only into March 2022.

### *Marine Heatwave Index*

Contributed by Emily Lemagie, [emily.lemagie@noaa.gov](mailto:emily.lemagie@noaa.gov), and Matt Callahan, [matt.callahan@noaa.gov](mailto:matt.callahan@noaa.gov). Marine Heatwaves (MHWs) in 2022 have been infrequent relative to 2021, and generally minor compared to recent years, with only a few brief and predominantly moderate events (Figure 19). No MHWs occurred between early fall 2021 and mid spring 2022. *Note:* this MHW index is based on SST, which is strongly influenced by sea ice and stratification in the Bering Sea, particularly over the middle shelf where surface and bottom temperature dynamics can be decoupled for much of the year (Ladd and Stabeno, 2012). Bottom temperature in the Bering Sea is an important ecosystem driver (Stabeno and Bell, 2019).

### *Annual and Seasonal SST Trends*

Contributed by Emily Lemagie, [emily.lemagie@noaa.gov](mailto:emily.lemagie@noaa.gov), and Matt Callahan, [matt.callahan@noaa.gov](mailto:matt.callahan@noaa.gov). The cumulative SSTs for 2022 were within a standard deviation of average for the first time since 2013 (Figure 20). Cumulative warming experienced in recent years may represent important conditions for the ecology of these systems as total thermal exposure for organisms was higher than historical conditions. Protracted warming may lead to elevated metabolic rates, higher growth rates, and higher prey demands.

At the seasonal level, mean SST patterns were more consistent with the long-term mean than with recent warm years (Figure 21). In most seasons there has been a cooling trend for the last 3 to 4 years, except during the spring in the NBS and SEBS where there was more year-to-year variability which could be related to the timing of sea-ice advance or retreat.

<sup>12</sup><https://github.com/MattCallahan-NOAA/ESR/tree/main/SST/EBS>

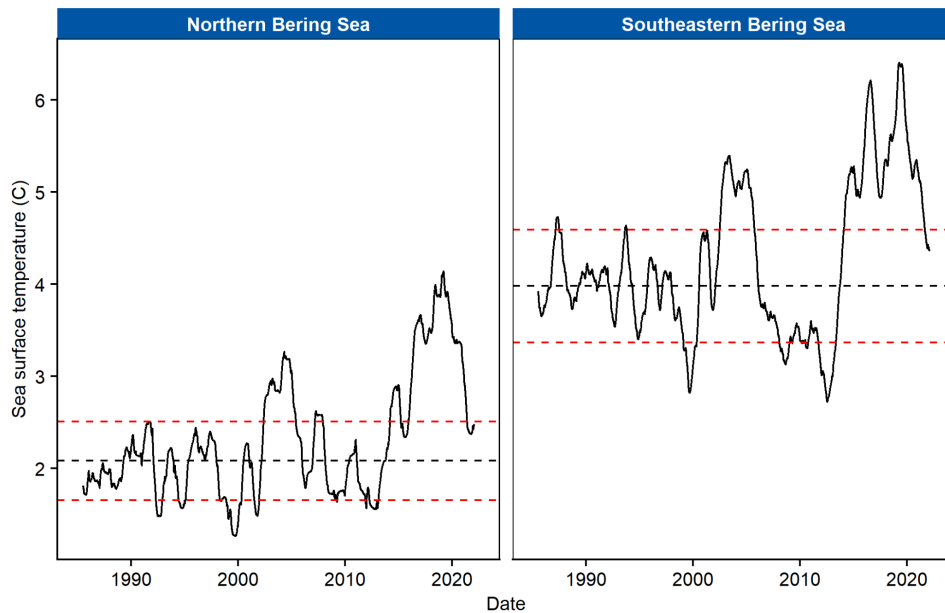


Figure 18: Time series trend of SST (seasonality and noise removed) for the northern (left) and southeastern (right) Bering Sea shelves. The black horizontal dotted line is the 30-year mean (1985–2014) of the trend and the red lines are  $\pm 1$  SD.

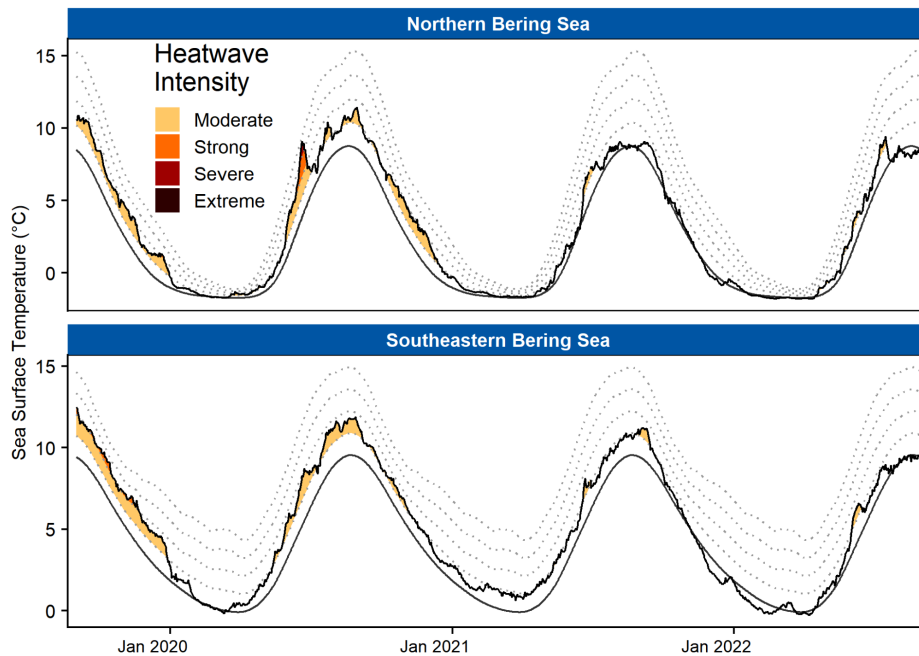


Figure 19: Marine heatwaves in the northern and southeastern Bering Sea since September 2019. The smoothed solid black line represents the baseline average temperature (i.e., climatology) for each day during the 30-yr baseline period (1 Sept 1985–31 Aug 2014). The jagged solid black line is the observed (satellite-derived) SST for each day. Dotted lines illustrate thresholds for increasing MHW intensity categories (moderate, strong, severe, extreme). Colored portions indicate periods during which MHW occurred, with intensity increasing as colors darken.

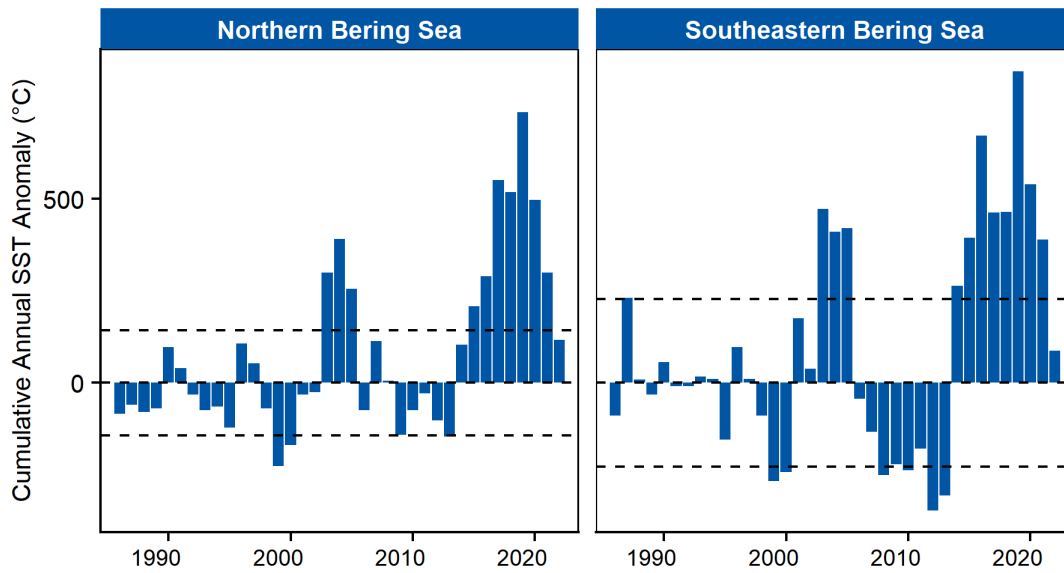


Figure 20: Cumulative annual SST anomalies (sum of daily temperatures). Horizontal lines are  $\pm 1$  SD from the mean during the 30-yr baseline period (1 Sept 1985-31 Aug 2014).

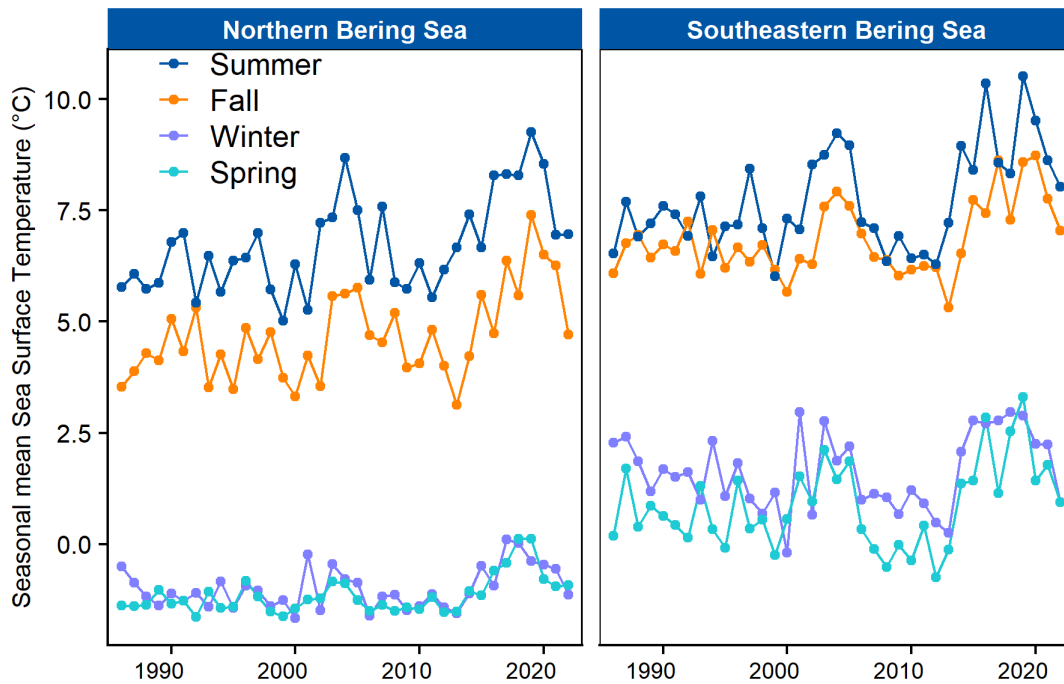


Figure 21: Seasonal mean SSTs for each year, apportioned by season: summer (Jun–Aug), fall (Sep–Nov), winter (Dec–Feb), and spring (Mar–May). Negative values are due to sea surface temperatures below zero.

### *Bering Sea SST and Bottom Temperature Trends*

Contributed by Emily Lemagie, *emily.lemagie@noaa.gov*, Matt Callahan, *matt.callahan@noaa.gov*, and Kelly Kearney, *kelly.kearney@noaa.gov*

Estimates of bottom temperature are derived from the Bering 10K Regional Ocean Modeling System (ROMS) hindcast simulation, which was extended to the near-present, using reanalysis-based input forcing. This hindcast simulation now extends from January 15, 1970 to August 16, 2022.

After an eight year warm stanza, SST over the past year (September 2021–August 2022) in the NBS and SEBS regions broadly returned to within a standard deviation of the 30-year baseline (1985–2014) across all domains (Figure 22). Exceptions to near-average thermal conditions include a relatively warm summer across all regions (close to 2021 conditions, see Figure 27) and a notably cool winter in the inner (10–50m) domain of the SEBS (Figure 23, top 2 rows).

Similar to SST, ROMS-estimated bottom temperatures in the NBS and SEBS were near historical averages much of the prior year over most domains (Figure 23, bottom 2 rows). Unlike SST, bottom temperatures were not significantly warmer than average during the 2022 summer, partially due to the seasonality of vertical thermohaline stratification. Particularly in the shallow coastal waters of the inner domain, where the water column tends to be well-mixed from top to bottom, this leads to a coupling of surface and bottom temperatures much of the year. Therefore, during the 2021–2022 winter, both surface and bottom temperatures in the inner SEBS were cooler than average. Beginning in mid-spring, a combination of freshwater melt and surface warming causes a stratification and decoupling between surface and bottom regimes, which allowed for the bottom temperatures to remain average while the surface waters warmed.

Bottom temperature was also cooler than average during the 2022 winter in the middle (51–100m) domain of the SEBS, due to similar seasonal stratification patterns present in the inner SEBS. The outer (101–200m) domain of the SEBS was cooler than average for virtually all of the past year. In the NBS, bottom temperature was more uniformly near historical averages, with the most notable exception in the outer NBS, where conditions were significantly warmer than average from approximately February to June, 2022.

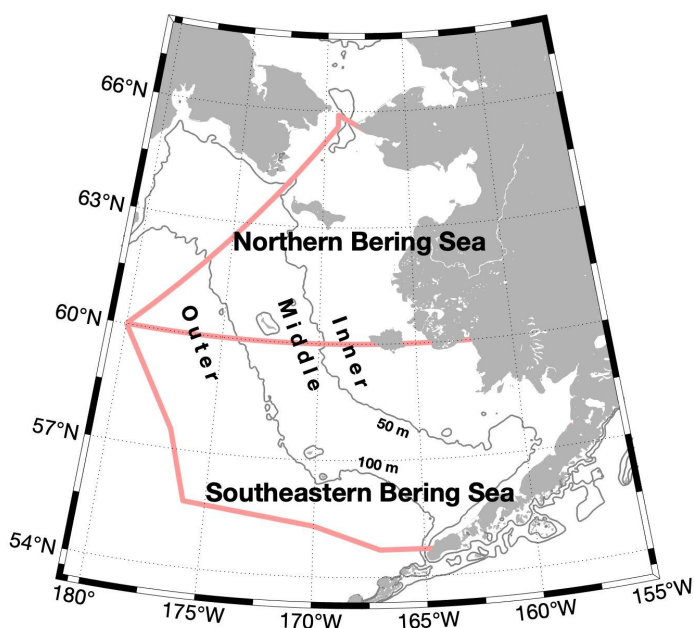


Figure 22: Map of the eastern Bering Sea. The inner (0–50m isobaths), middle (50–100m isobaths), and outer (100–200m isobaths) domains are shown. The southeastern and northern Bering Sea are delineated at 60°N.

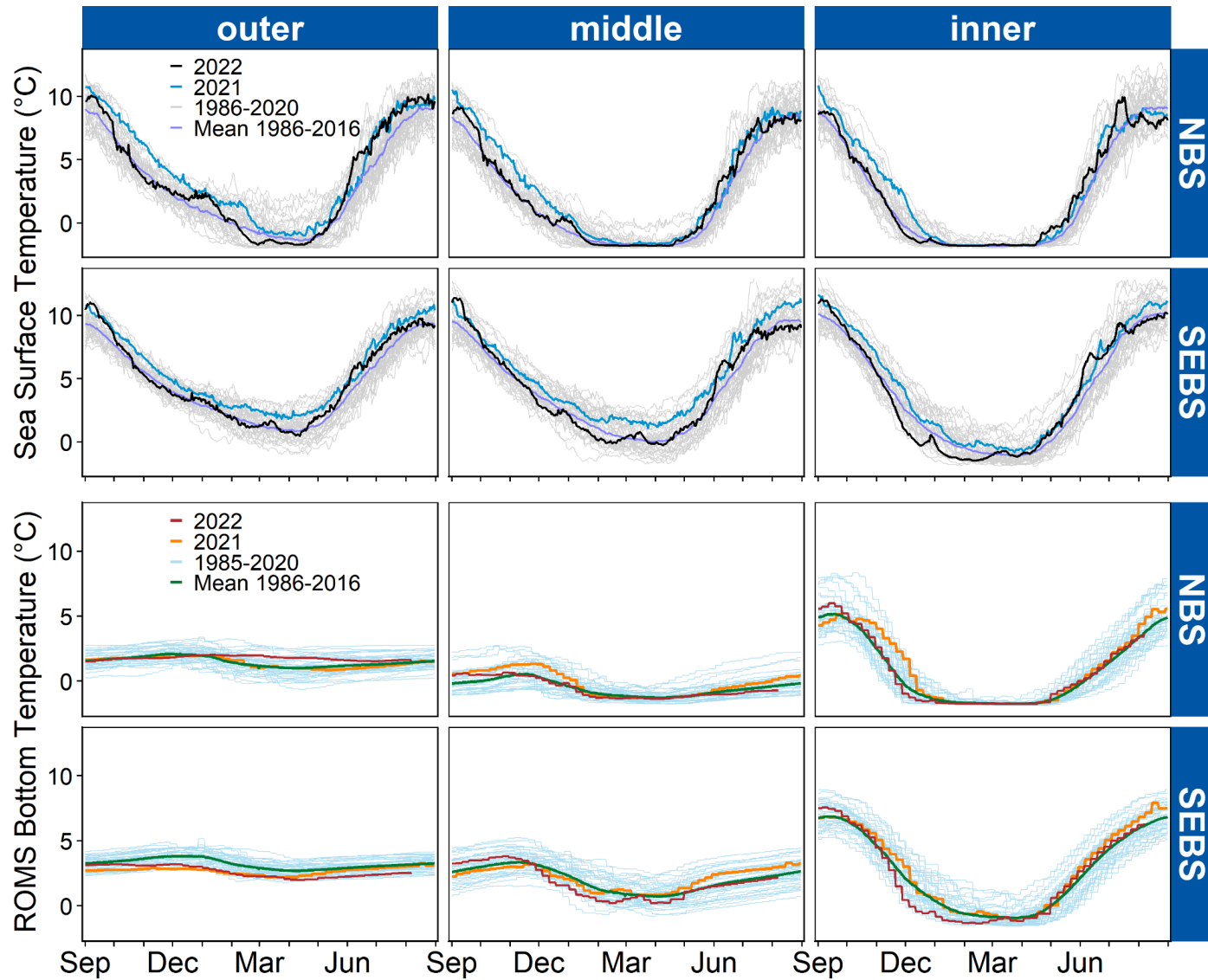


Figure 23: Top 2 rows: Mean daily SST for the northern (NBS) and southeastern (SEBS) outer, middle, and inner shelf domains. The most recent year (2021–2022; through Aug 31, 2022) is shown in black, 2020–2021 is shown in blue, and the historical mean is shown in purple. Individual years in the time series are shown in light gray. Bottom 2 rows: Mean weekly bottom temperature for the NBS and SEBS outer, middle, and inner shelf domains. The most recent year (2021–2022; through Aug 7, 2022) is shown in dark red, 2020–2021 is shown in orange, and the historical mean is shown in green. Individual years in the time series are shown in light blue.

*St. Paul Island Temperature, Salinity, and Chlorophyll-a*

Contributed by Seth Danielson, [sldanielson@alaska.edu](mailto:sldanielson@alaska.edu), Lauren Divine, [lmdivine@aleut.com](mailto:lmdivine@aleut.com), Aaron Lestenkof, and Tyler Hennon

Community-led monitoring of temperature and salinity from North Dock on the St. Paul Island breakwater have been made since 2014 using CTD data loggers (Figure 24). Instrumentation used since 2015 has also had a sensor for chlorophyll-a fluorescence, which provides a measure of phytoplankton concentration. Water depth at the sample site is approximately 8m. Water column profiles are collected nominally weekly and have been averaged into monthly means with the annual signal removed (Figure 25).

Following the trends exhibited elsewhere, temperature anomalies over the last ~12 months show relatively cool conditions compared to the preceding years. Anomalies in the last 12 months occasionally exceed 2°C cooler than the seasonal average (Figure 25). It is important to note, however, that across the North Pacific as a whole, 2014 through 2021 has been appreciably warmer than the long-term average, such that the baseline temperature in this record is significantly warmer than other time series with a longer period-of-record (e.g., Danielson et al. (2020)).

Though salinity has generally been increasing throughout the period of record, observations in late 2021 and 2022 show a potential reversal of this trend, with some of the lowest salinities on record (Figure 25). Contributing factors to salinity variability on the EBS shelf include river discharge, precipitation, evaporation, ice advection, inflows from the Gulf of Alaska, and cross-slope exchanges with the basin (Aagaard et al., 2006). At the moment it is unclear what is driving this freshening, though we note it does loosely coincide with the rapid springtime retreat of sea ice that occurred across the Bering Sea (Figure 31).

Chlorophyll-a fluorescence measurements show year-to-year variations in the timing of the spring phytoplankton bloom. While several years (e.g., 2018, 2019) show a relatively late and weak bloom, the chlorophyll-a data from St. Paul in 2022 exhibit, at least locally, a strong and early bloom (Figure 26), corroborating trends detected from sensors deployed at mooring M2 (56.9°N, -164.1°W; see p. 68).

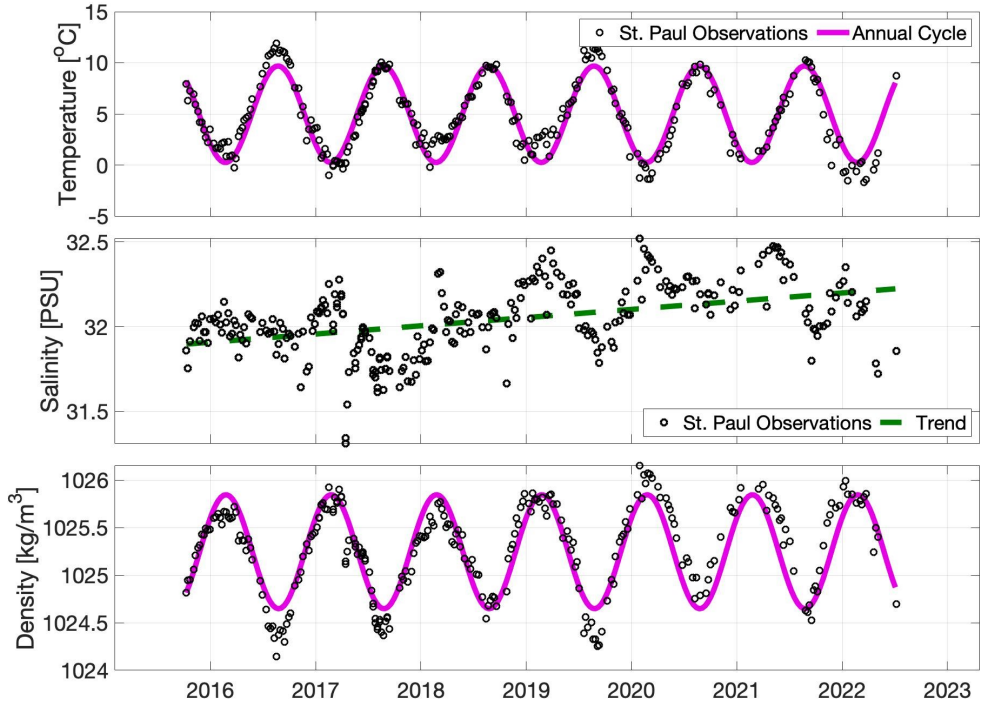


Figure 24: Observations of temperature (top), salinity (middle), and density (bottom) collected at St. Paul Island (black dots). Fitted annual cycles in temperature and density are in magenta, and the long term linear trend in salinity over the time series is represented by the dashed green line ( $p < 0.01$ ).

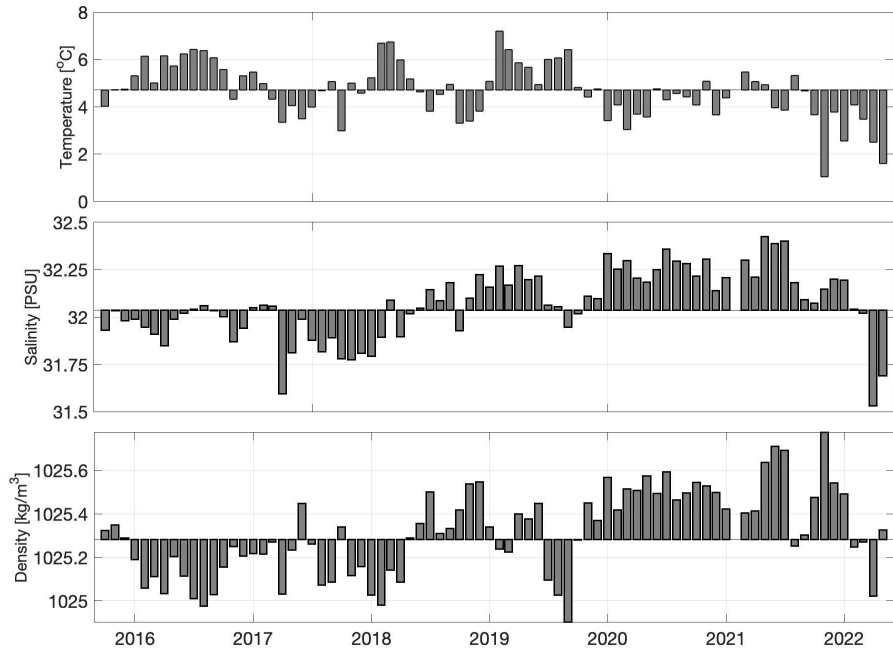


Figure 25: Monthly averages with the seasonal cycle removed for temperature (top), salinity (middle), and density (bottom) from St. Paul Island.

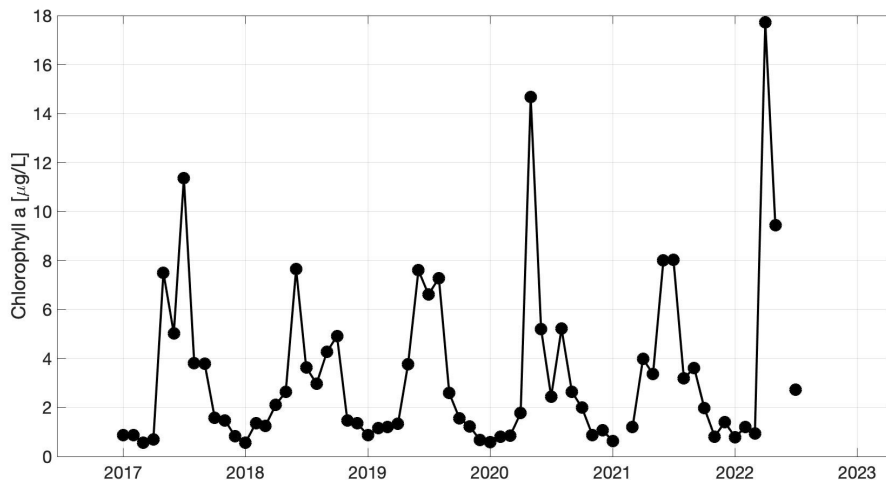


Figure 26: Monthly average of chlorophyll concentrations collected at St. Paul Island through July 2022.

### Summer SST and Bottom Temperatures

Contributed by Sean Rohan, [sean.rohan@noaa.gov](mailto:sean.rohan@noaa.gov), and Lewis Barnett, [lewis.barnett@noaa.gov](mailto:lewis.barnett@noaa.gov)

Mean surface and bottom temperatures are calculated from spatially interpolated data collected during AFSC summer bottom trawl surveys of the EBS shelf (1982–2022, except 2020) and NBS (2010, 2017, 2018, 2019, 2021). Temperature data are not adjusted for effects of seasonal heating. Temperature data are interpolated using ordinary kriging with Stein’s parameterization of the Matérn semivariogram model (Rohan et al., in review). Code, figures, and data products presented in this contribution are provided in the coldpool R package<sup>13</sup>.

In the EBS, the mean surface temperature (7.46°C) was 0.2°C higher than in 2021, but near the time series average (6.76°C). The mean bottom temperature in the EBS (2.56°C) was near the time series mean (2.50°C) in 2022 (Figure 27). This near-average bottom temperature in 2022 represents a change from recent years (2016–2021) with four of the five warmest years in the times series. In the NBS (data not shown), the mean surface temperature (8.05°C) was slightly below the time series average (9.18°C) and the mean bottom temperature (3.92°C) was near the time series average (3.94°C). However, the time series for the NBS is extremely short compared to that for the EBS.

In 2022, bottom temperatures were lower throughout the EBS and NBS survey areas compared to the three previous surveys in 2018, 2019, and 2021 (Figure 28). The coldest bottom temperatures ( $\leq -1^{\circ}\text{C}$ ) within the combined EBS shelf and NBS survey areas were along the U.S.-Russia maritime boundary between St. Matthew Island and St. Lawrence Island. In 2018 and 2019, extremely cold bottom temperatures ( $\leq 0^{\circ}\text{C}$ ) were confined to a small area along the U.S.-Russia Convention Line, but the size of this area increased in 2021 and again in 2022. The warmest bottom temperatures were along the coast of the Alaska mainland between Nunivak Island and Norton Sound. However, the area north of Nunivak Island at 60.5°N is sampled at the end of the survey and reflects seasonal warming since sampling occurs 35–45 days later than in the area directly to the south.

<sup>13</sup><https://github.com/afsc-gap-products/coldpool>

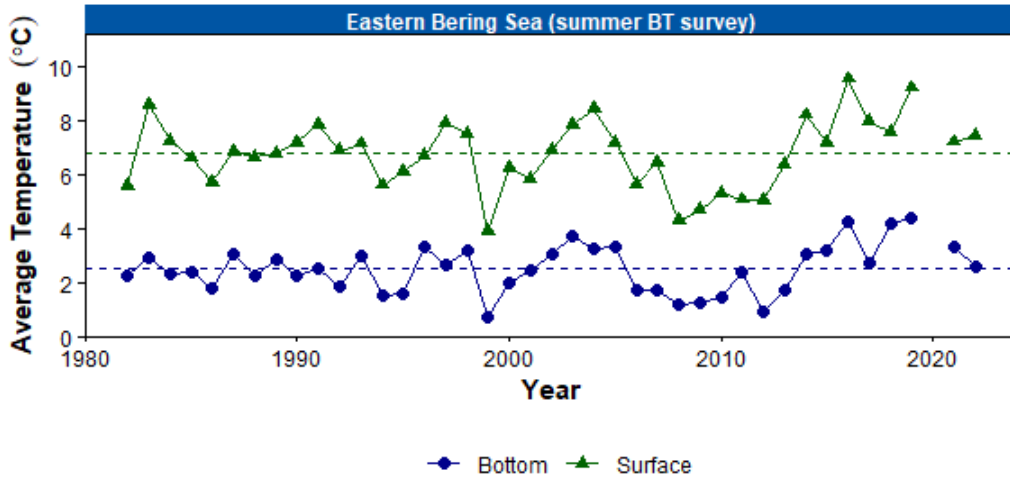


Figure 27: Average summer surface (green triangles) and bottom (blue circles) temperatures (°C) on the eastern Bering Sea shelf based on data collected during standardized summer bottom trawl surveys from 1982–2022. Dashed lines represent the time series mean.

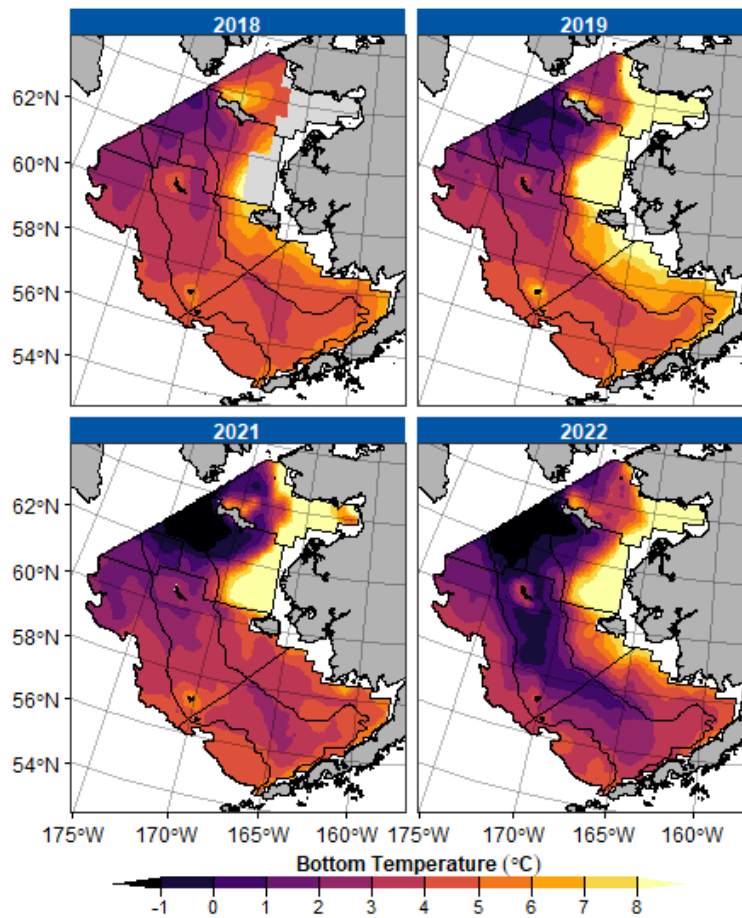


Figure 28: Contour maps of bottom temperatures from the 2018, 2019, 2021, and 2022 eastern Bering Sea shelf and northern Bering Sea bottom trawl surveys.

## 5. Sea Ice

Contributed by Rick Thoman, *rthoman@alaska.edu*

### *Early Season Sea-Ice Extent*

While the annual mean sea-ice extent in the Bering Sea (both eastern and western) has shown no significant trend until recently (see Figure 30), this is not the case for early season ice. The presence or absence of early sea ice in the Bering Sea is important because, at least during the passive microwave era, nearly all ice in the Bering Sea is first year ice. Therefore Bering Sea sea-ice thickness is related to both the air temperature and the age of the ice.

Below-average sea surface temperatures in the EBS in October 2021 were followed by one of the coldest Novembers on record and produced rapid sea-ice growth near Alaska. As a result, the early season ice extent in 2021 was the highest since 2012 (Figure 29).

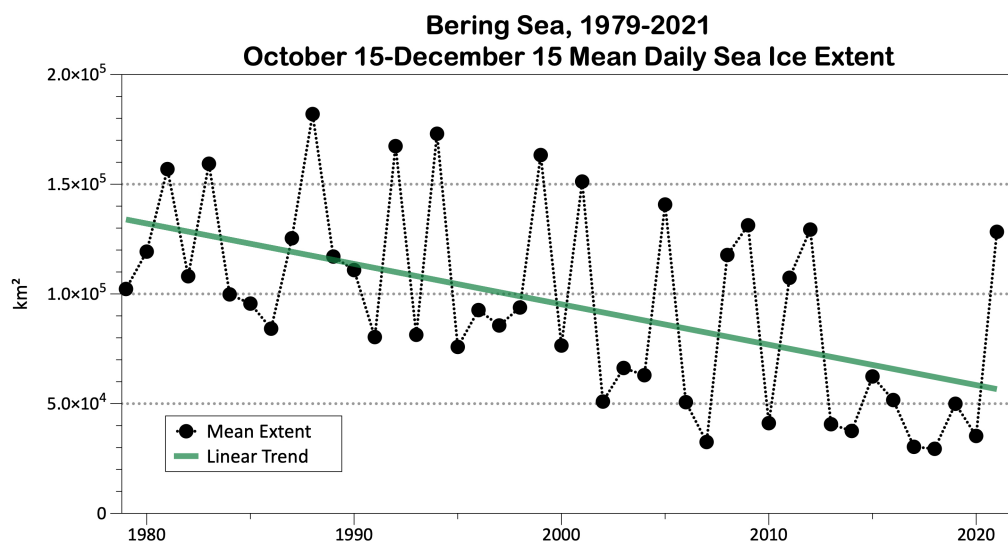


Figure 29: Early (15 Oct-15 Dec) mean sea-ice extent in the Bering Sea, 1979–2021. Source: National Snow and Ice Data Center Sea Ice Index version 3.

### *Annual Bering Sea Sea-Ice Extent*

The Bering Sea has historically been ice-free in the middle and late summer, with ice developing during the second half of October. To account for this seasonal cycle, the Bering Sea ice year is defined as 1 August to 31 July. Bering Sea ice extent data are from the National Snow and Ice Center’s Sea Ice Index, version 3 (Fetterer et al., 2017), and use the Sea Ice Index definition of the Bering Sea (effectively south of the line from Cape Prince of Wales to East Cape, Russia).

Annual mean daily sea-ice extent in the Bering Sea exhibits no significant long-term trend, although interannual variability has increased significantly since the mid-1990s (Figure 30). In the 2021–2022 season, the average extent was the highest since 2012–2013, mostly on the strength of early season ice growth near Alaska fueled by one of the coldest Novembers on record.

### *Bering Sea Daily Sea-Ice Extent*

Tracking the seasonal progression and retreat of sea ice highlights the interactive roles of water temperature (i.e., warmth in the system) and winds (Figure 31). Rapid sea-ice growth in November and dramatic sea-ice loss in April were the highlights of the 2021–2022 season. The maximum ice extent for the season was reached on February 17, almost a month earlier than the 1979–2021 median. Sea ice briefly reached St. George in the Pribilof Islands in late March for the first time since 2017.

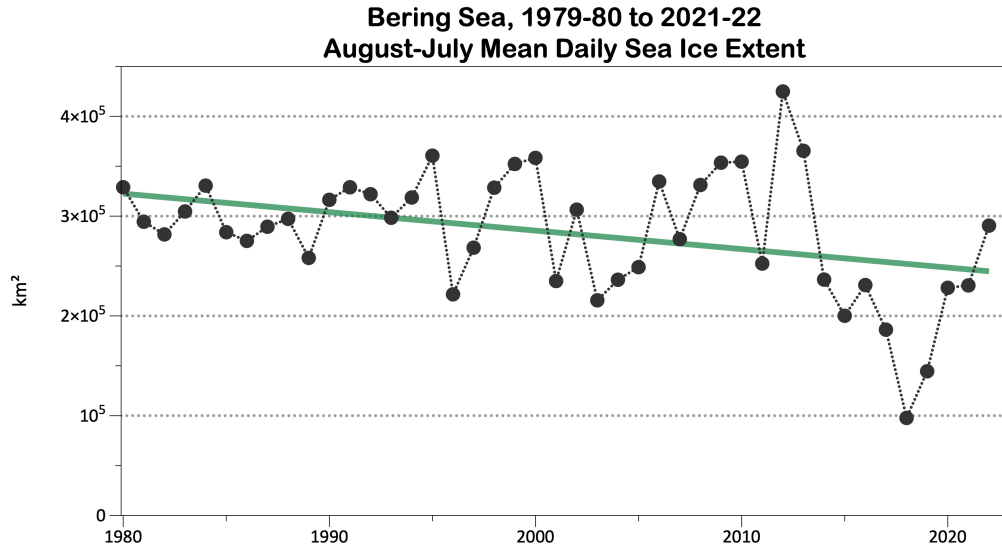


Figure 30: Mean sea-ice extent in the Bering Sea from 1 August to 31 July, 1979/1980–2021/2022.

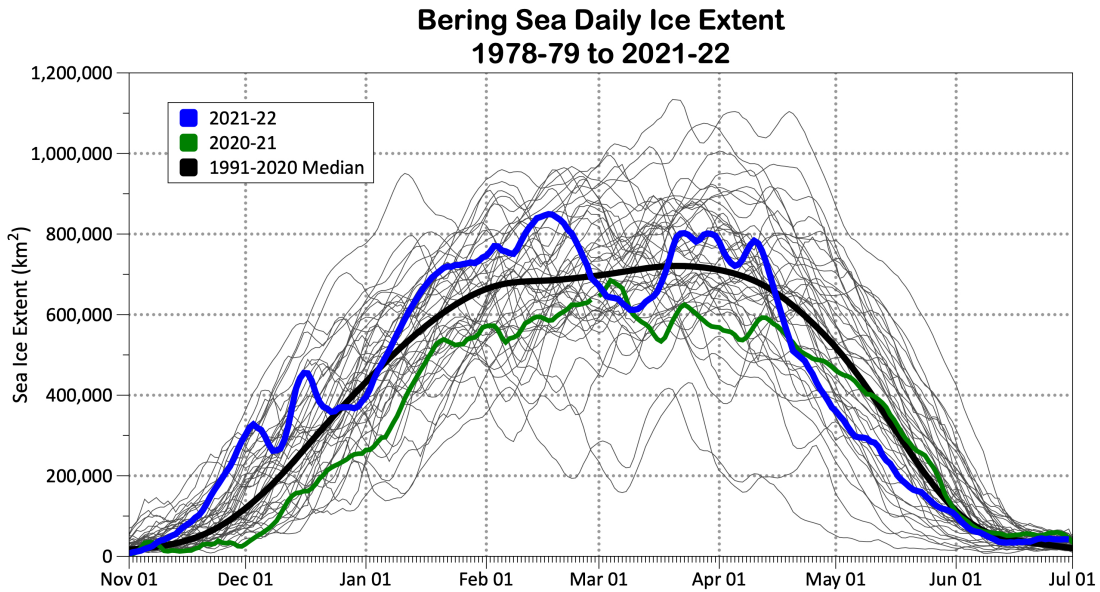


Figure 31: Daily ice extent in the Bering Sea. The most recent year (2021–2022) is shown in blue, 2020–2021 in green, and the historical median in black. Individual years in the time series are shown in gray.

### *Sea-Ice Thickness*

Bering Sea sea-ice thickness was calculated for the 3<sup>rd</sup> week in March using merged SMOS/CryoSat-2 sea-ice thickness estimates. SMOS is the Soil Moisture and Ocean Salinity satellite and CryoSat-2 is the Sea Ice Radar Altimetry from the European Space Agency CryoSat-2 satellite. SMOS estimates are most reliable at ice thickness  $\leq 1\text{m}$ , while CryoSat-2 is more reliable for ice thickness  $\geq 1\text{m}$ . Ice thickness was calculated for five areas over the Bering Sea: Gulf of Anadyr (Bering W), Bering Strait, Norton Sound, St. Lawrence Island to St. Matthew Island (Bering NC), and St. Matthew Island to St. Paul Island (Bering S) (Figure 32). Details on how uncertainty in sea-ice thickness was quantified are available at: <https://www.meereiportal.de/en/>.

While sea-ice extent in 2021-2022 was greater in the Bering Sea than in the past several years, in the NBS mid-March sea-ice thickness was lower in 2022 than 2021. In particular, Norton Sound sea-ice thickness was second lowest in the 12-year period of record. The only area with higher sea-ice thickness in mid-March 2022 than 2021 was the St. Matthew Island to St. Paul Island area, which had very little ice in spring 2021 (Figure 33).

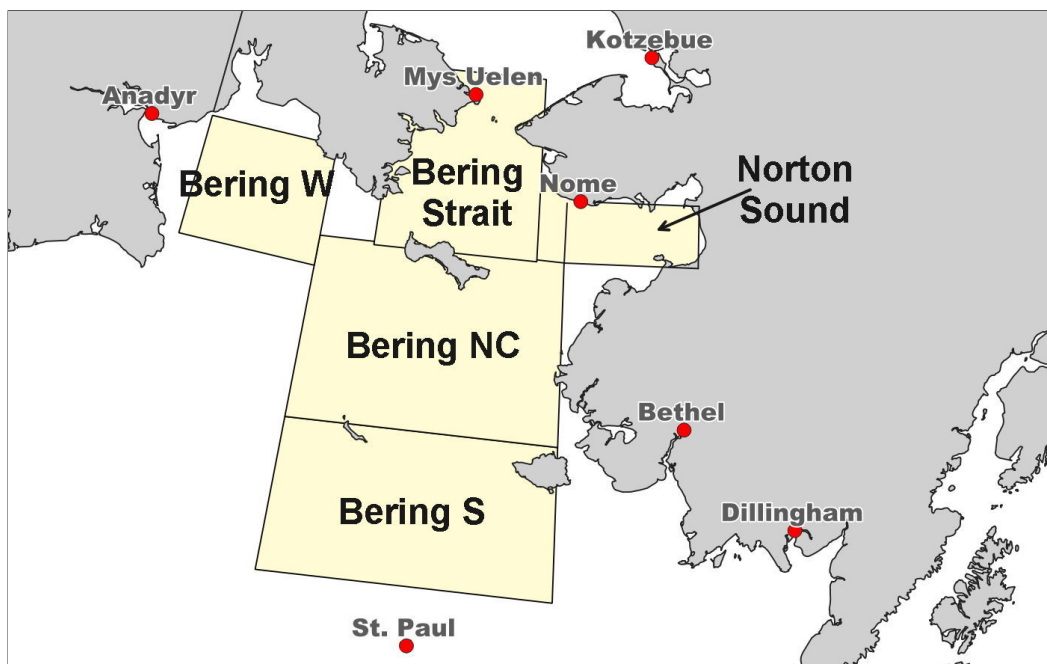
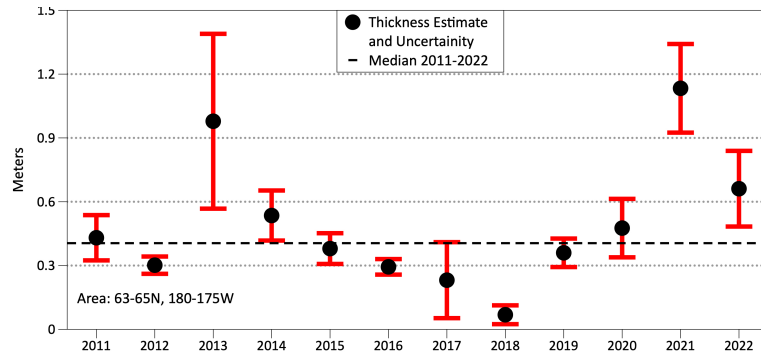
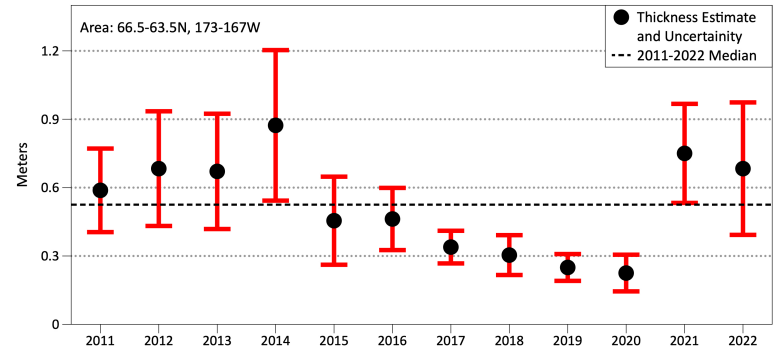


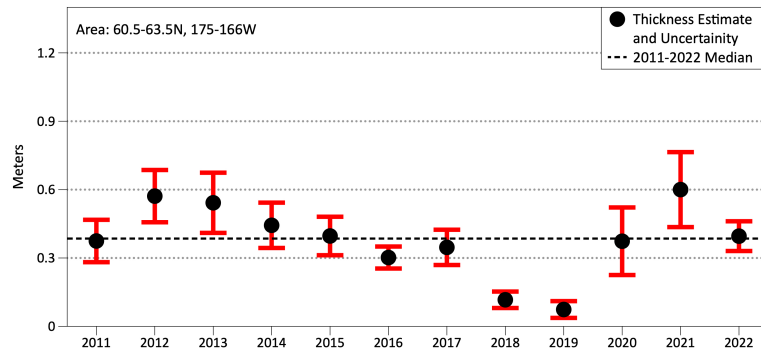
Figure 32: Map showing the five areas over the Bering Sea within which ice thickness indices were calculated: Gulf of Anadyr (Bering W), Bering Strait, Norton Sound, St. Lawrence Island to St. Matthew Island (Bering NC), and St. Matthew Island to St. Paul Island (Bering S).



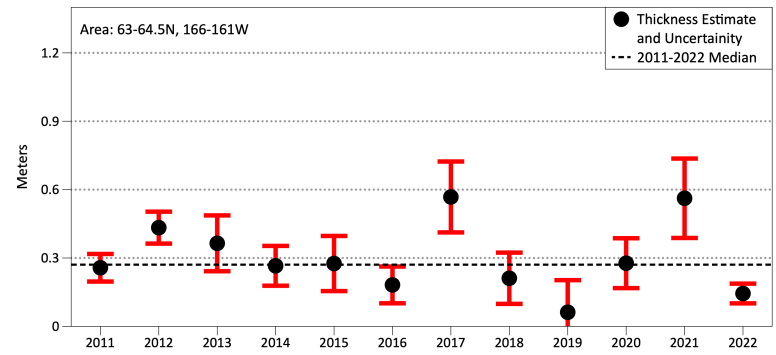
(a) Gulf of Anadyr



(b) Bering Strait



(c) St. Lawrence Island to St. Matthew Island



(d) Norton Sound

Figure 33: Sea-ice thickness in the Bering Sea for (a) Gulf of Anadyr, (b) Bering Strait, (c) St. Lawrence Island to St. Matthew Island, and (d) Norton Sound. Source: Alfred Wegener Institute. Details on how uncertainty in sea-ice thickness was quantified are available at: <https://www.meereisportal.de/en/>

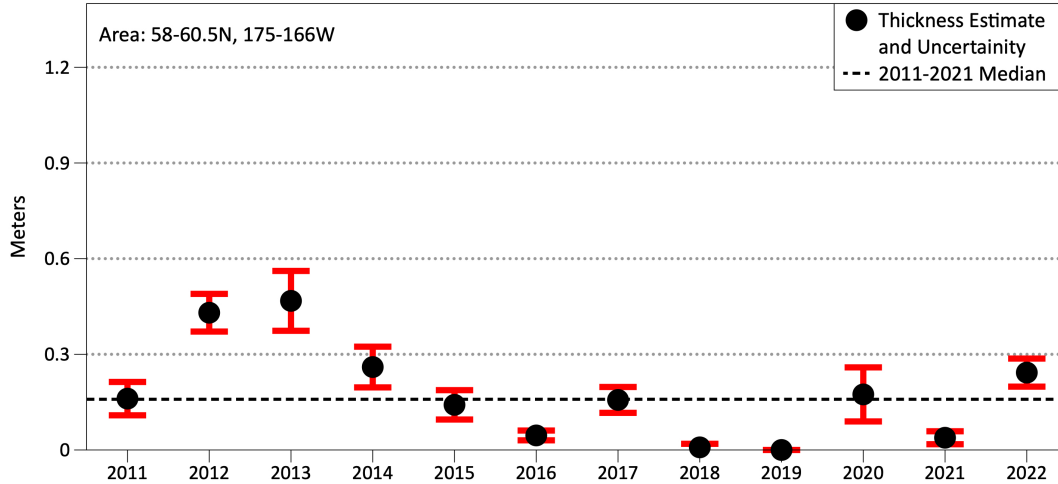


Figure 34: Sea-ice thickness between St. Matthew Island and St. Paul Island. Source: Alfred Wegener Institute. Details on how uncertainty in sea-ice thickness was quantified are available at: <https://www.meereisportal.de/en/>

## 6. Cold Pool

### *Cold Pool Extent - ROMS*

Contributed by Kelly Kearney, [kelly.kearney@noaa.gov](mailto:kelly.kearney@noaa.gov)

The Bering 10K Regional Ocean Modeling System (ROMS) hindcast simulation was extended to the near-present, using reanalysis-based input forcing. This hindcast simulation now extends from January 15, 1970–August 16, 2022.

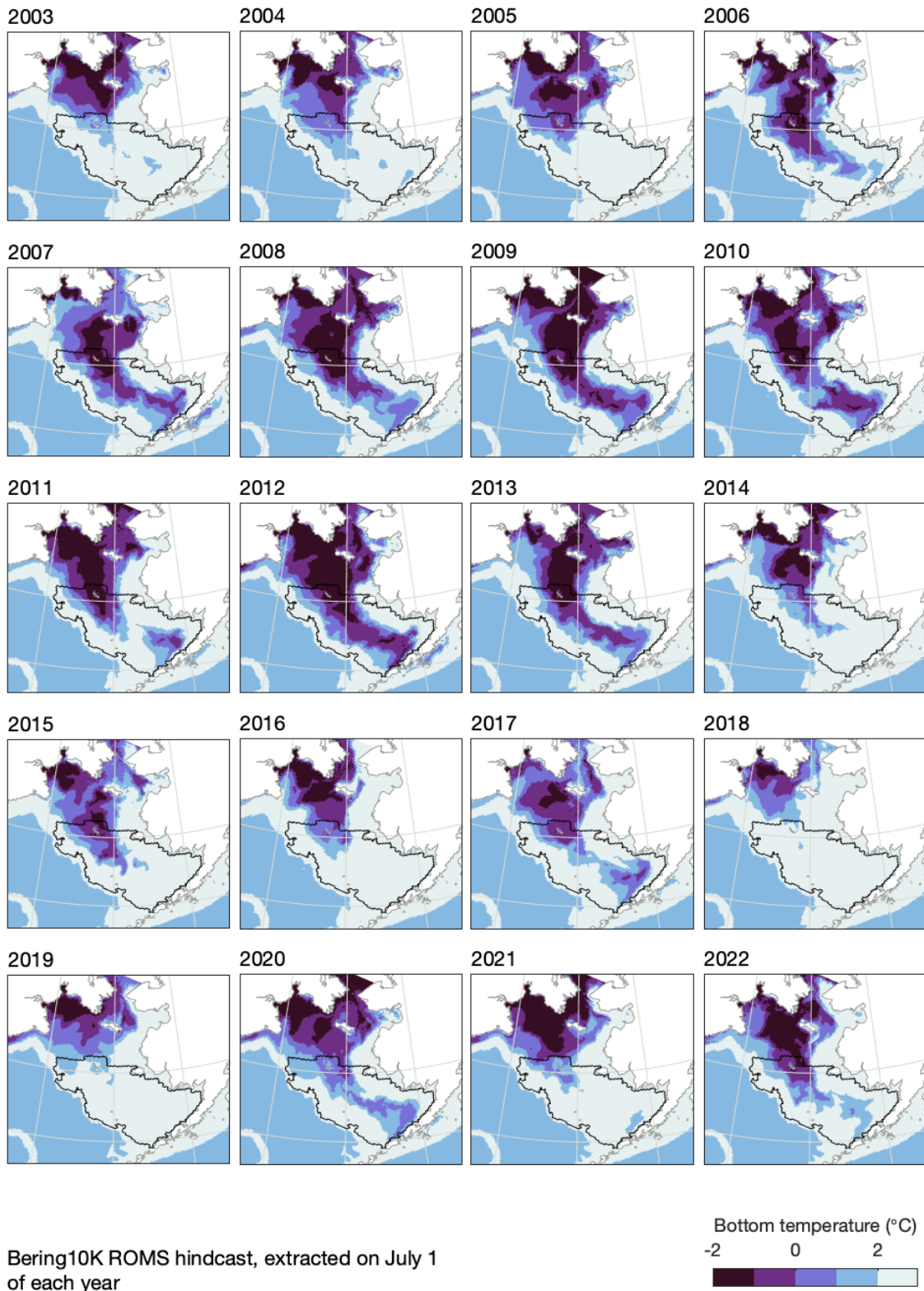
Simulated 2022 conditions were very near the historical (1971–2022) average (Figure 35). The mean SEBS bottom temperature in July was 2.53°C, just below the mean of 2.78°C. The 2°C cold pool index was 0.39, likewise just to the cool side of the mean of 0.35. For the first time since 2017, below-0°C water remained in the northern part of the SEBS region in the summer, resulting in a 0°C cold pool index of 0.09 (historical mean 0.11). 2022 resembles other average-to-cool years, with a spatial pattern characterized by summer <2°C water across much of the southeast middle shelf, patches of <1°C water in both the northern and southern parts of the southeast middle shelf, and some <0°C water in the northern southeast middle shelf. The closest recent analogue showing a similar pattern was 2017.

### *Cold Pool Extent - AFSC Bottom Trawl Survey*

Contributed by Sean Rohan, [sean.rohan@noaa.gov](mailto:sean.rohan@noaa.gov), and Lewis Barnett, [lewis.barnett@noaa.gov](mailto:lewis.barnett@noaa.gov)

The cold pool extent is calculated from spatially interpolated bottom temperature data collected during AFSC summer bottom trawl surveys of the EBS shelf (1982–2022, except 2020). See ‘Summer SST and Bottom Temperatures’ contribution above for more details.

The spatial footprint of the cold pool in 2022 was similar to the most recent near-average years in 2011 and 2017 (Figure 36). North of ~57°N, the cold pool covered nearly the entire middle domain of the survey area between the 50m and 100m isobaths. The extents of the ≤-1°C (12,075 km<sup>2</sup>), ≤0°C (45,000 km<sup>2</sup>), and ≤1°C (107,300 km<sup>2</sup>) isotherms were larger than during the three prior surveys and near their time-series averages (23,505 km<sup>2</sup>, 53,951 km<sup>2</sup>, and 102,706 km<sup>2</sup>, respectively).



Bering10K ROMS hindcast, extracted on July 1 of each year

Figure 35: Bering 10K ROMS hindcast of cold pool extent, extracted on July 1 of each year, for the Bering Sea, 2003–2022. The black outline denotes the standard bottom trawl survey grid.

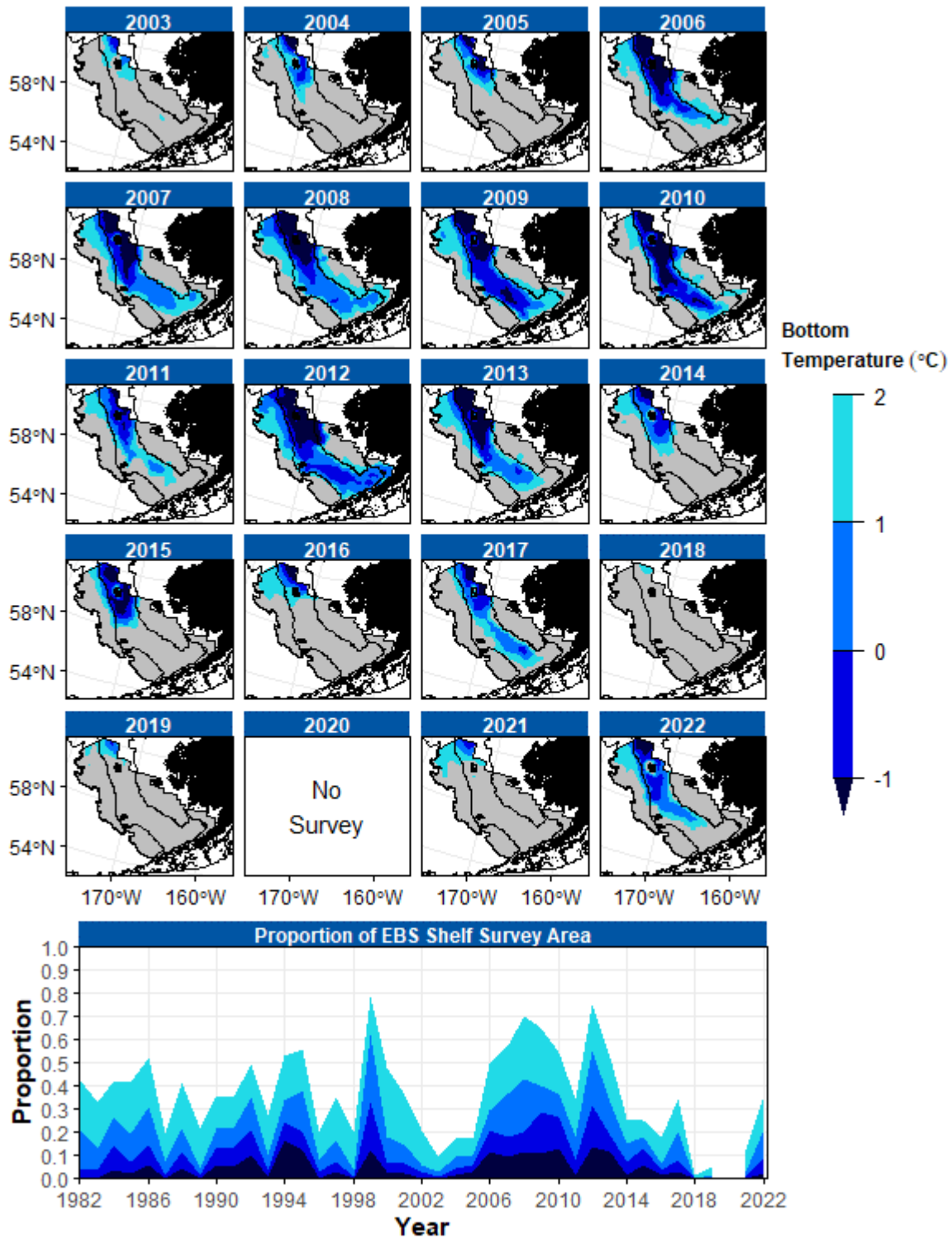


Figure 36: Cold pool extent in the eastern Bering Sea (EBS), as measured using observations from the EBS bottom trawl survey. Upper panels: Maps of cold pool extent in the EBS shelf survey area from 2003–2022. Lower panel: Extent of the cold pool in proportion to the total EBS shelf survey area from 1982–2022. Fill colors denote bottom temperatures  $\leq 2^\circ\text{C}$ ,  $\leq 1^\circ\text{C}$ ,  $\leq 0^\circ\text{C}$ , and  $\leq -1^\circ\text{C}$ .

**Implications:** The cold pool has a strong influence on thermal stratification and, overall, changes in surface and bottom temperatures influence the spatial structure of the demersal community (Kotwicki and Lauth, 2013; Stevenson and Lauth, 2019; Thorson et al., 2020), trophic structure of the EBS food web (Mueter and Litzow, 2008; Spencer et al., 2016), and demographic processes of fish populations (Grüss et al., 2021). When the cold pool is small, species with warm-water affinity (e.g., arrowtooth flounder, *Atheresthes stomias*) are distributed more widely over the EBS shelf with expansion across the shelf and to the north because there is no thermal barrier to migration. In contrast, the distribution of species with cold water affinity (e.g., Arctic cod, *Boreogadus saida*; Bering flounder, *Hippoglossoides robustus*) contract to the north when the cold pool is small. While the cold pool area is defined based on the 2°C isotherm, recent studies suggest that a more ecologically relevant temperature for several subarctic fishes and crabs is the 1°C isotherm (Kotwicki and Lauth, 2013) or the 0°C isotherm for walleye pollock (*Gadus chalcogrammus* and Pacific cod *G. macrocephalus*) (Baker, 2021; Eisner et al., 2020). Similar to the most recent near-average cold-pool-extent year in 2017 (Stevenson and Lauth, 2019), the NBS bottom trawl survey encountered considerable densities of adult walleye pollock and Pacific cod in the NBS in 2022, which suggests the larger cold pool and extents of  $\leq 0^\circ\text{C}$  and  $\leq 1^\circ\text{C}$  isotherms may not have posed a significant barrier to northward migration for these species.

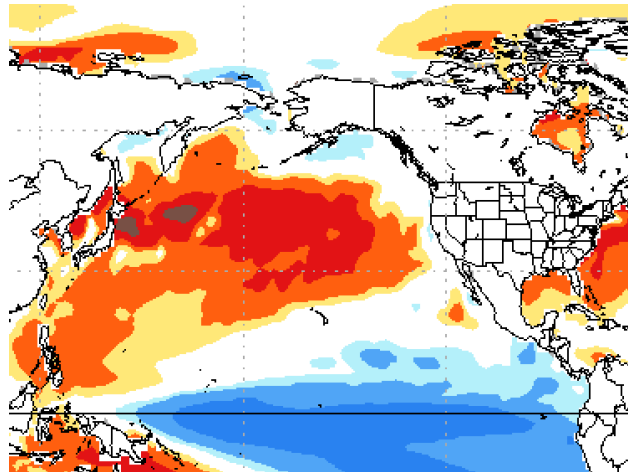
## 7. Seasonal Projections from the National Multi-Model Ensemble (NMME)

Contributed by Nick Bond, [nicholas.bond@noaa.gov](mailto:nicholas.bond@noaa.gov)

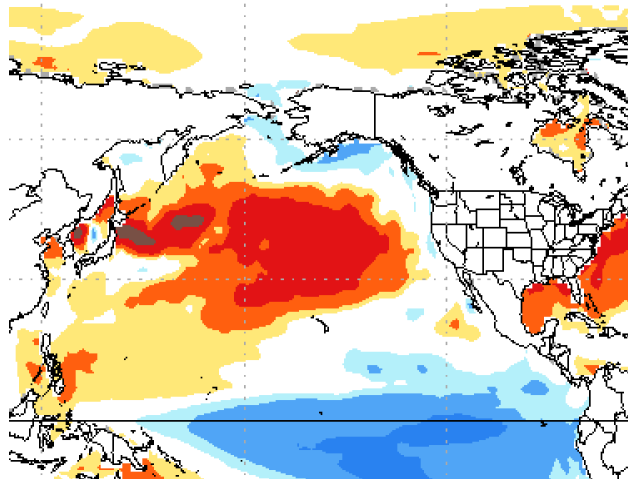
Seasonal projections of SST from the National Multi-Model Ensemble (NMME) are shown in Figures 37, a-c. An ensemble approach incorporating different models is particularly appropriate for seasonal and longer-term simulations; the NMME represents the average of eight climate models. The uncertainties and errors in the predictions from any single climate model can be substantial. More detail on the NMME, and projections of other variables, are available at the following website: <http://www.cpc.ncep.noaa.gov/products/NMME/>.

First, the model projections from a year ago are reviewed. The consensus of the model forecasts from September 2021 for the following fall and winter indicated a continuation of positive SST anomalies across the North Pacific south of 50°N and modest warmth on the southeast Bering Sea shelf. They also indicated weak cool anomalies in the GOA. The extended range projections for spring 2022 included continued cooling of the GOA to anomaly values of 0.5–1°C and near-average temperatures on the SEBS shelf. The performance of the climate models as a group was fairly good in an overall sense. For the first period considered, October through December 2021, they correctly forecast warmth in the central North Pacific and negative anomalies in the GOA and Chukchi Sea. But the GOA was actually cooler than predicted and the southeast Bering Sea shelf was cool instead of warm as forecast. The overall SST anomaly pattern was forecast to remain similar for the following winter (Dec-Feb). As with the previous forecast, the models captured the overall pattern for the North Pacific, but under-predicted the cool temperatures in the GOA and on the SEBS shelf. The consensus of the model forecasts for February–April 2022 included slight additional cooling of the GOA and southeast Bering Sea shelf whereas in reality the temperatures in these regions moderated. In summary, the model predictions were quite good for the tropics and mid-latitude North Pacific, but were less skillful for the SEBS shelf, perhaps due to the early and unanticipated onset of cold weather for Alaska and the waters to its west and south in autumn 2021.

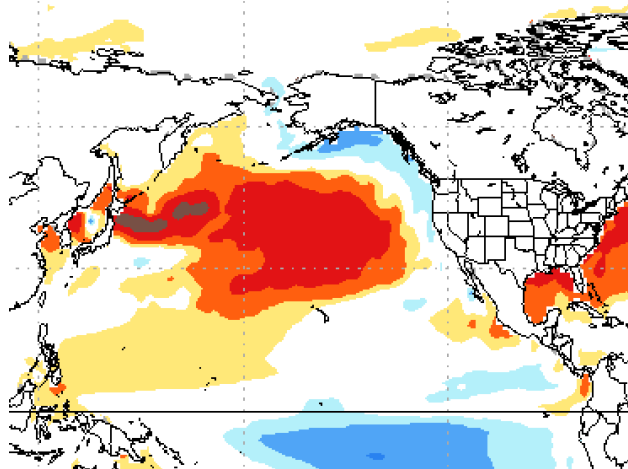
These NMME forecasts of three-month average SST anomalies indicate a continuation of a large region of relatively warm water in the central and western North Pacific south through the end of the calendar year (Oct-Dec 2022; Figure 37a). Near-average temperatures are predicted for Alaskan waters with the exception of the western Aleutian Islands, where positive anomalies are also predicted. The models also are indicating an atmospheric circulation pattern that would bring enhanced storminess to the GOA. The ensemble of model predictions for December 2022 through February 2023 is quite similar to that of the earlier period, with the exception of cooling for the GOA (Figure 37b) as compared with climatological norms. This change is consistent with what has occurred in past La Niña winters; the models as a group are predicting tropical Pacific temperatures commensurate with a weak-moderate La Niña. The projection for February through April of 2023 (Figure 37c) features a rather static pattern in the SST anomalies aside from weakening of the equatorial Pacific cold anomalies. Based on the spread in the forecasts among the models for Alaskan waters, it appears that the forecasts for the SEBS shelf are more uncertain than elsewhere, with the various model predictions yielding a range from moderately below-average to moderately above-average temperatures. Nevertheless, most of the models suggest reasonably average conditions relative to the last 20–30 years that would result in sea ice extending south of 60°N perhaps all the way to M2, and as far south as Bristol Bay along the west coast of Alaska.



(a) Months Oct-Nov-Dec



(b) Months Dec-Jan-Feb



(c) Months Feb-Mar-Apr

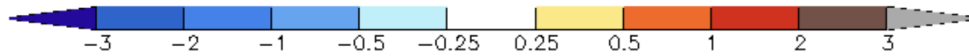


Figure 37: Predicted SST anomalies ( $^{\circ}\text{C}$ ) from the National Multi-Model Ensemble (NMME) for Oct-Dec 2022 (1 month lead), Dec 2022-Feb 2023 (3-month lead), and Feb-Apr 2023 (5-month lead). See text for details.

## Habitat

### Structural Epifauna - Eastern Bering Sea Shelf

Contributed by Thaddaeus Buser

Resource Assessment and Conservation Engineering Division, Alaska Fisheries Science Center

National Marine Fisheries Service, NOAA

Contact: thaddaeus.buser@noaa.gov

**Last updated: September 2022**

**Description of indicator:** Groups considered to be structural epifauna include: sea whips, corals, anemones, and sponges. Corals are rarely encountered on the eastern Bering Sea shelf so they were not included here. Relative CPUE by weight (kg per hectare) was calculated and plotted for each species group by year for 1982–2022. Relative CPUE was calculated by setting the largest biomass in the time series to a value of 1 and scaling other annual values proportionally. The standard error ( $\pm 1$ ) was weighted proportionally to the CPUE to produce a relative standard error.

**Status and trends:** Relative catch rates for sea anemones (Actiniaria) returned to levels similar to those observed during 2010–2015, compared to lower catch rates observed from 2016–2021. Sea whip (Pennatulacea) estimates for 2022 are similar to those observed in 2021, which together represent an increase from 2019 observations and a return to a catch rate similar to that observed 1999–2005 and 2013–2016. The catch rate of sponges in 2022 (Porifera) continues the very low catch level observed in 2021, which was the lowest level observed in the time series, but similar to results observed intermittently during the early years of the time series, 1984–1992. These trends should be viewed with caution, however, because the consistency and quality of their enumeration have varied over the time series (Stevenson and Hoff, 2009; Stevenson et al., 2016). Moreover, the identification of trends is uncertain given the large variability in relative CPUE (Figure 38).

**Factors influencing observed trends:** Further research in several areas would benefit the interpretation of structural epifauna trends including systematics and taxonomy of Bering Sea shelf invertebrates, survey gear selectivity, and the life history characteristics of the epibenthic organisms captured by the survey trawl.

**Implications:** Understanding the trends as well as the distribution patterns of structural epifauna is important for modeling habitat to develop spatial management plans for protecting habitat, understanding fishing gear impacts, and predicting responses to future climate change (Rooper et al., 2016). More research on the eastern Bering Sea shelf will be needed to determine if there are definitive links.

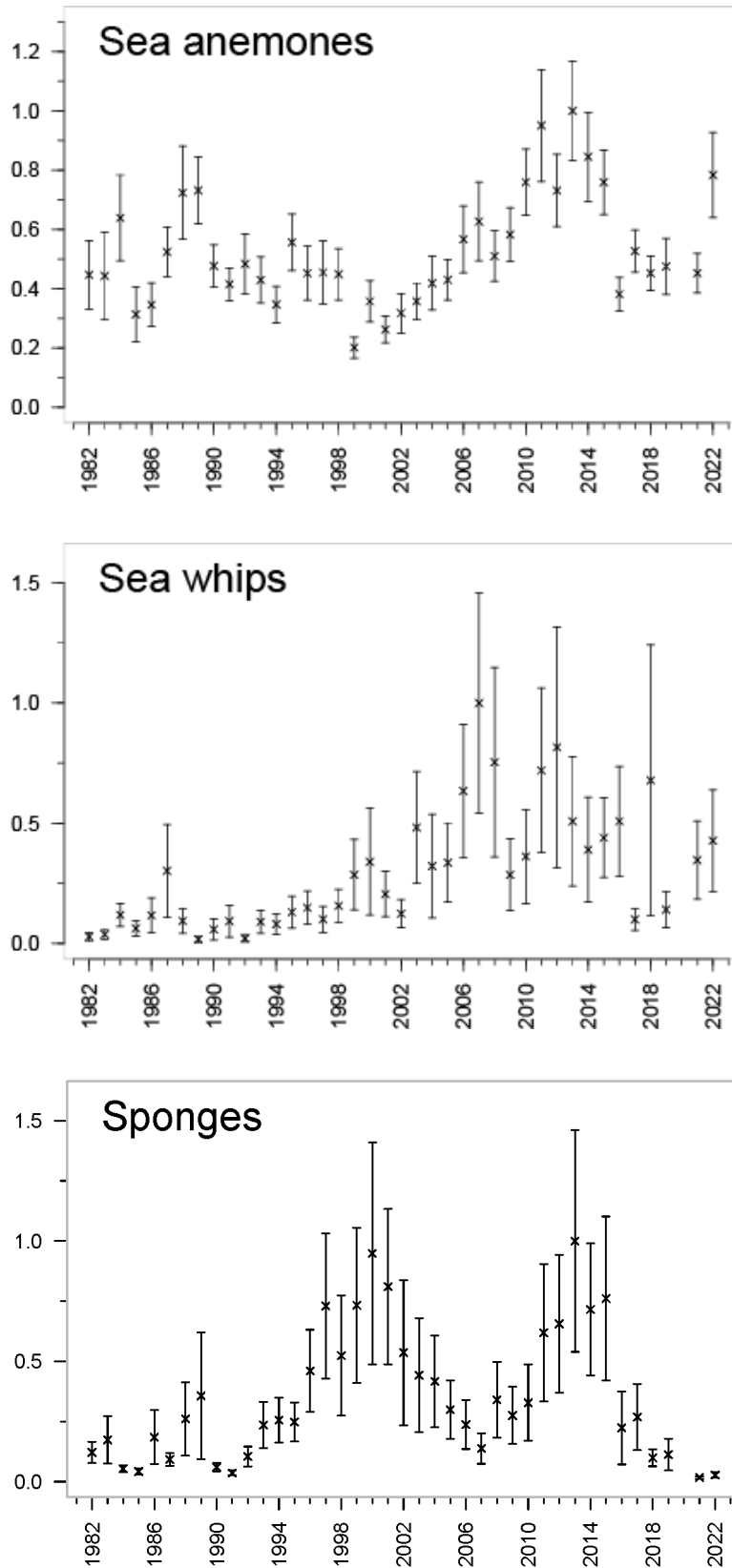


Figure 38: AFSC eastern Bering Sea shelf bottom trawl survey relative CPUE for three groups of benthic epifauna during the May to August time period from 1982–2022.

# Primary Production

## Spring Satellite Chlorophyll-a Concentrations in the Eastern Bering Sea

Contributed by Jens M. Nielsen<sup>1,2</sup>, Lisa Eisner<sup>3</sup>, Jordan Watson<sup>4</sup>, Jeanette C. Gann<sup>3</sup>, Matt W. Callahan<sup>5</sup>, Calvin W. Mordy<sup>2,6</sup>, Shaun W. Bell<sup>2,6</sup>, and Phyllis Stabeno<sup>6</sup>

<sup>1</sup>Resource Assessment and Conservation Engineering Division, Alaska Fisheries Science Center, NOAA Fisheries

<sup>2</sup>Cooperative Institute for Climate, Ocean, and Ecosystem Studies (CICOES), University of Washington, Seattle, WA

<sup>3</sup>Auke Bay Laboratories, Alaska Fisheries Science Center, NOAA Fisheries

<sup>4</sup>Pacific Islands Ocean Observing System, University of Hawai'i Manoa, 1680 East West Rd. POST 815, Honolulu, HI 96822, USA

<sup>5</sup>Pacific States Marine Fisheries Commission - Alaska Fish Information Network

<sup>6</sup>Pacific Marine Environmental Laboratory, NOAA Research, Seattle, WA, USA

Contact: jens.nielsen@noaa.gov

**Last updated: September 2022**

**Description of indicator:** In subarctic systems, such as the eastern Bering Sea, the timing and magnitude of the spring bloom can have large and long-lasting effects on biological production, with subsequent impacts on higher trophic levels including commercial fish stocks (Platt et al., 2003). The fate of the spring bloom (pelagic grazing or sinking to benthos), and its timing, impact benthic feeders in the Bering Sea (Hunt et al., 2002). Recent climatic changes in the Bering Sea have included reduced sea ice and warming ocean temperatures (Stabeno and Bell, 2019), with consequent changes to the food web (Duffy-Anderson et al., 2019; Hunt et al., 2020). Understanding annual changes in spring phytoplankton biomass and peak timing dynamics are thus important metrics for depicting ecosystem changes.

Here, we used ocean color satellite data from 2003–2022 available from the MODIS (Moderate Resolution Imaging Spectroradiometer) satellite at a 4x4 km resolution composites<sup>14</sup> to estimate: 1) average spring (Apr–Jun) chlorophyll-a concentrations (chl-a, an estimate of phytoplankton biomass in the surface layer), and 2) peak timing of the spring open water bloom for major regions in the eastern Bering Sea. In the southeastern Bering Sea, sustained observations at the M2 mooring (56.9°N, -164.1°W) provide good representation of the south middle shelf biophysical conditions. Thus, the long-term chlorophyll-a fluorescence mooring measurements were compared to the bloom peak timing estimates calculated from the satellite data.

We focus on the spring period as this is an important time for providing basal resources for zooplankton and thus energy for higher trophic level species. The April–June time period was chosen as this period consistently includes the pelagic spring bloom. We further divided the eastern Bering Sea into 8 distinct regions split between approximately north and south of 60°N and defined by oceanographic fronts and water mass characteristics based on Ortiz et al. (2012) (Figure 39). There are several advantages of satellite data, including high spatial and temporal coverage. However, these products are also limited to measurements within the surface ocean and also have missing data due to ice and cloud cover, particularly in high latitude systems such as the Bering Sea. We used 8-day composite data for the biomass and spring bloom peak timing estimates.

Open water spring bloom peak timing was estimated from data binned to individual ADF&G groundfish statistical areas (~0.5° latitude x 1° longitude spatial grid cells)<sup>15</sup>. We then calculated the average and standard deviation of all estimated bloom peaks within a specific region, which allowed for calculation of variability for each of the 8 areas. Grid cells with less than 66% seasonal coverage were excluded.

---

<sup>14</sup>[coastwatch.pfeg.noaa.gov/erddap/griddap/erdMBchla8day.html](https://coastwatch.pfeg.noaa.gov/erddap/griddap/erdMBchla8day.html)

<sup>15</sup><http://www.adfg.alaska.gov/index.cfm?adfg=fishingCommercialByFishery.statmaps>

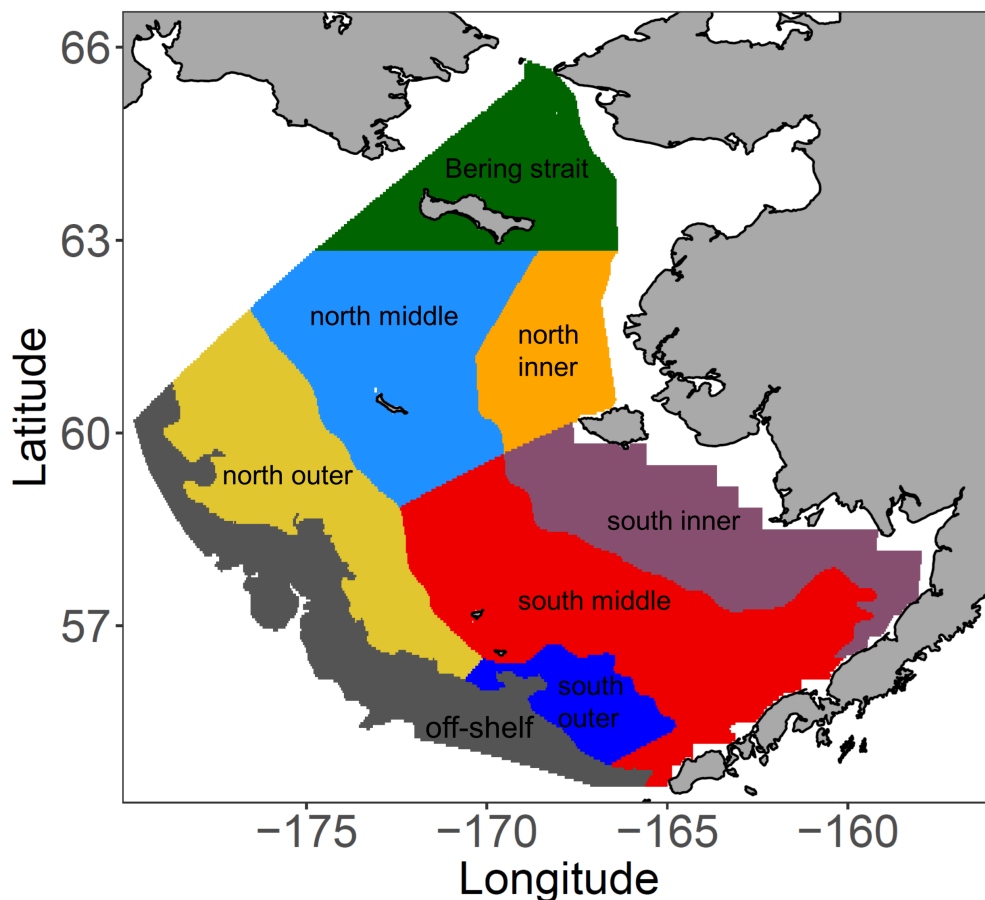


Figure 39: Map of the 8 shelf regions used for satellite chlorophyll-a analyses: south inner (purple), south middle (red), south outer (dark blue), off-shelf (dark gray), north inner (orange), north middle (light blue), north outer (yellow), and the Bering Strait (dark green). Off-shelf denotes regions on the shelf break and slope deeper than 200m (Ortiz et al., 2012).

**Status and trends:** There was a high degree of interannual variability in satellite chlorophyll-a from 2003–2022. Both the south inner (<50m) and south outer shelf (100–180m) had below-average values in 2022, similar to values in the period 2016–2019. Values in the south middle (50–100m), north inner, and north middle shelf region were close to median. Values along the shelf-break (off-shelf region) were low in 2022, continuing an apparent decreasing trend since 2014 (Figure 40). Data coverage in the southern regions was generally good across all years; however further north, in some years data from April were particularly scarce due to extended ice coverage (Figure 41, blank spaces). Consequently, estimates in spring should be considered with caution during the years when coverage was limited.

Preliminary analyses of the pelagic spring bloom peak timing suggest that 2022 was similar to the long-term averages in the south inner, south middle, and south outer shelf regions (Figure 42). For the south middle shelf region, there was evidence of 2 peaks, the largest around 4 May (day 125) and a substantial but smaller peak around 24 May (Figures 41 and 42). Peak bloom timing estimated from the M2 mooring clearly showed the later peak ~24 May. *Note:* mooring peak timing in 2022 was estimated from the 10m fluorescence sensor. This sensor was deployed after the first peak (~4 May). Overall, annual timing estimates from 2003 to 2022 from the M2 mooring align well with estimates based on satellite chlorophyll-a at the mooring (0.5 lon x 0.5 lat box with M2 in the center). In the off-shelf region, the bloom peak in 2022 was fairly close to the long-term average but later than 2021. However, the magnitude of off-shelf spring chlorophyll-a concentrations were low overall (Figure 40). No bloom satellite peak estimates were done for the northern regions.

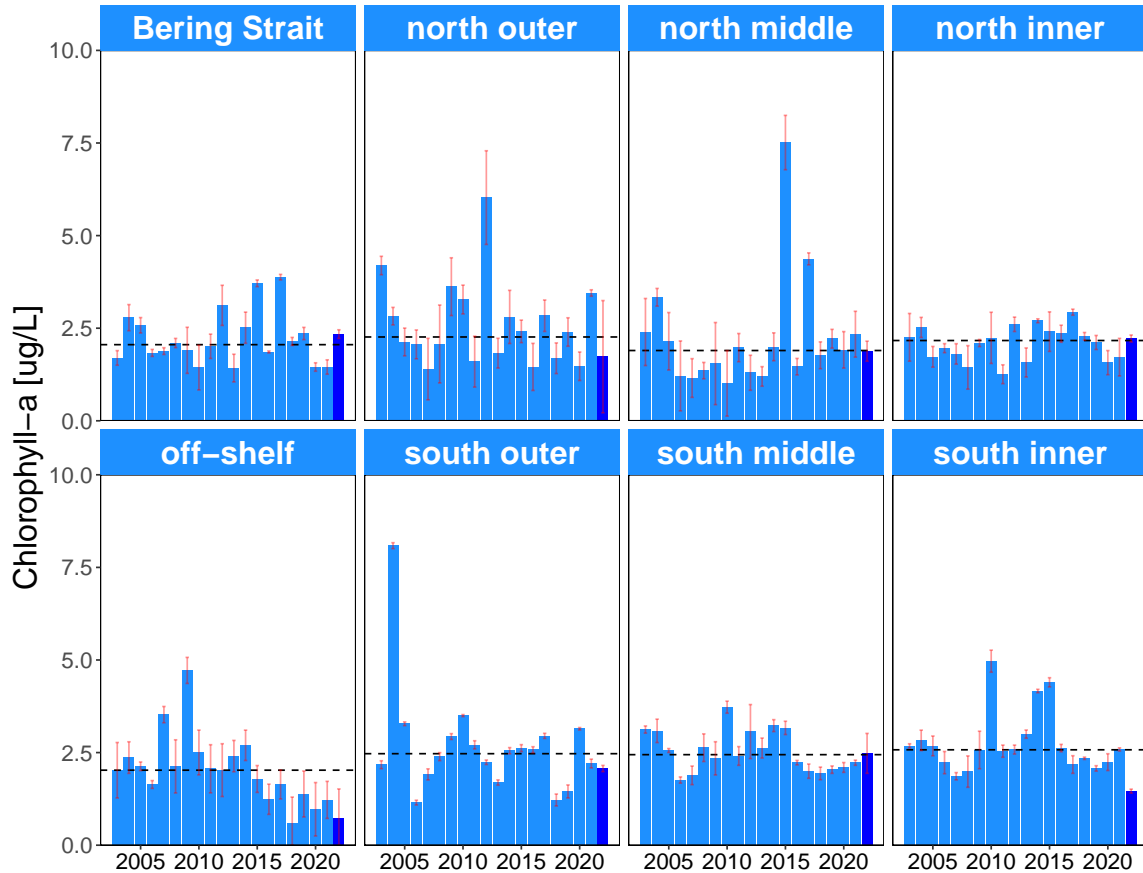


Figure 40: Average and standard deviation (SD) from spring (Apr-Jun) chlorophyll-a concentrations for 8 regions in the eastern Bering Sea. Dotted black line denotes the long-term median (2003–2021) for each region. **Note:** For plotting purposes, the minimum error bar is set at 0.01 and the maximum at 9.99. In a few cases, the +standard deviation was >10 (south outer in 2004 was 18.9; north middle in 2015 was 13.8; south outer in 2012 was 11.6).

**Factors influencing observed trends:** Previous studies have highlighted the strong coupling between temperature and sea-ice dynamics and spring bloom timing. For example, in the southern Bering Sea, ice present after mid-march commonly results in an early and prominent ice-associated bloom, while lack of ice normally results in a delayed open water bloom in mid- to late-May (Sigler et al., 2014). On the southern middle shelf, we observed an earlier spring bloom in the cold years of 2007–2012 (excluding 2009) and in the average years of 2013 and 2017. However, spring bloom timing varied considerably in recent warm years (2018–2021), suggesting that the timing of the bloom in those years was impacted by other factors besides ice. Open water blooms were prevalent in the most southern areas in 2022, including at M2. For these open water blooms, variations in springtime winds may influence the setup of stratification (e.g., higher winds can delay stratification, Stabeno et al. (2016)), which in turn affects light availability and the timing of the bloom. However, ice was present in April as far south as latitude 57°N and then retracted rapidly in April. While blooms appeared to form predominantly as ice-associated it is unclear how the rapid ice retreat and likely thin ice influenced overall phytoplankton production associated with the spring bloom. Analysis of chlorophyll-a biomass, though informative in depicting spring bloom timing, does not directly provide information of primary productivity (growth rates), though biomass levels in spring generally align with the timing of production peak estimates. Since biomass is a balance between production and losses, lower biomass levels could also indicate enhanced grazing by microzooplankton and mesozooplankton, or sinking to the benthos.

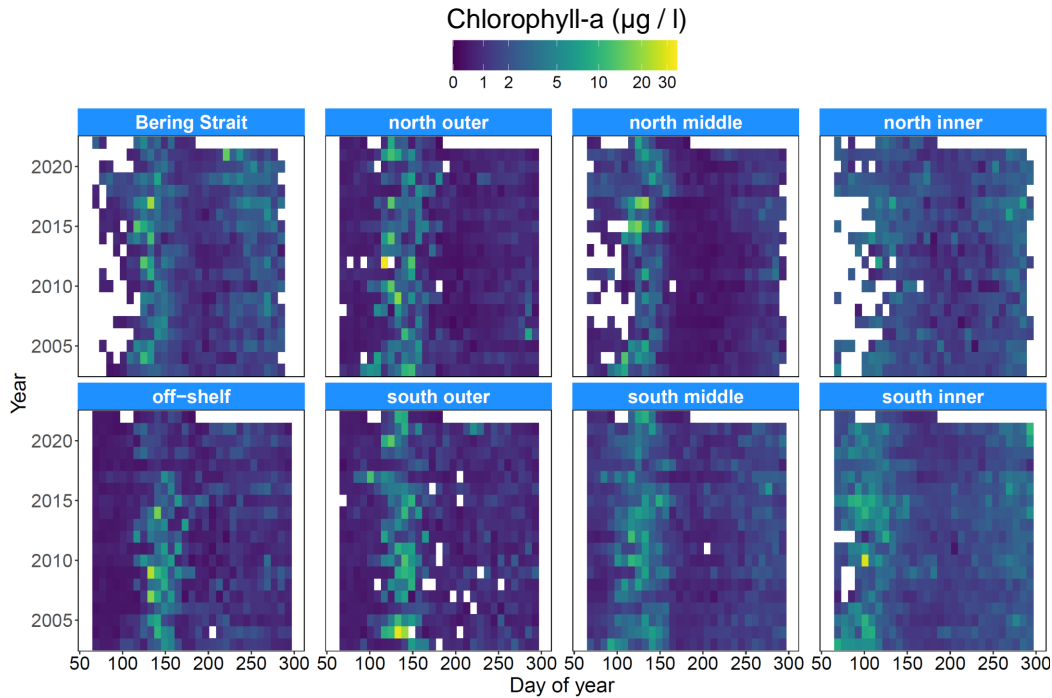


Figure 41: Heatmap of satellite 8-day composite chlorophyll-a concentrations for each year and region. Color scale is logged.

**Implications:** Primary producers provide fundamental energy and nutrients for zooplankton grazers and higher trophic level species. Understanding how climatic perturbations, and particularly the recent warm period, influence phytoplankton dynamics is a critical component in understanding ecosystem dynamics in the Bering Sea. Large, lipid-rich copepods, *Calanus* spp. were in higher abundance in summer 2017 (see Kimmel et al., p. 79), a year with an early spring bloom (and average ice cover), which may have offered an early food resource for zooplankton reproduction and survival. Our analyses show no significant long-term change in the bloom peak timing among low and high ice years combined for most of the southern Bering Sea (<60°N). For the Northern Bering Sea, bloom timing is occurring earlier as ice retreat advances with warming (Waga et al., 2021), except in the years 2018–2019 where ice retreated so early that open water blooms formed in large areas in this region (Nielsen et al., in prep.).

If warming temperatures during winter and spring accelerate development rates of zooplankton (Coyle and Gibson, 2017) it may also reduce the duration of diapause leading to earlier emergence (Pierson et al., 2013). Thus the timing of the spring bloom has important implications for consumers such as zooplankton, and in turn their predators such as fish larvae. Reduction of sea ice, and thus lack of ice-associated phytoplankton blooms also shifts the community composition in favor of pelagic phytoplankton over ice algae; changes that likely have strong impacts on benthic-pelagic energy fluxes (Hunt et al., 2002) and the nutritional composition of basal resources for consumers. The declining trends in chlorophyll-a biomass observed along the shelf-break in recent warm years (2015–2022) deserves further investigation. This area includes the “greenbelt”, an area known for high production (Springer et al., 1996), and it will be important to understand the mechanism behind these apparent changes.

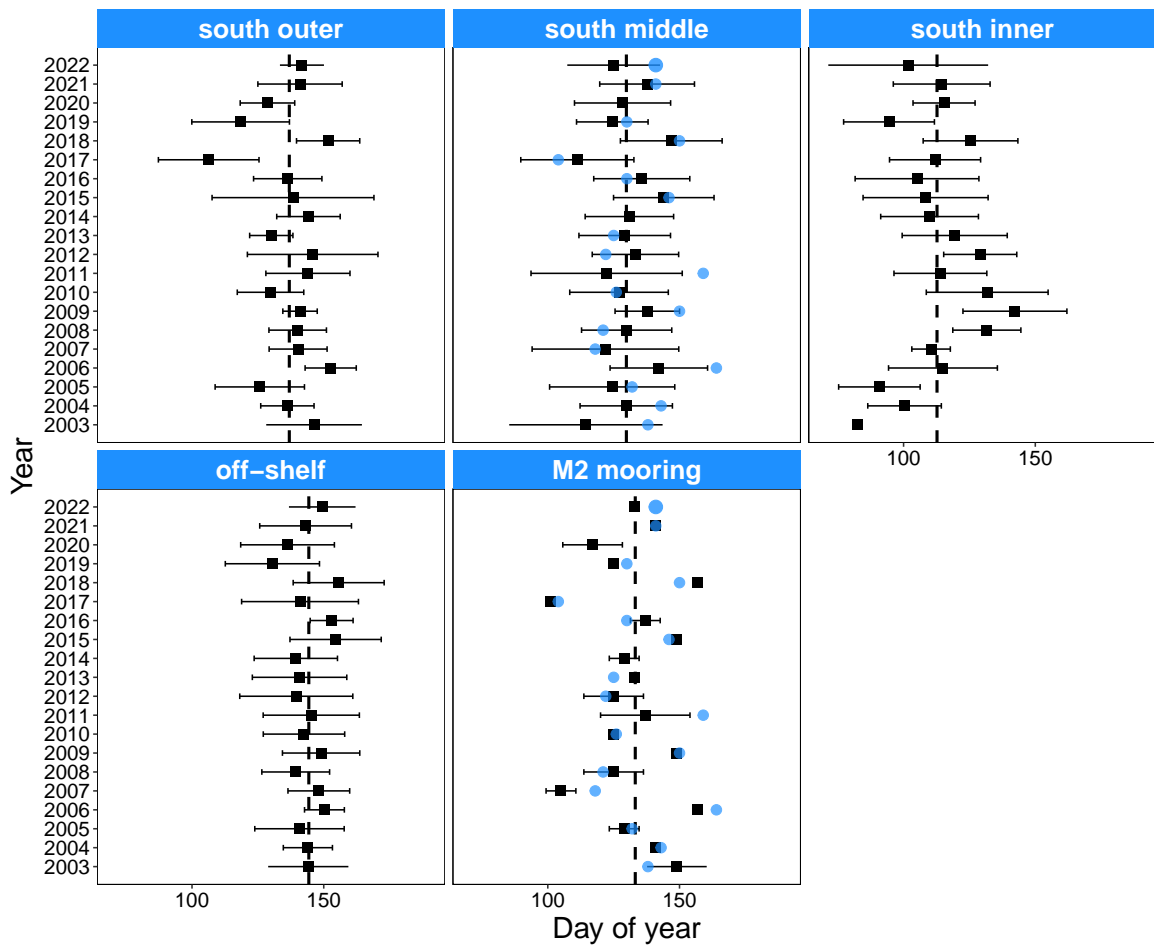


Figure 42: Average and SD of peak spring bloom timing estimated from areas within 4 southern regions in the eastern Bering Sea. Red dots are the M2 fluorescence peak timing estimates, which are compared to both the south middle shelf data and specifically to satellite data near M2 [ $1^\circ$  latitude x  $1^\circ$  longitude].

## Coccolithophores in the Bering Sea

Contributed by Jens Nielsen<sup>1,2</sup> and Lisa Eisner<sup>3</sup>

<sup>1</sup>Resource Assessment and Conservation Engineering Division, Alaska Fisheries Science Center, NOAA Fisheries

<sup>2</sup>Cooperative Institute for Climate, Ocean, and Ecosystem Studies (CICOES), University of Washington, Seattle, WA

<sup>3</sup>Auke Bay Laboratories, Alaska Fisheries Science Center, NOAA Fisheries

Contact: jens.nielsen@noaa.gov

**Last updated: October 2022**

**Description of indicator:** Blooms of coccolithophores, a unicellular calcium carbonate-producing phytoplanktonic organism, are easily observed by satellite ocean color instruments due to their high reflectivity. Coccolithophores produce calcium carbonate plates (coccoliths) that contribute to particulate inorganic carbon (PIC) in the ocean (Matson et al., 2019). Blooms are most commonly observed and cloud cover is typically lower during September than in other months, allowing for better quantification (Iida et al., 2012). An interannual index of the average area (km<sup>2</sup>) covered by coccolithophores during the month of September is calculated with monthly average mapped PIC data (Balch et al., 2005; Gordon et al., 2001) from satellite observations. This year we have updated our index and now use monthly PIC data from the blended (multi-sensor) GlobColour product<sup>16</sup>. This update extends our time series from 1997 to the present. Comparisons of the new GlobColour calculations show very similar trends to estimates from previous years based on MODIS-Aqua satellite data (2003–2020,  $r^2 = 0.96$ – $0.98$ ) and from the VIIRS-SNPP satellite (2012–2021,  $r^2 = 0.97$ – $0.98$ ) provided by NASA Goddard Space Flight Center, Ocean Ecology Laboratory (NASA, 2019).

PIC > 0.0011 mol/m<sup>3</sup> was used to estimate the location of the influence of coccolithophore blooms. This threshold was derived by Matson et al. (2019). Highly reflective waters in shallow water near the coast can be due to re-suspended diatom frustules rather than coccoliths (Broerse et al., 2003). Thus, the index is calculated from the region south of 60°N and deeper than 30m depth to avoid contamination by shallow regions around St. Matthew and St. Lawrence islands and along the Alaskan coast, as well as sediment associated with the Yukon River. Because blooms are often largely confined to either the middle shelf or the inner shelf (Ladd et al., 2018), two indices are calculated, one for the middle shelf (50–100m depth) and one for the inner shelf (30–50m depth).

Before 1997, coccolithophore blooms in the eastern Bering Sea were rare. A large bloom (primarily *Emiliania huxleyi*) occurred in 1997 (Napp and Hunt, 2001; Stockwell et al., 2001) and for several years thereafter. During the 1997 bloom, the bloom was associated with a die-off of short-tailed shearwaters (*Puffinus tenuirostris*), a seabird commonly seen in these waters (Baduini et al., 2001). It was thought that the bloom may have made it difficult for the shearwaters to see their zooplankton prey from the air (Lovvorn et al., 2001). Since then, coccolithophore blooms in the eastern Bering Sea have become more common. Satellite ocean color data suggest that blooms are only found where water depths are between 20 and 100m. Blooms typically peak in September and interannual variability is related to both very weak and strong stratification (Iida et al., 2012; Ladd et al., 2018).

**Status and trends:** Annual images (Figure 43) show the spatial and temporal variability of coccolithophore blooms in September. Annual indices are obtained from satellite data by averaging spatially over the inner and middle shelf (Figure 44). Coccolithophore blooms were particularly large during the early part of the record, 1997, 1998, and 2000 (Figure 44). The index was low and remained low (<80,000 km<sup>2</sup>) through 2006. In 2007, the index rose to almost double that observed in 2006 (~125,000 km<sup>2</sup>). A higher index (>100,000 km<sup>2</sup>) was observed in 2007, 2009, 2011, 2014, 2016, 2020, 2021, and 2022 for the middle shelf and in 2011, 2014, and 2022 (> 40,000 km<sup>2</sup>) for the inner shelf. In 2022, the coccolithophore index for both the inner and middle shelf was among the highest ever observed in the timeseries (Figures 43 and 44). Commonly for years with high index values (e.g., 2014, 2016, 2020, and 2022) blooms are also observed in August (e.g., scientists

<sup>16</sup><https://hermes.acri.fr/index.php?class=archive>

conducting shipboard sampling on the middle shelf noted an extensive bloom in August 2022). September 2017 exhibited the lowest index of the record. The bloom index remained below average in 2018 and 2019 but increased, particularly on the middle shelf, in 2020, 2021, and especially in 2022.

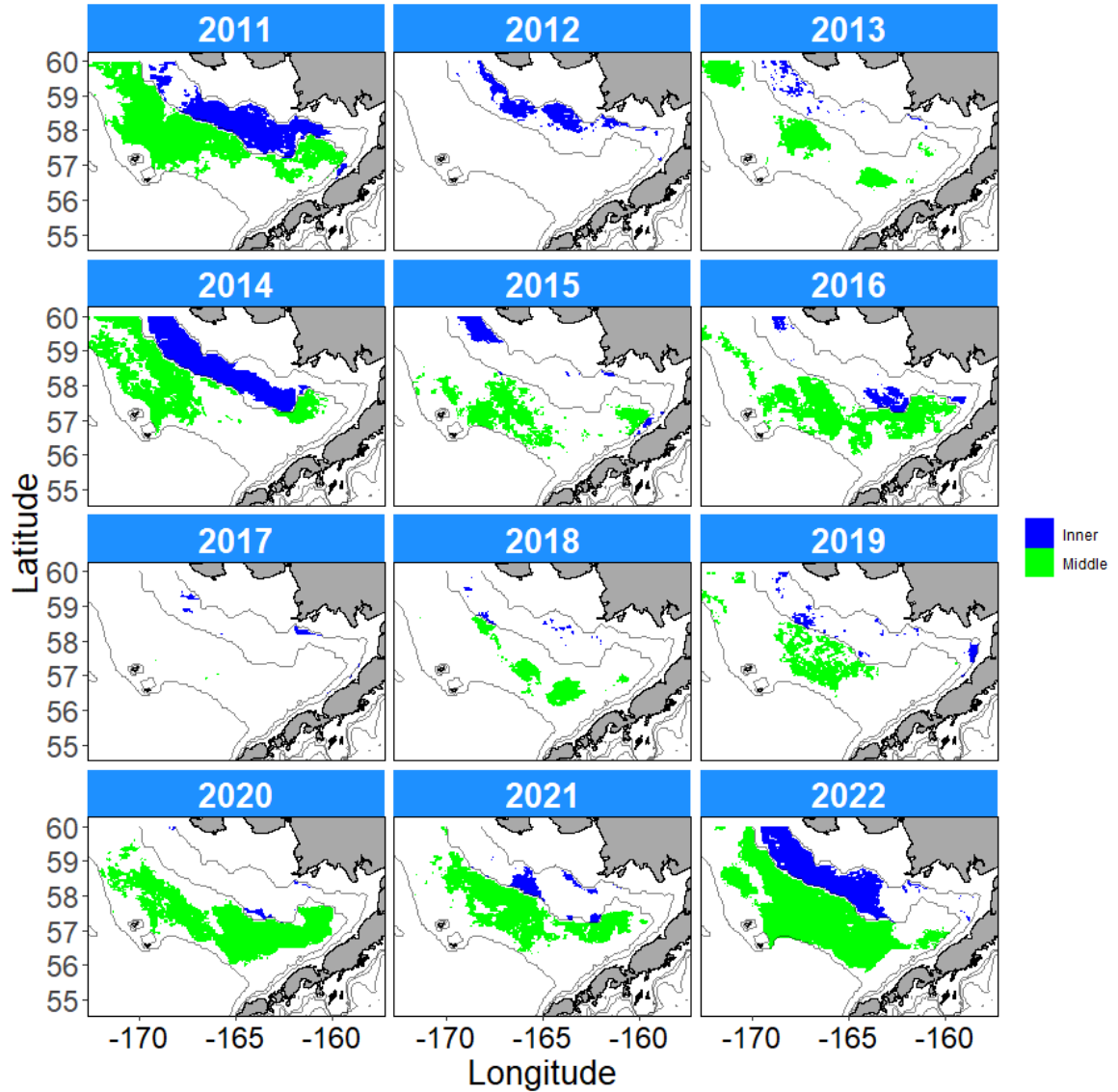


Figure 43: Maps illustrating the location and extent of coccolithophore blooms in September of each year from globcolour data. Color: satellite ocean color pixels exceeding the threshold ( $PIC > 0.0011 \text{ mol/m}^3$ ) indicating coccolithophore bloom conditions. Blue: inner shelf (30–50m depth), Green: middle shelf (50–100m depth). These data are used to calculate the areal index in Figure 44.

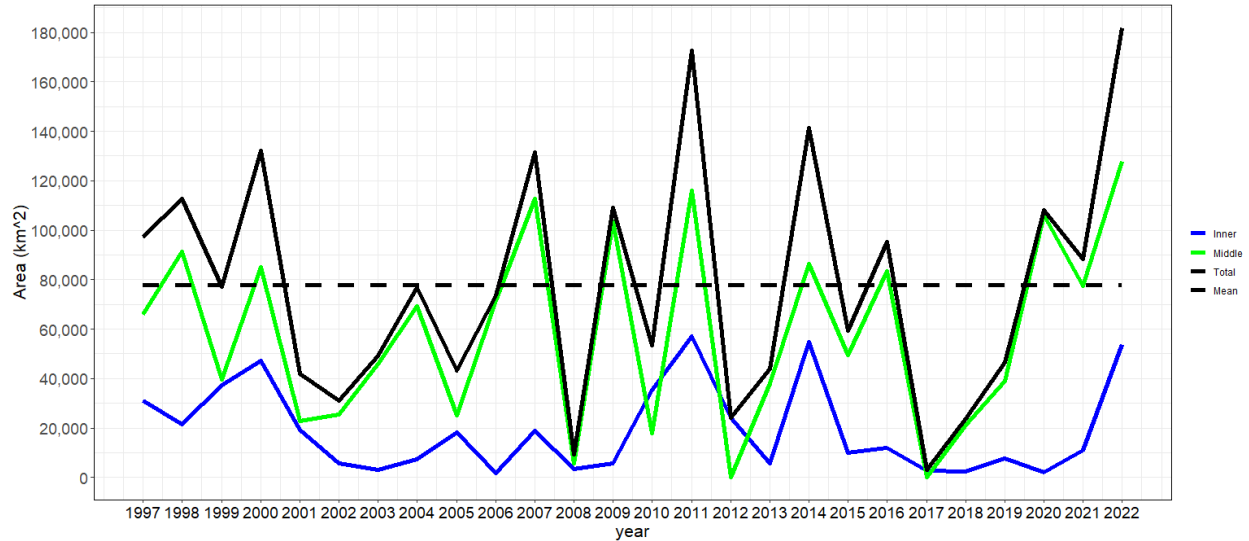


Figure 44: Cocolithophore index for the southeastern Bering Sea shelf (south of 60°N) calculated from the GlobColour blended PIC product. Blue: average over the inner shelf (30–50m depth), Green: average over the middle shelf (50–100m depth), Black: total. The black dashed line is the long-term average.

**Factors influencing observed trends:** It has been suggested that the strength of density stratification is the key parameter controlling variability of coccolithophore blooms in the eastern Bering Sea (Iida et al., 2012; Ladd et al., 2018). Stratification influences nutrient supply to the surface layer. Stratification in this region is determined by the relative properties (both temperature and salinity) of two water masses formed in different seasons, the warm surface layer formed in summer and the cold bottom water influenced by ice distributions the previous winter. Thus, the strength of stratification is not solely determined by summer temperatures and warm years can have weak stratification and vice versa (Ladd and Stabeno, 2012).

**Implications:** Coccolithophore blooms can have important biogeochemical implications. The Bering Sea can be either a source or a sink of atmospheric CO<sub>2</sub>, with the magnitude of coccolithophore blooms and the associated calcification playing a role (Iida et al., 2012). In addition, variability in the dominant phytoplankton (diatoms vs. coccolithophores) is likely to influence trophic connections with the smaller coccolithophores resulting in longer trophic chains. Coccolithophores may be a less desirable food source for microzooplankton in this region (Olson and Strom, 2002). As noted previously, the striking milky aquamarine color of the water during a coccolithophore bloom can also reduce foraging success for visual predators, such as surface-feeding seabirds and fish.

# Zooplankton

## Continuous Plankton Recorder Data from the Eastern Bering Sea

Contributed by Clare Ostle<sup>1</sup> and Sonia Batten<sup>2</sup>

<sup>1</sup>CPR Survey, The Marine Biological Association, The Laboratory, Citadel Hill, Plymouth, Devon, PL1 2PB, UK

<sup>2</sup>PICES, 4737 Vista View Cr, Nanaimo, BC, V9V 1N8, Canada

Contact: claost@mba.ac.uk

**Last updated: August 2022**

**Description of indicator:** Continuous Plankton Recorders (CPRs) have been deployed in the North Pacific routinely since 2000. Two transects are sampled seasonally, both originating in the Strait of Juan de Fuca, one sampled monthly (~April–September) which terminates in Cook Inlet, the second sampled 3 times per year (in spring, summer, and autumn) which follows a great circle route across the Pacific terminating in Asia. Several indicators are now routinely derived from the CPR data and updated annually.

In addition, the icebreaker *Sir Wilfrid Laurier* (SWL) has sampled a transect through the Bering Strait, and the western Chukchi and Beaufort Seas during the summer months of 2018–2021. The SWL is currently towing a CPR in the same region for 2022. We do not (at present) have the funds to complete the sample analysis for the year 2022; however, we are looking for long-term funding to continue sampling in these areas in the future, as they provide important information on this transition area.

This report highlights the Arctic route that started in 2018 and transects the Bering Strait during the summer months of July and September. We present CPR data from the eastern Bering Sea region (Figure 45) as the following indices: the abundance per sample of large diatoms (the CPR only retains large, hard-shelled phytoplankton so while a large proportion of the community is not sampled, the data are internally consistent and may reveal trends), mean Copepod Community Size (see Richardson et al. (2006) for details but essentially the length of an adult female of each species is used to represent that species and an average length of all copepods sampled calculated) as an indicator of community composition, and mesozooplankton biomass (estimated from taxon-specific weights and abundance data). Annual anomaly time series of each index have been calculated using a standard z-score calculation:  $z\text{-score} = (x - \mu) / \sigma$  where  $x$  is the value and  $\mu$  is the mean, and  $\sigma$  is the standard deviation (Glover et al., 2011). Scores of zero are equal to the mean, positive scores signify values above the mean, and negative scores values below the mean.

**Status and trends:** Figure 46 shows that the copepod community size and annual anomaly for 2021 was positive, where it had been negative in 2020. The mean diatom abundance and mesozooplankton biomass anomalies were negative in 2021.

**Factors influencing observed trends:** As there are only four years of consistent data from the EBS, it is difficult to determine any trend. Analysis of summer CPR data in this region has revealed a general alternating (and opposing) pattern of high and low abundance of diatoms and large copepods (indicated in Figure 46 by copepod community size). This is a similar finding to the analysis from Batten et al. (2018) which was carried out in the southern Bering Sea and Aleutian Islands and concluded that this alternation was the result of a trophic cascade caused by maturing pink salmon present in the region. The zooplankton data in Figure 46 consist of more taxa than just large copepods, but it is likely that there is also some top-down influence of pink salmon present in these data.

**Implications:** This region appears to be subjected to top-down influence by pink salmon as well as bottom-up forcing by ocean climate, the combination of which is particularly challenging to interpret. Changes in community composition (e.g., abundance and composition of large diatoms, prey size as indexed by mean copepod community size) may reflect changes in the nutritional quality of the organism to their predators. Changes in abundance or biomass, together with size, influences availability of prey to predators.

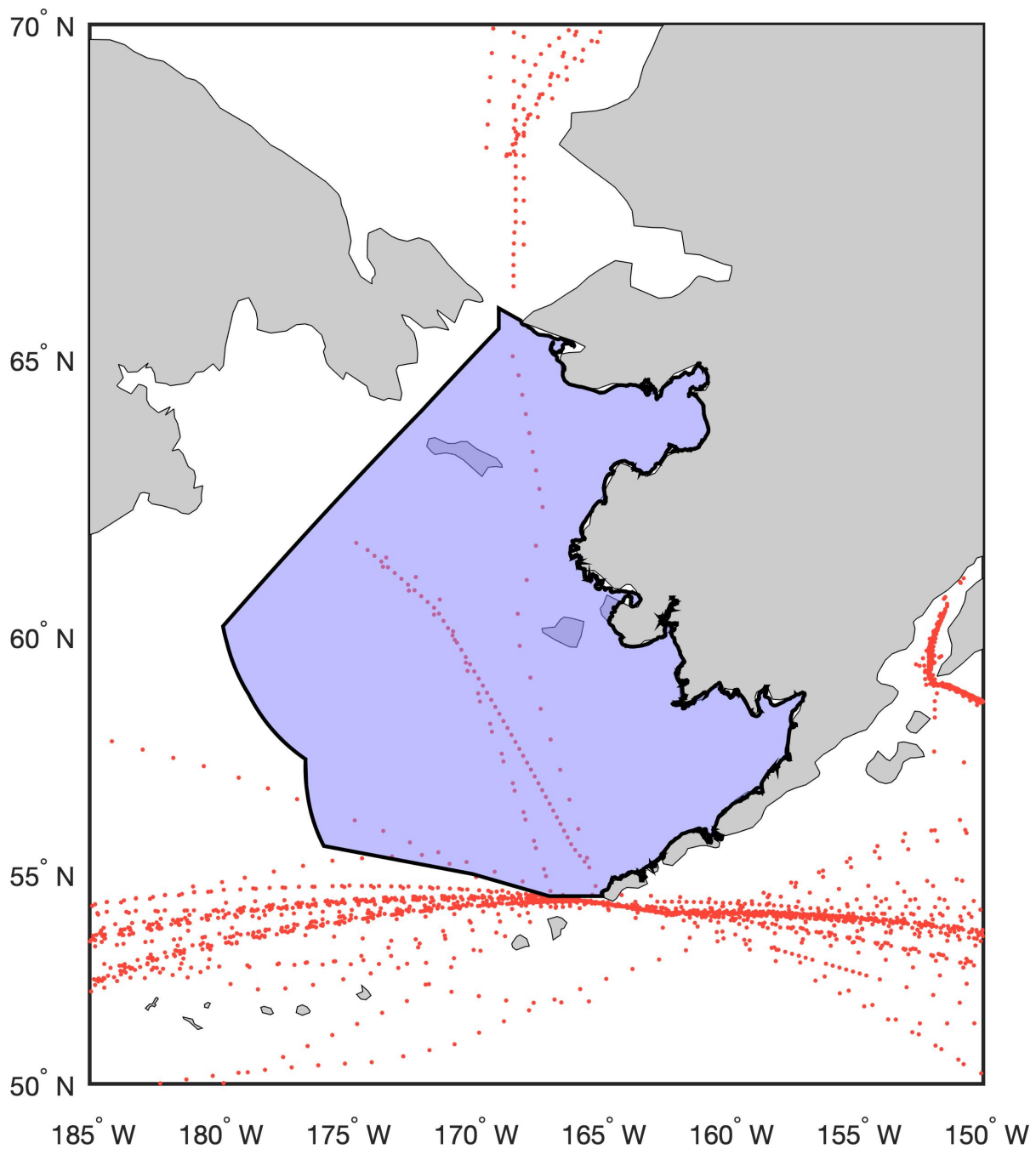


Figure 45: Location of CPR data. The EBS region selected for analysis is highlighted in purple. Red dots indicate actual sample positions and may overlay each other.

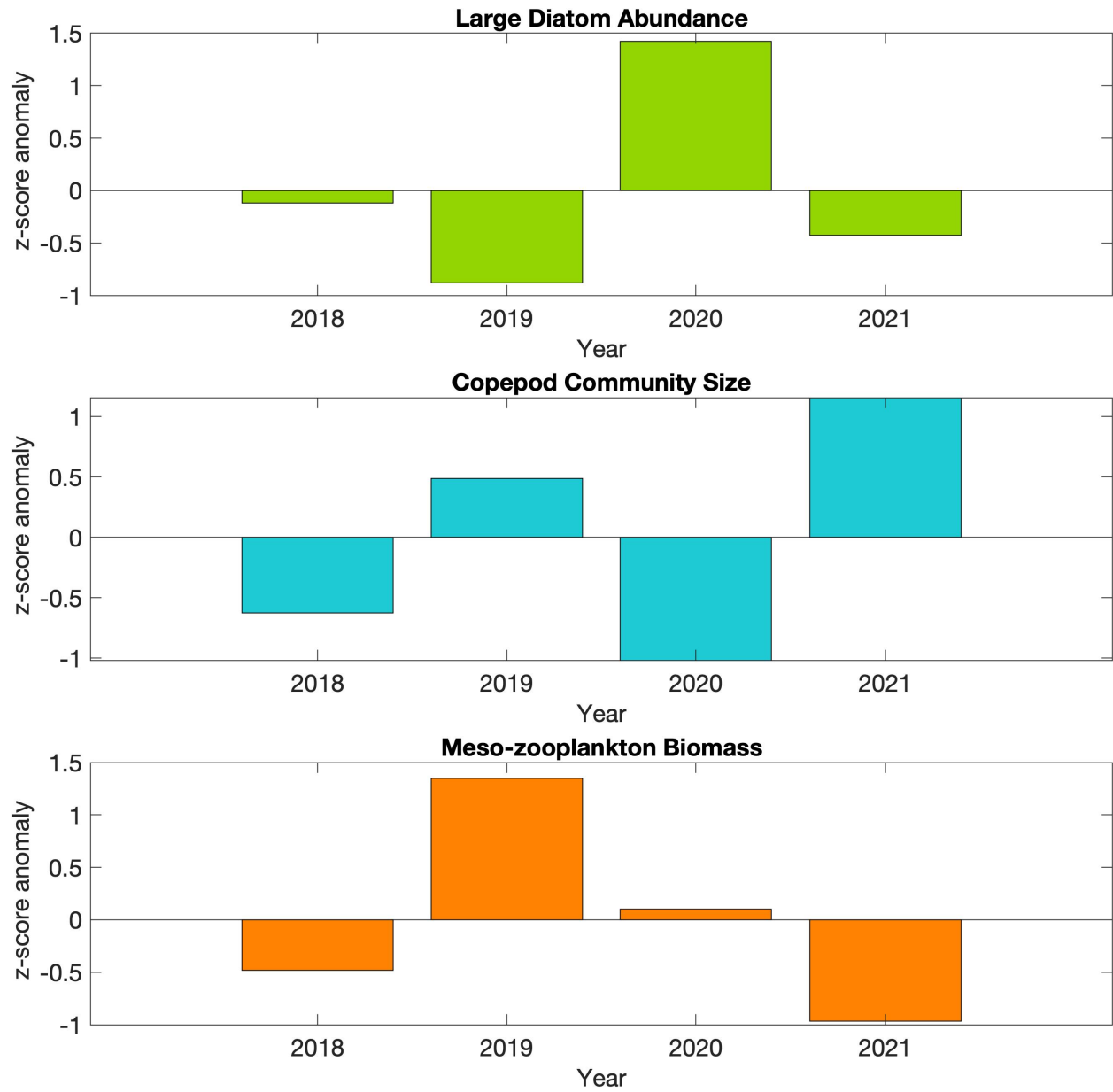


Figure 46: Annual anomalies of three indices of lower trophic levels (see text for description and derivation) for the region shown in Figure 45.

## Current and Historical Trends for Zooplankton in the Bering Sea

Contributed by David Kimmel<sup>1</sup>, Jenna Barrett<sup>1</sup>, Daniel Cooper<sup>1</sup>, Deana Crouser<sup>1</sup>, Alison Deary<sup>1</sup>, Lisa Eisner<sup>2</sup>, Jesse Lamb<sup>1</sup>, James Murphy<sup>2</sup>, Cody Pinger<sup>2</sup>, Bryan Cormack<sup>2</sup>, Steven Porter<sup>1</sup>, Wesley Strasburger<sup>2</sup>, and Robert Suryan<sup>2</sup>

<sup>1</sup>Resource Assessment and Conservation Engineering Division, Alaska Fisheries Science Center, National Marine Fisheries Service, NOAA

<sup>2</sup>Auke Bay Laboratories, Alaska Fisheries Science Center, National Marine Fisheries Service, NOAA

Contact: david.kimmel@noaa.gov

**Last updated: October 2022**

**Description of indicator:** In 2015, NOAA’s Alaska Fisheries Science Center (AFSC) implemented a method for an at-sea Rapid Zooplankton Assessment (RZA) to provide leading indicator information on zooplankton composition in Alaska’s Large Marine Ecosystems. The rapid assessment, which is a rough count of zooplankton (from paired 20/60 cm oblique bongo tows from 10m from bottom or 300m, whichever is shallower), provides preliminary estimates of zooplankton abundance and community structure. The method employed uses coarse categories and standard zooplankton sorting methods (Harris et al., 2000). The categories are small copepods (<2mm; example species: *Acartia* spp., *Pseudocalanus* spp., and *Oithona* spp.), large copepods (>2mm; example species: *Calanus* spp. and *Neocalanus* spp.), and euphausiids (<15mm; example species: *Thysanoessa* spp.). Small copepods were counted from the 153 $\mu$ m mesh, 20cm bongo net. Large copepods and euphausiids were counted from the 505 $\mu$ m mesh, 60cm bongo net. Other, rarer zooplankton taxa were present but were not sampled effectively with the on-board sampling method.

RZA abundance estimates may not closely match historical estimates of abundance as methods differ between laboratory processing and ship-board RZA, particularly for euphausiids which are difficult to quantify accurately (Hunt et al., 2016). Rather, RZA abundances should be considered estimates of relative abundance trends overall. Detailed information on these taxa is provided after in-lab processing protocols have been followed (1 year post survey). We adjusted the inclusion of euphausiid estimates to more closely match the RZA to net samples by comparing total adults and juveniles estimated from the RZA to total adults and juveniles from the counted samples. Previously we had reported the abundance of earlier life-history stages (furcilia, calyptopis), which had caused the two time-series to differ at times. We believe this adjustment makes the RZA a better estimator of adult and juvenile euphausiid abundance.

Here, we show RZA maps for three surveys: (1) the spring 70m isobath survey (May 2022), (2) the Bering Arctic Subarctic Integrated Survey (BASIS, Aug-Sep 2022), and (3) the northern Bering Sea survey (NBS, Sep 2022). We also show time-series of each RZA category for the southern middle shelf of the Bering Sea (Ortiz et al., 2012) in spring and summer as well as the north Bering Sea in summer. The total lipid content from RZA samples is also reported for all surveys. Total lipid is reported for designated zooplankton categories of large copepods and euphausiids (>15mm), which were collected separately in glass vials from each station, stored frozen, and analyzed at NOAA’s Auke Bay Laboratories. Briefly, the measured lipid content was compared to the respective wet-mass for the zooplankton in each vial. Lipid analysis was performed via a rapid colorimetric technique employing a modified version of the sulfo-phospho-vanillin (SPV) assay. This method was proven to be highly accurate for analyzing zooplankton lipids in a recent inter-laboratory cross validation study (Pinger et al., 2022).

### Status and trends:

#### *Southeastern Bering Sea*

In 2022, abundances of large and small copepods were low along the 70m isobath overall, with increased abundances near the M2 mooring. Euphausiids were also in low abundance, with many stations lacking euphausiids (Figure 47). Relative to prior years, large copepod abundances in 2022 were reduced in comparison to the last cold period which ended in 2012. Small copepod numbers remained elevated compared to abundances during the cold period from 2006-2012. Euphausiid estimates remained low as is common

during the spring (Figure 48). Lipid content for large copepods was low overall, with only one station having elevated lipid values. Euphausiid lipid content was low in the southeastern portion of the 70m isobath and increased in the northern portion of the 70m isobath (Figure 49). *Note*: lipid estimates for euphausiids are reported for stations with no euphausiid abundance reported. This is due to size differences, i.e. euphausiids >15mm were present and sampled for lipid content but no euphausiids <15mm were recorded.

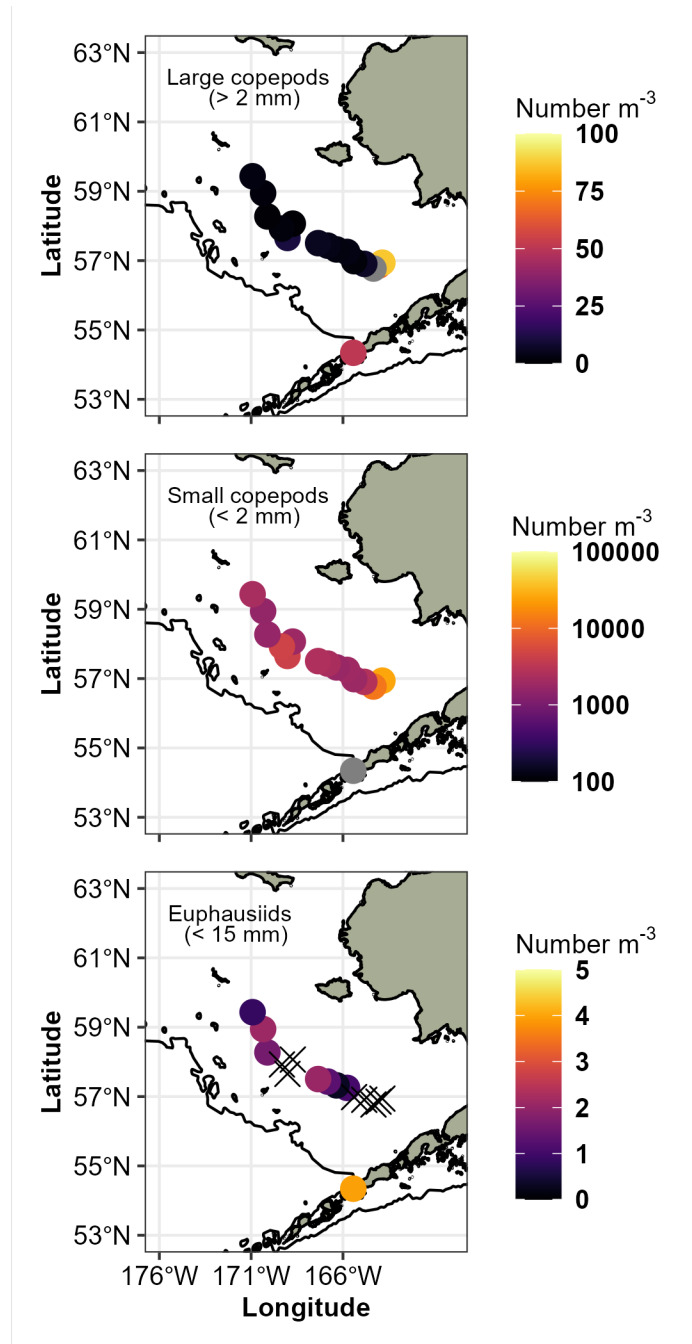


Figure 47: Maps show the abundance of large copepods (>2 mm), small copepods (<2 mm), and euphausiids (<15 mm) estimated by the RZA during the spring 2022 70m isobath survey. **Note** all maps have different abundance scales (Number  $m^3$ ). X indicates a sample with an abundance of zero individuals  $m^3$ .

Abundances of large copepods were low during the BASIS survey, particularly in the southern portion of the middle shelf. Small copepod abundances were also low in the southern portion, but were substantially higher in the northern section of the BASIS survey area. Euphausiids were moderately abundant throughout the survey area (Figure 50). Compared to historical abundances, large copepod numbers were very low overall and matched the abundances observed in the recent warm period. Small copepods numbers were reduced compared to prior year abundances, whereas euphausiid numbers were higher relative to recent RZA estimates from 2015–2020, with the exception of 2017 (Figure 51). Lipid provisioning in *Calanus* spp. was higher during this late-summer survey, averaging  $16.7 \pm 2.4\%$  (standard deviation [SD]) compared to  $4.8 \pm 3.5\%$  (SD) in spring. Euphausiid lipid content was similar on average  $5.1 \pm 2.2\%$  (SD) to that of spring,  $4.1 \pm 2.3\%$  (SD) (Figure 52).

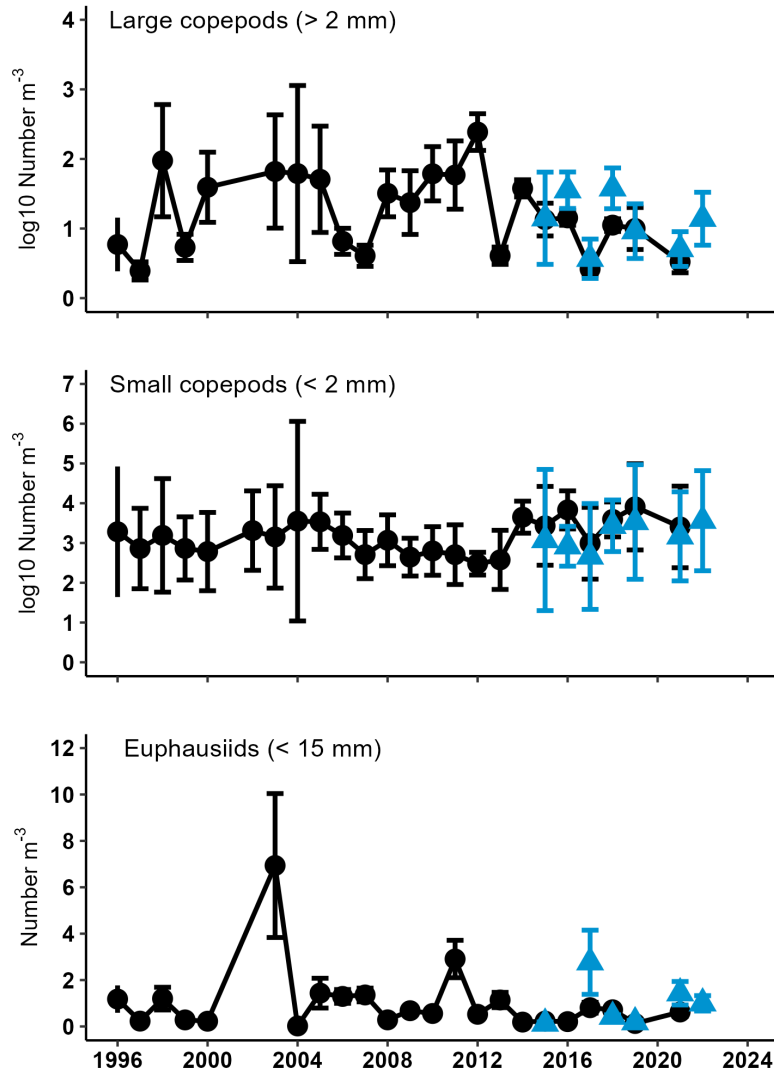


Figure 48: Mean abundance ( $\pm$  standard error of the mean) of large copepods (>2 mm), small copepods (<2 mm), and euphausiids (<15 mm) during the spring 2022 70m isobath survey. Black circles represent archived data, blue triangles represent RZA data. **Note** differences in scale for the different taxa.

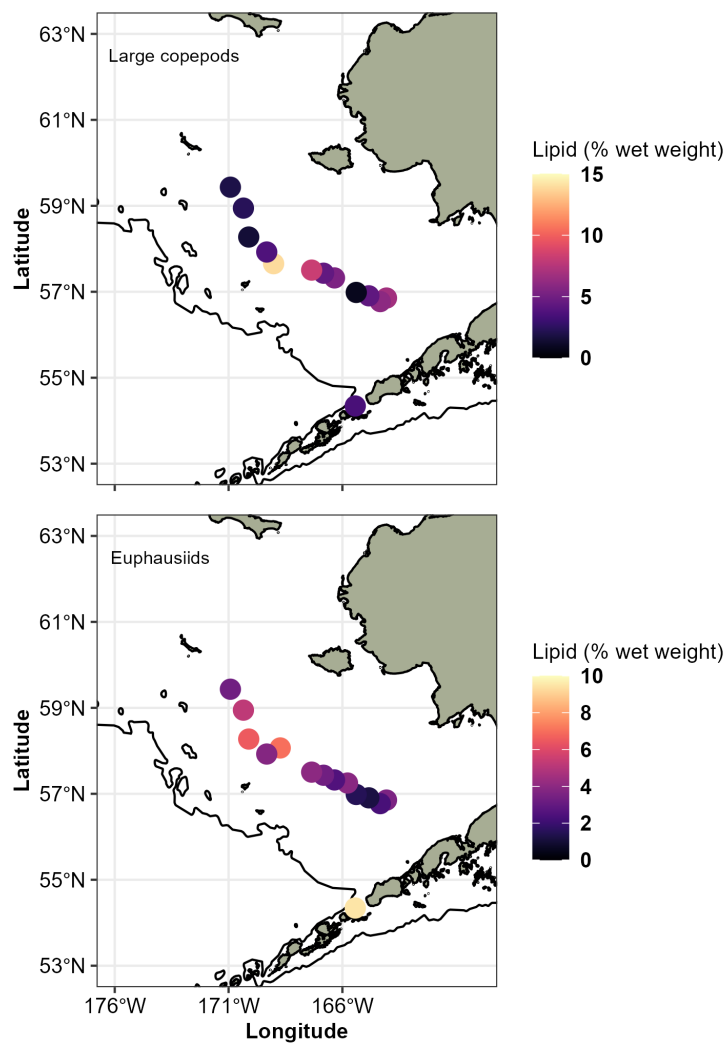


Figure 49: Maps show the lipid content (% wet mass) for large copepods (>2 mm; *Calanus* spp.) and euphausiids (>15 mm) during the spring 2022 70m isobath survey. **Note** maps have different scales.

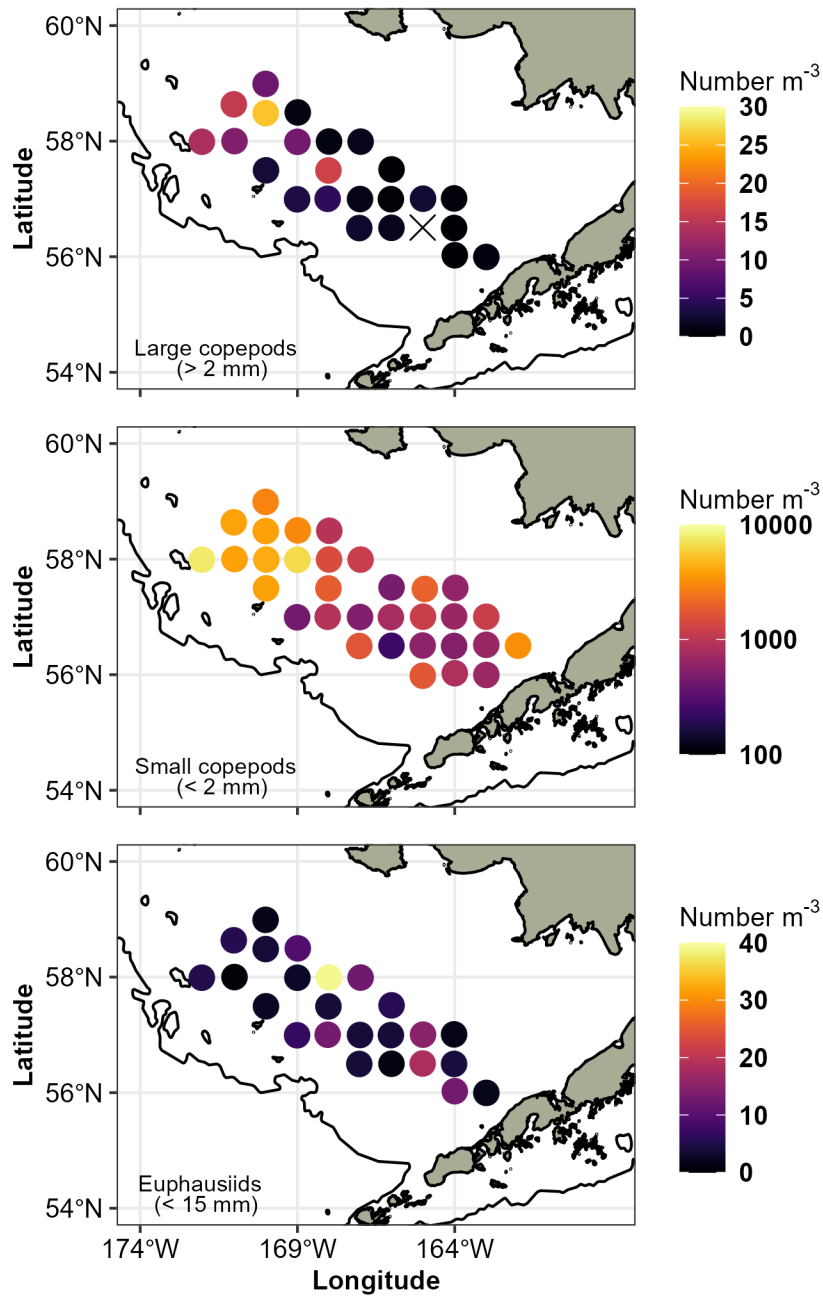


Figure 50: Maps show the abundance of large copepods (>2 mm), small copepods (<2 mm), and euphausiids (<15 mm) estimated by the RZA during the late-summer 2022 BASIS survey. **Note** all maps have different abundance scales ( $\text{Number m}^3$ ). X indicates a sample with an abundance of zero individuals  $\text{m}^3$ .

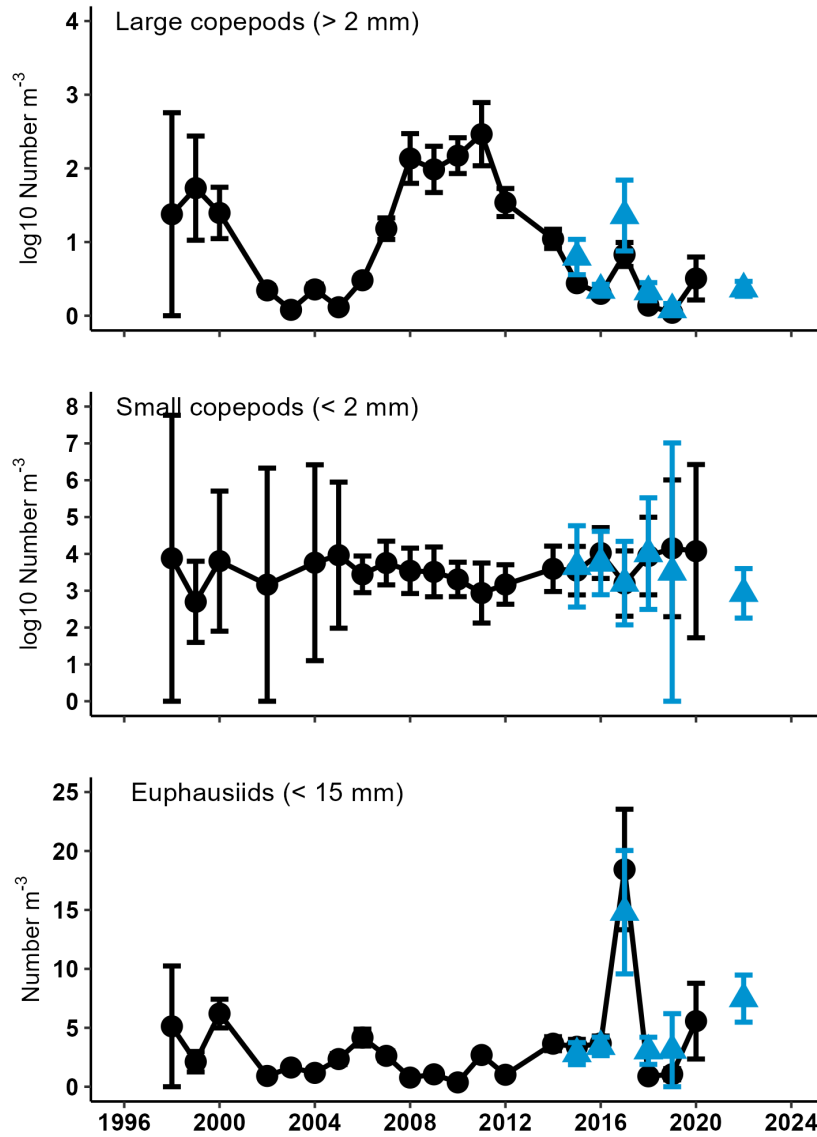


Figure 51: Mean abundance ( $\pm$  standard error of the mean) of large copepods (>2 mm), small copepods (<2 mm), and euphausiids (<15 mm) for the middle shelf in late-summer 2022. Black circles represent archived data, blue triangles represent RZA data. **Note** differences in scale for the different taxa.

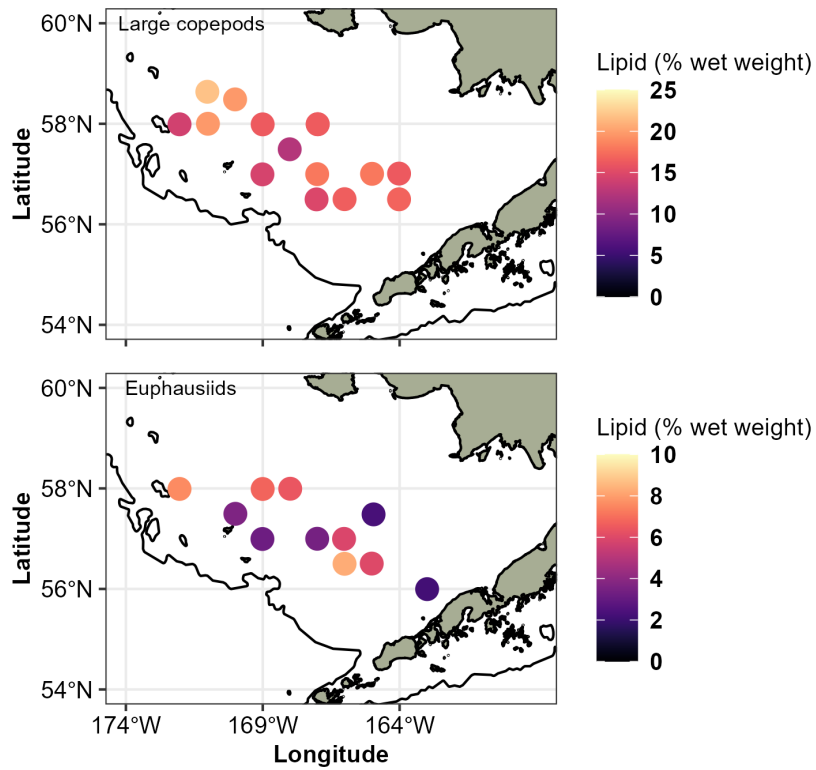


Figure 52: Maps show the lipid content (% wet mass) for large copepods (>2 mm; *Calanus* spp.) and euphausiids (>15 mm) for the late-summer 2022 BASIS survey. Note maps have different scales.

### *Northern Bering Sea*

Abundances of large copepods in the NBS were higher than those observed on the BASIS survey overall, with increased numbers on the western edge of the survey grid, particularly at the station south of St. Lawrence Island. Euphausiids followed a similar spatial pattern, with higher numbers in the more western stations. In contrast, the number of small copepods numbers was low overall (Figure 53). Abundances of large copepods were greater than those observed in 2018 and 2019, but below those of earlier years. Small copepods declined by nearly an order of magnitude on average compared to prior years. Euphausiid estimated abundances were higher compared to prior years and have increased every year since 2018 (Figure 54). Lipid values were spatially variable for copepods, with much higher lipid values recorded in the NE portion of the NBS survey region (Figure 55). On average, the lipid content was similar to that of the BASIS survey, for both copepods ( $15.3 \pm 6.2\%$  (SD) lipid by wet mass) and euphausiids ( $6.7 \pm 3.3\%$  (SD) lipid by wet mass).

**Factors influencing observed trends:** We had three snapshots of the zooplankton community in the Bering Sea during 2022. The larger extent of sea ice observed in 2022 rapidly retreated in April, leaving behind cooler water that appeared to limit the development of the zooplankton community in spring with larger abundances only beginning to appear at the M2 mooring location (Figure 47). That being said, copepod abundances resembled those of recent warm years (Figure 48). Lipid content during the spring was low, as is expected, as large copepods such as *Calanus* spp. were represented by earlier life-history stages and euphausiids were preparing for spring reproduction, meaning energy was not being stored as lipid (Figure 49). In prior years, the lipid content of *Calanus* spp. in spring has averaged around 4% by wet mass.

The BASIS survey revealed low large zooplankton abundance throughout the survey area (Figure 50) and these low abundances matched recent estimates of large copepod abundances during warm periods (Figure 51). This was not expected as there was a cold pool present in 2022, which correlated with increased *Calanus* spp. abundances in the past (Eisner et al., 2018). Two possibilities for this observation are: (1) abundances of large copepods were higher along the middle shelf further north and not sampled by the BASIS or NBS surveys; and/or (2) despite increased ice cover in 2022 and lower temperatures in spring, the region warmed over the summer accelerating large copepod growth and causing earlier entry into diapause. Also, a lag of at least one year has been observed between warm year abundances and the return of abundances typically associated with the cold pool (Eisner et al., 2018). Interestingly, warmer temperatures typically result in increased small copepod abundances; however, small copepod populations were low near the southern portion of the BASIS survey (Figure 50), and lower on average compared to recent estimates (Figure 51). This suggests reduced overall zooplankton productivity in the Bering Sea during summer of 2022. Euphausiid abundances were higher than recent estimates and this observation supports the hypothesis that increased euphausiid abundances during warm years may compensate for lower large copepod abundances (Duffy-Anderson et al., 2017). Despite the low abundance of large copepods, those that were sampled appeared to be accumulating lipids. Lipid content for copepods increased compared to spring, with nearly a four-fold increase in percent lipid, on average (Figure 52). Lipid content was consistent over the survey grid. Euphausiid lipids were more variable spatially (Figure 52), but were similar to spring estimates, on average.

Similar trends were observed in the NBS survey, with reduced large and small copepod abundances (Figure 53). Again, this suggests lower overall productivity, at least for the inner shelf sampled by the NBS survey. As with the BASIS survey, euphausiid numbers were slightly higher compared to recent estimates (Figure 54). This suggests that euphausiids increase in number when larger copepods are not present. Lipid content of copepods showed a strong spatial pattern with the more southern stations having reduced lipid content relative to the northern stations (Figure 55). Average lipid content for copepods was similar to that observed in the BASIS survey; however, the copepods in the northern portion had very high lipid storage and this suggests that these copepods were nearing diapause. Euphausiid lipid content was similar to those observed in the 70m isobath and BASIS surveys and did not display the spatial variability of the copepods (Figure 55).

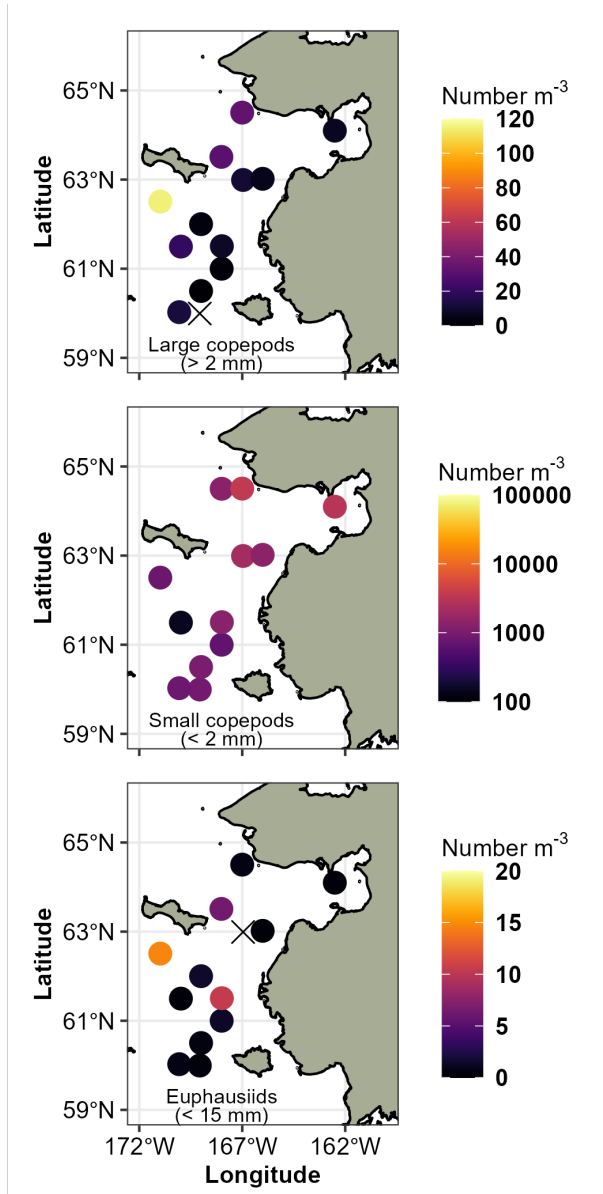


Figure 53: Maps show the abundance of large copepods (>2 mm), small copepods (<2 mm), and euphausiids (<15 mm) estimated by the RZA during the late-summer 2022 NBS survey. **Note** all maps have different abundance scales (Number m<sup>3</sup>). X indicates a sample with an abundance of zero individuals m<sup>3</sup>.

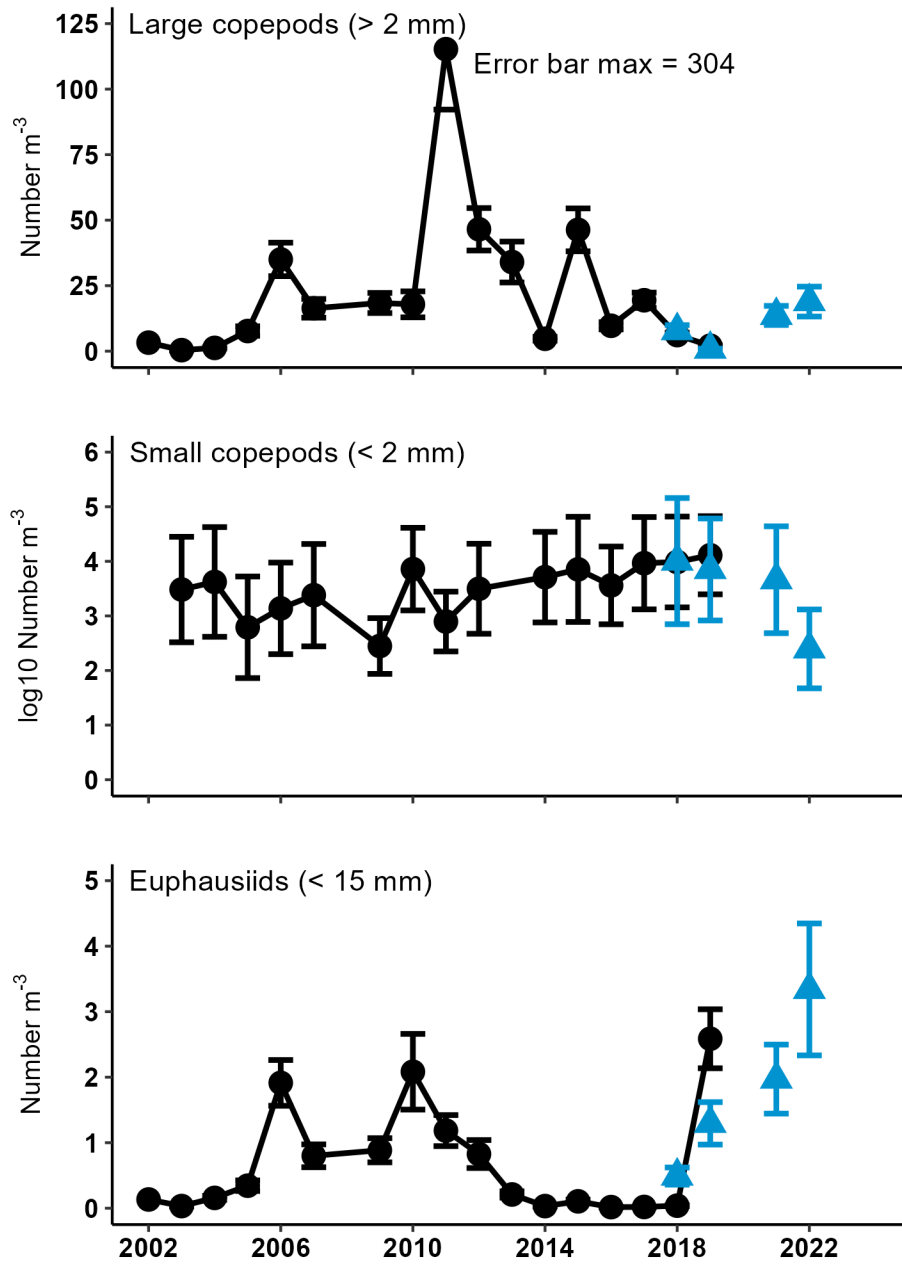


Figure 54: Mean abundance ( $\pm$  standard error of the mean) of large copepods (>2 mm), small copepods (<2 mm), and euphausiids (<15 mm) during the late-summer 2022 NBS survey. Black circles represent archived data, blue triangles represent RZA data. **Note** differences in scale for the different taxa.

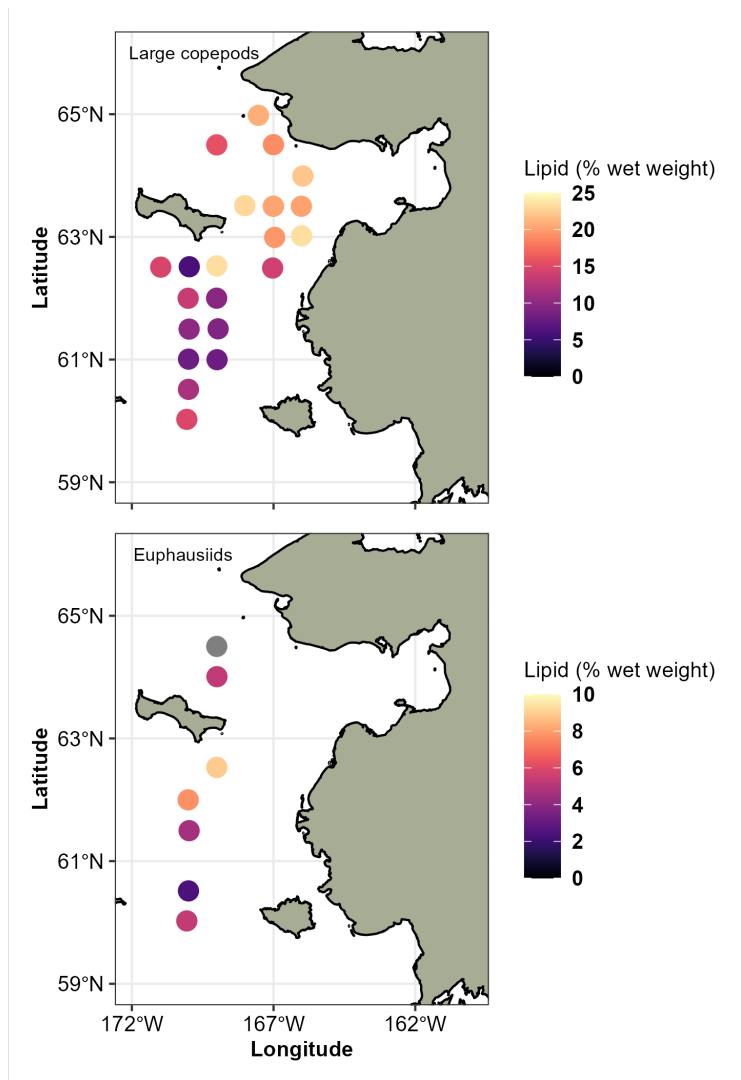


Figure 55: Maps show the lipid content (% wet mass) for large copepods (>2 mm; *Calanus* spp.) and euphausiids (>15 mm) in the NBS in late-summer 2022. **Note** maps have different scales and this grid differs from that of Figure 53 as lipid sampling did not necessarily occur at RZA stations and *vice versa*.

**Implications:** Smaller copepods and their early life history stages (nauplii) form the prey base for larval to early juvenile Walleye pollock, as well as other fish species, during spring on the eastern Bering Sea middle shelf. While small copepods were reduced in the southern portion of 70m isobath, numbers did increase farther north resulting in average abundances that were high. This suggests that adequate food for larval fish was present during spring 2022, but that there was spatially variability in zooplankton availability.

On the middle shelf, *Calanus* spp. were in very low numbers in summer. The main center of biomass for *Calanus* spp. may have been located farther north ( $>60^{\circ}\text{N}$ ) and therefore not captured in the surveys. The lack of large copepods in the NBS survey is less surprising as this survey is restricted to primarily the inner shelf where *Calanus* spp. are not typically located. In both locations, lipid content of the *Calanus* spp. sampled was high, averaging near 16% by wet mass. We have been able to estimate the % lipid by dry mass and these copepods were near 50% lipid by dry mass, which is similar to values measured in European waters (Mayzaud et al., 2016). This suggests that the copepods sampled were nearing diapause, particularly those in the northern portion of the NBS survey (Figure 55). Many of these copepods were in excess of 60% lipid by dry mass. Low abundances of large copepods are less critical to the survival of age-0 pollock in the spring, but very important later in the year (Hunt et al., 2011). The low abundance of large, lipid rich *Calanus* spp. observed during the BASIS survey may indicate a poor recruitment class of pollock as the abundance of *Calanus* spp. has been linked to pollock abundances at age-3 (Eisner et al., 2020). However, a drop in overall productivity may also be occurring as the small copepod abundances were lower on the middle shelf and inner shelf. This suggests that less trophic transfer from primary producers occurred which would have resulted in larger zooplankton standing stocks or that consumption of zooplankton had increased during summer of 2022.

Euphausiid numbers were slightly higher in the BASIS and NBS surveys relative to prior years; however, exact estimates of euphausiid abundances remain semi-quantitative. Euphausiid estimates should be treated with caution as the bongo nets are effectively avoided by euphausiids. Furthermore, it should be noted that the RZA and processed estimates of abundances do differ and this is expected due to the patchy nature of euphausiid distribution and the difficulty in accurately estimating euphausiid abundances (Hunt et al., 2016). Lipid values for euphausiids were consistent across all three surveys, though those captured in the NBS had the highest lipid content. Dry mass estimates place the euphausiid values at  $19.1 \pm 8.1\%$  (SD),  $22.2 \pm 9.1\%$  (SD), and  $25.8 \pm 10.2\%$  (SD), for spring 70m isobath, BASIS, and NBS surveys, respectively. These values also highlight the difference in total lipids between *Calanus* spp. and euphausiids, with *Calanus* spp. providing nearly double the lipid content per unit mass. In prior years with low large copepod numbers, the proportion of euphausiids increased in age-0 pollock diets; however, this correlated with lower overall condition of age-0 pollock (Heintz et al., 2013).

In summary, recent trends in the zooplankton community for the Bering Sea match those observed during warm conditions, with the notable exception of reduced small copepod numbers observed during the summer of 2022. This suggests that larval fish in the early portion of the year experienced adequate forage; however, the lack of large copepods later in the year may impact age-0 pollock recruitment if there is not sufficient overlap with these large copepod prey (Siddon et al., 2013).

## Eastern Bering Sea Euphausiids ('Krill')

Contributed by Patrick Ressler

Midwater Assessment and Conservation Engineering Program (MACE), Resource Assessment and Conservation Engineering Division, Alaska Fisheries Science Center (AFSC), National Marine Fisheries Service, NOAA

Contact: patrick.ressler@noaa.gov

**Last updated: September 2022**

**Description of indicator:** Ressler et al. (2012) developed a survey of the abundance and biomass of euphausiids on the middle and outer shelf of the eastern Bering Sea using acoustic and Methot trawl data from 2004–2010 surveys of midwater Walleye pollock (*Gadus chalcogrammus*, e.g., Honkalehto et al. (2018)). The method has been used to estimate an index of euphausiid abundance on a biennial schedule since that time. Acoustic backscatter at 120 kHz classified as euphausiids was used to compute the mean numerical density (no. m<sup>3</sup>) of euphausiids in 0.5 nmi intervals along acoustic-trawl survey transects (Figure 56); these values were then averaged across the surveyed area to produce annual averages (Figure 57). Because few trawl samples were available in the early years of the times series, the parameter used to convert euphausiid backscatter to numerical density (target strength; Smith et al. (2013)) was modeled using the average of length and species composition from samples collected over the time series. There is large uncertainty about the abundance of euphausiids in the eastern Bering Sea, with acoustic estimates being much higher than those from net capture in an absolute sense (Hunt et al., 2016), but the relative trends in the index presented here are probably robust. Error bars on annual values indicate 95% confidence intervals computed from geostatistical estimates of relative estimation error due to sampling variability (Petitgas, 1993).

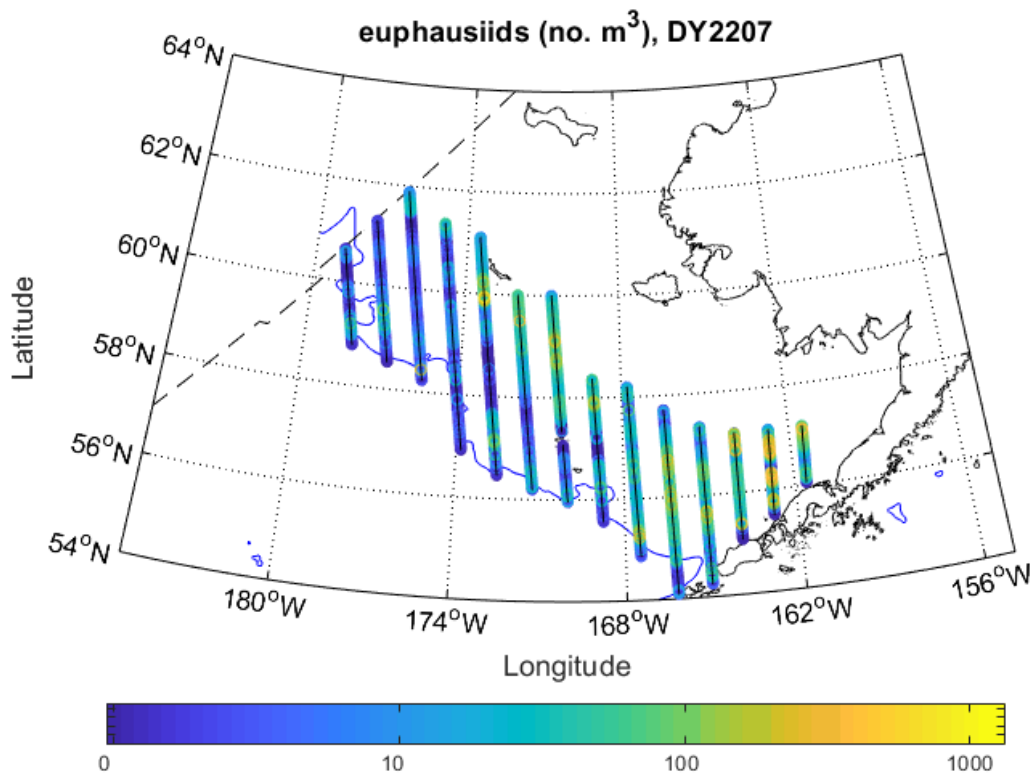


Figure 56: Water column averages of estimated euphausiid density (no. m<sup>3</sup>) in the 2022 NOAA-AFSC eastern Bering Sea summer acoustic-trawl survey.

Since the previous update to this index, euphausiid backscatter observations from the 2022 acoustic-trawl survey of pollock were added to the time series. At this time no euphausiid estimate is available from summer 2020 because the survey was canceled by the COVID-19 pandemic. Net catches collected from 2004–2016 were used to estimate the average length and species composition of euphausiids (length and species composition from trawl samples collected in 2018 and 2022 are not yet available); they indicated euphausiid layers in 2004–2016 were dominated numerically by euphausiids (mean 87%) of average length between 18 and 20 mm, and that euphausiid species *Thysanoessa inermis* dominated the species composition on the outer shelf, and *T. raschii* dominated inshore. These observations of length and species composition are consistent with what is known from the literature (Smith, 1991; Coyle and Pinchuk, 2002). There is some indication that euphausiids were smaller in 2004–2009 and in 2016 (by 1-2 mm), and that there was an increase in relative abundance of *T. spinifera* in 2016 compared to other years in the time series. Overall though, no radical changes in length or species composition of euphausiid scattering layers have been indicated in our samples. De Robertis et al. (2010) advocated the use of a mean normal deviate (z-score) of the frequency response to judge the quality of the multifrequency backscatter classification process used here, where a value of 1 indicates that the observed frequency response is within 1 standard deviation of the known response for a given class of acoustic targets. For euphausiids, this value has averaged 0.86 (range 0.75–1.15) in the 2004–2022 time series given here; the 2022 value was 0.80, indicating consistent performance of the method.

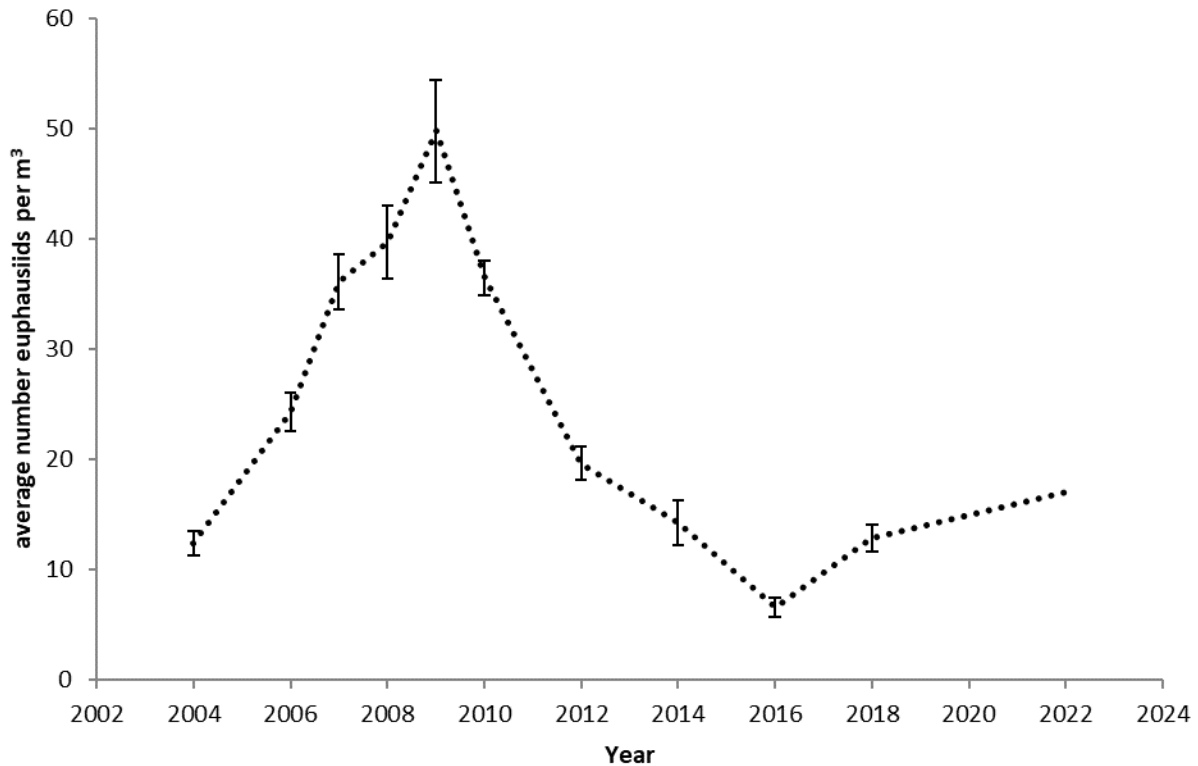


Figure 57: Acoustic estimate of average euphausiid abundance (no. m<sup>3</sup>) from NOAA-AFSC EBS summer acoustic-trawl surveys. Error bars are approximate 95% confidence intervals computed from geostatistical estimates of sampling error (Petitgas, 1993). The 2022 estimate is preliminary; error bars have not yet been calculated.

**Status and trends:** Summertime euphausiid density increased on the eastern Bering from 2004–2009, then subsequently declined 2010 through 2016, when the lowest value in the time series was reported. Euphausiid density increased slightly in summers 2018 and 2022 from 2016, but remains below the average of the time series.

**Factors influencing observed trends:** Factors controlling annual changes in euphausiid abundance in the north Pacific are not well understood; possible candidates include bottom-up forcing by temperature and food supply, and top-down control through predation (Hunt et al., 2016). When factors including temperature, pollock abundance, primary production, and spatial location have been considered in spatially-explicit multiple regression models, temperature has been the best predictor, with increases in euphausiid abundance associated with cold temperatures in the eastern Bering Sea (Ressler et al., 2014), but not in the Gulf of Alaska (Simonsen et al., 2016). The summers of 2014–2019 were warmer than average on the Bering Sea shelf (see p. 31) and in the acoustic-trawl survey area (McCarthy et al., 2020), but 2022 was more moderate and a substantial cold pool was observed (Stienessen et al. in prep.). The biomass of eastern Bering Sea pollock (an abundant predator of euphausiids) has been near or above the historical mean over the past decade (Ianelli et al., 2021), though euphausiid abundance has not been strongly correlated with pollock biomass in multiple regression models of euphausiid biomass in either the eastern Bering Sea or the Gulf of Alaska (Ressler et al., 2014; Simonsen et al., 2016).

**Implications:** Euphausiids are food for many species of both ecological and commercial importance in the eastern Bering Sea, including pollock (Aydin and Mueter, 2007). The data presented here suggest that euphausiid availability as prey is below average in 2022, but it remains greater than at the lowest points in the time series.

## Jellyfish

### Trends in the Biomass of Jellyfish in the Southeastern and Northeastern Bering Sea During the Late-Summer Surface Trawl Survey, 2003–2022

Contributed by Ellen Yasumiishi, Alex Andrews, Jim Murphy, Andrew Dimond, Ed Farley, and Elizabeth Siddon

Ecosystem Monitoring and Assessment Program, Auke Bay Laboratories, Alaska Fisheries Science Center  
Contact: ellen.yasumiishi@noaa.gov

**Last updated: October 2022**

**Description of indicator:** Annual indices of juvenile groundfish, forage fish, salmon, and jellyfish biomass (kg) and abundance (numbers) of juvenile sockeye salmon (*Oncorhynchus nerka*) in surface waters are produced from the Alaska Fisheries Science Centers' (AFSC) Bering Arctic Subarctic Integrated Survey (BASIS). BASIS is an integrated fisheries oceanography survey in the southeastern and northeastern Bering Sea during late summer, 2003–2022. Primary fish caught include age-0 pollock (*G. chalcogrammus*), age-0 Pacific cod (*Gadus macrocephalus*), capelin (*Mallotus villosus*), herring (*Clupea pallasii*), juvenile Chinook salmon (*O. tshawytscha*), juvenile sockeye, juvenile chum salmon (*O. keta*), juvenile pink salmon (*O. gorbuscha*), and juvenile coho salmon (*O. kisutch*). Primary jellyfish taxa include *Chrysaora melanaster*, *Aequorea* spp., *Aurelia labiata*, *Phacellophora camtschatica*, and *Staurophora mertensii*. Unidentified or non-dominant jellyfish species were included in the total jellyfish catch.

Pelagic fish and jellyfish were sampled using a trawl net towed in the upper 25m of the water column (for detailed trawl methods, see Farley and Moss (2009)). For the estimates of species abundance, the BASIS survey (373,404 km<sup>2</sup>) was within the region south to north from 54.54°N to 59.50°N and west to east from -173.08°W to -159.00°W for years 2002–2012, 2014, 2016, 2018, and 2022. The northern Bering Sea survey (197,868 km<sup>2</sup>) was within the region south to north from 59.97°N to 65.50°N and west to east from -172.00°W to -161.50°W for years 2003–2007, 2009–2019, 2021–2022. A trawl was towed for approximately 30 minutes. Area swept was estimated from horizontal net opening and distance towed.

Annual indices of relative biomass (kg) and numbers (abundance) were estimated using a single-species spatio-temporal model with the VAST package version 3.10.0, INLA version 22.04.16, TMB version 1.9.1, FishStatsUtils version 2.12.0, R software version 4.11.3, and RStudio version 2022.02.3 (Team, 2020; Thorson et al., 2015; Thorson and Kristensen, 2016; Thorson, 2019a). We used the VAST package to reduce bias in biomass estimates due to spatially unbalanced sampling across years, while propagating uncertainty resulting from predicting density in unsampled areas. Spatial and spatio-temporal variation for both encounter probability and positive catch rate components were specified at a spatial resolution of 500 knots. We used a Poisson-link, or conventional, delta model and a gamma distribution to model positive catch rates (Thorson et al., 2019). Parameter estimates were within the upper and lower bounds and final gradients were less than 0.0005. Julian day was added as a normalized covariate with a spatially constant and linear response due to changes in the timing of the survey among years.

**Status and trends:** During 2022, the estimated biomass of jellyfish in pelagic waters was low in both the northeastern and southeastern Bering Sea during late summer (Figure 58). Trends in jellyfish biomass were similar in the north and south, except during 2012–2018. Higher levels of jellyfish biomass occurred in the south during 2012, 2014, 2016, and 2018.

**Factors influencing observed trends:** Jellyfish feed primarily on small fish and zooplankton, and jellyfish production tracks forage fish production (see Yasumiishi et al., p. 97). Lower forage fish biomass, such as age-0 pollock, during 2022 may have contributed to lower jellyfish production. In addition, the higher levels of jellyfish biomass in the south from 2012–2018 corresponded with a relatively warm period and higher biomass of age-0 pollock (see Andrews et al., p. 97) and forage fish.

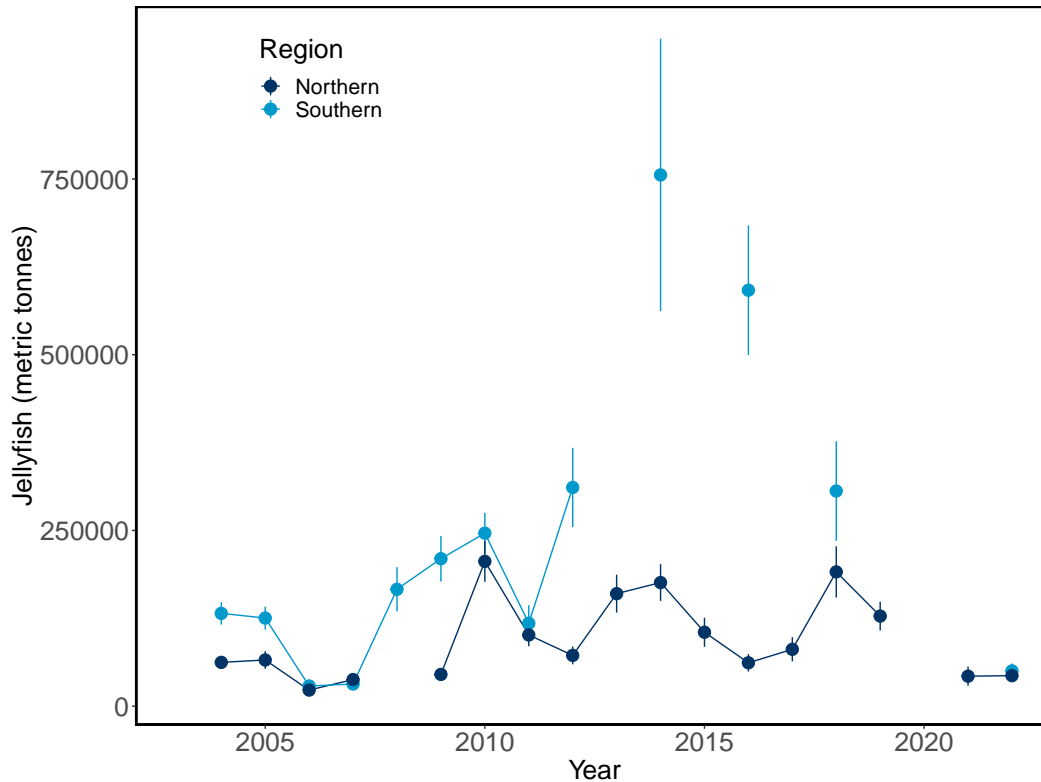


Figure 58: Estimated biomass (kg) of jellyfish in surface waters surveyed in the eastern Bering Sea during late summer, 2003–2022.

**Implications:** Jellyfish are competitors, predators, and act as shelter for forage fishes. During 2022, the lower abundance of jellyfish may indicate poor environmental conditions for the growth and survival of jellyfish and other species in the eastern Bering Sea during late summer. Lower jellyfish biomass may also favor other species by reduced competition for food and predation pressure.

## Jellyfishes - Eastern Bering Sea Shelf

Contributed by Thaddaeus Buser

Resource Assessment and Conservation Engineering Division, Alaska Fisheries Science Center

National Marine Fisheries Service, NOAA

Contact: thaddaeus.buser@noaa.gov

**Last updated: September 2022**

**Description of indicator:** The time series for jellyfishes (Scyphozoa, but primarily *Chrysaora melanaster*) relative CPUE by weight (kg per hectare) was updated for 2022 (Figure 59). Relative CPUE was calculated by setting the largest biomass in the time series to a value of 1 and scaling other annual values proportionally. The standard error ( $\pm 1$ ) was weighted proportionally to the CPUE to produce a relative standard error.

**Status and trends:** The relative CPUE for jellyfishes in 2022 increased  $\sim 75\%$  from the 2021 survey estimate, similar to the catch rates observed 1992–1999 and in 2018. There is an apparent pattern of cyclical rise and fall of CPUE values across the time series. The relatively low biomass estimated throughout the 1980's was followed by a period of increasing biomass of jellyfishes throughout the 1990's (Brodeur et al., 1999). A second period of relatively low CPUE estimates from 2001 to 2008 was then followed by a second

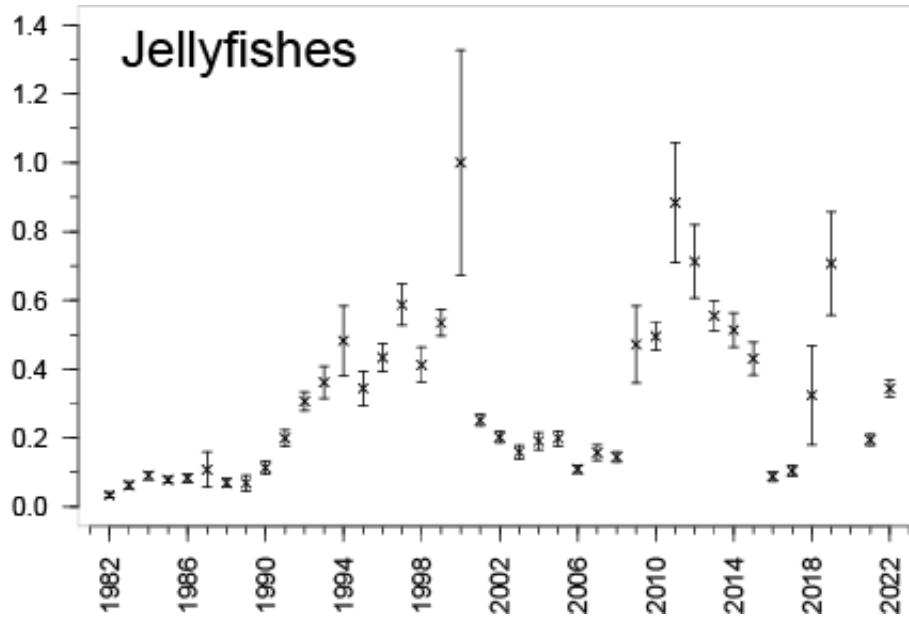


Figure 59: AFSC eastern Bering Sea shelf bottom trawl survey relative CPUE for jellyfish during the May to August time period from 1982-2022.

period with relatively higher CPUE values from 2009 to 2015. Jellyfish CPUE estimates in the EBS have been relatively inconsistent over the past five survey years.

**Factors influencing observed trends:** The fluctuations in jellyfish biomass and their impacts on forage fish, juvenile Walleye pollock (*Gadus chalcogrammus*), and salmon in relation to other biophysical indices were investigated by Cieciel et al. (2009) and Brodeur et al. (2002, 2008). Ice cover, sea surface temperatures in the spring and summer, and wind mixing all influence jellyfish biomass, and affect jellyfish sensitivity to prey availability (Brodeur et al., 2008).

**Implications:** Jellyfish are pelagic consumers of zooplankton, larval and juvenile fishes, and small forage fishes. A large influx of pelagic consumers such as jellyfish can decrease zooplankton and small fish abundance, which in turn can affect higher trophic levels causing changes to the community structure of the ecosystem.

## Ichthyoplankton

There are no updates to Ichthyoplankton indicators in this year's report. See the contribution archive for previous indicators at: <http://access.afsc.noaa.gov/reem/ecoweb/index.cfm>.

## Forage Fish

### Trends in the Biomass of Forage Fish Species in the Southeastern and Northeastern Bering Sea During the Late-Summer Surface Trawl Survey, 2003–2022

Contributed by Ellen Yasumiishi, Alex Andrews, Andrew Dimond, and Jim Murphy  
Ecosystem Monitoring and Assessment Program, Auke Bay Laboratories, Alaska Fisheries Science Center  
Contact: [ellen.yasumiishi@noaa.gov](mailto:ellen.yasumiishi@noaa.gov)

**Last updated: October 2022**

**Description of indicator:** See 'Description of indicator' on p. 94. This forage fish contribution includes a combined index of age-0 pollock, age-0 Pacific cod, capelin, herring, and juvenile chum, Chinook, coho, pink, and sockeye salmon biomass.

**Status and trends:** During 2022, the biomass of forage fishes in pelagic waters was low in both the southeastern and northeastern Bering Sea during late summer. Temporal trends in forage fish biomass indicated higher productivity during the recent warm years 2014–2018 and lower during the cold year (2007–2013), especially for the southern forage fish. In the southern region, the trends in biomass were dominated by age-0 pollock (2004, 2005) and juvenile sockeye salmon (2014–2018) and in the northern region by herring (2014–2019) (Figure 60).

**Factors influencing observed trends:** Low forage fish biomass corresponded with cooling conditions during 2022. During cool years, age-0 pollock typically distribute deeper in the water column (i.e., below the surface trawl net), which may be driving the 2022 trend of lower forage fish biomass (Spear and Andrews III, 2021). Species composition in the north generally changes from herring during warm years to capelin during cool years, and in the south from higher to lower abundances of juvenile sockeye salmon and age-0 pollock (Yasumiishi et al., 2020).

**Implications:** Forage fishes are small pelagic fish eaten by larger predators. Lower biomass of forage fish may impact food availability for piscivores such as other fish, jellyfish, seabirds, and mammals during 2022.

### Trends in the Biomass of Age-0 Walleye Pollock in the Southeastern and Northeastern Bering Sea During the Late-Summer Surface Trawl Survey, 2003–2022

Contributed by Alex Andrews<sup>1</sup>, Ellen Yasumiishi<sup>1</sup>, Adam Spear<sup>2</sup>, Jim Murphy<sup>1</sup>, Elizabeth Siddon<sup>1</sup>, and Andrew Dimond<sup>1</sup>

<sup>1</sup>Ecosystem Monitoring and Assessment Program, Auke Bay Laboratories, Alaska Fisheries Science Center

<sup>2</sup>Recruitment Processes Program, Resource Assessment and Conservation Engineering Division, Alaska Fisheries Science Center

Contact: [alex.andrews@noaa.gov](mailto:alex.andrews@noaa.gov)

**Last updated: October 2022**

**Description of indicator:** See 'Description of indicator' on p. 94.

**Status and trends:** The 2022 age-0 Walleye pollock relative biomass estimates in the southeastern and northeastern regions of the Bering Sea were below estimates from the recent warm period (2014–2018), and

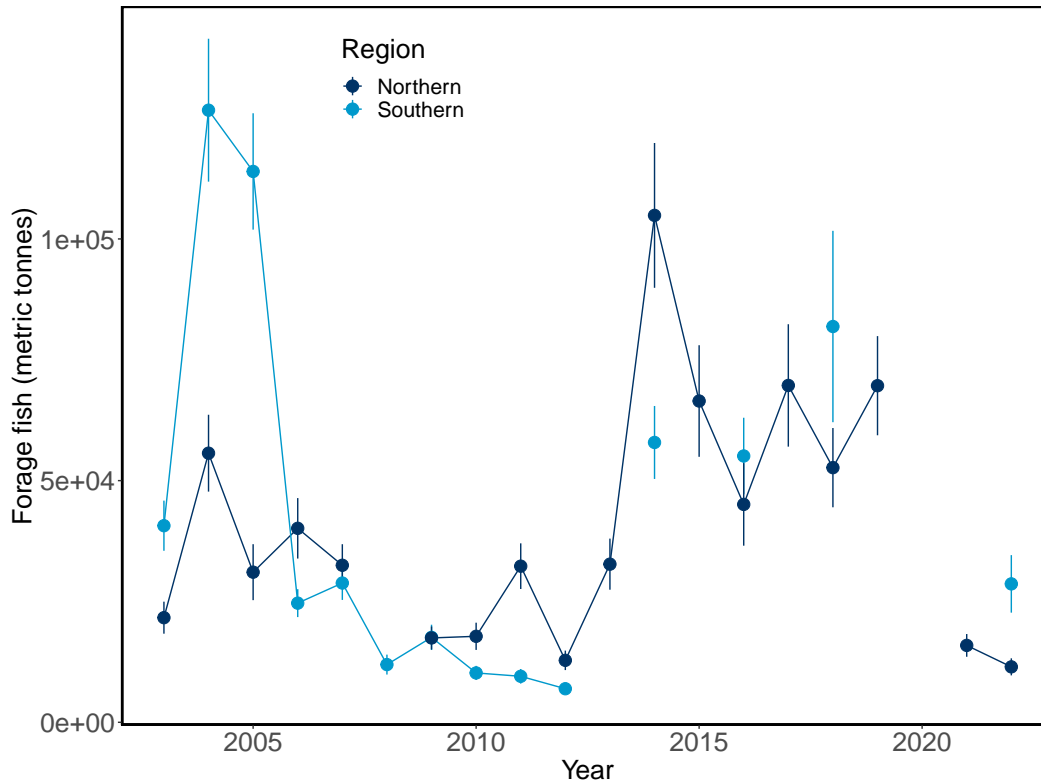


Figure 60: Estimated biomass (kg) of forage fish in surface waters surveyed in the eastern Bering Sea during late summer, 2003–2022.

were slightly greater than the cold period from 2007–2013 (Figure 61). Earlier in the time series, in the southeastern Bering Sea, higher estimates appeared to be related to warm periods with reduced cold pool extents. In the northeastern Bering Sea, biomass increased in 2014, 2015, and 2018 (three warm years), but has otherwise remained low compared to the southeast.

**Factors influencing observed trends:** Changes in climate-mediated oceanographic conditions, such as water column temperatures, may influence the vertical distribution of age-0 pollock and therefore the resulting surface trawl catches. Results from water-column trawls demonstrated that age-0 pollock densities were higher in representative warm years (2014, 2016) than in cold years (2011, 2012), and that age-0 pollock were found closer to the surface in warm years (Spear and Andrews III, 2021). However, warm periods with increased age-0 pollock biomass do not always correlate with strong recruitment, which is likely a result of the lack of high quality prey during warm years (Heintz et al., 2013).

**Implications:** A significant increase in biomass of age-0 pollock in the northeast relative to the southeast region could indicate a northward movement of adult spawning aggregations or improved juvenile habitat. Monitoring changes in biomass estimates along with vertical distribution may provide a better understanding of overall biomass and spatial distribution of age-0 pollock in the EBS. In addition, age-0 pollock are a major source of prey for upper trophic level guilds including fish, birds, and mammals.

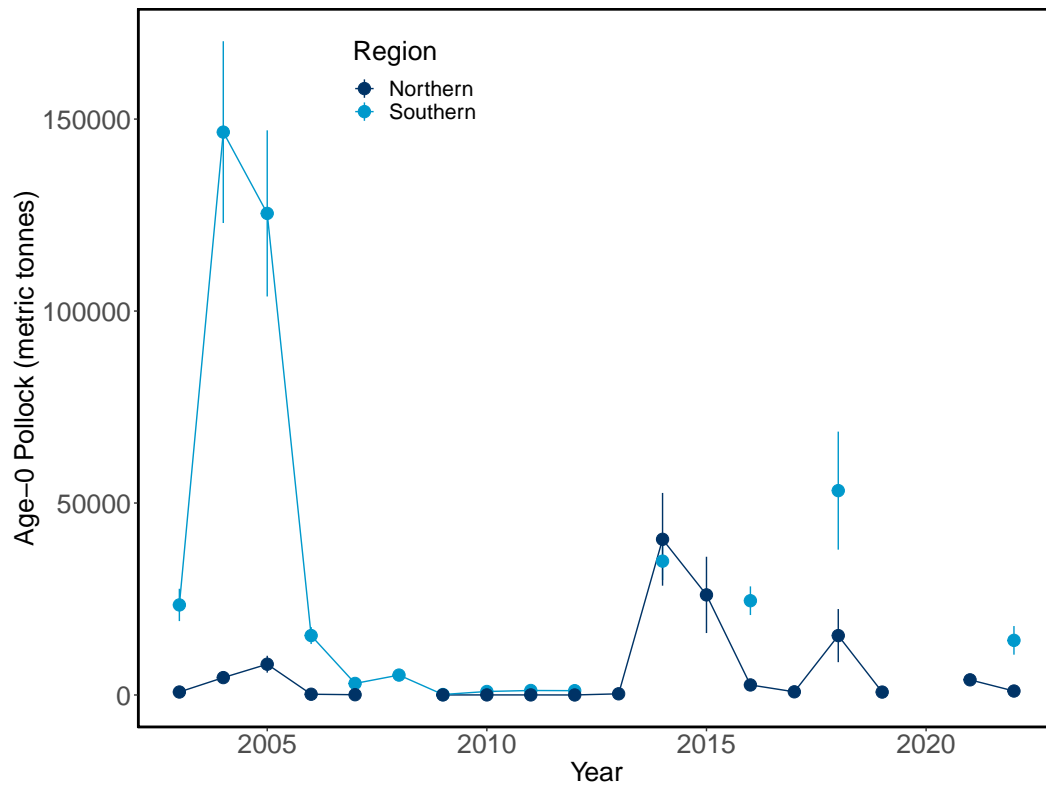


Figure 61: Estimated biomass (kg) of age-0 Walleye pollock in surface waters surveyed in the eastern Bering Sea during late summer, 2003–2022.

## Herring

### Trends in the Biomass of Pacific Herring and Capelin in the Southeastern and Northeastern Bering Sea During the Late-Summer Surface Trawl Survey, 2003–2022

Contributed by Alex Andrews<sup>1</sup>, Ellen Yasumiishi<sup>1</sup>, Jim Murphy<sup>1</sup>, Elizabeth Siddon<sup>1</sup>, Andrew Dimond<sup>1</sup>, and Rob Suryan<sup>2</sup>

<sup>1</sup>Ecosystem Monitoring and Assessment Program, Auke Bay Laboratories, Alaska Fisheries Science Center

<sup>2</sup>Recruitment Energetics and Coastal Assessment Program, Auke Bay Laboratories, Alaska Fisheries Science Center

Contact: alex.andrews@noaa.gov

Last updated: October 2022

**Description of indicator:** See 'Description of indicator' on p. 94.

**Status and trends:** During the BASIS survey, juvenile and adult Pacific herring (i.e., age-0 and age-1+) as well as capelin are predominantly caught in the northeastern region of the survey area (Andrews III et al., 2016). Herring relative biomass estimates remain at lower levels in the southeast while estimates slightly increased in the northeast (Figure 62). That said, relative biomass estimates of herring in 2022 remain lower than previous estimates in the time series. Relative biomass estimates of capelin in 2022 are lower than previous estimates in the time series, though biomass increased in the northeast in 2022 relative to 2021.

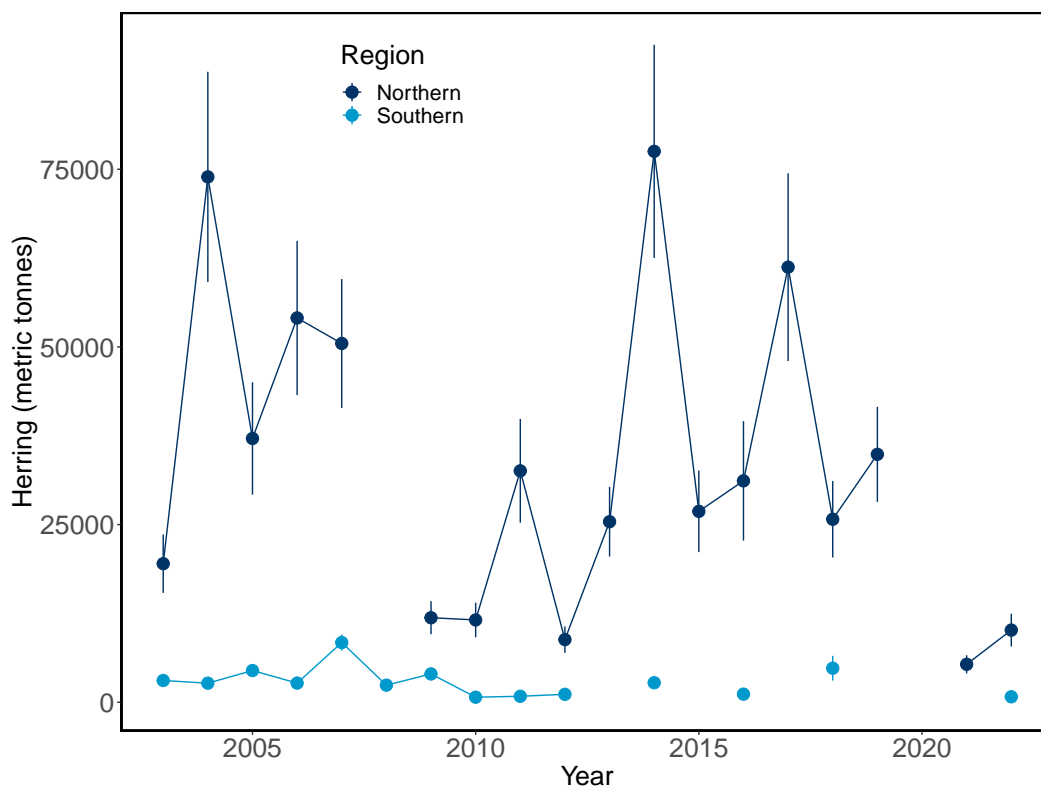


Figure 62: Estimated biomass (kg) of Pacific herring in surface waters surveyed in the eastern Bering Sea during late summer, 2003–2022.

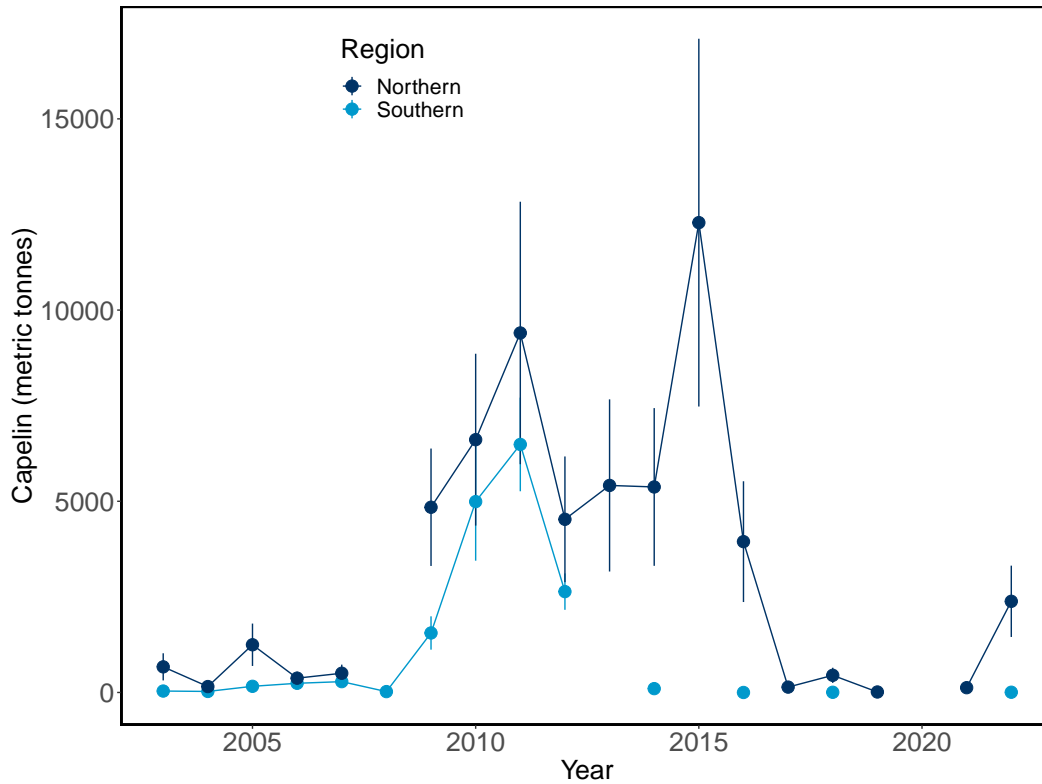


Figure 63: Estimated biomass (kg) of capelin in surface waters surveyed in the eastern Bering Sea during late summer, 2003–2022.

**Factors influencing observed trends:** Favorable conditions for herring recruitment are linked to warm temperatures, wind direction, and prey availability (see Dressel et al., p. 102, Williams and Quinn (2000); Wespestad and Gunderson (1991)). High relative biomass estimates in 2014, 2017, and 2019 occurred during a series of warm years in the EBS. In particular, the highest relative biomass estimate in 2017 may be an early indicator of a high model estimate for age-4 recruit strength in 2021 (see Dressel et al., p. 102).

Capelin relative biomass estimates are generally higher in the eastern Bering Sea (EBS) during cold periods when the cold pool extends over the southern shelf. The highest catches in the time series occurred in 2015, closely following a series of cold years associated with large cold pool extents.

**Implications:** Herring and capelin are both important prey species for upper trophic level guilds including fish, birds, and mammals. In addition, herring is an important resource for both subsistence and commercial harvesters. Monitoring relative biomass estimates can provide important information for changes in distribution patterns and abundance and the impacts of climate change in the eastern Bering Sea.

## Togiak Herring Population Trends

Contributed by Sherri Dressel<sup>1</sup>, Sara Miller<sup>1</sup>, Caroline Brown<sup>2</sup>, Jack Erickson<sup>1</sup>, and Phil Joy<sup>1</sup>

<sup>1</sup>Alaska Department of Fish & Game, Commercial Fisheries Division

<sup>2</sup>Alaska Department of Fish & Game, Subsistence Section

Contact: sherri.dressel@alaska.gov

**Last updated: September 2022**

**Description of indicator:** A time-series of catch-at-age model estimates of mature Pacific herring (*Clupea pallasii*) biomass (1980–2021) spawning in the Togiak District of Bristol Bay serves as an index of mature population size. An integrated statistical catch-at-age model is used to estimate Togiak herring biomass (Funk et al., 1992; Funk and Rowell, 1995). The data used in the model include aerial survey estimates of biomass (Lebida and Whitmore, 1985) weighted by a confidence score (Figure 64), age composition and weight-at-age information collected from the fishery, and harvest from the purse seine and gillnet fisheries.

Recruitment of Togiak herring to the fishery begins at age-4 and fish are estimated to be fully recruited into the fishery at age-8. Togiak herring are an important prey species for piscivorous fish, seabirds, and marine mammals, an important resource for subsistence harvesters (herring and spawn on kelp historically have composed measurable percentages of the total non-salmon fish harvests for the area), the basis for a directed Togiak commercial herring sac roe fishery and a directed commercial Dutch Harbor bait fishery, as well as being prohibited species catch (PSC) in the EBS groundfish fisheries. The PSC limit for BSAI groundfish fisheries is set at 1% of the EBS mature herring biomass (age 4+) forecast, and Togiak herring comprise a majority of the nine-stock combined EBS mature herring biomass.

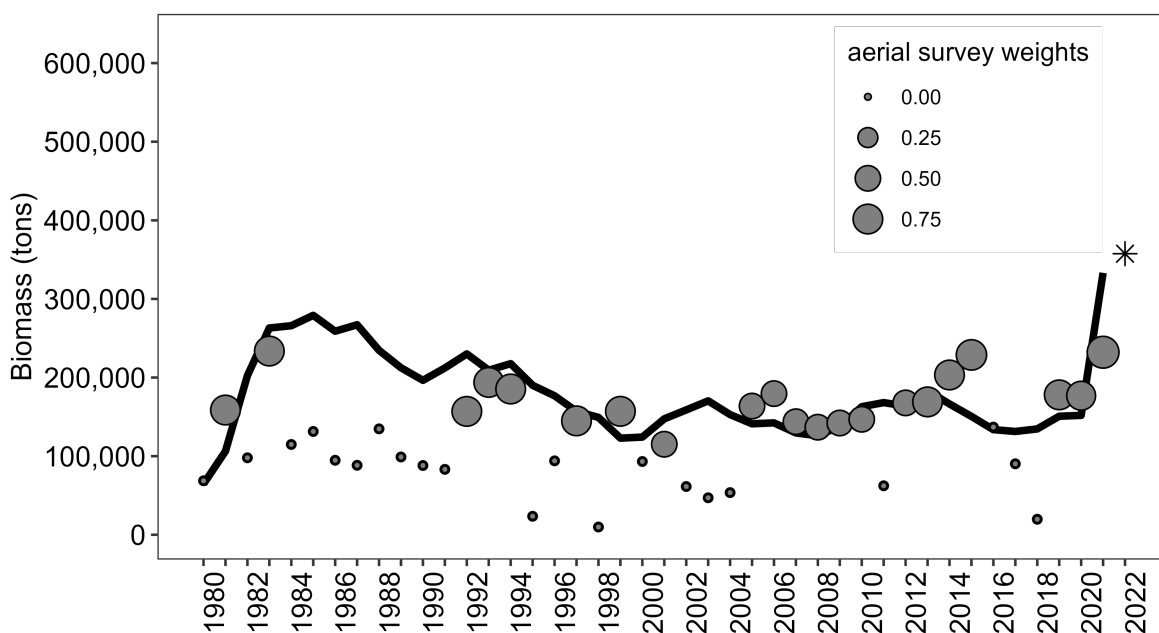


Figure 64: Aerial survey-estimated herring biomass plus pre-peak catch were included in the model (grey points), model-estimated mature biomass (black solid line), and model-estimated mature biomass forecast (black asterisk). The size of the grey points reflects the confidence weighting of each aerial survey estimate in the model based on weather, number of surveys, quality of surveys, and timing of surveys relative to the spawn (ranging from 0=no confidence to 1=complete confidence). The confidence ranking in 2021 was 0.90 out of 1.0.

**Status and trends:** Mature Togiak herring biomass, as estimated by the model, increased steeply from 1980 to 1983 (Figure 64) due to large age-4 recruitments in 1981 and 1982 (Figure 65). The biomass then declined through the late-1990s and has remained stable through 2020. A large age-4 recruitment in 2021 (2017 year class), currently estimated to be the largest since 1980 (Figure 65), combined with increased maturation of the 2016 year class resulted in a large population increase in 2021 (Figure 64). While the 2017 year class has only been observed once, and its magnitude is highly uncertain, model estimates suggest that the population has increased to near or above population levels that occurred in the mid-1980s. While the magnitude of the 2017 year class is uncertain, the high PSC in the EBS pollock fishery in 2020 supports a strong increase in young EBS herring at this time (Siddon et al., 2020). ADF&G subsistence surveys and studies of Togiak herring spawn on kelp show variable harvest pounds per capita from 1999–2019 (Coiley-Kenner et al., 2003; Fall et al., 2012; Jones et al., 2021), but Togiak respondents noted that the quantity of herring spawn on kelp available for harvest was improved in 2019 in comparison to resource availability since the early 1990s. An anecdotal report suggests that the 2020 harvest was also good. There is currently no information for 2021 and 2022.

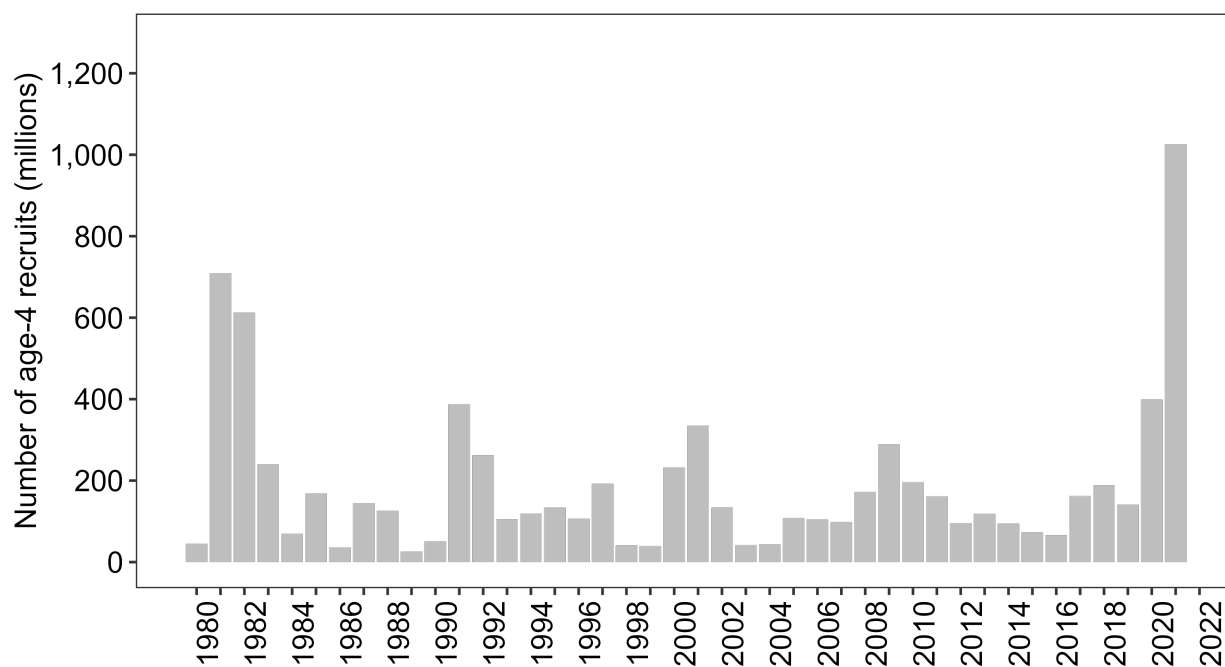


Figure 65: Model estimates of age-4 herring recruit strength (millions of age-4 mature and immature fish).

**Factors causing observed trends:** Togiak herring biomass trends are dependent upon highly variable recruitment and are influenced by the environment. The large biomass estimates in 1983–1987 and 2021 resulted from the largest age-4 recruitments in 1981, 1982, and 2021. Williams and Quinn (2000) demonstrated that Pacific herring populations in the North Pacific are closely linked to environmental conditions, particularly water temperature. Tojo et al. (2007) demonstrate how the complex reproductive migration of EBS herring is related to temperature and the retreat of sea ice and how it has changed since the 1980s. Wespestad and Gunderson (1991) suggest that recruitment variation in the EBS relates to the degree of larval retention in near-coastal nursery areas where temperatures and feeding conditions are optimal for rapid growth. Specifically, they indicate that above-average year-classes occur in years with warm sea surface temperatures when the direction of transport is north to northeast (onshore) and wind-driven transport velocity is low. The shift to anomalously warm sea surface temperatures from 2014 to 2020 (Watson, 2020) and the northward onshore springtime drift in June 2017 (Wilderbuer, 2017) may have contributed to support the exceptional 2017 year class. The warm sea surface temperatures and predominant northward and eastward drift in 2018 (Cooper and Wilderbuer, 2020) are promising for the upcoming 2018 year class as well.

**Implications:** The exceptional recruitment of age-4 Togiak herring in 2021 combined with the recruitment in 2020 were primarily responsible for the largest Togiak herring forecast on record (324,351 metric tons) in 2022 (forecasting began in 1993; Brannian et al. (1993)). The large forecast resulted in increased allowable harvest in State of Alaska 2022 directed sac roe and Dutch Harbor food and bait fisheries and may have resulted in increased spawn on kelp available for subsistence harvest. The recruitment also led to a large increase in the forecast of 2022 EBS mature population biomass (approximately a 40% increase) and the resultant PSC limit for 2022 groundfish fisheries. However, the EBS pollock fleet had a high incidental catch of herring, exceeding their PSC limits in 2020. As Togiak herring have historically comprised a majority of the nine-stock EBS mature herring biomass, it is likely that a large proportion of the 2020 PSC were Togiak herring from this exceptional 2017 year class that had not yet matured. Therefore, they were neither observed on the spawning grounds in 2020, nor included in the estimated mature herring biomass (age-4+) on which the 2020 PSC limit was based (an explanation not included as one of the three hypotheses in Siddon et al. (2020)). The observation of the exceptional 2017 year class in the 2021 Togiak spawning population supports the conclusion of pollock fishermen that the increased bycatch in 2020 was due to an increased abundance of herring on the grounds (Siddon et al., 2020). While a PSC limit set based on the size of the mature EBS herring biomass may be constraining again in the future if exceptional recruitment occurs, historical estimates of recruitment (Figure 65) indicate that such an occurrence has been extremely rare (the 2017 year class was the largest in the 42-year time series and the only recruitments similar in magnitude were in 1981 and 1982).

## Salmon

### Trends in the Abundance of Juvenile Sockeye Salmon in the Southeastern and Northeastern Bering Sea During the Late-Summer Surface Trawl Survey, 2003–2022

Contributed by Alex Andrews, Ellen Yasumiishi, Ed Farley, Jim Murphy, and Andrew Dimond  
Ecosystem Monitoring and Assessment Program, Auke Bay Laboratories, Alaska Fisheries Science Center  
Contact: alex.andrews@noaa.gov  
**Last updated: October 2022**

**Description of indicator:** See 'Description of indicator' on p. 94.

**Status and trends:** Juvenile sockeye salmon relative abundance has remained high in the southeastern Bering Sea (Figure 66). In 2022, the relative abundance was the second highest in the time series. The highest relative abundance occurred in 2018. Relative abundances in the northeastern Bering Sea, compared with the southeastern, tend to be relatively low, with the exception of 2019, when SSTs were high and the cold pool extent was at a near minimum extent.

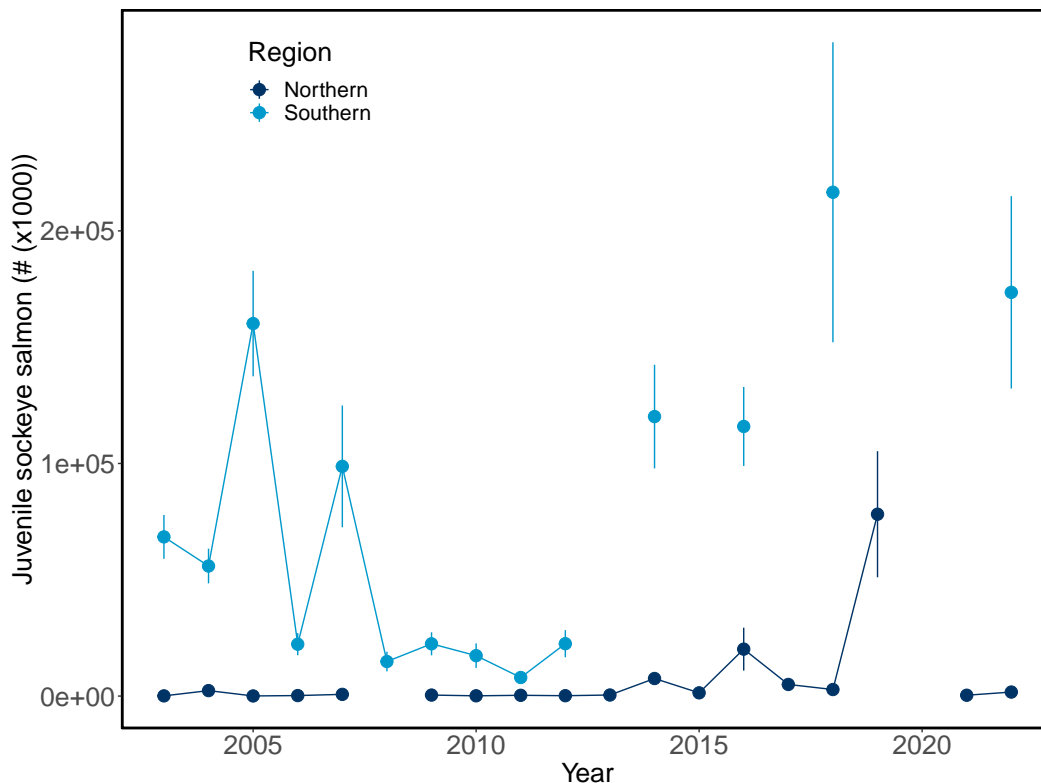


Figure 66: Estimated abundance of juvenile sockeye salmon in surface waters surveyed in the eastern Bering Sea during late summer, 2003–2022.

**Factors influencing observed trends:** Bristol Bay sockeye salmon adult returns in the last 5–10 years have been above the long-term average, with a record high in 2022 (see Cunningham et al., p. 109). Juvenile sockeye salmon are likely benefiting from a combination of good freshwater rearing habitat and good early marine survival (Farley et al., 2011) and high abundances of age-0 pollock in surface waters during warm years, a major prey item of juvenile sockeye salmon during warm years (Yasumiishi et al. in revision). From

2003–2018, juvenile sockeye salmon in these surveys incurred warming-related increases in biomass, shifts in their distribution northward and westward, and increases in area occupied (Yasumiishi et al., 2020). Further research into the predominant age classes of the juvenile salmon encountered during this survey would benefit the interpretation of these relative abundances. In addition, genetic analyses confirming that the juvenile sockeye salmon captured in the NBS are of Bristol Bay origin would help to determine if, during periods of warm SSTs and reduced cold pool extent, Bristol Bay juvenile sockeye salmon are able to benefit from expanding distributions into the NBS.

**Implications:** A continuation of relatively high Bristol Bay juvenile sockeye salmon abundance, along with favorable ocean conditions, suggests that adult returns will continue to be above average.

## Northern Bering Sea Juvenile Salmon Abundance Indices

Contributed by Jim Murphy<sup>1</sup>, Sabrina Garcia<sup>2</sup>, Dan Cooper<sup>3</sup>, Ed Farley<sup>1</sup>, Elizabeth Lee<sup>2</sup>, Andrew Dimond<sup>1</sup>, and Kathrine Howard<sup>2</sup>

<sup>1</sup>Auke Bay Laboratories, Alaska Fisheries Science Center, NOAA

<sup>2</sup>Alaska Department of Fish & Game, Anchorage, AK

<sup>3</sup>Resource Assessment and Conservation Engineering Division, Alaska Fisheries Science Center

Contact: jim.murphy@noaa.gov

**Last updated: October 2022**

**Description of indicator:** Mixed-stock juvenile (first year at sea) Chinook (*Oncorhynchus tshawytscha*) and pink (*O. gorbuscha*) salmon abundance indices are estimated from late summer surface trawl catch-per-unit-effort (CPUE) data and adjusted for mixed-layer depth in the northern Bering Sea (NBS). The mixed-stock index for Chinook salmon provides a rapid assessment of all juvenile Chinook salmon stocks present in the NBS and is different than the stock-specific abundance of Yukon River Chinook salmon. Abundance indices for Yukon River Fall chum salmon (*O. keta*, Upper Yukon River genetic stock group) are based on CPUE data from surveys in both the northern and southern Bering Sea. The preliminary 2022 abundance index was generated using the average genetic stock proportion from 2016 to 2021 and will change once stock compositions from 2022 become available.

**Status and trends:** The mixed-stock abundance of juvenile Chinook salmon in the NBS was below average in 2022 (1.8 million), and has ranged from 1.4 million to 5.8 million with an overall average of 3.0 million (Figure 67). The stock-specific CPUE index for the Fall chum salmon stock group ranged from a low of 17 in 2022 to a high of 122 in 2019, with an average of 51 (Figure 68). The juvenile pink salmon CPUE index ranged from a low of 0.9 during 2021 to a high of 5.4 during 2015, with an average of 2.9 (Figure 69).

**Factors influencing observed trends:** Early life-history (freshwater and early marine) survival and adult spawning escapement are the key factors influencing juvenile salmon abundance in the northern Bering Sea.

**Implications:** Juvenile abundance has been related to adult returns (Murphy et al., 2017; Howard et al., 2019, 2020; Farley Jr et al., 2020; Murphy et al., 2021). Below-average juvenile abundance is expected to contribute to below-average adult Chinook and chum salmon returns three to four years in the future (juveniles typically remain at sea for three to four years before returning to freshwater to spawn) and the following year for pink salmon (juveniles remain at sea for one year). Below-average returns of Chinook salmon may result in subsistence fishery restrictions in the NBS (Yukon River and Norton Sound Chinook salmon) and could contribute to reduced Chinook salmon bycatch caps in the eastern Bering Sea pollock fisheries. Fall chum salmon from the Yukon River are an important subsistence resource and are increasingly important when Chinook salmon runs are low, especially for the people of the Upper Yukon River. Continued marine research on juvenile salmon is necessary to understand how rapid changes to the marine environment affect chum salmon population dynamics.

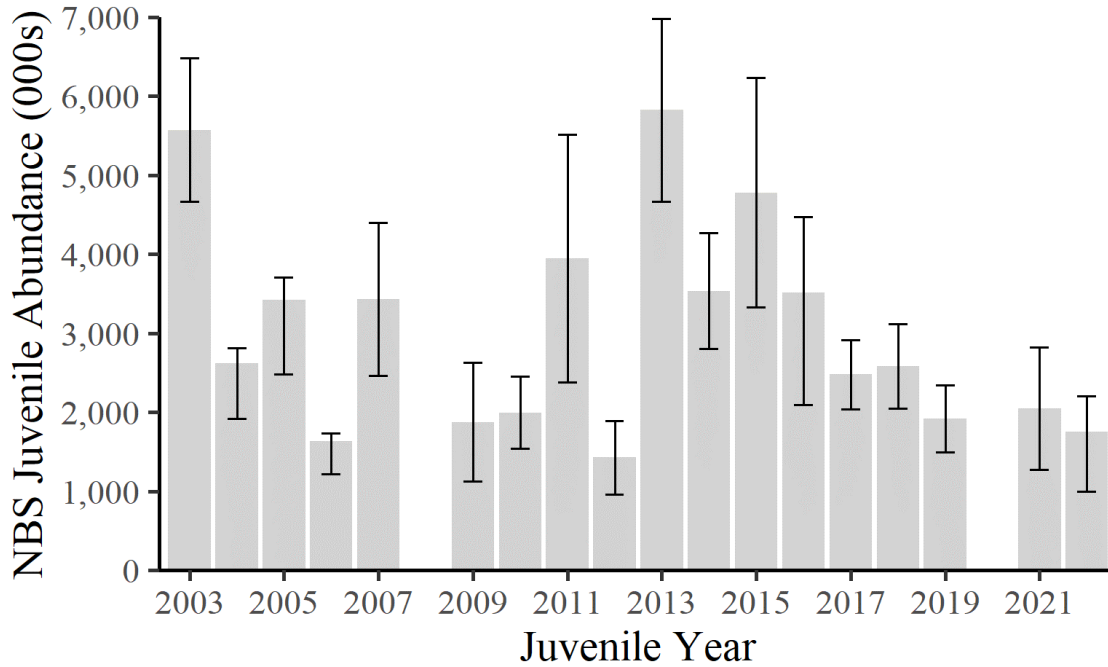


Figure 67: Juvenile Chinook salmon abundance estimates in the northern Bering Sea, 2003–2022. Error bars are one standard deviation above and below juvenile abundance estimates.

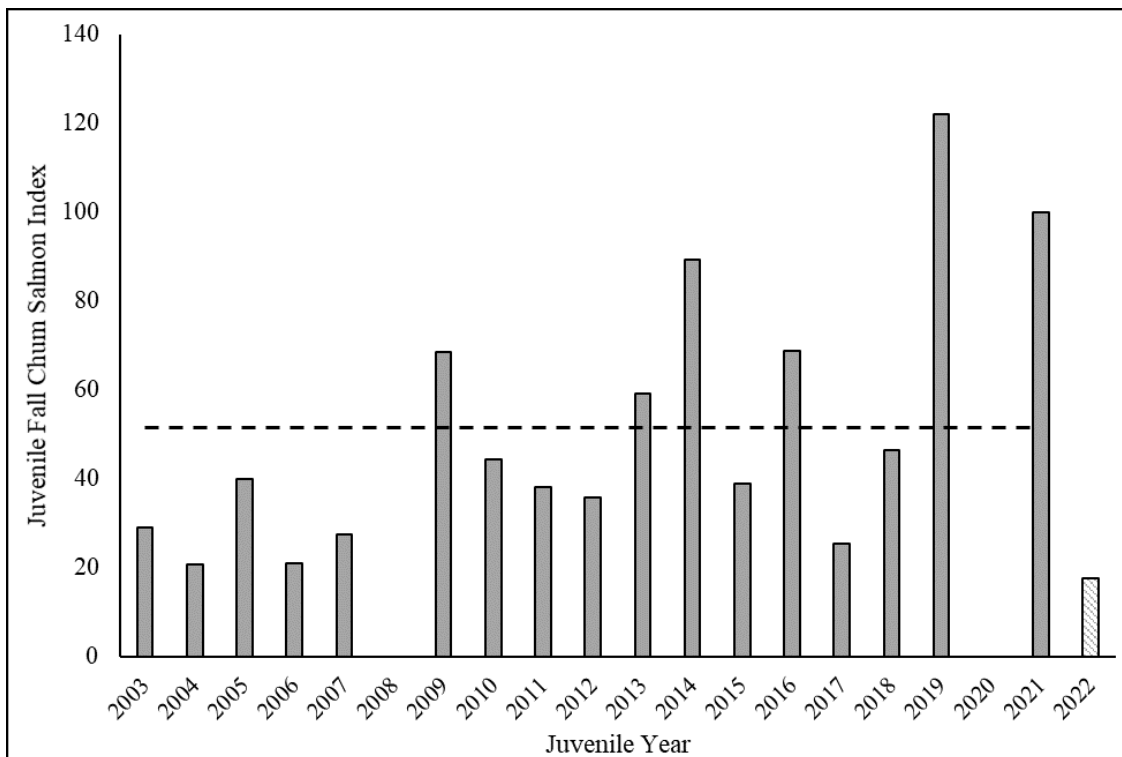


Figure 68: Juvenile chum salmon abundance index ( $\#/km^2$ ) for the Upper Yukon River (fall chum) stock group, 2003–2022. Dashed line indicates the average juvenile chum salmon index across years 2003–2021. No surveys occurred in 2008 and 2020. The 2022 abundance index was generated using the average genetic stock proportion from 2016 to 2021 and will change once stock compositions from 2022 become available. Additionally, the 2022 abundance index does not include southern Bering Sea survey data as they were not yet available.

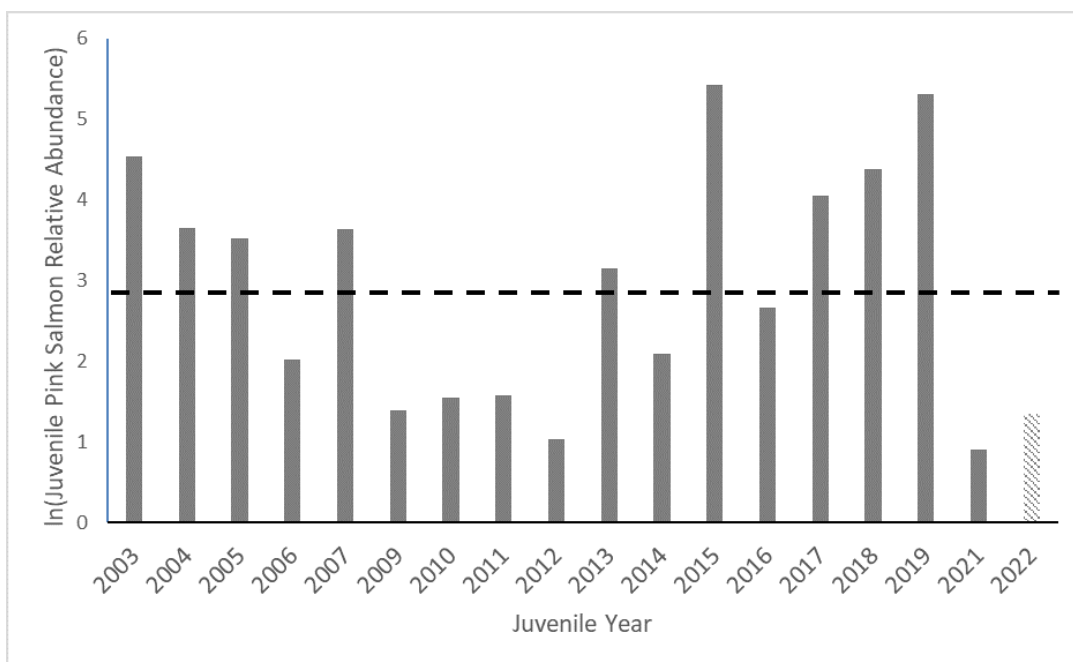


Figure 69: Juvenile pink salmon relative abundance index for the northern Bering Sea, 2003–2022. Dashed line indicates the average relative abundance index from 2003–2022. No surveys were conducted in 2008 or 2020. The dashed bar is the preliminary juvenile pink salmon relative abundance index for 2022.

## Temporal Trend in the Annual Inshore Run Size of Bristol Bay Sockeye Salmon (*Oncorhynchus nerka*)

Contributed by Curry J. Cunningham<sup>1</sup>, Stacy Vega<sup>2</sup>, and Jordan Head<sup>2</sup>

<sup>1</sup>College of Fisheries and Ocean Sciences, University of Alaska Fairbanks, Juneau, Alaska

<sup>2</sup>Alaska Department of Fish & Game, Anchorage, Alaska

Contact: cjcunningham@alaska.edu

**Last updated: October 2022**

**Description of indicator:** The annual abundance of adult sockeye salmon (*Oncorhynchus nerka*) returning to Bristol Bay, Alaska is enumerated by the Alaska Department of Fish and Game (ADF&G). The total inshore run in a given year is the sum of catches in five terminal fishing districts plus the escapement of sockeye to nine major river systems. Total catch is estimated based on the mass of fishery offloads and the average weight of individual sockeye within time and area strata. Escapement is the number of fish successfully avoiding fishery capture and enumerated during upriver migration toward the spawning grounds, or through post-season aerial surveys of the spawning grounds (Elison et al., 2018). Although there have been slight changes in the location and operation of escapement enumeration projects and methods over time, these data provide a consistent index of the inshore return abundance of sockeye salmon to Bristol Bay since 1963.

**Status and trends:** The 2022 Bristol Bay salmon preliminary inshore run estimate of 79.0 million sockeye is the largest on record since 1963 and is 55.1% higher than the recent 10-year average of 50.9 million sockeye, and 127.7% higher than the 1963–2020 average of 34.7 million sockeye. The temporal trend in Bristol Bay sockeye salmon indicates a large increase during the recent 8-year period, with inshore run sizes in 2015–2022 all exceeding 50 million salmon and above recent and long-term averages. The current period of high Bristol Bay sockeye salmon production now exceeds the previous high production stanza that occurred 1989–1995.

*Note:* At the time of printing, the 2022 Bristol Bay inshore run size numbers are preliminary and subject to change.

**Factors influencing observed trends:** The return abundance of Bristol Bay sockeye salmon is positively correlated with the Pacific Decadal Oscillation (Hare et al., 1999), specifically with the Egegik and Ugashik district run sizes increasing after the 1976/1977 regime shift (Figure 71). However, recent research has highlighted that relationships between salmon population dynamics and the PDO may not be as consistent as once thought, and may in fact vary over time (Litzow et al., 2020*a,b*). The abundance and growth of Bristol Bay sockeye salmon has also been linked to the abundance of pink salmon (*Oncorhynchus gorbuscha*) in the North Pacific (Ruggerone and Nielsen, 2004; Ruggerone et al., 2016).

**Implications:** The high inshore run of Bristol Bay sockeye salmon in 2022 and in the preceding 7-year period indicate positive survival conditions for these stocks while in the ocean. Given evidence that the critical period for sockeye salmon survival occurs during the first summer and winter at sea (Beamish and Mahnken, 2001; Farley et al., 2007, 2011) and the predominant age classes observed for Bristol Bay stocks are 1.2, 1.3, 2.2, and 2.3 (European designation: years in freshwater – years in the ocean), the large 2022 Bristol Bay sockeye salmon inshore run suggests these stocks experienced positive conditions at entry into the eastern Bering Sea in the summers of 2019 and 2020, and winters of 2019–2020 and 2020–2021.

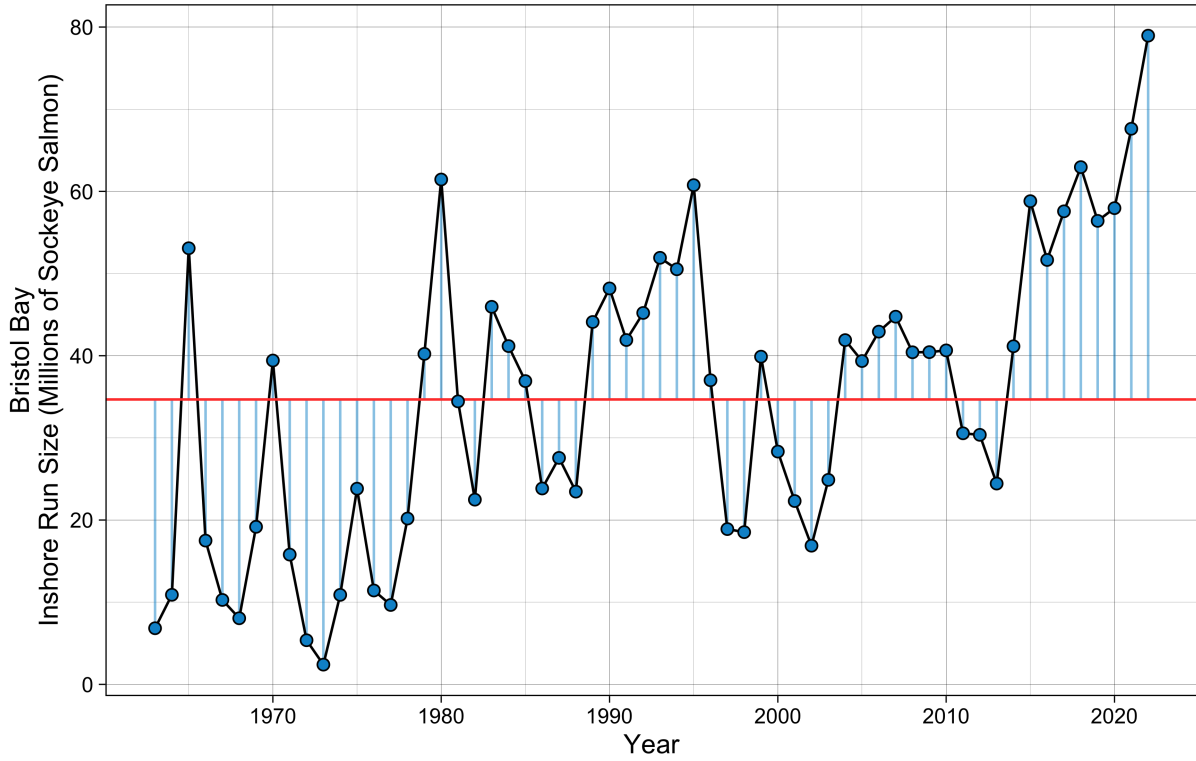


Figure 70: Annual Bristol Bay sockeye salmon inshore run size 1963–2022. Red line is the time series average of 34.7 million sockeye.

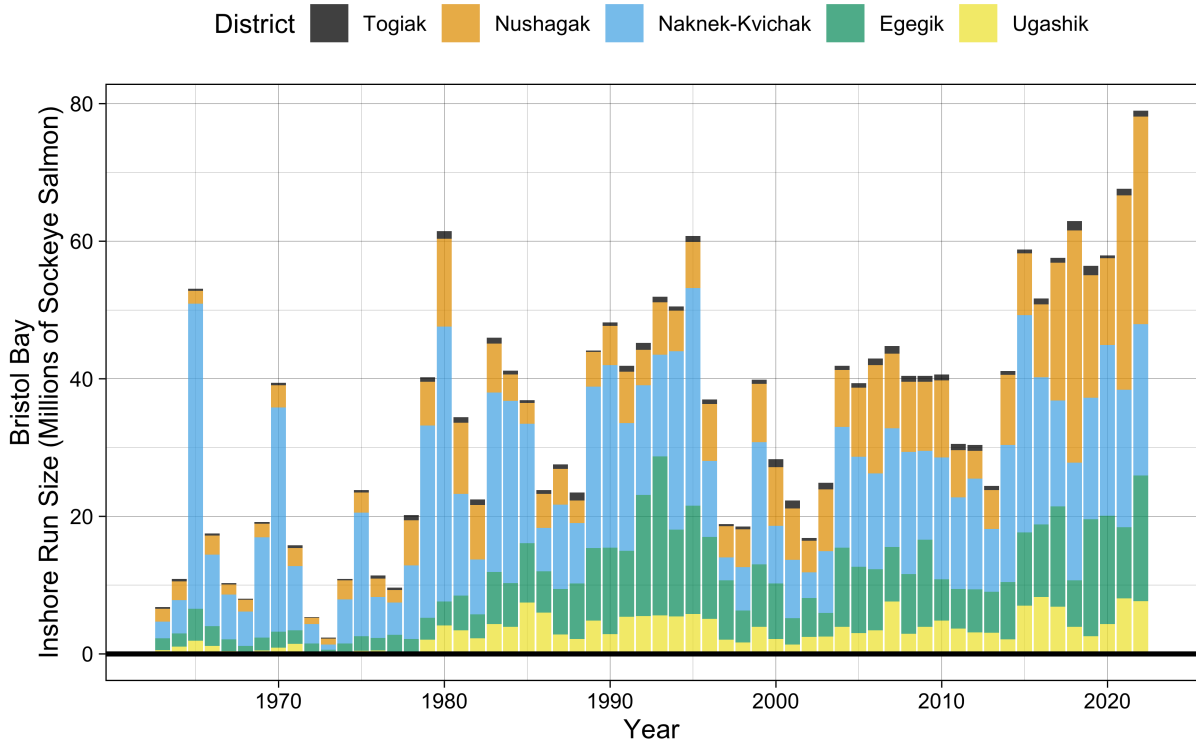


Figure 71: Annual Bristol Bay sockeye salmon inshore run size 1963–2022 by commercial fishing district.

## Trends in Alaska Commercial Salmon Catch – Bering Sea

Contributed by George A. Whitehouse

Cooperative Institute for Climate, Ocean, and Ecosystem Studies (CICOES), University of Washington, Seattle WA

Contact: andy.whitehouse@noaa.gov

**Last updated: October 2022**

**Description of indicator:** This contribution provides historic and current commercial catch information for salmon of the Bering Sea. This contribution summarizes data and information available in current Alaska Department of Fish & Game (ADF&G) agency reports (e.g., Brenner et al. (2022)) and on their website<sup>17</sup>.

Pacific salmon in Alaska are managed in four regions based on freshwater drainage basins<sup>18</sup>: Southeast/Yakutat, Central (encompassing Prince William Sound, Cook Inlet, and Bristol Bay), Arctic-Yukon-Kuskokwim, and Westward (Kodiak, Chignik, and Alaska peninsula). ADF&G prepares harvest projections for all areas rather than conducting run size forecasts for each salmon run. There are five Pacific salmon species with directed commercial fisheries in Alaska; they are sockeye (*Oncorhynchus nerka*), pink (*O. gorbuscha*), chum (*O. keta*), Chinook (*O. tshawytscha*), and coho (*O. kisutch*) salmon.

### Status and trends:

#### *Statewide*

Catches from directed fisheries on the five salmon species have fluctuated over recent decades but in total have been generally strong statewide (Figure 72). The commercial harvests from 2021 totaled 235.2 million fish, which was 45.1 million more than the preseason forecast of 190.1 million fish. The 2021 total commercial harvest was elevated by the harvest of 161.8 million pink salmon, primarily from Prince William Sound and Southeast Alaska. Preliminary data from ADF&G for 2022 indicates a statewide total commercial salmon harvest of about 154 million fish (as of 22 September 2022), which is below the preseason projection of 160.6 million fish. The 2022 harvest has been bolstered by the catch of 74.5 million sockeye salmon, primarily from Bristol Bay.

#### *Bering Sea*

Salmon harvests in the Bering Sea are numerically dominated by the catch of sockeye in Bristol Bay (Figure 73). The 2021 Bristol Bay sockeye salmon run of 67.7 million was the largest ever, and the harvest of 41.99 million was the third highest ever. Escapement goals for sockeye salmon in 2021 were met or exceeded in every drainage in Bristol Bay where escapement was defined. Preliminary data for 2022 from ADF&G indicates that the commercial harvest of Bristol Bay sockeye salmon is strong again, at more than 60 million fish. For more information on 2022 Bristol Bay sockeye salmon, see Cunningham et al., p. 109.

Chinook salmon abundance in the Arctic-Yukon-Kuskokwim region has been low since the mid-2000s and remains low. From 2008 to 2021 no commercial periods targeting Chinook salmon were allowed in the Yukon Management Area. Preliminary data for 2022 indicate that Chinook salmon escapement goals will not likely be met for the Yukon Area. In 2021, Chinook salmon did meet the drainage-wide sustainable escapement goal for the Kuskokwim River. For more information on factors affecting the 2022 Western Alaska Chinook salmon runs and subsistence harvest, see Whitworth et al., p. 24.

Summer chum salmon did not meet any escapement goals in the Yukon Area in 2021 and there was no commercial harvest. Additionally, there were no commercial harvests for salmon during fall 2021 in the Yukon Management Area due to the low run size for fall chum and coho salmon. Preliminary data for the Yukon River in 2022 indicates that fall chum are again unlikely to meet escapement goals.

---

<sup>17</sup><https://www.adfg.alaska.gov/>

<sup>18</sup><https://www.adfg.alaska.gov/index.cfm?adfg=commercialbyfisherysalmon.salmonareas>

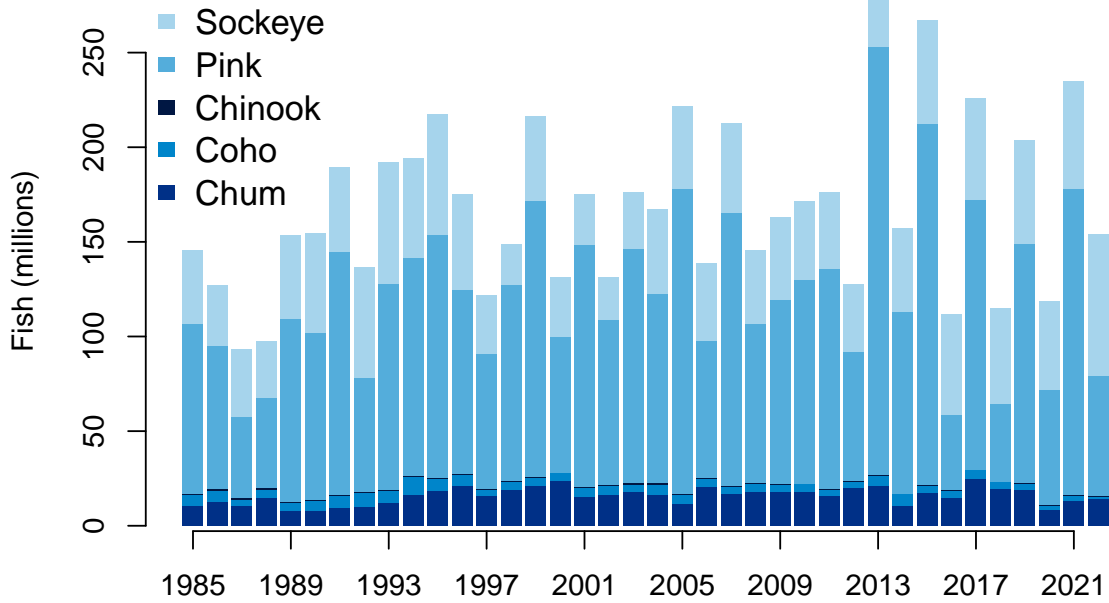


Figure 72: Alaska statewide commercial salmon catches, 2022 values are preliminary. Source: ADF&G, <http://www.adfg.alaska.gov>. ADF&G not responsible for the reproduction of data, subsequent analysis, or interpretation.

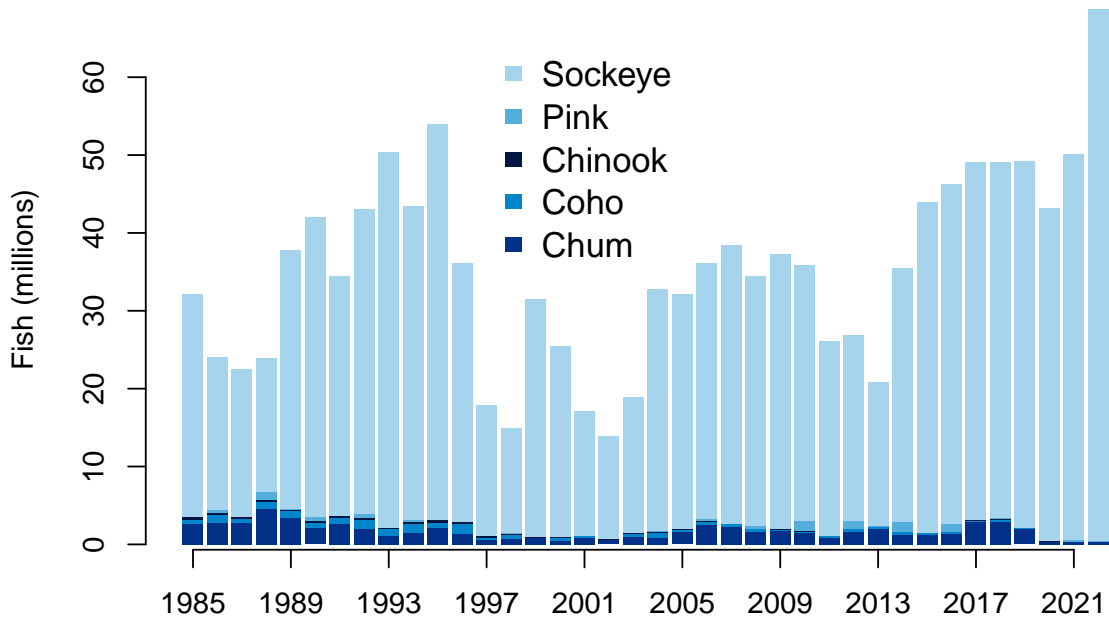


Figure 73: Commercial salmon catches in the eastern Bering Sea, 2022 values are preliminary. Source: ADF&G; <http://www.adfg.alaska.gov>. ADF&G not responsible for the reproduction of data, subsequent analysis, or interpretation.

**Factors influencing observed trends:** Salmon have complex life histories and are subject to stressors in the freshwater and marine environments, and anthropogenic pressures. These forces do not affect all species and stocks equally or in the same direction, and resolving what is driving the population dynamics of a particular stock is challenging (Rogers and Schindler, 2011). Interannual variation in Alaska statewide total salmon abundance is partly due to the even-year, odd-year cycle in pink salmon, particularly production from the Prince William Sound stock of pink salmon, which typically has larger runs in odd years. Chinook runs have been declining statewide since 2007. Size-dependent mortality during the first year in the marine environment is thought to be a leading contributor to low Chinook run sizes (Beamish and Mahnken, 2001; Graham et al., 2019). Additionally, rising sea temperatures and loss of sea ice may lead to slower growth for juvenile Chinook salmon in the eastern Bering Sea (Yasumiishi et al., 2020).

Salmon are also caught as bycatch in Bering Sea groundfish trawl fisheries, most of which are Chinook and chum salmon. The North Pacific Fishery Management Council has implemented management measures and incentives that have largely been successful at reducing Chinook salmon bycatch in groundfish trawl fisheries since their peak in 2007 (Stram and Ianelli, 2015). However, the bycatch of non-chinook salmon (i.e., chum) has trended upward since 2012 and in 2021 was at its highest level since 2005<sup>19</sup>.

In the Bering Sea, sockeye salmon are the most abundant salmonid and since the early 2000s, they have had consistently strong runs, which have supported large harvests. Bristol Bay sockeye salmon display a variety of life history types. For example, their spawning habitat is highly variable and demonstrates the adaptive and diverse nature of sockeye salmon in this area (Hilborn et al., 2003). Therefore, productivity within these various habitats may be affected differently depending upon varying conditions, such as climate (Mantua et al., 1997), so more diverse sets of populations provide greater overall stability (Schindler et al., 2010). The abundance of Bristol Bay sockeye salmon may also vary over centennial time scales, with brief periods of high abundance separated by extended periods of low abundance (Schindler et al., 2006).

**Implications:** Salmon have important influences on Alaska marine ecosystems through interactions with marine food webs as predators on lower trophic levels and as prey for other species such as Steller sea lions. In years of great abundance, salmon may exploit prey resources more efficiently than their competitors. A negative relationship between seabird reproductive success and years of high pink salmon abundance has been demonstrated (Springer and van Vliet, 2014). Directed salmon fisheries are economically important for the state of Alaska. The trend in total statewide salmon catch in recent decades has been for generally strong harvests, despite annual fluctuations.

Measures to reduce salmon bycatch can affect the spatial distribution of groundfish trawl fisheries through area closures and incentives to avoid bycatch. When the aggregate Chinook salmon run size in the Kuskokwim, Unalakleet, and Upper Yukon Rivers is less than 250,000, a lower limit to Chinook bycatch is imposed on the pollock fishery.

---

<sup>19</sup><https://www.npfmc.org/wp-content/PDFdocuments/bycatch/BeringSeaSalmonBycatchFlyer.pdf>

# Groundfish

## Eastern and Northern Bering Sea Groundfish Condition

Contributed by Sean Rohan, Bianca Prohaska, and Cecilia O’Leary  
Resource Assessment and Conservation Engineering Division  
Alaska Fisheries Science Center, NOAA Fisheries

Contact: sean.rohan@noaa.gov  
Last updated: October 2022

**Description of indicator:** Morphometric condition indicators based on length-weight relationships characterize variation in somatic growth and can be considered indicators of prey availability, growth, general health, and habitat condition (Blackwell et al., 2000; Froese, 2006). This contribution presents two morphometric condition indicators based on length-weight relationships: a new relative condition indicator that is estimated using a spatio-temporal model and the historical indicator based on residuals of the length-weight relationship.

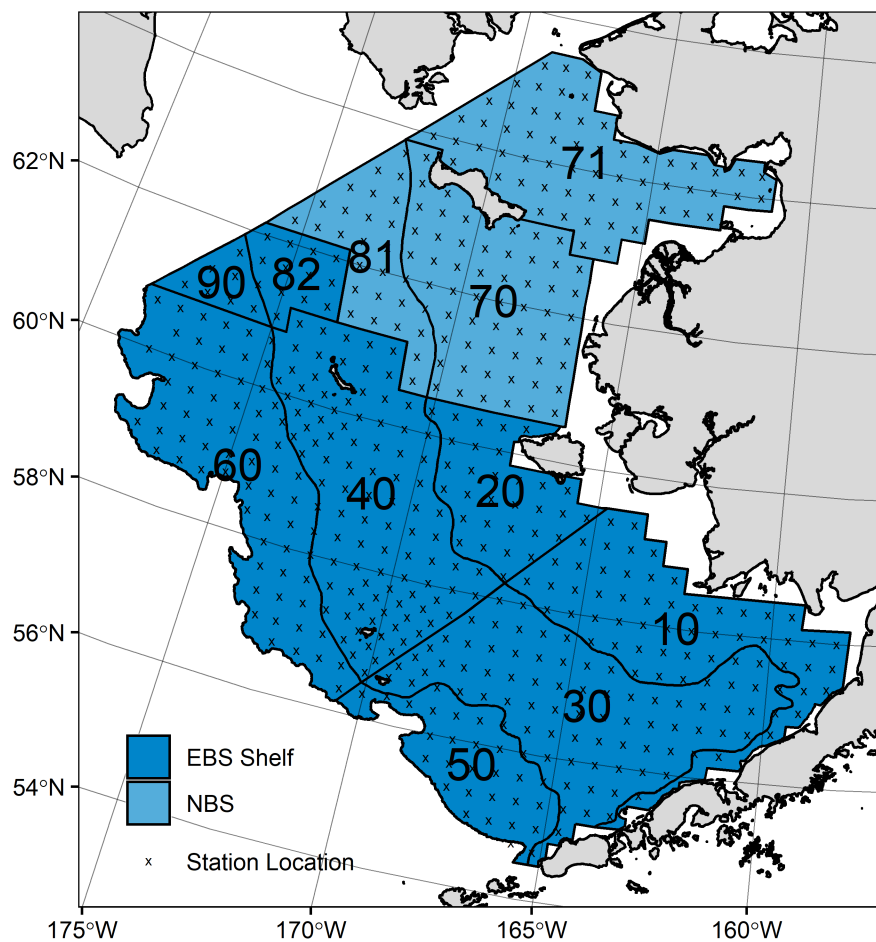


Figure 74: NOAA Alaska Fisheries Science Center summer bottom trawl survey strata (10–90) and station locations (x) on the eastern Bering Sea (EBS) shelf and in the northern Bering Sea (NBS).

The new model-based relative condition indicator (VAST relative condition) is the ratio of fish weight-at-length relative to the time series mean based on annual allometric intercepts,  $a_{year}$ , in the length-weight equation ( $W = aL^b$ ;  $W$  is mass (g),  $L$  is fork length (cm)), i.e.,  $condition = a_{year}/\bar{a}$ . Relative condition greater than one indicates better condition (i.e., heavier per unit length) and relative condition less than one indicates poorer condition (i.e., lighter per unit length).

The historical length-weight indicator based on residuals of the length-weight relationship represents how heavy a fish is per unit body length compared to the time series mean (Brodeur et al., 2004). Positive length-weight residuals indicate better condition (i.e., heavier per unit length) and negative residuals indicate poorer condition (i.e., lighter per unit length) (Froese, 2006). Fish condition calculated in this way reflects realized outcomes of intrinsic and extrinsic processes that affect fish growth, which can have implications for biological productivity through direct effects on growth and indirect effects on demographic processes such as, reproduction, and mortality (e.g., Rodgveller (2019); Barbeaux et al. (2020)).

The model-based relative condition indicator was estimated using a spatio-temporal model with spatial random effects, implemented in the software VAST v3.8.2 (Grüss et al., 2020; Thorson, 2019a). Allometric intercepts,  $a_{year}$ , are estimated as fixed effects using a multivariate generalized linear mixed model that jointly estimates spatial and temporal variation in  $a$  and catch per unit effort (numbers of fish per area). Density-weighted average  $a_{year}$  is a product of population density, local  $a$ , and area. Spatial variation in  $a_{year}$  was represented using a Gaussian Markov random field. The model approximates  $a_{year}$  using a log-link function and linear predictors (Grüss et al., 2020). Parameters are estimated by identifying the values that maximize the marginal log-likelihood.

The historical indicator was estimated from residuals of linear regression models based on a log-transformation of the exponential growth relationship from 1999 to 2022 (EBS: 1999–2022, NBS: 2010, 2017–2019, 2022). A unique slope ( $b$ ) was estimated for each survey stratum (Figure 74) to account for spatial-temporal variation in growth and bottom trawl survey sampling. Survey strata 31 and 32 were combined as stratum 30; strata 41, 42, and 43 were combined as stratum 40; and strata 61 and 62 were combined as stratum 60. Northwest survey strata 82 and 90 were excluded from these analyses due to sample size considerations. Length-weight relationships for juvenile length walleye pollock (100–250mm fork length, corresponding with ages 1–2 years) were calculated separately from adult walleye pollock (> 250mm). Residuals for individual fish were obtained by subtracting observed weights from bias-corrected weights-at-length that were estimated from regression models.

For the EBS shelf, individual length-weight residuals were averaged for each stratum and weighted in proportion to total biomass in each stratum from area-swept expansion of bottom-trawl survey catch per unit effort (CPUE; i.e., design-based stratum biomass estimates). Analysis for the NBS was conducted separately from the EBS because of the shorter time series and the NBS was treated as a single stratum without biomass weighting. To minimize the influence of unrepresentative samples on indicator calculations, combinations of species, stratum, and year with sample size <10 were used to fit length-weight regressions but were excluded from calculating length-weight residuals in the EBS.

Both condition indicators were calculated from paired fork lengths and weights of individual fishes that were collected during bottom trawl surveys of the eastern Bering Sea (EBS) shelf and northern Bering Sea (NBS) which were conducted by the Alaska Fisheries Science Center’s Resource Assessment and Conservation Engineering (AFSC/RACE) Groundfish Assessment Program (GAP). Fish condition analyses were applied to walleye pollock (*Gadus chalcogrammus*), Pacific cod (*G. macrocephalus*), arrowtooth flounder (*Atheresthes stomias*), yellowfin sole (*Limanda aspera*), flathead sole (*Hippoglossoides elassodon*), northern rock sole (*Lepidopsetta polyxystra*), and Alaska plaice (*Pleuronectes quadrituberculatus*) collected in bottom trawls at standard survey stations (Figure 74).

#### *Methodological Changes:*

The historical length-weight residual indicator (used in 2020 and 2021) and new VAST relative condition indicator (Grüss et al., 2020) are both presented this year to allow comparison between methods. Overall, trends were similar between historical and new indicators based on the strong correlation ( $r > 0.85$ ) between indicators for most species (Figures 76, 77, and 79). An exception was large walleye pollock (> 250 mm)

in the NBS ( $r = 0.33$ ), which may be due to the small sample size ( $n = 4$ ) collected exclusively from the southern end of the NBS survey area in 2010. Mean estimates and confidence intervals for the new condition indicator are likely more reliable than the historical indicator because the new indicator affords more precise expansion of individual samples to the population. This indicator also better accounts for spatially and temporally unbalanced sampling that is characteristic of historical bottom trawl survey data due to changes in sampling protocols (e.g., transition from sex-and-length stratified to random sampling).

**Status and trends:** Fish condition, indicated by the model-based condition indicator (VAST relative condition), has varied over time for all species examined (Figures 75 and 78). In 2019 in the EBS, an upward trend in VAST relative condition was observed for most species relative to 2017–2018; however, in 2021 VAST relative condition had a downward trend in most species examined. In 2022 in the EBS, VAST relative conditions were near the historical mean, or positive for all species examined, except for arrowtooth flounder and large walleye pollock ( $>250$  mm), and while their VAST relative conditions were negative, the mean for both groups fell within one standard deviation of the historical mean (Figure 75).

In the NBS in 2022, VAST relative condition of all species examined, including large ( $>250$ mm) and small (100–250mm) walleye pollock, were negative; however, despite being below the historical average, the VAST relative condition of all species were within one standard deviation of the time series mean (Figure 78).

**Factors influencing observed trends:** Temperature appears to influence morphological condition of several species in the EBS and NBS, so near-average cold pool extent and water temperatures in 2022 likely played a role in the near-average condition (within  $\pm 1$  standard deviation of the mean) for most species. Historically, particularly cold years tend to correspond with negative condition, while particularly warm years tend to correspond to positive condition. For example, water temperatures were particularly cold during the 1999 Bering Sea survey, a year in which negative condition was observed for all species for which data were available. In addition, spatio-temporal factor analyses suggest the morphometric condition of age-7 walleye pollock is strongly correlated with cold pool extent in the EBS (Grüss et al., 2021). In recent years, warm temperatures across the Bering Sea shelf, since the record low seasonal sea-ice extent in 2017–2018 and historical cold pool area minimum in 2018 (Stabeno and Bell, 2019), may have influenced the positive trend in the condition of several species from 2016 to 2019.

Although warmer temperatures may increase growth rates if there is adequate prey to offset temperature-dependent increases in metabolic demand, growth rates may also decline if prey resources are insufficient to offset temperature-dependent increases in metabolic demand. The influence of temperature on growth rates depends on the physiology of predator species, prey availability, and the adaptive capacity of predators to respond to environmental change through migration, changes in behavior, and acclimatization. For example, elevated temperatures during the 2014–2016 marine heatwave in the Gulf of Alaska led to lower growth rates of Pacific cod and lower condition because available prey resources did not make up for increased metabolic demand (Barbeaux et al., 2020).

Other factors that could affect morphological condition include survey timing, stomach fullness, fish movement patterns, sex, and environmental conditions (Froese, 2006). The starting date of annual length-weight data collections has varied from late May to early June and ended in late July-early August in the EBS, and mid-August in the NBS. Although we account for some of this variation by using spatially-varying coefficients in the length-weight relationship, variation in condition could relate to variation in the timing of sample collection within survey strata. The affect of survey timing on fish condition can be further compounded by seasonal fluctuations in reproductive condition with the buildup and depletion of energy stores (Wuenschel et al., 2019). Another consideration is that fish weights sampled at sea include gut content weights, so variation in gut fullness may influence weight measurements. Since feeding conditions vary over space and time, prey consumption rates and the proportion of total body weight attributable to gut contents may be an important factor influencing the length-weight residuals.

Finally, although the condition indicators characterize temporal variation in morphometric condition for important fish species in the EBS and NBS they do not inform the mechanisms or processes behind the observed patterns.

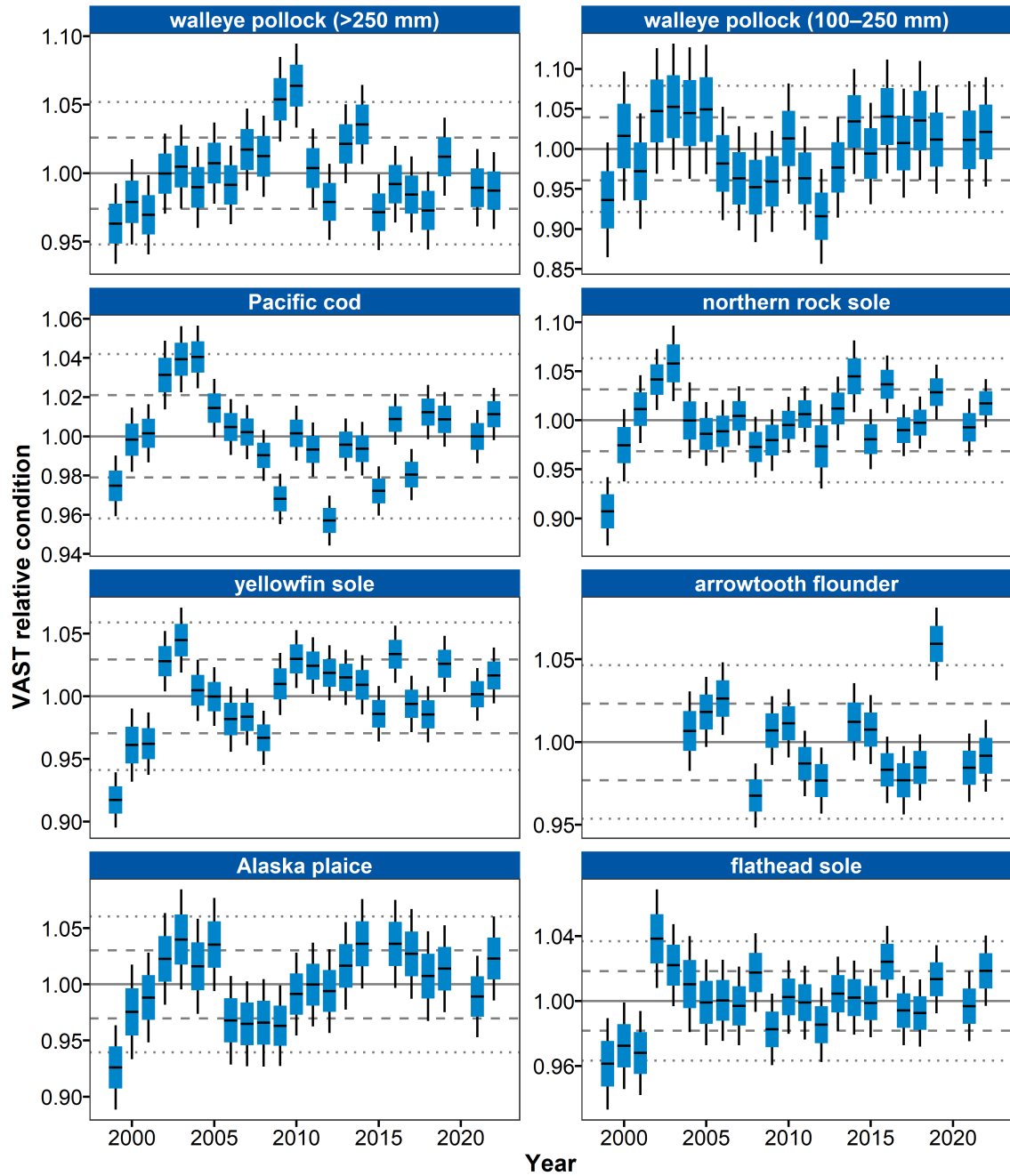


Figure 75: VAST relative condition for groundfish species collected during AFSC/RACE GAP standard summer bottom trawl surveys of the eastern Bering Sea shelf, 1999–2022. The dash in the blue boxes denote the mean for that year, the box denotes one standard error, and the lines on the boxes denote two standard errors. Lines on each plot represent the historical mean, dashed lines denote one standard deviation, and dotted lines denote two standard deviations.

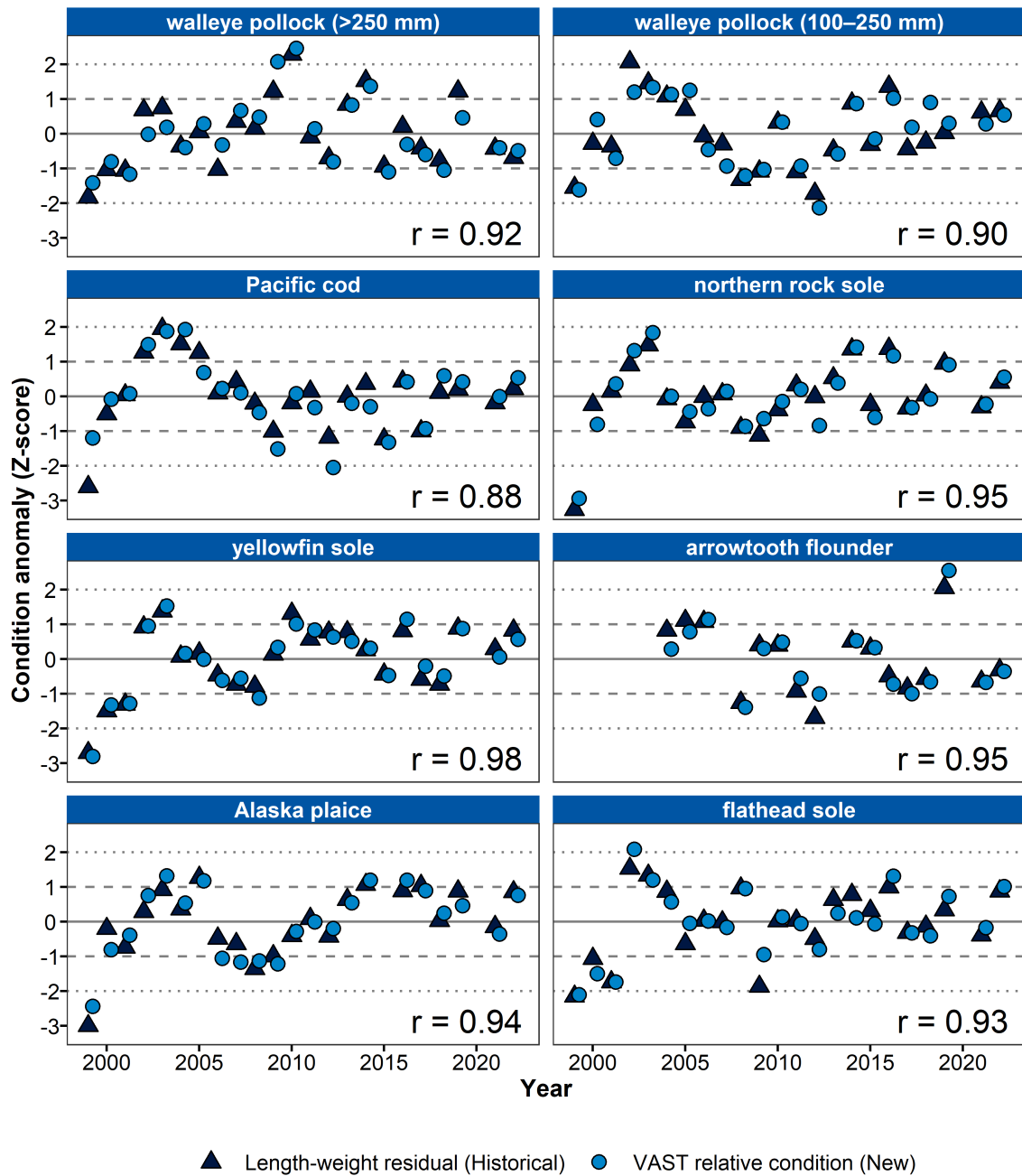


Figure 76: Time series of VAST relative condition and length-weight residual condition anomalies for the eastern Bering Sea. Triangles denote the length-weight residual, while circles denote the VAST relative condition. Lines represent the historical mean, dashed lines denote one standard deviation, and dotted lines denote two standard deviations. The Pearson correlation coefficient ( $r$ ) is shown at the bottom right of each panel.

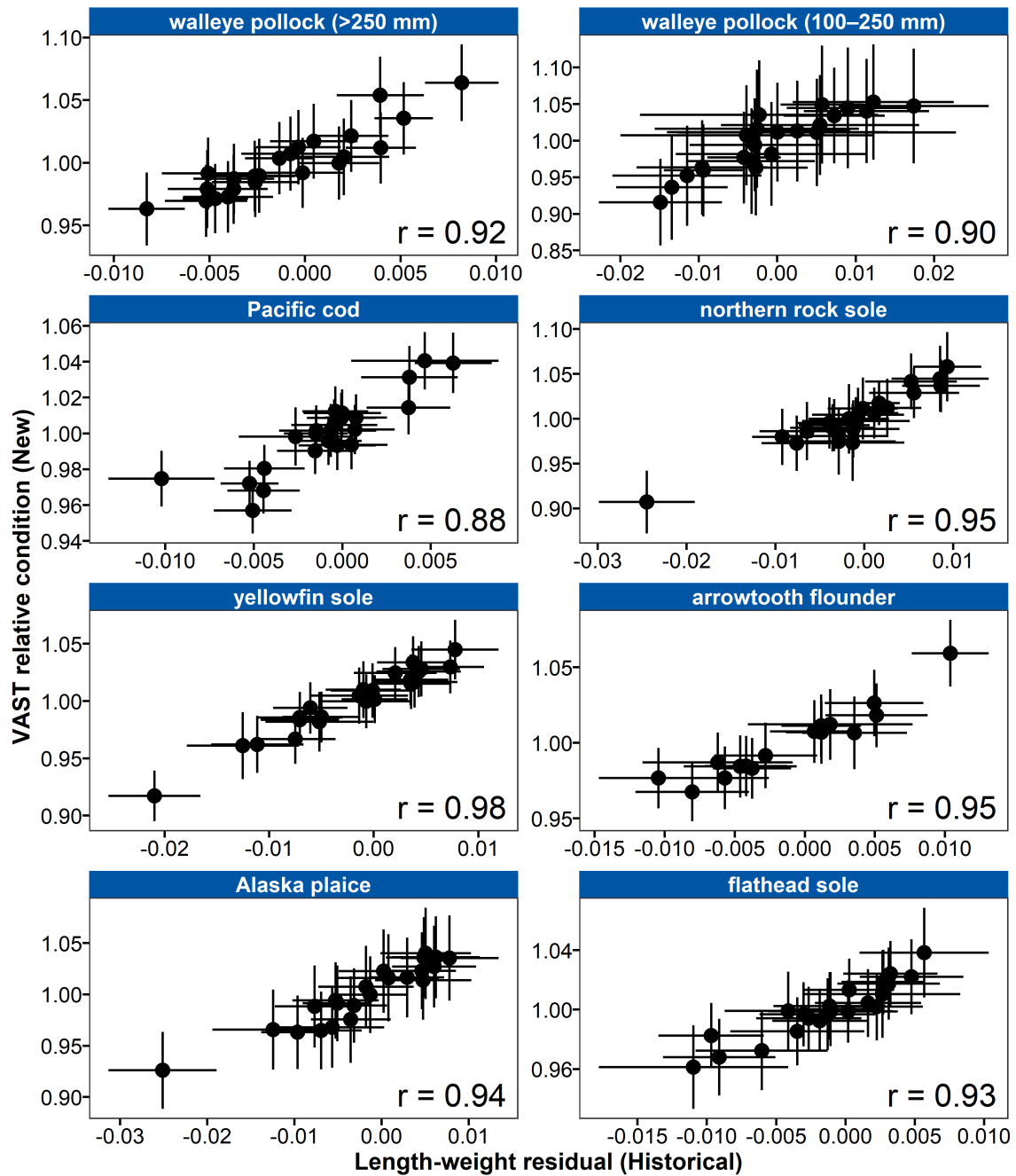


Figure 77: Length-weight residual condition versus VAST relative condition for the eastern Bering Sea. Points denote the mean, error bars denote two standard errors. The Pearson correlation coefficient ( $r$ ) is shown at the bottom right of each panel.

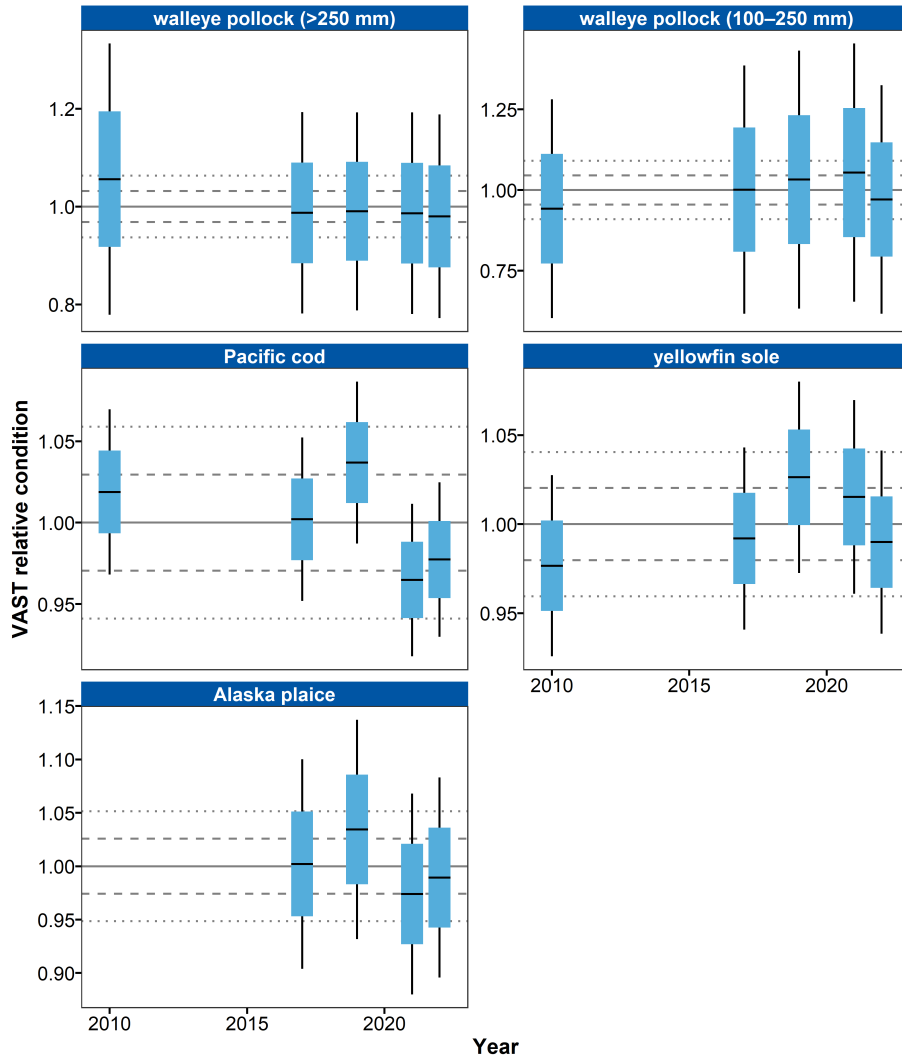


Figure 78: VAST relative condition for groundfish species collected during AFSC/RACE GAP summer bottom trawl surveys of the northern Bering Sea, 2010 and 2017 to 2022. The dash in the blue boxes denote the mean for that year, the box denotes one standard error, and the lines on the boxes denote two standard errors. Lines on each plot represent the historical mean, dashed lines denote one standard deviation, and dotted lines denote two standard deviations.

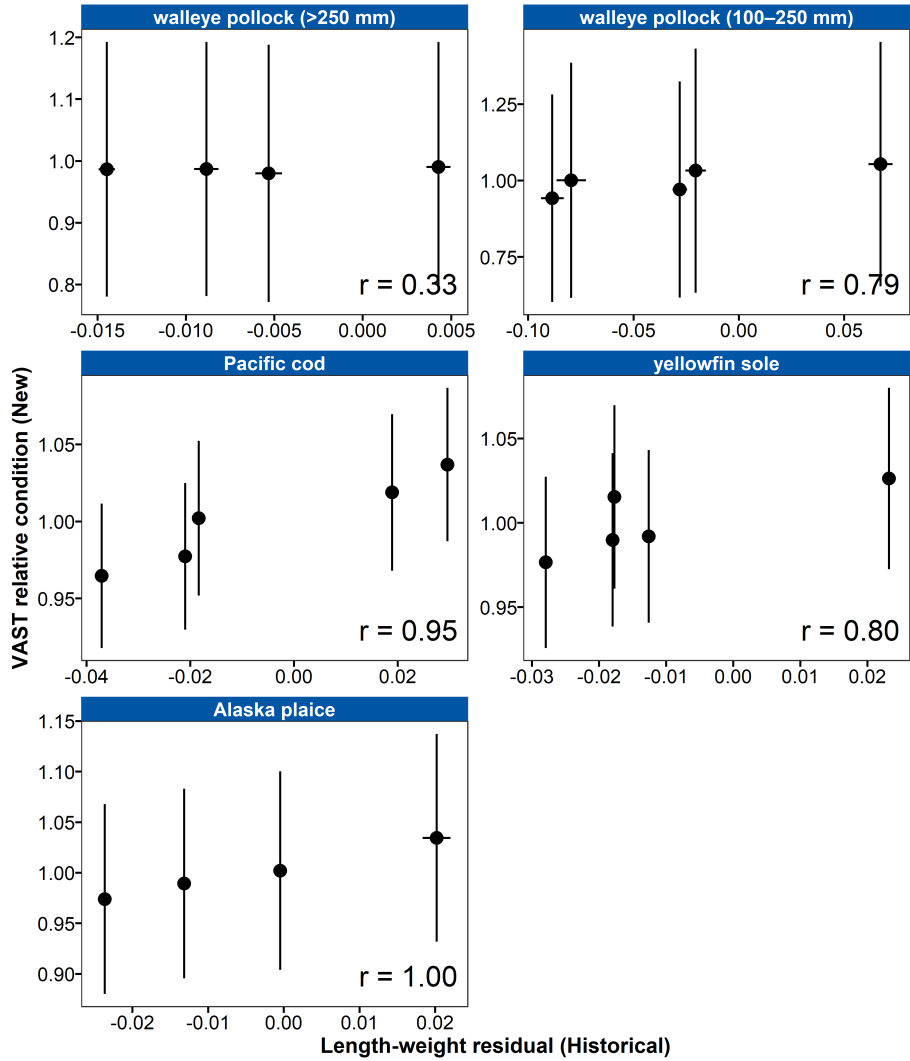


Figure 79: Length-weight residual condition versus VAST relative condition for the northern Bering Sea (NBS). Points denote the mean, error bars denote two standard errors. The Pearson correlation coefficient ( $r$ ) is shown at the bottom right of each panel. NBS length-weight residuals are not weighted by stratum biomass.

**Implications:** Fish morphometric condition can be considered an indicator of ecosystem productivity with implications for fish survival, maturity, and reproduction. For example, in Prince William Sound, the pre-winter condition of herring may determine their overwinter survival (Paul and Paul, 1999), differences in feeding conditions have been linked to differences in morphometric condition of pink salmon in Prince William Sound (Boldt and Haldorson, 2004), variation in morphometric condition has been linked to variation in maturity of sablefish (Rodgveller, 2019), and lower morphometric condition of Pacific cod was associated with higher mortality and lower growth rates during the 2014–2016 marine heat wave in the Gulf of Alaska (Barbeaux et al., 2020). Thus, the condition of EBS and NBS groundfishes may provide insight into ecosystem productivity as well as fish survival, demographic status, and population health. However, survivorship is likely affected by many factors not examined here.

Another important consideration is that fish condition was computed for all sizes of fishes combined, except in the case of walleye pollock. Examining condition of early juvenile stage fishes not yet recruited to the fishery, or the condition of adult fishes separately, could provide greater insight into the value of length-weight residuals as an indicator of individual health or survivorship (Froese, 2006), particularly since juvenile and adult walleye pollock exhibited opposite trends in condition in the EBS this year.

The near-average condition for most species in 2022 may be related to the near historical average temperatures observed. However, trends in recent years such as prolonged warmer water temperatures following the marine heat wave of 2014–2016 (Bond et al., 2015) and reduced sea-ice and cold pool areal extent in the eastern Bering Sea (Stabeno and Bell, 2019) may affect fish condition in ways that have yet to be determined. As we continue to add years of length-weight data and expand our knowledge of relationships between condition, growth, production, survival, and the ecosystem, these data may increase our understanding of the health of fish populations in the EBS and NBS.

*Research priorities:*

The new model-based condition indicator (VAST relative condition) will be further explored for biases and sensitivities to data, model structure, and parameterization. Research is also being planned and implemented across multiple AFSC programs to explore standardization of statistical methods for calculating condition indicators, and to examine relationships among putatively similar indicators of fish condition (i.e., morphometric, bioenergetic, physiological). Finally, we plan to explore variation in condition indices between life history stages alongside density dependence and climate change effects (Bolin et al., 2021; Oke et al., 2022).

## Patterns in Foraging and Energetics of Walleye Pollock, Pacific Cod, Arrowtooth Flounder, and Pacific Halibut

Contributed by Kirstin K. Holsman<sup>1</sup>, Cheryl Barnes<sup>1</sup>, Kerim Aydin<sup>1</sup>, Ben Laurel<sup>2</sup>, Tom Hurst<sup>2</sup>, Ron Heintz<sup>3</sup>

<sup>1</sup>NOAA Fisheries, Alaska Fisheries Science Center, Resource Ecology and Fishery Management Division

<sup>2</sup>NOAA Fisheries, Alaska Fisheries Science Center, Resource Assessment and Conservation Engineering Division

<sup>3</sup>Sitka Sound Science Center

Contact: kirstin.holsman@noaa.gov

**Last updated: November 2022**

**Description of indicator:** We report trends in metabolic demand from an adult bioenergetics model for groundfish in SEBS (Ciannelli et al., 1998; Holsman et al., 2019; Holsman and Aydin, 2015) and patterns in diet composition from the NOAA Fisheries Alaska Fisheries Science Center’s Food Habits database of fish diets collected during summer bottom trawl surveys in the eastern Bering Sea (EBS). This work is part of an in prep manuscript and the authors request that the images and data reported herein not be duplicated or shared outside of the ESR until the publication is complete. Bioenergetics-based indices were calculated for individual predator stomach samples using bioenergetics models. Samples were averaged by 5-cm predator bins across stations within a strata and then extrapolated to the population level using annual proportional biomass for each bin in each strata based on bottom trawl surveys (see Ciannelli et al. (1998); Holsman et al. (2019); Holsman and Aydin (2015), and Livingston et al. (2017) for more information).

Bioenergetic diet indices collectively indicate changes in foraging and growing conditions; relative foraging rate (RFR) reflects the ratio of observed food consumption (specific consumption rate; C\_ggd) to a theoretical temperature and size-specific maximum consumption rate from laboratory feeding experiments. Declines in this index can reflect decreases in prey availability or prey switching to more energetically valuable prey. Therefore we also present mean diet energy density (mnEDJ\_g) which reflects the average energetic density of prey in stomachs sampled from across the EBS in a given year. Less favorable foraging patterns would be reflected in declines in RFR when mnEDJ\_gg remains the same or also declines in a given year. Metabolic demand (R\_gg) generally increases with temperature and indicates the basal energetic requirements of the fish. Finally, scope for growth (G\_ggd) integrates metabolic demand, prey energy, and relative consumption rates to indicate how changes in temperature and foraging collectively influence (potential) growth.

**Status and trends:** We observe directional trends in consumption and potential growth that reflect climate driven changes to metabolic demand and trophic interactions and which indicate declining conditions for groundfish in the southeastern Bering Sea (SEBS) during and following anomalously warm conditions. All five indices suggest poor conditions for Walleye pollock (*Gadus chalcogrammus*; hereafter “pollock”) and Pacific cod (*Gadus macrocephalus*) in recent years relative to historical rates (1982–2010).

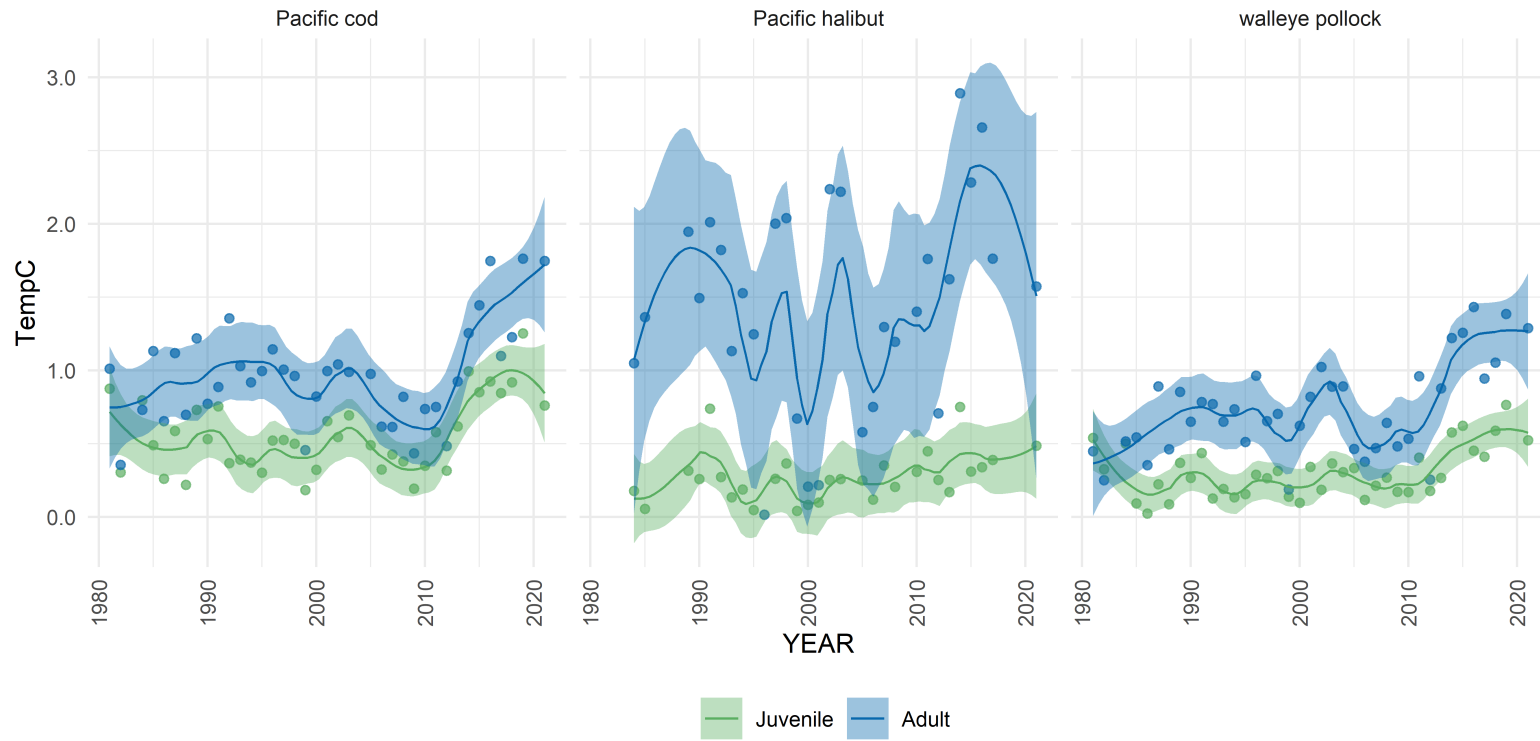


Figure 80: Average biomass weighted (by strata) thermal experience (TempC) for juvenile and adult fish. Data is based on biomass-weighted bottom temperature for samples collected during the AFSC bottom-trawl summer surveys.

Thermal experience (biomass weighted bottom temperature) of all four groundfish species in the SEBS has increased in recent years (Figure 80), with Pacific cod and pollock recent thermal experience remaining near the highest levels in the 30+ year time series. Relative energetic demand of pollock, Pacific cod, and Pacific halibut (*Hippoglossus stenolepis*; hereafter “halibut”) reflect climate-driven changes to metabolic demand with marked increases in metabolic demand since 2005–2010 (“R\_ggd” for respiration). Accordingly, metabolic demand for (juvenile and adult) pollock and Pacific cod continues to increase relative to historical (1982–2010) rates with 2015–2021 rates approximately 20%, 19%, and 25% higher than historical (1982–2010) baseline values for pollock, Pacific cod, and halibut, respectively.

Meanwhile, relative foraging rates for juvenile pollock and Pacific cod declined markedly in recent years (2015–2019) relative to historical rates (1982–2010) but rebounded slightly in 2021 with cooler conditions. Relative to historical baseline rates, average relative foraging rates over the past 5 years changed by 9% and -15% for juvenile pollock and Pacific cod, respectively (Figure 81).

The mean energetic value of sampled diets dropped during and following recent anomalously warm years (2015–2019) but has rebounded slightly in 2021 reflecting a shift to more energetically valuable prey. Mean energetic density of prey for pollock and Pacific cod is approximately 27% higher than historical baseline years (1982–2010). The integrated outcome of these changes is an overall decline in scope for growth for both pollock and juvenile Pacific cod over time (Figure 81), especially for juvenile Pacific cod, where in recent years scope for growth remains below the long-term average (1982-2010; Figure 82).

**Factors influencing observed trends:** Metabolic demands for ectothermic fish like pollock, Pacific cod, Arrowtooth flounder, and halibut are largely a function of thermal experience and body size and tend to increase exponentially with increasing temperatures. Fish can minimize metabolic costs through behaviors such as movement to thermally optimal temperatures, or can increase consumption of food energy to meet increasing metabolic demands. The latter requires sufficient access to abundant or high energy prey resources.

**Implications:** For both species in the EBS during recent anomalously warm years, metabolic demands were elevated while foraging rates and scope for growth were reduced (Figures 80 and 81), this pattern was most pronounced for juvenile and adult pollock, and juvenile Pacific cod (Figure 82). This has important implications, as to offset metabolic demands these fish would have had to (1) consume more food or more energetically rich food, (2) access energetic reserves leading to net body mass loss, or (3) move to more energetically favorable foraging grounds. There are a few lines of evidence to support all three of these potential responses to climate-driven changes in the EBS, including observations of large numbers of Pacific cod in the NEBS surveys in 2017–2019.

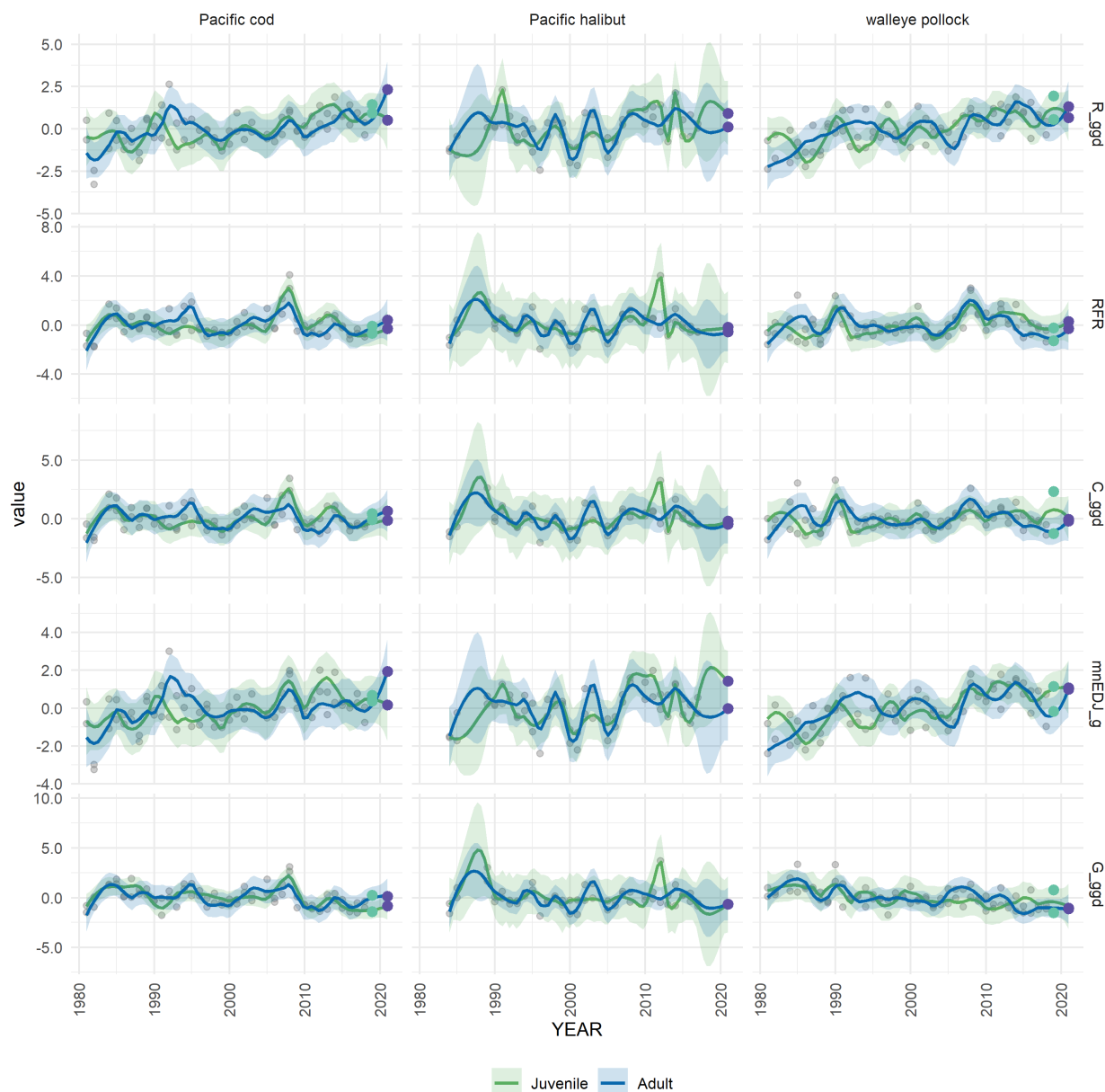


Figure 81: Normalized (i.e., Z-score scaled) bioenergetic diet indices for groundfish species over time including relative foraging rate (RFR), specific consumption rate ( $C_{\text{ggd}}$ ), mean diet energy density ( $\text{mnEDJ}_g$ ), scope for growth ( $G_{\text{ggd}}$ ), and metabolic demand ( $R_{\text{ggd}}$ ). Mean values for each year and bin are shown as light gray points, recent years are highlighted as larger points for reference. The spline represents a loess smoother for juvenile and adult fish. Data is based on strata biomass-weighted indices for samples collected during NOAA NMFS AFSC bottom-trawl summer surveys.

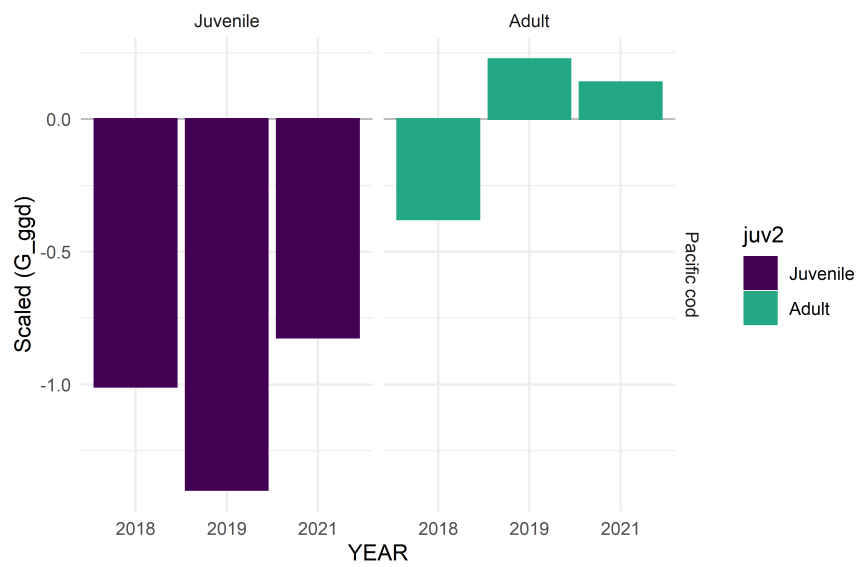


Figure 82: Normalized (i.e., Z-score scaled) bioenergetic (potential) scope for growth ( $G_{ggd}$ ) for juvenile and adult fish in recent years. Data is based on strata biomass-weighted indices for samples collected during NOAA NMFS AFSC bottom-trawl summer surveys.

## Multispecies Model Estimates of Time-varying Natural Mortality

Contributed by Kirstin K. Holsman, Jim Ianelli, Kerim Aydin, Kalei Shotwell, Kelly Kearney, Ingrid Spies, Steve Barbeaux, and Grant Adams

Resource Ecology and Fishery Management Division, Alaska Fisheries Science Center, National Marine Fisheries Service, NOAA

Contact: [kirstin.holsman@noaa.gov](mailto:kirstin.holsman@noaa.gov)

**Last updated: November 2022**

**Description of indicator:** We report trends in age-1 total mortality for Walleye pollock (*Gadus chalcogrammus*, ‘pollock’), Pacific cod (*Gadus macrocephalus*, ‘P. cod’) and Arrowtooth flounder (*Atheresthes stomias*, ‘Arrowtooth’) from the eastern Bering Sea. Total mortality rates are based on residual mortality inputs (M1) and model estimates of annual predation mortality (M2) produced from the multi-species statistical catch-at-age assessment model (known as CEATTLE; Climate-Enhanced, Age-based model with Temperature-specific Trophic Linkages and Energetics). See Appendix 1 of the BSAI pollock stock assessment for 2022 as well as Holsman et al. (2016), Holsman and Aydin (2015), Ianelli et al. (2016), and Jurado-Molina et al. (2005) for more information.

**Status and trends:** The CEATTLE model estimates of age-1 natural mortality (i.e., M1+M2) for pollock, P. cod, and Arrowtooth continue to decline from the 2016 peak mortality. For all three species, age-1 predation mortality rates have remained similar to 2021. At  $1.43 \text{ yr}^{-1}$ , age-1 mortality estimated by the model was greatest for pollock and lower for P. cod and Arrowtooth, with total age-1 natural mortality at approximately  $0.67$  and  $0.64 \text{ yr}^{-1}$  for P. cod and Arrowtooth, respectively. The 2022 age-1 natural mortality across species is 10% to 40% lower than in 2016 and is near average for pollock (relative to the long-term mean) (Figure 83). Similarly, P. cod and Arrowtooth age-1 mortality are well below the long-term mean.

Patterns in the total biomass of each species consumed by all three predators in the model (typically 1–3 yr old fish) is similar to patterns in age-1 natural mortality but with slight differences in 2022. Pollock and Arrowtooth biomass consumed by all predators in the model is approximately equal to the long-term average and slightly higher than that of 2021, while P. cod biomass consumed is well below average (Figure 84).

**Factors influencing observed trends:** Temporal patterns in natural mortality reflect annually varying changes in predation mortality that primarily impact age-1 fish (and to a lesser degree impact ages 2 and 3 fish in the model). Pollock are primarily consumed by older conspecifics, and pollock cannibalism accounts for 60% (on average) of total age-1 predation mortality, with the exception of the years 2006–2008 when predation by Arrowtooth marginally exceeded cannibalism as the largest source of predation mortality of age-1 pollock (Figure 85). The relative proportion of age-1 pollock consumed by older pollock and Arrowtooth increased slightly in 2022, while the relative proportion consumed by P. cod declined slightly.

Combined annual predation demand (annual ration) of pollock, P. cod, and Arrowtooth in 2022 was 8.63 million tons, down slightly from the 9.77 million t annual average during the warm years and large maturing cohorts of 2014–2016 (note there is an increase in this estimate relative to the 2021 index that reflects increased predation accounted for in the 2022 assessment from the inclusion of NBS survey data (2010, 2017–2019, 2022)). Pollock represent approximately 79% of the model estimates of combined prey consumed with a long-term average of 5.48 million tons of pollock consumed annually by all three predators in the model. From 2015–2019, individual annual rations were above average for all three predator species, driven by anomalously warm water temperatures in the eastern Bering Sea during those years. However, cooler temperatures in 2022 have resulted in annual rations at or below the long-term average (Figure 86).

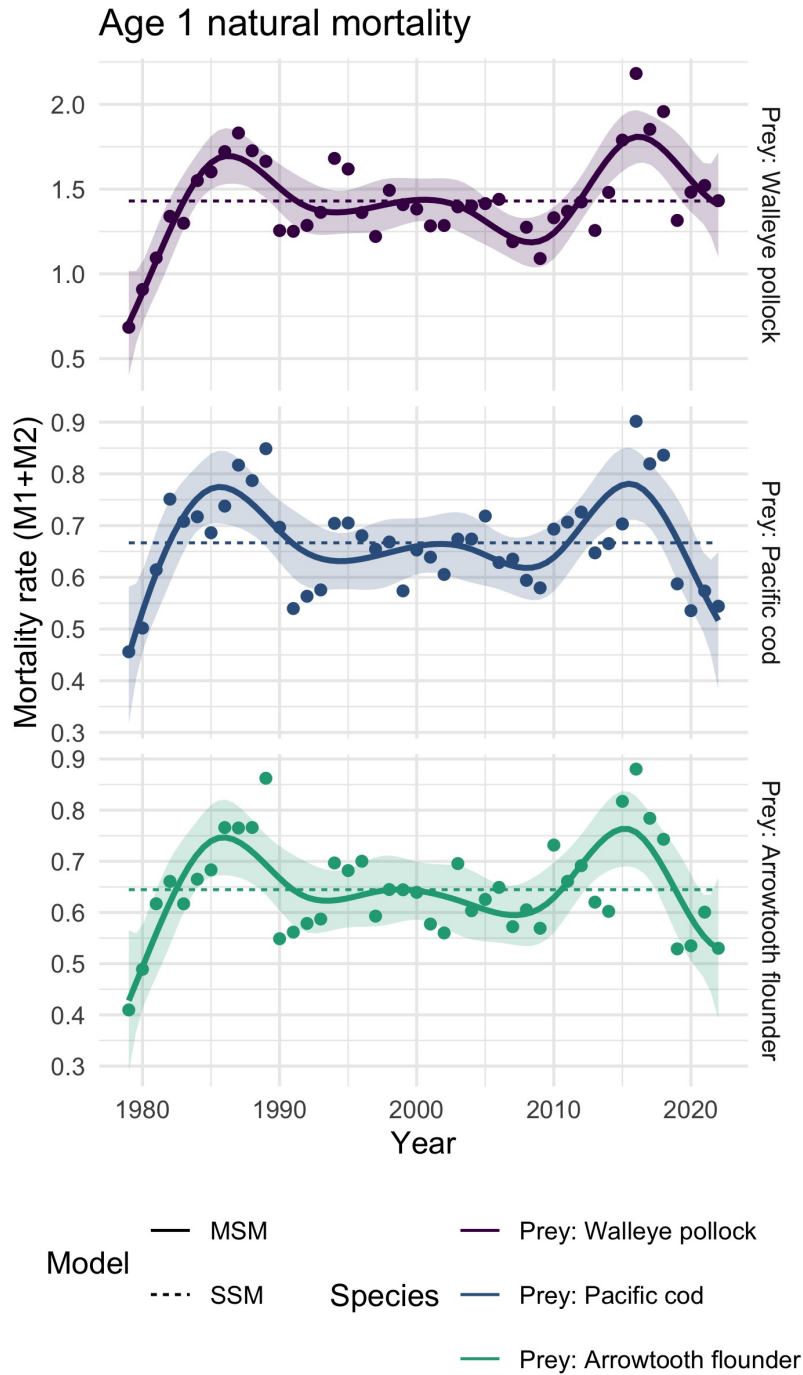


Figure 83: Annual variation in total mortality ( $M_{1i1} + M_{2i1,y}$ ) of age-1 pollock (as prey) (a), age-1 P. cod (as prey) (b), and age-1 Arrowtooth (as prey) (c) from the single-species models (dashed gray line) and the multi-species models with temperature (black line). Updated from Holsman et al. (2016); more model detail can be found in Appendix 1 of the BSAI pollock stock assessment for 2022. Solid lines are a 10-y (symmetric) loess polynomial smoother indicating trends in age-1 mortality over time.

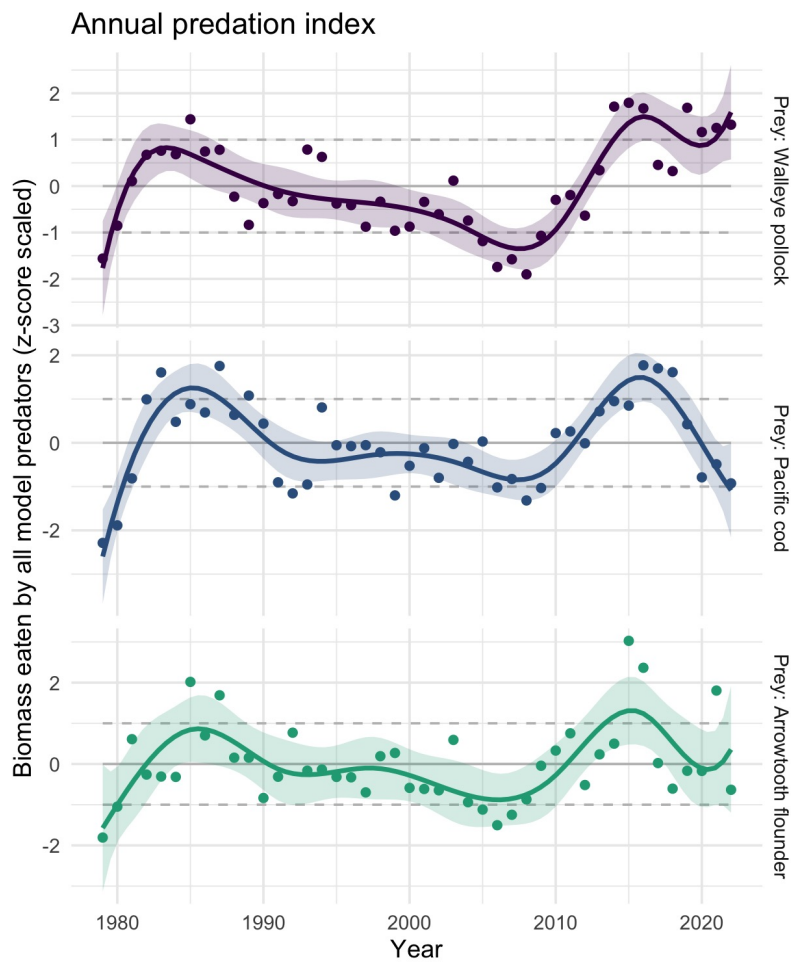


Figure 84: Multispecies estimates of prey species biomass consumed by all predators in the model: a) total biomass of pollock consumed by predators annually; b) total biomass of P. cod consumed by predators annually; c) total biomass of Arrowtooth consumed by predators annually. Gray lines indicate 1979–2022 mean estimates for each species; dashed lines represent 1 standard deviation of the mean. Solid lines are a 10-y (symmetric) loess polynomial smoother indicating trends in biomass consumed over time.

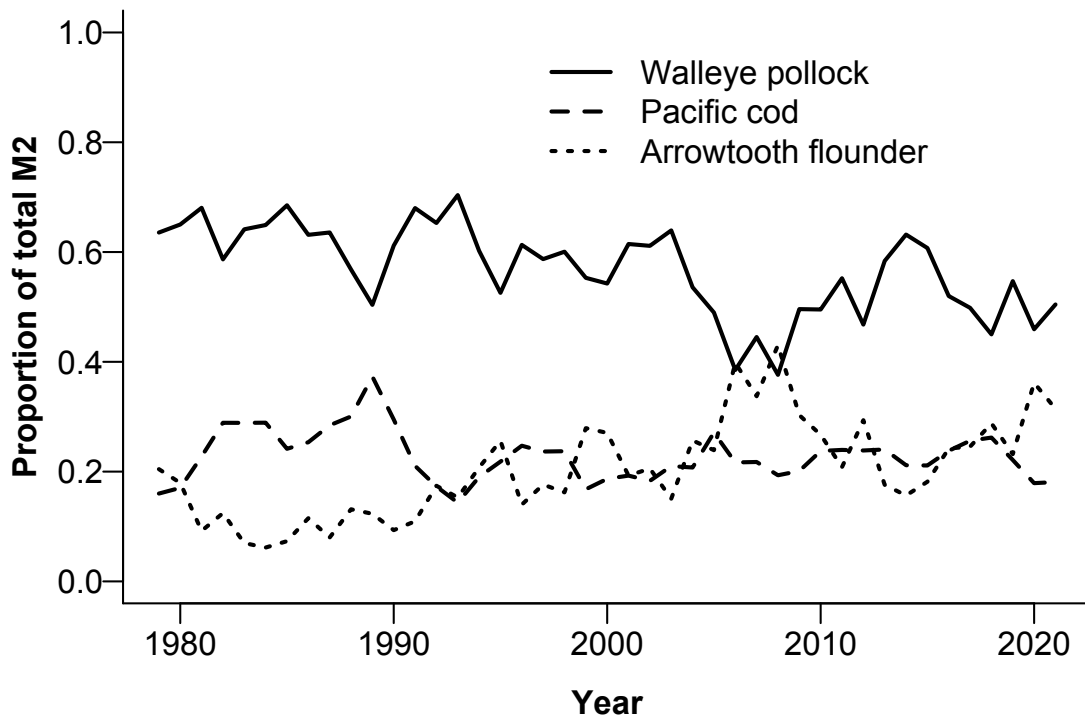


Figure 85: Proportion of total predation mortality for age-1 pollock from pollock (solid), P. cod (dashed), and Arrowtooth (dotted) predators across years. Updated from Holsman et al. (2016); more model detail can be found in Appendix 1 of the BSAI pollock stock assessment for 2022.

**Implications:** We find evidence of continued declines in predation mortality of age-1 pollock, P. cod, and Arrowtooth relative to recent high predation years (2014–2016). While warm temperatures continue to lead to high metabolic (and energetic) demand of predators 2016–2021, declines in total predator biomass are contributing to a net decrease in total consumption (relative to 2016) and therefore reduced predation rates and mortality in 2020–2022. In 2022, cooler conditions have further driven declines in annual predation of age-1 fish. This pattern indicates improving top-down conditions for juvenile groundfish survival in 2021 through predator release due to declining biomass of groundfish and more favorable thermal conditions in 2022.

Between 1980 and 1993, relatively high natural mortality rates for pollock reflect patterns in combined annual demand for pollock prey by all three predators that was highest in the mid 1980’s (collectively 9.37 million t per year). The peak in predation mortality of age-1 pollock in 2016 corresponds to warmer than average conditions and higher than average energetic demand of predators combined with the maturation of the large 2010–2012 year classes of pollock and P. cod (collectively with Arrowtooth 9.79 million t per year).

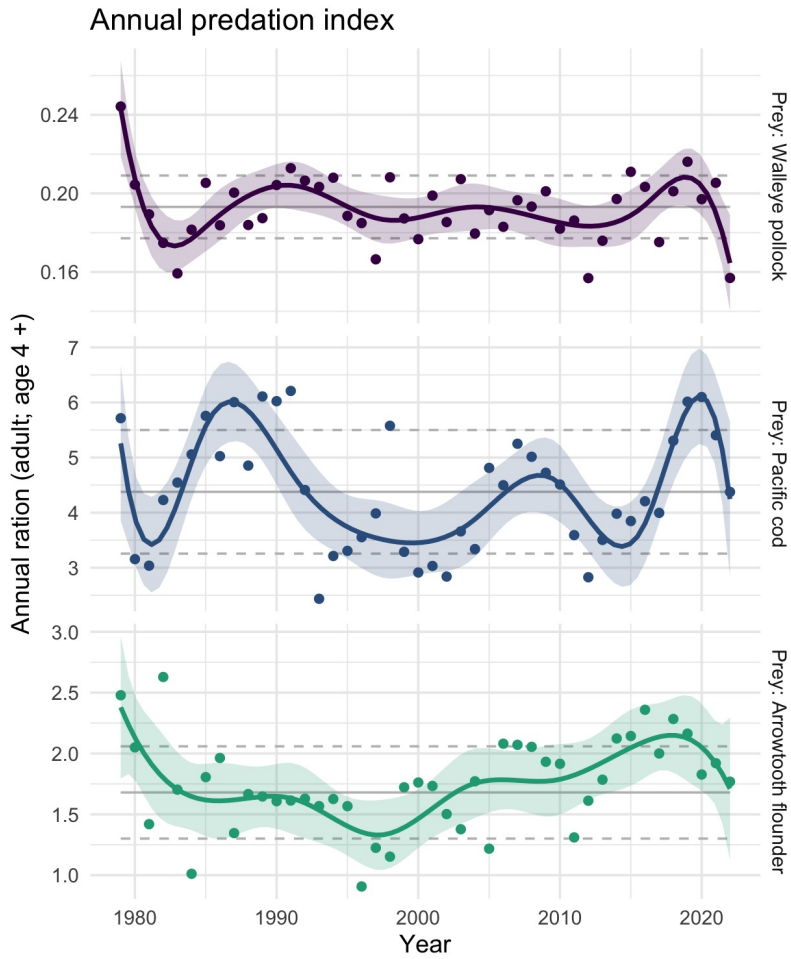


Figure 86: Multispecies estimates of annual ration (kg consumed per individual per year) for adult (age-4+) predators: a) pollock, b) P. cod, and c) Arrowtooth. Gray lines indicate 1979–2022 mean estimates for each species; dashed lines represent 1 standard deviation of the mean. Solid lines are a 10-y (symmetric) loess polynomial smoother indicating trends in ration over time.

# Groundfish Recruitment Predictions

## Temperature Change Index and the Recruitment of Bering Sea Pollock

Contributed by Ellen Yasumiishi

Auke Bay Laboratories, Alaska Fisheries Science Center, NOAA Fisheries

Contact: ellen.yasumiishi@noaa.gov

Last updated: July 2022

**Description of indicator:** The temperature change (TC) index is a composite index for the pre- and post-winter thermal conditions experienced by Walleye pollock (*Gadus chalcogrammus*) from age-0 to age-1 in the southeastern Bering Sea (Martinson et al., 2012). The TC index (year t) is calculated as the difference in the average monthly sea surface temperature in June (t+1) and August (t) (Figure 87) in an area of the southern region of the eastern Bering Sea (56.2°N to 58.1°N by 166.9°W to 161.2°W). Time series of average monthly sea surface temperatures were obtained from the NOAA Earth System Research Laboratory Physical Sciences Division website. Sea surface temperatures were based on NCEP/NCAR gridded reanalysis data (Kalnay et al. (1996), data obtained from <http://www.esrl.noaa.gov/psd/cgi-bin/data/timeseries/timeseries1.pl> (accessed July 25, 2022)). We specify Variable SST and Analysis level Monolevel Variables. Less negative values represent a cool late summer during the age-0 phase followed by a warm spring during the age-1 phase for pollock.

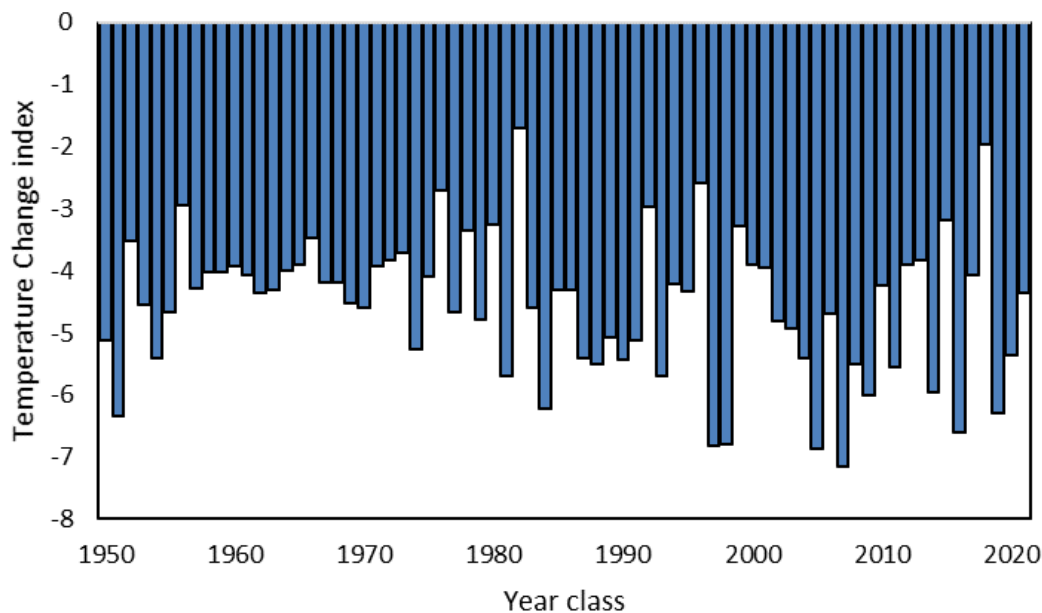


Figure 87: The Temperature Change index values for the 1950 to 2021 year classes of pollock. Values represent the differences in sea temperatures on the southeastern Bering Sea shelf experienced by the 1950–2021 year classes of pollock. Less favorable conditions (more negative values) represent a warm summer during the age-0 life stage followed by a relatively cool spring during the age-1 life stage. More favorable conditions (less negative values) represent a cool summer during the age-0 life stage followed by a relatively warm spring during the age-1 life stage.

**Status and trends:** The 2021 year class TC index value is -4.36, higher than the 2020 year class TC index value of -5.37, indicating slightly improved conditions for pollock survival from age-0 to age-1 from 2021 to 2022 than from 2020 to 2021. The average expected survival is due to the smaller relative difference in sea temperature from late summer (warm) to the following spring (warm). The late summer sea surface temperature (August 10.8°C) in 2021 was 0.9°C higher than the longer-term average (9.9°C) and spring sea temperature (June 6.4°C) in 2022 was warmer than the long-term average of 5.3°C in spring since 1949.

**Factors causing observed trends:** According to the original Oscillating Control Hypothesis (OCH), warmer spring temperatures and earlier ice retreat led to a later oceanic and pelagic phytoplankton bloom and more food in the pelagic waters at an optimal time for use by pelagic species (Hunt et al., 2002). The revised OCH indicated that age-0 pollock were more energy-rich and have higher overwintering survival to age-1 in a year with a cooler late summer (Coyle et al., 2011; Heintz et al., 2013). Therefore, the warmer later summers during the age-0 phase followed by warmer spring temperatures during the age-1 phase are assumed average for the survival of pollock from age-0 to age-1. The 2021 year class of pollock experienced above-average summer temperatures in 2021 during the age-0 stage and a warm spring in 2022 during the age-1 stage indicating average conditions for overwintering survival from age-0 to age-1.

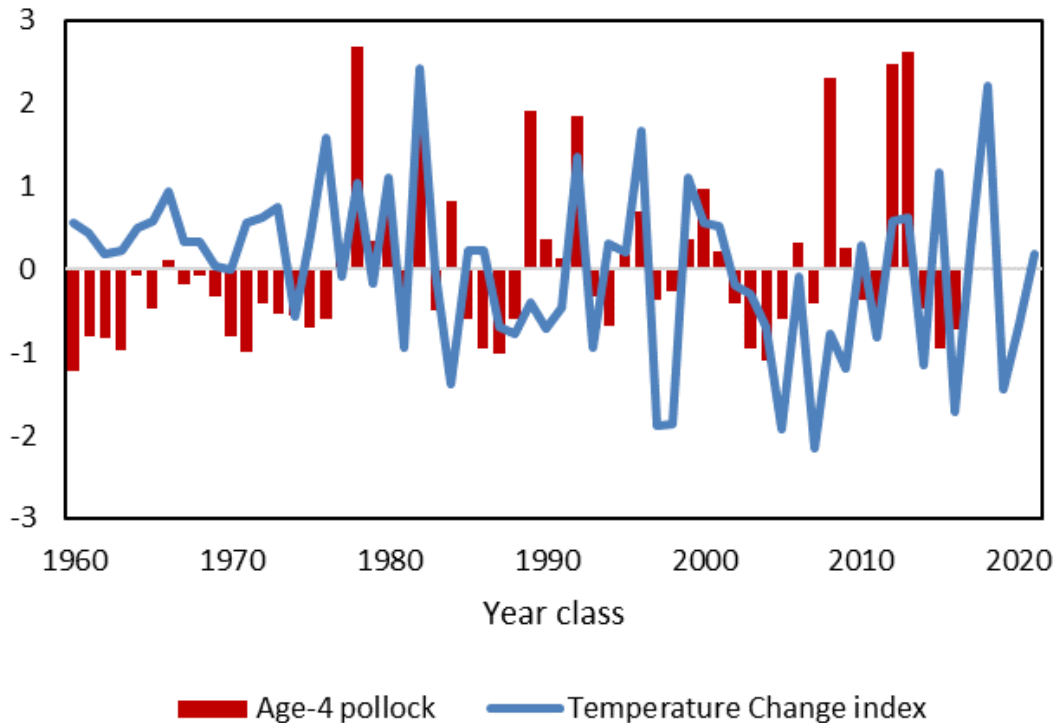


Figure 88: Normalized time series values of the temperature change index indicating conditions experienced by the 1960–2021 year classes of pollock during the summer age-0 and spring age-1 life stages. Normalized values of the estimated abundance of age-4 pollock in the southeastern Bering Sea from 1964–2021 for the 1960–2017 year classes. Age-4 pollock estimates are from Table 29 in Ianelli et al. (2020). The TC index indicates average conditions for the 2021 year class of pollock.

**Implications:** The 2021 TC index value of -4.36 was similar to the long-term average of -4.59, therefore we expect average recruitment of pollock to age-4 in 2025 from the 2021 year class (Figure 88).

## Large Copepod Abundance (Sample-Based and Modeled) as an Indicator of Pollock Recruitment to Age-3 in the Southeastern Bering Sea

Contributed by Ellen Yasumiishi<sup>1</sup>, Lisa Eisner<sup>1</sup>, and David Kimmel<sup>2</sup>

<sup>1</sup>Auke Bay Laboratories, Alaska Fisheries Science Center, NOAA Fisheries

<sup>2</sup>Resource Assessment and Conservation Engineering Division, Alaska Fisheries Science Center, NOAA Fisheries

Contact: Ellen.Yasumiishi@noaa.gov

**Last updated: August 2022**

**Description of indicator:** Interannual variations in large copepod abundance during the age-0 pollock life stage were compared to age-3 pollock (*Gadus chalcogrammus*) abundance for the 2002–2018 year classes on the southeastern Bering Sea shelf, south of 60°N, <200m bathymetry (Eisner et al., 2020). The large copepod index sums the abundances of *Calanus marshallae/glacialis* (copepodite stage 3 (C3)–adult), *Neocalanus* spp. (C3–adult), and *Metridia pacifica* (C4–adult), taxa important in age-0 pollock diets (Coyle et al., 2011). Zooplankton samples were collected with oblique bongo tows using 60 cm, 505  $\mu\text{m}$  mesh nets for 2002–2011, and 20 cm, 153  $\mu\text{m}$  mesh or 60 cm, 505  $\mu\text{m}$  nets, depending on taxa and stage for 2012–2020.

Data were collected on the BASIS surveys (2002–2012, 2014–2016, 2018) and along the 70-m isobath (2002–2012, 2014–2020) during August and September for four warm (2002–2005), one average (2006), six cold (2007–2012), four warm (2014–2016, 2018), and an average (2017, 70-m isobath only) year using methods in Eisner et al. (2014) and Kimmel et al. (2018). Zooplankton data were not available for 2013. Age-3 pollock abundance was obtained from the stock assessment report for the 2002–2018 year classes (Ianelli et al., 2021). Two estimates of large copepod abundances from the BASIS survey data were calculated, the first using means among stations (sample-based), and the second using the means estimated from the geostatistical VAST model, package version 13.0.1 (Thorson et al., 2015). We specified 30 knots, a log normal distribution, and the delta link function between probability of encounter and positive catch rate in VAST.

**Status and trends:** Positive significant relationships were found between large copepods collected during the age-0 stage of pollock (2002–2018 year classes) and stock assessment estimates of age-3 pollock three years later (2005–2021). For the BASIS survey, the stronger relationship of age-3 pollock with the large copepod index using the VAST model compared to observed means among stations ( $r^2=0.57$  vs.  $r^2=0.27$ ) is partially due to the VAST model filling in data for survey areas missed in some years (e.g., 2008). The copepod index from the 70-m isobath explained 42% of the variation in the stock assessment estimates of pollock (Figure 89).

Fitted means and standard errors of the age-3 pollock abundances were estimated from the linear regression model using large copepod estimates from the BASIS VAST means and BASIS and 70-m isobath sample based means, and compared to the pollock stock assessment estimates from Ianelli et al. (2021) (Figure 90). Copepod indices were similar to estimates of age-3 pollock for the 2017 year class but under estimated age-3 pollock for the 2018 year class relative to the stock assessment estimates, indicating additional mechanisms driving the recruitment of pollock to age-3 for the 2018 year class. Copepod indices from the 70-m isobath during 2019 and 2020 predict below-average recruitment of age-3 pollock in 2022 and 2023.

**Factors influencing observed trends:** Increases in sea-ice extent and duration were associated with increases in large zooplankton abundances on the shelf (Eisner et al., 2014, 2015, 2020), increases in large copepods and euphausiids in pollock diets (Coyle et al., 2011) and increases in age-0 pollock lipid content (Heintz et al., 2013). The increases in sea ice and associated ice algae and phytoplankton may provide an early food source for large crustacean zooplankton reproduction and growth (Baier and Napp, 2003; Hunt et al., 2011). These large zooplankton taxa contain high lipid concentrations (especially in cold, high-ice years) which in turn increases the lipid content in their predators such as age-0 pollock and other fish that forage on these taxa. Increases in energy density (lipids) in age-0 pollock allow them to survive their first winter (a time of high mortality) and eventually recruit into the fishery. Accordingly, a strong relationship has been shown for energy density in age-0 fish and age-3 pollock abundance (Heintz et al., 2013).

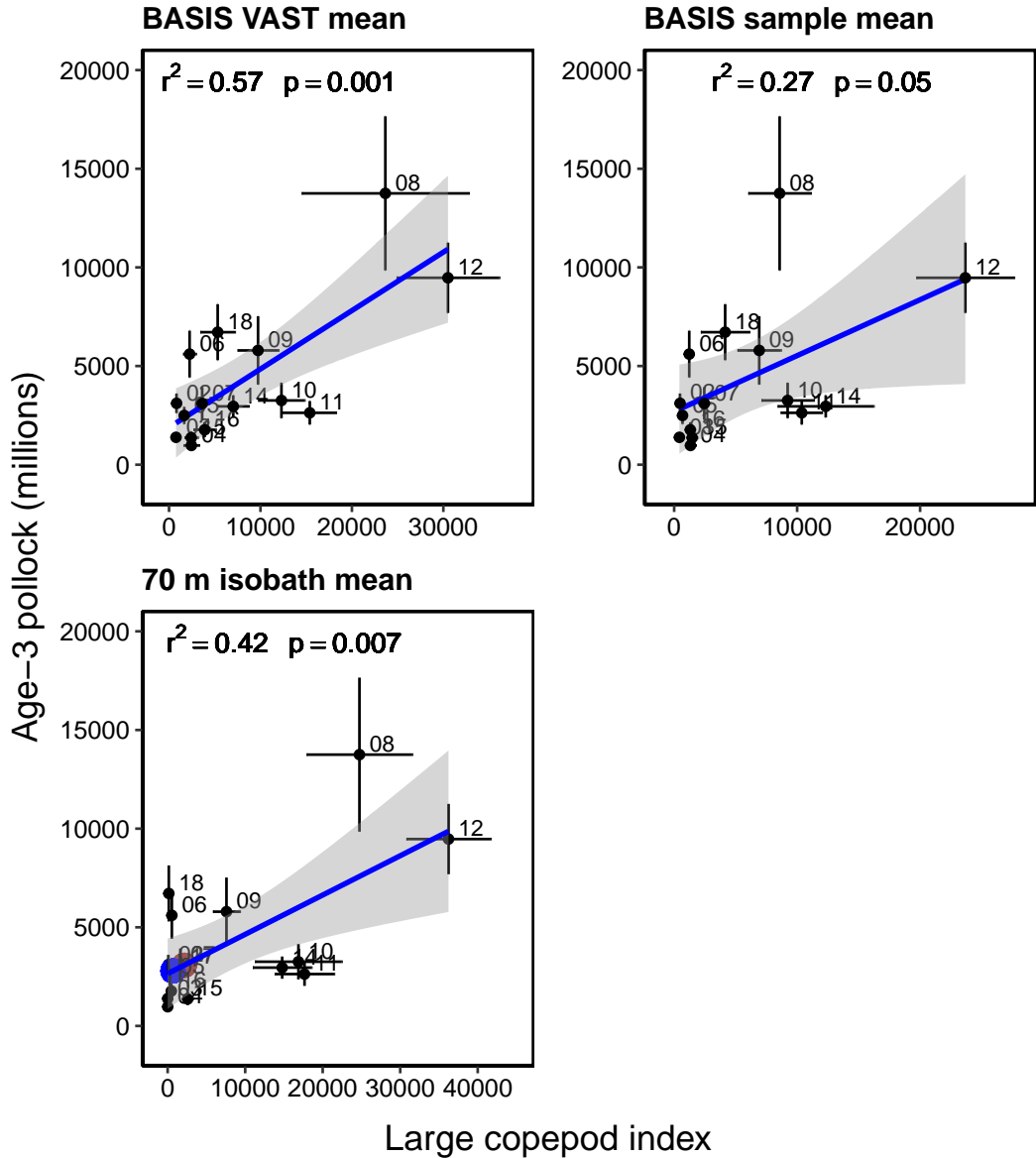


Figure 89: Linear relationships between sample-based (top) from the BASIS and 70-m isobath surveys and BASIS VAST-model (bottom) estimated mean abundance of large copepods (C+MN, sum of *Calanus marshallae/glacialis*, *Metridia pacifica*, and *Neocalanus* spp.) during the age-0 life stage of pollock, and the estimated abundance (millions) of age-3 pollock from Ianelli et al. (2021) for 2002–2018 year classes. No zooplankton data were available for 2013. Dots represent the predicted pollock values based on the 70-m isobath large copepod index for year-classes 2018 (brown) and 2019 (blue).

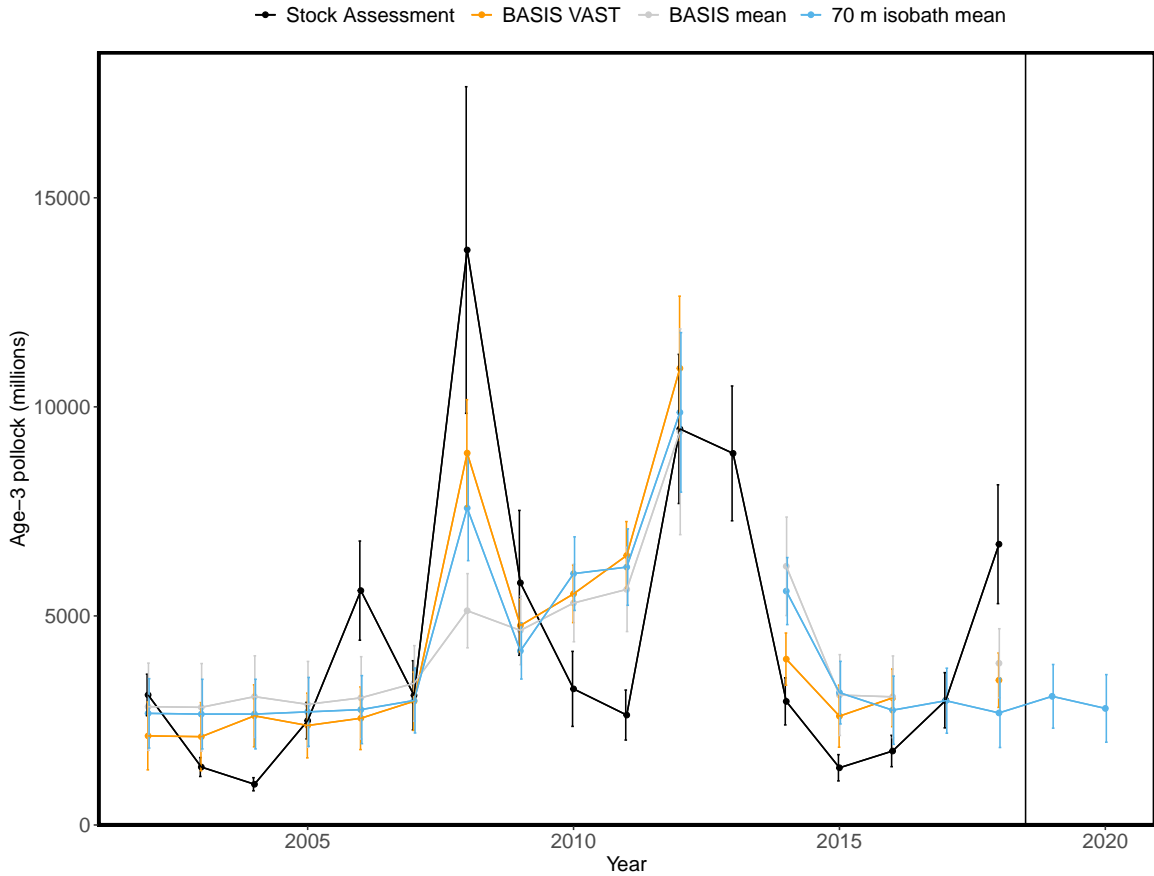


Figure 90: Fitted means and standard errors of the age-3 pollock abundance estimated from the linear regression models using VAST estimates of large copepods (orange), sample mean abundance of large copepods from BASIS (gray) and at the 70-m isobath stations (blue), and means from the pollock stock assessment estimates (black) from Ianelli et al. (2021). Predicted estimates of age-3 pollock (recruited into fishery as age 3's in 2022 and 2023) based on data from the 70-m isobath are shown for the 2019 and 2020 year classes.

**Implications:** Our results suggest low availability of large copepod prey for age-0 pollock during the first year of life in 2019 and 2020. These conditions may not be favorable for age-0 pollock overwinter survival and recruitment to age-3. However, in 2018 there was an increase in euphausiids in BASIS age-0 pollock diets (Andrews III et al., 2019), which may have compensated for the lack of large copepods, and enhanced overwinter survival and subsequent recruitment of the 2018 year class. Information from the 70-m isobath survey may be useful in years without a BASIS survey in the southeast Bering Sea. If the relationship between large copepods and age-3 pollock remains significant in our analysis, the index can be used to predict the recruitment of pollock three years in advance of recruiting to age-3, from zooplankton data collected three years prior. This relationship also provides further support for the revised oscillating control hypothesis that suggests as the climate warms, reductions in the extent and duration of sea ice could be detrimental large crustacean zooplankton and subsequently to the pollock fishery in the southeastern Bering Sea (Hunt et al., 2011).

# Benthic Communities and Non-target Fish Species

## Miscellaneous Species - Eastern Bering Sea Shelf

Contributed by Thaddaeus Buser

Resource Assessment and Conservation Engineering Division, Alaska Fisheries Science Center

National Marine Fisheries Service, NOAA

Contact: thaddaeus.buser@noaa.gov

Last updated: September 2022

**Description of indicator:** “Miscellaneous” species fall into three groups: eelpouts (fishes of the Family Zoarcidae), poachers (fishes of the Family Agonidae), and sea stars (Class Asteroidea). The three species comprising the majority of the eelpout group are the wattled eelpout (*Lycodes palearis*) and shortfin eelpout (*L. brevipes*) and to a lesser extent the marbled eelpout (*L. varidens*). The biomass of poachers is dominated by a single species, the sturgeon poacher (*Podothecus acipenserinus*) and to a lesser extent the sawback poacher (*Leptagonus frenatus*). The composition of sea stars in shelf trawl catches are dominated by the purple-orange sea star (*Asterias amurensis*), which is found primarily in the inner/middle shelf regions, and the common mud star (*Ctenodiscus crispatus*), which is primarily an inhabitant of the outer shelf. Relative CPUE by weight (kg per hectare) was calculated and plotted for each species or species group by year for 1982–2022. Relative CPUE was calculated by setting the largest biomass in the time series to a value of 1 and scaling other annual values proportionally. The standard error ( $\pm 1$ ) was weighted proportionally to the CPUE to produce a relative standard error.

**Status and trends:** The 2022 relative CPUE estimate for eelpouts showed a modest increase from 2021, just above the average of the estimates over the last 10 years. For poachers, CPUE increased marginally ( $\sim 12\%$ ) from 2021, continuing an increasing trend following the multiyear decrease observed from 2015 to 2018. The 2022 poacher estimate matches the average for the time series. The sea stars, as a group, increased by  $\sim 3\%$  from 2021 to 2022, and the 2022 CPUE ranked as the 2<sup>nd</sup> highest since 1982, continuing an overall increasing trend that started in 2013 (Figure 91).

**Factors causing observed trends:** Determining whether these trends represent real responses to environmental change or are simply an artifact of standardized survey sampling methodology (e.g., temperature-dependent catchability) will require more specific research on survey trawl gear selectivity relative to inter-annual differences in bottom temperatures and on the life history characteristics of these epibenthic species.

**Implications:** Eelpouts have important roles in the energy flow within benthic communities. For example, eelpouts are a common prey item of Arrowtooth flounder (*Atheresthes stomias*). However, it is not known at present whether these changes in CPUE are related to changes in energy flow.

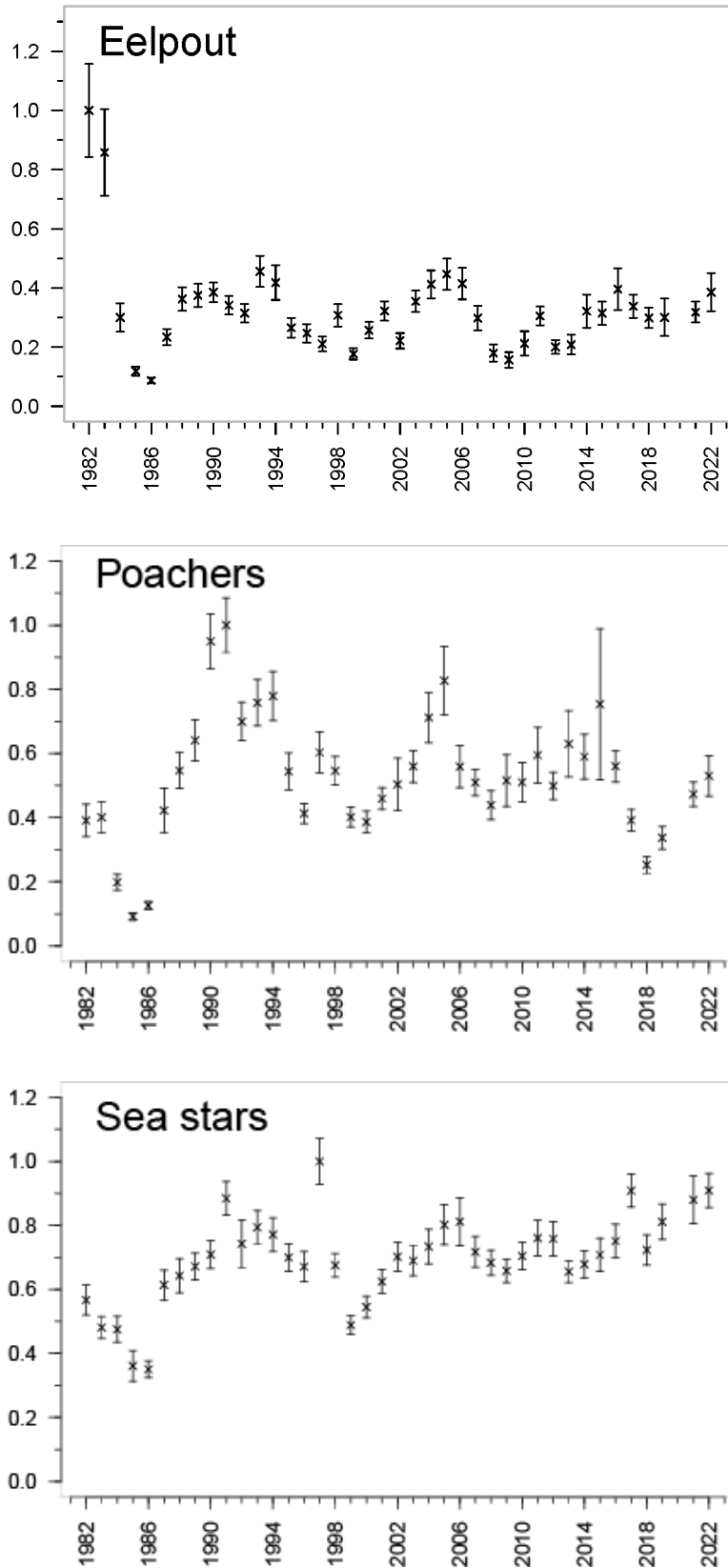


Figure 91: AFSC eastern Bering Sea shelf bottom trawl survey relative CPUE for miscellaneous fish species during the May to August time period from 1982–2022.

## Eastern Bering Sea Commercial Crab Stock Biomass Indices

Contributed by Jon Richar

Kodiak Laboratory, Alaska Fisheries Science Center, National Marine Fisheries Service, NOAA

Contact: jon.richar@noaa.gov

**Last updated: September 2022**

**Description of indicator:** This indicator is the commercial crab species biomass time series in the eastern Bering Sea. The eastern Bering Sea bottom trawl survey has been conducted annually since 1975 by the Resource Assessment and Conservation Engineering Division of the Alaska Fisheries Science Center. The purpose of this survey is to collect data on the distribution and abundance of crab, groundfish, and other benthic resources in the eastern Bering Sea. The data provided here include the time series of results from 1998 to the present. In 2022, 375 standard stations were sampled on the eastern Bering Sea shelf from 30 May to 29 July. The observed trends in crab biomass may be indicative of trends in either benthic production, or benthic response to environmental variability. The commercial crab biomass is also indicative of trends in exploited resources over time.

**Status and trends:** The historical trends of commercial crab biomass and abundance are highly variable (Figure 92). In 2022, Bristol Bay mature male red king crab biomass increased by 37% relative to 2021 estimates, which, while continuing a recent moderate rebound trend, represents a -55% decline since 2014. Mature female red king crab biomass increased by 3%, although abundance increased by 19%, with the discrepancy being due to an influx of smaller recruits. Numbers however remain near the historical low points. The St. Matthew blue king crab adult male stock increased by 3% relative to 2021 estimates, marking a pause in a declining trend observed since 2014. Female blue king crab biomass is not adequately sampled during this survey due to a nearshore distribution around St. Matthew Island. Mature male Tanner biomass trends were mixed, with the eastern district seeing a 73% increase, although this was partially offset by a -9% decline in the western district. The increase in the eastern district mature male biomass marks a departure from a recent declining trend which has seen biomass decline by -78% since 2014. The reduction in western district mature males continues a decline observed since 2019. Mature females declined in both the western district (-15%) and the eastern district (-36%). Total snow crab biomass increased by 2% relative to 2021, representing a pause in an 86% decline since 2018. This was driven by declines in mature females (-30%), immature males (-23%), legal males (-44%), and mature males (-16%), which are offset by a dramatic increase in immature female biomass (+8712%), and a moderate increase in industry preferred male biomass (+8%). Pribilof Islands' crab stocks remain extremely depressed with highly variable survey biomass estimates due to trawl survey limitations related to crab habitat and the patchy crab distribution.

**Factors influencing observed trends:** Environmental variability and exploitation affect trends in commercial crab biomass over time. Recent modeling analyses suggest that environmental variability is largely driving inter-annual variability in crab stock recruitment, although a mortality event may be occurring with snow crab, the direct driver of which is unknown.

**Implications:** The implications of the observed variability in crab stocks are dramatic inter-annual and inter-decadal variability in benthic predators and ephemeral (seasonal) pelagic prey resources when crab are in larval stages in the water column or as juveniles in the benthos. Although it is unclear at what life stage crab stock variability is determined, it is likely that environmental variability affecting larval survival and changes in predation affecting juvenile survival are important factors. As such, the environmental conditions affecting larval crab may also be important for larval demersal groundfish and the availability of crab as prey may be important for demersal fish distributions and survival. Disease may also be a factor, although this is speculative.

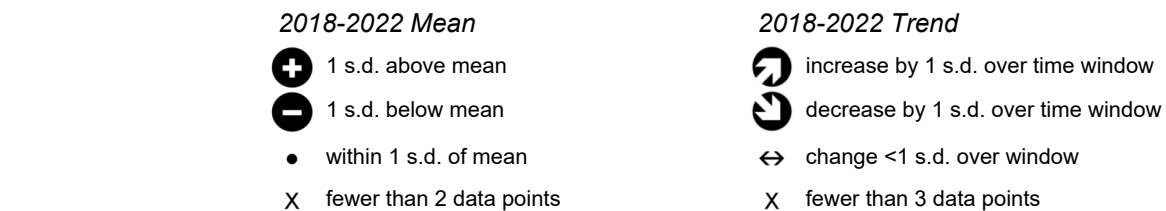


Figure 92: Historical biomass for commercial crab stocks caught on the National Marine Fisheries Service eastern Bering Sea bottom trawl survey, 1998–2022.

# Seabirds

## Integrated Seabird Information

This integration is in response to ongoing collaborative efforts within the seabird community and contains contributions from (in alphabetical order):

**David Akeya** - Savoonga, St. Lawrence Island, Alaska

**Sistoq Ahkinga** - Inalik, Little Diomede Island, Alaska

**Lauren Divine** - Ecosystem Conservation Office at Aleut Community of St. Paul Island

**Timothy Jones** - Coastal Observation and Seabird Survey Team [COASST], Washington

**Lucy Kingeekuk** - Savoonga, St. Lawrence Island, Alaska

**Aaron Lestenkof** - Island Sentinel, Ecosystem Conservation Office at Aleut Community of St. Paul Island

**Jackie Lindsey** - Coastal Observation and Seabird Survey Team [COASST], Washington

**Trevor Niksik** - Savoonga, St. Lawrence Island, Alaska

**Veronica Padula** - Ecosystem Conservation Office at Aleut Community of St. Paul Island

**Delbert Pungowiwi** - Savoonga, St. Lawrence Island, Alaska

**Heather Renner** - U.S. Fish and Wildlife Service, Alaska Maritime National Wildlife Refuge, Homer, AK

**Alexis Will** - World Wildlife Fund US Arctic Program, University of Alaska Fairbanks

**Last updated: November 2022**

### Summary Statement

Seabirds at the Pribilof Islands in the southeastern Bering Sea were monitored by Alaska Maritime Refuge for the first time since 2019. All monitored species at the Pribilofs had an exceptional year in terms of reproductive success, except thick-billed murres. Seabirds generally bred earlier and had better reproductive success in 2022 than compared to very poor years in 2016–2018. Reproductive success can represent food availability around the colony during the breeding season (summer), therefore indicating sufficient prey abundance and/or high-quality prey over the southeastern Bering Sea shelf. Colony attendance counts were relatively high for most species, although species that experienced recent population loss (least auklets and common murres) have not recovered.

On St. Lawrence Island in the northern Bering Sea, qualitative observations indicate that planktivorous seabirds did well, though abundances were also low. For example, auklet adults were attending nests and carrying food loads. Piscivorous seabirds, however, did not do well. Kittiwake reproduction failed completely while murres were in lower abundance and those that laid eggs were several weeks late.

### Introduction

Seabirds can be viewed as indicators of ecosystem changes in productivity therefore population-level responses can signal shifts in prey availability that may similarly affect commercial fish populations. In this Seabird Integration section, we synthesize information and observations from a variety of sources to provide an overview of environmental impacts to seabirds and what that may indicate for ecosystem productivity as it pertains to fisheries management. We merge across information sources to derive regional summaries within the southeastern and northern Bering Sea and interpret changes in seabird dynamics with respect to understanding ecosystem productivity.

## Approach

We focus on several attributes of seabirds that may serve as broader ecosystem indicators important to fisheries managers. We interpret these attributes as reflective of seabirds' life history and how they sample the ecosystem, either as fish-eating or plankton-eating species.

1. *Breeding timing* can represent conditions prior to breeding and/or phenological variation in the environment. Birds arriving to breed at an earlier date can reflect favorable winter and/or spring foraging conditions, or earlier peaks in ocean productivity.
2. *Reproductive success* can represent food availability around the colony during the breeding season (summer), with a higher number of fledged chicks generally reflecting an increase in the local abundance of high-quality prey.
3. *Mortality* which gives insight into environmental conditions and ecosystem impacts beyond breeding colonies and the breeding season.

## Breeding and Reproductive Success

### Southeastern Bering Sea (Pribilof Islands)

**Common murre**s had the highest reproductive success in a decade at both of the Pribilof islands (Figure 93). Counts of common murre on attendance plots remain quite low after a substantial reduction in 2015–2016, but higher than the last count in 2017. **Thick-billed murre**s had lower-than-average reproductive success (Figure 94), but numbers of birds attending the colony were similar to recent years (relatively high on St. George/increasing in recent decades; relatively low on St. Paul/continued decline over recent decades). Thick-billed murre did not undergo the massive population loss in 2015–2016 like common murre did.

**Least auklets** at the Pribilof Islands continued the recent trend of earlier mean hatch dates, and very low colony attendance. As of November 1, community members reported that there were still no least auklets at East Landing, where they once nested, and confirmed seemingly low colony attendance at Antone Lake. On St. George Island, least auklets experienced their highest reproductive performance ever recorded, although numbers of nesting crevices remained apparently low (crevices were hard to find). The 2022 mean hatch date was 11 days earlier than the long-term mean. Finally, the mean count of least auklets at colony attendance plots on St. George in 2022 was higher than in 2019, but remained nearly an order of magnitude lower than the long-term mean.

Both **black-legged and red-legged kittiwake** species showed significant increases in reproductive success in 2022 at both islands. This is noteworthy because kittiwakes experienced four years of complete, or near complete, reproductive failure from 2015–2018. Both species had reproductive success well above average and well above recent years. Timing was average for both species. Attendance was also quite high, with St. Paul showing the highest numbers of red-legged kittiwakes present since the 1970s.

**Red-faced cormorant** reproductive success at St. Paul Island in 2022 was well above the long-term mean, and all metrics of productivity (laying success, clutch size, egg success, fledglings/nest start) were very high. While monitored less intensively at St. George, cormorants did well there, too.

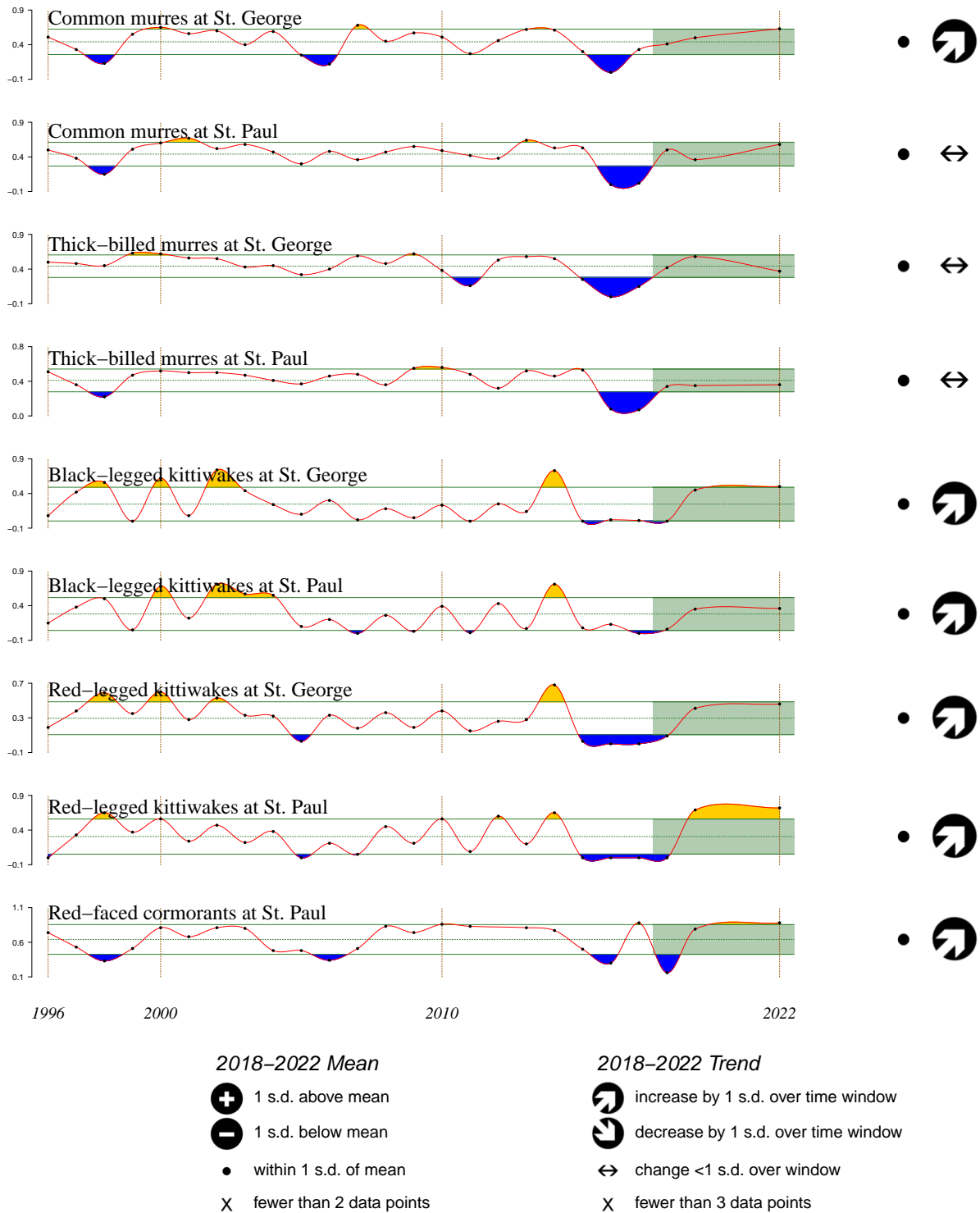


Figure 93: Reproductive success of five seabird species at St. George and St. Paul Islands between 1996–2022.

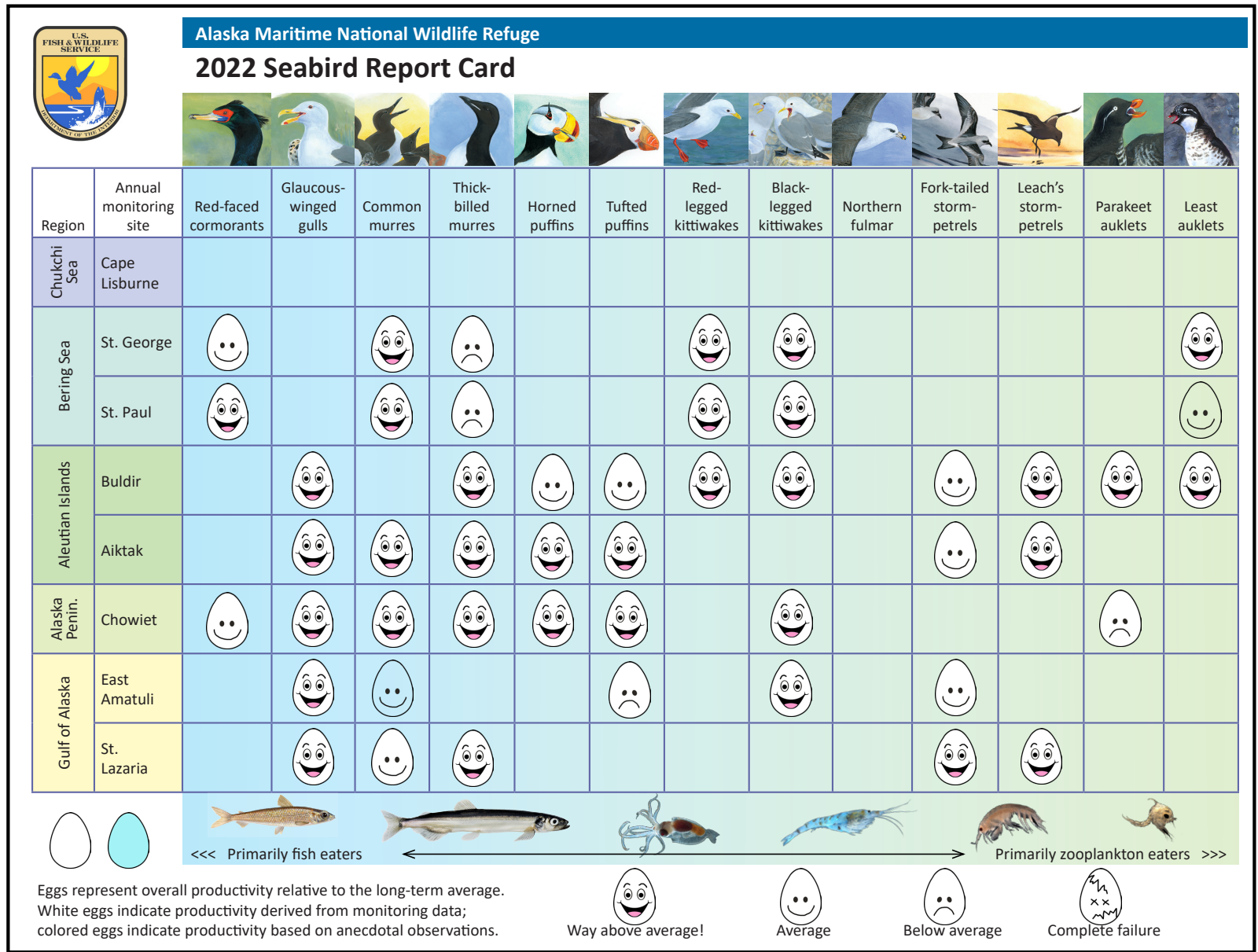


Figure 94: 2022 Seabird Report Card showing a summary of seabird productivity across Alaska Maritime National Wildlife Refuge monitored colonies.

### **Northern Bering Sea (St. Lawrence Island and Little Diomed Island)**

In 2022 there was only a short period of field work on St. Lawrence Island. At the time of writing this report only qualitative observations are available (sample and other data analysis still pending). The colony at Kitnik was visited in early August (2–9, 2022). **Crested auklets** hatched in early August, and **least auklets** appeared to have mostly hatched in late July (about a week prior to Aug 3 colony visit). In general both species of auklets appeared to be doing well in 2022 (no reproductive success data available this year), adults were attending nests (not necessarily the case in previous years of reproductive failure), the majority of attending adults were carrying food loads, and the colony was bustling in a way it hadn't since 2017. Preliminary analysis of auklet food loads indicates that some copepods were again available to breeding least auklets. Based on an informal assessment of chick diets crested auklets were provisioning chicks with euphausiids, and least auklets were provisioning chicks with a mix of copepods, amphipods, and euphausiids. However, the numbers of auklets at the colony were noticeably low, an observation corroborated by people in Savoonga who also commented that the colony nearest to town was almost completely empty. While the number of auklets at colonies near Savoonga were markedly low, on Little Diomed there was an unusually large number of auklets attending the breeding colony. It is not clear whether these trends are interlinked (auklets moving) or independent (gains and losses in population).

**Murres** were late laying this year, by some estimates several weeks later than usual (e.g., they typically lay ~June 21, this year some birds were still laying in early July). At our Kevipak study plots numbers were much lower than in previous years, but reproductive success is unknown at the time of this report.

In early August there were no **kittiwakes** breeding at Kevipak, when birds would usually have medium-sized chicks.

*General observations:* There were a lot of what was described as “krill”, perhaps large amphipods, in the ocean near Savoonga in early August. Halibut and cod pulled up from lines set out for three hours were nearly completely eaten (down to the skeleton) by these organisms. Cod were caught more often than halibut. Shearwaters were seen near the island, flying and foraging near shore. Some old shearwater carcasses were seen on beaches, this is not necessarily unusual if there were large numbers of shearwaters in the area then some mortality can be normal.

### **Mortality**

#### **Eastern Bering Sea**

Monitoring by the Coastal Observation and Seabird Survey Team (COASST) and regional partners provides a standardized measure of relative beached bird abundance. Surveys began in the Eastern Bering Sea in 2006, and since that time over 1300 surveys have taken place across 25 beaches; in 2022, 49 surveys took place across 7 beaches in Nome and the Pribilof Islands. Detailed methods for beached bird surveys can be found in Jones et al. (2019).

In 2022, surveyors reported relatively few carcasses across beaches in the Bering Sea, despite typical survey effort. Encounter rates (all <1 per km) were not indicative of a die-off event. (See monthly encounter rates for 2007 and 2019 in Figure 95 for examples of elevated encounter rates indicative of an unusual mortality event - typically defined as 5x the baseline rate.)

In addition to monthly, effort-based surveys for beachcast seabirds, opportunistic reports of seabird mortality from beachwalkers, fishermen, and seasonal researchers are assembled by regional state, federal, tribal, and community partners each year. They are collated into a map of carcass reports by COASST (Figure 96). Species (if known), count, and location is required for each report, but standardized effort (outside of COASST and National Park Service surveys) is rarely available.

In 2022 most opportunistic reports of carcasses in the eastern Bering Sea were from aerial surveys (covering 50km) led by National Park Service and ABR along the northeast side of the Seward Peninsula. These surveys are indicated with dashed circles in Figure 96, indicating the difference in survey methodology. The number of opportunistic reports received in 2022 is not indicative of a major die-off event in this region. Similar maps from years with large-scale mortality events depicted thousands of birds.

### Beached Bird Relative Abundance: Bering Sea

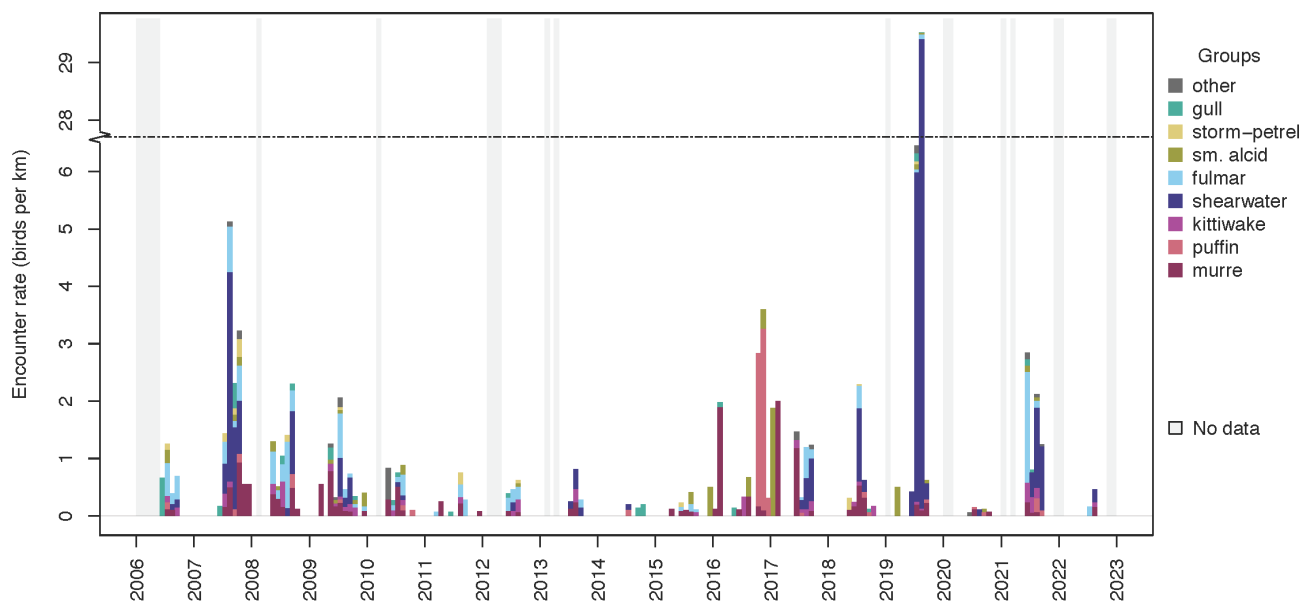


Figure 95: Month-averaged beached bird abundance, standardized per km of survey effort, for the eastern Bering Sea. Species groups (gull, storm-petrel, small alcid, fulmar, shearwater, kittiwake, puffin, murre) are depicted with different colors within each bar, with gray bars indicating months where no survey was conducted. **Note:** break in the y-axis between 6 and 28 birds/km, indicated by the dashed line, shows the magnitude of the 2019 die-off while still being able to distinguish patterns among other years. Credit: COASST.

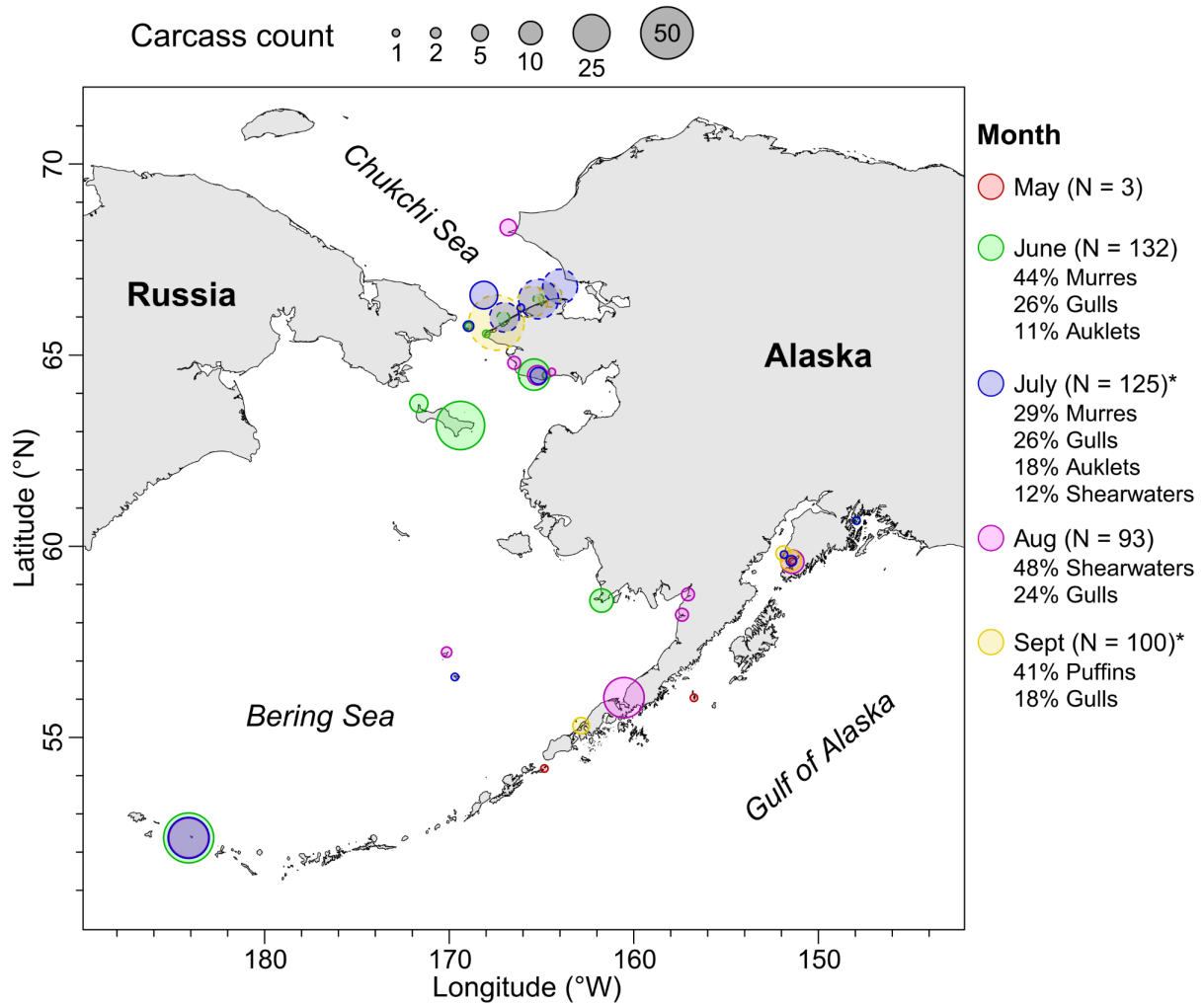
In 2022, reports of Highly Pathogenic Avian Influenza (HPAI) in wild seabirds and marine mammals across North America put the seabird mortality reporting community on high alert. While researchers prepared to document and collect seabirds on colonies for testing, large die-off events like those reported in the North Atlantic and EU were not documented in Alaska. Individual reports of seabirds with HPAI from 2021–2022 (confirmed by laboratory test results) are collated by USGS<sup>20</sup>.

#### Implications

Fish-eating, surface feeding seabirds include black-legged kittiwakes who feed on small schooling fish that are available at the surface (e.g., capelin, Arctic cod, juvenile pollock and juvenile herring), making them potential indicators of processes affecting juvenile groundfish that migrate to the surface to feed. Fish eating, diving seabirds include common murres who feed on small schooling fish (age-0 and age-1 pollock) to depths up to 90m, thus they have access to fish throughout the water column and to the ocean bottom in shallow areas. Both species had high reproductive success at the Pribilof Islands in 2022, indicating local availability of small schooling forage fish.

Planktivorous seabirds include least and crested auklets, which feed primarily on copepods and euphausiids. Shearwaters and thick-billed murres also consume euphausiids, along with larvae and small fish. All of these species are indicators of feeding conditions for planktivorous groundfish species, including the larvae and juveniles of fish-eating species. The factors contributing to the poor reproductive success of thick-billed murres at the Pribilof Islands in 2022 are not fully understood at this time. Other planktivorous species (e.g., auklets) had high reproductive success at the Pribilof Islands and appeared to be doing well on St. Lawrence Island where it was noted that adults were carrying food loads to provision chicks. Chick diets of crested auklets included euphausiids and least auklets were provisioning chicks with a mix of copepods, amphipods, and euphausiids.

<sup>20</sup>[https://www.usgs.gov/centers/nwhc/science/distribution-highly-pathogenic-avian-influenza-north-america-2021-2022?utm\\_source=Newsletter&utm\\_medium=Email&utm\\_campaign=usgs-econews--vol-3--issue-2&utm\\_term=Image](https://www.usgs.gov/centers/nwhc/science/distribution-highly-pathogenic-avian-influenza-north-america-2021-2022?utm_source=Newsletter&utm_medium=Email&utm_campaign=usgs-econews--vol-3--issue-2&utm_term=Image)



\* : species composition is of birds identified to species/group. However, in July/Sept a large proportion (38%, 83%) of birds were unidentified

Note: Circles represent reports of seabird carcass abundance and are not standardized for variable observer effort among locations. The absence of reports in certain locations may indicate gaps in current knowledge OR an actual absence of bird carcasses. Reports from aerial surveys (dashed circles) are distinguished from other beach-based reports (solid circles) due to major differences in area observed.

Figure 96: Map of seabird carcass reports for Alaska during May-September 2022. Data provided by COASST participants and National Park Service staff, and coastal community members reporting to ADFG, USFWS, UAF-Alaska Sea Grant, and Kawerak, Inc. Bubble sizes indicate number of carcasses counted (between 1 and 50) and bubble color indicates month of report. Species composition is reported monthly, aggregated to species groups.

## Marine Mammals

### Marine Mammal Stranding Network: Eastern Bering Sea

Contributed by Mandy Keogh and Kate Savage  
NOAA Fisheries, Protected Resources Division, Alaska Regional Office  
Contact: [mandy.keogh@noaa.gov](mailto:mandy.keogh@noaa.gov)  
**Last updated: September 2022**

**Description of indicator:** Since 1985, members of the NMFS Alaska Marine Mammal Stranding Network (AMMSN) have collected and compiled reports on marine mammal strandings throughout the state. These reports are indices of events witnessed by members of the stranding network, the scientific community, and the general public, with varying degrees of knowledge regarding marine mammal biology and ecology. A marine mammal is considered “stranded” if it meets one of the following criteria: 1) dead, whether found on the beach, ice, or floating in the water; 2) alive on a beach (or ice) but unable to return to the water; 3) alive on a beach (or ice) and in need of apparent medical attention; or 4) alive in the water and unable to return to its natural habitat without assistance. The causes of marine mammal strandings are often unknown but some causes include disease, exposure to contaminants or harmful algal blooms, vessel strikes, and entanglement in or ingestion of human-made gear.

When a stranded marine mammal is reported, information is collected including species, location, age class or size. In some cases, the initial photos and observations reported to AMMSN may be the only opportunity to collect information on the event. When possible, trained and authorized AMMSN members respond and collect life history data and samples as part of a partial or full necropsy. Photos and carcasses are evaluated for potential human interactions such as entanglement. These responses are conducted under the Marine Mammal Protection Act authorization either under a 112c agreement issued by NMFS to AMMSN members through a Stranding Agreement or under 109 (h) authority exercised by local, state, federal or tribal entities. All responses involving ESA-listed species fall under the Marine Mammal Health and Stranding Program Permit # 18786.

**Status and trends:** The number of confirmed strandings in Alaska has increased over time. As of August 31, 2022, 190 confirmed stranded marine mammals have been reported for the year within Alaska, of which 72 were in the eastern Bering Sea region (Table 1). The majority of reports were from more populated areas where AMMSN members are located. Further, increased outreach and dedicated surveys associated with high priority species or events (e.g., 2018 ice seal Unusual Mortality Event; entanglement surveys on St. Paul Island) also contributed to reported strandings in some areas and years. Reported strandings in the eastern Bering Sea region since 2017 varied between years without an overall pattern or consistent increase in reports (Table 1). The 2022 stranding data include confirmed strandings reported between January 1, 2022 and August 31, 2022. These data are preliminary and the details may change as we review reports and receive additional information.

**Factors influencing observed trends:** It is important to recognize that stranding reports represent effort that has varied substantially over time and location. Human population and activity in an area influences the potential for a carcass or stranded marine mammal to be observed and reported. Overall, this effort has increased across Alaska and particularly in areas with higher human population densities. Unusual Mortality Events (UME) including the 2018 ice seal UME and the 2019 gray whale UME can have large influence on variability between years in this area (Table 1). Under the Marine Mammal Protection Act, an UME is defined as “a stranding that is unexpected; involves a significant die-off of any marine mammal population; and demands immediate response.” The ice seal and gray whale UMEs continued through 2022, though the number of confirmed strandings within the eastern Bering Sea region in 2022 are comparable to pre-UME reports (e.g., 2017).

Other factors that may influence the number and species of marine mammals being reported include changing populations of some species including the increase in northern fur seals using Bogoslof Island for breeding.

Further, the number of stranded marine mammals in an area can vary due to the potential conflict with fishery resources either directly through prey competition or indirectly through interactions with fishing gear such as increased pinniped entanglements. Within the Eastern Bering Sea region, there was a dramatic increase in stranded northern fur seals in 2022 (Table 1). All forty northern fur seals were alive and disentangled by the Ecosystem Conservation Office (ECO) of the Aleut Community of St. Paul Island. Under the Examiners Guide<sup>21</sup>, the level A and human interaction forms are completed for free-swimming entangled pinnipeds when a response is conducted and the animal is in-hand. Observations of entangled pinnipeds with no response are captured with an Alaska Regional form and by ECO database but these observations are not part of the national stranding database. In 2021, the Aleut Community of St. Paul Island increased ECO team efforts which allowed entangled northern fur seals observed during their weekly entanglement surveys or subsistence efforts to be captured and disentangled. Therefore, the increase in stranded northern fur seals in 2022 in this region may be due, at least in part, to reporting requirements and the successful capture and disentanglement of northern fur seals rather than solely due to an increase in entanglements.

**Implications:** Across Alaska, reported marine mammal strandings have varied by year and location. In 2018, the increase in ice seal strandings in the eastern Bering Sea and Arctic regions led to the declaration of an UME and in 2019 the increase in gray whale strandings across the migration route between Mexico and Alaska led to the declaration of an UME. Increases in confirmed strandings of marine mammals may signal changes in the environment or other stressors (e.g., entanglements). Marine mammal stranding data can be paired with other data sets and may give clues to ecosystem-wide changes.

---

<sup>21</sup>[https://media.fisheries.noaa.gov/2021-07/EXAMINERS%20GUIDE\\_2024%20FINAL.pdf?](https://media.fisheries.noaa.gov/2021-07/EXAMINERS%20GUIDE_2024%20FINAL.pdf?)

Table 1: Reported stranded NMFS marine mammal species for the last five years in the eastern Bering Sea by species and year.

	2017	2018	2019	2020	2021	2022 <sup>22</sup>
Bowhead whale						1
Bairds beaked whale						
beluga whale	12	11	14	13	6	2
Harbor porpoise	3	4	6	3		3
Bowhead whale						
Fin whale				2		
Gray whale	7	7	14	15	4	4
Humpback whale	2	4	3	1	1	1
Minke whale			2	1		1
Killer whale		2		1	2	
Sperm whale						
Unidentified cetacean	8		1	2	1	2
Striped dolphin <sup>23</sup>					1	
Unidentified small cetacean	2					
Unidentified large whale	7	7	11	2	4	2
<b>Total cetaceans</b>	<b>41</b>	<b>35</b>	<b>51</b>	<b>40</b>	<b>19</b>	<b>16</b>
Harbor seal		1	4	2	2	
Northern fur seal	6	10	18	2	8 <sup>24</sup>	40 <sup>24</sup>
Bearded seal	1	32	20	8	3	7
Ribbon seal			2			
Ringed seal	8	31	8	2		2
Steller sea lion	3	1		4	1	3
Spotted seal	5	17	14	4	1	2
Unidentified pinniped	3	19	26	8		2
Unidentified marine mammal	7	5	2			
<b>Total pinnipeds</b>	<b>33</b>	<b>116</b>	<b>94</b>	<b>30</b>	<b>15</b>	<b>56</b>
<b>Total Cetaceans and Pinnipeds</b>	<b>74</b>	<b>151</b>	<b>145</b>	<b>70</b>	<b>34</b>	<b>72</b>

<sup>22</sup>2022 stranding data includes confirmed strandings reported between January 1, 2022 and August 31, 2022

<sup>23</sup>An unidentified dolphin sampled on St. Paul Island in an advanced state of decomposition was identified as a female striped dolphin through genetic analysis by NOAA Fisheries Southwest Fisheries Science Center

<sup>24</sup>All northern fur seals in the eastern Bering Sea region in 2021 and 2022 were alive and entangled in fishing gear or debris. Seals were captured, disentangled, and immediately released

## Ecosystem or Community Indicators

### Aggregated Catch-Per-Unit-Effort of Fish and Invertebrates in Bottom Trawl Surveys on the Eastern and Northern Bering Sea Shelf, 1982–2022

Contributed by Franz Mueter

University of Alaska Fairbanks, 17101 Point Lena Loop Road, Juneau, AK 99801

Contact: fmueter@alaska.edu

**Last updated: October 2022**

**Description of indicator:** The index provides a measure of the overall biomass of demersal and benthic fish and major invertebrate species. I estimated annual mean catch-per-unit-effort (CPUE in kg ha) of all demersal fish and major invertebrate taxa using all successful hauls completed during standardized bottom trawl surveys on the eastern Bering Sea shelf (EBS) from 1982–2022 and on the northern Bering Sea shelf (NBS) in 2010, 2017, 2019, 2021, and 2022. Total CPUE for each haul was computed as the sum of the CPUEs of all fish and major invertebrate taxa. To obtain an index of average CPUE by year for each survey region, I modeled log-transformed total CPUE ( $N = 14,842$  hauls in the EBS,  $N = 716$  hauls in the NBS) as a smooth function of Julian Day and location (latitude/longitude), with year-specific intercepts, using an Additive Model. The CPUE index does not account for gear or vessel differences, which are confounded with interannual differences and may affect results prior to 1990. Therefore, I only show trends from 1990–2022. To highlight differences between recent trends in the EBS and NBS, I also computed the mean CPUE by region and year for the five years with complete surveys in the NBS using an additive model to account for seasonal trends (smooth function of Julian day) and account for spatially correlated errors that were assumed to decrease exponentially with distance.

**Status and trends:** Total log(CPUE) in the EBS shows no significant trend (linear regression, accounting for temporal autocorrelation:  $t=0.287$ ,  $p=0.776$ ) (Figure 97, top), but there were large fluctuations between 1990 and 2022. The highest observed value in the time series occurred in 2014 and total CPUE declined thereafter with a sharp and significant drop between 2017 and 2018. Total log(CPUE) increased again in 2019, followed by another significant decrease between 2019 and 2021 to the lowest level since 2009. CPUE increased again in 2022 to near its 30-year average. Total CPUE in the NBS increased between 2010 and 2019, and decreased substantially after 2019 to very low values in 2021 and 2022 (Figure 97, bottom).

**Factors influencing observed trends:** Commercially harvested species accounted for approximately 95% of survey catches. Fishing is expected to be a major factor determining trends in survey CPUE, but environmental variability is likely to account for a substantial proportion of the observed variability in CPUE through variations in recruitment, growth, distribution, and catchability. The increase in survey CPUE in the early 2000s in the EBS primarily resulted from increased abundances of Walleye pollock (*Gadus chalcogrammus*) and a number of flatfish species (Arrowtooth flounder, *Atheresthes stomias*; Yellowfin sole, *Limanda aspera*; Rock sole, *Lepidopsetta bilineata*; and Alaska plaice, *Pleuronectes quadrituberculatus*) due to strong recruitments in the 1990s. Decreases in 2006–2009 and subsequent increases are largely a result of fluctuations in pollock recruitment and abundance. Models including bottom temperature suggest that, in the EBS, CPUE tends to be lower in years with low bottom water temperatures, as evident in reduced CPUEs in 1999 and 2006–2013, when the cold pool covered a substantial portion of the shelf. Overall, there is a moderate positive relationship between average bottom temperatures and CPUE in the same year ( $r=0.46$ ,  $p=0.0075$ ), but not in the following years. Reduced CPUE during cold periods is likely due to a combination of temperature-dependent changes in catchability of certain species (e.g., flatfish, crab), changes in distribution as a result of the extensive cold pool displacing species into shallower (e.g., red king crab) or deeper waters (e.g., Arrowtooth flounder), or changes in vertical distribution of semi-demersal species. The large decrease in the EBS in 2018 was primarily due to a decrease in the CPUE of pollock, as well as that of Pacific cod (*G. macrocephalus*) and most flatfish species, except Arrowtooth flounder. The subsequent increase from 2018 to 2019 and decrease from 2019 to 2021 were primarily due to changes in pollock catches, whereas the CPUE of other dominant species remained stable. Total CPUE increased again in 2022 for

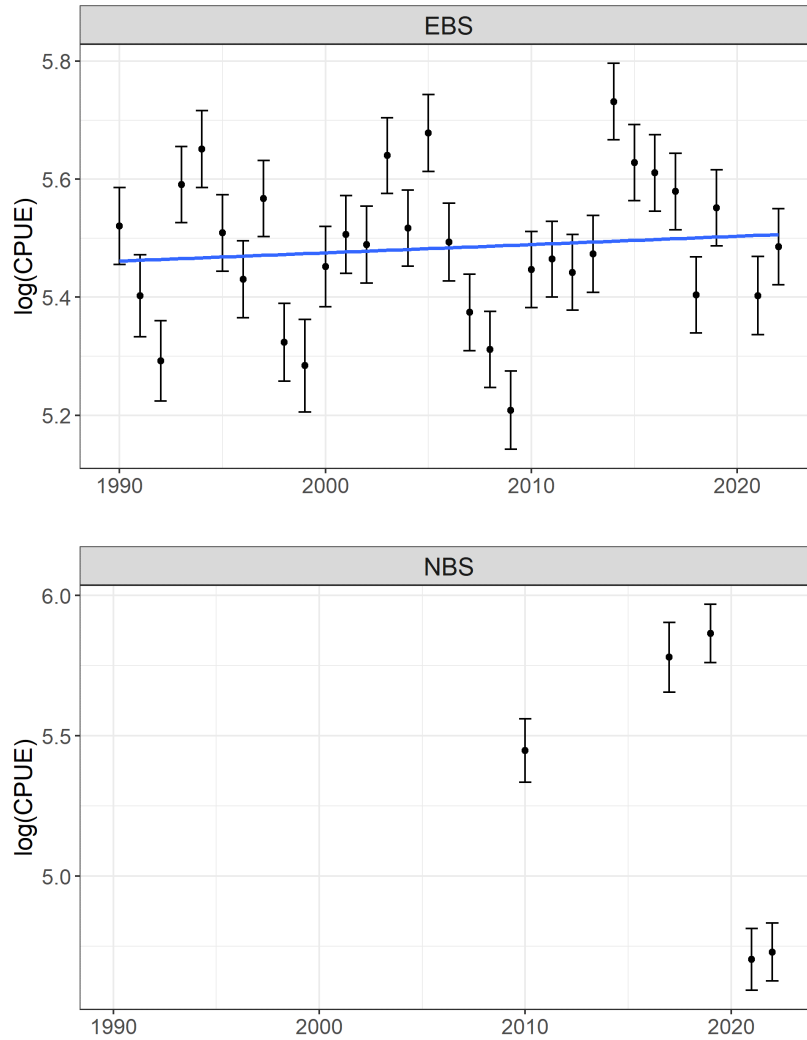


Figure 97: Model-based estimates of total log(CPUE) for major fish and invertebrate taxa captured in bottom trawl surveys from 1990 to 2022 in the eastern Bering Sea (EBS) and northern Bering Sea (NBS) with approximate pointwise 95% confidence intervals and linear time trend (EBS only). Estimates were adjusted for differences in day of sampling and sampling locations among years. The linear time trend was estimated using a generalized least squares regression assuming 1<sup>st</sup> order auto-correlated residuals and was not statistically significant ( $t=0.287$ ,  $p=0.777$ ). Note differences in y-axis scales.

all major taxa, but particularly for pollock. The drop in total CPUE in the NBS between 2019 and 2021 was much more pronounced compared to the EBS (Figure 98) and reflected large decreases in all of the dominant species, including pollock, Yellowfin sole, Alaska plaice, Pacific cod, snow crab, and skates (Figure 99). Moreover, while CPUE increased substantially in 2022 in the EBS, there was no corresponding increase in the NBS (Figure 98).

**Implications:** This indicator likely reflects changes in the overall productivity and carrying capacity of a system with relatively moderate exploitation rates, and also addresses concerns about maintaining an adequate biomass of prey for upper trophic level species and other ecosystem components. Relatively stable or increasing trends in the total biomass of demersal fish and invertebrates suggest that the prey base has remained stable over recent decades, but displays substantial fluctuations over time, largely as a result of variability in pollock biomass.

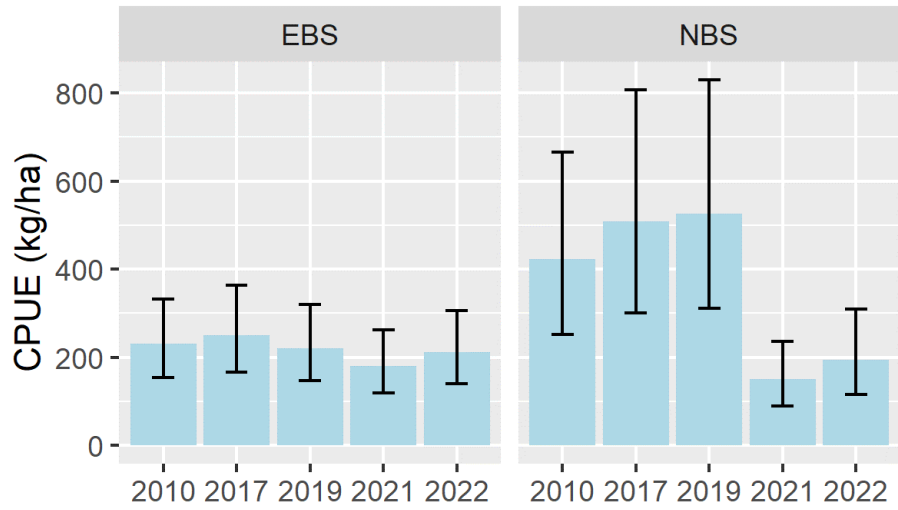


Figure 98: Mean CPUE of all fish and invertebrates sampled during bottom trawl surveys in 2010, 2017, 2019, 2021, and 2022 with 95% confidence intervals. Estimates by region and year, adjusted for day of sampling, based on additive model with spatially auto-correlated errors (exponential correlation structure).

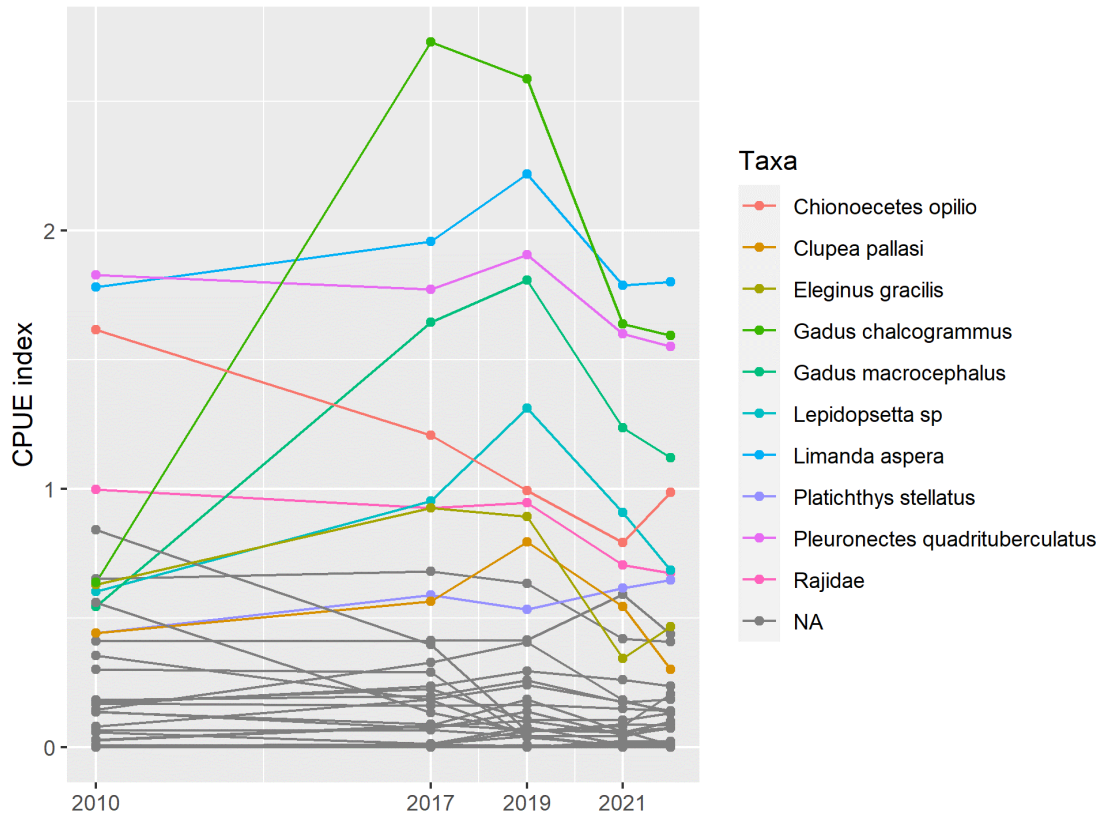


Figure 99: Changes in mean, fourth-root transformed CPUE of 41 major taxa in the northern Bering Sea based on surveys conducted in 2010, 2017, 2019, 2021 and 2022. 'NA' denotes all other taxa.

## Spatial Distribution of Groundfish Stocks in the Eastern Bering Sea

Contributed by Franz Mueter

University of Alaska Fairbanks, 17101 Point Lena Loop Road, Juneau, AK 99801

Contact: fmueter@alaska.edu

**Last updated: October 2022**

**Description of indicator:** I provide indices of changes in the spatial distribution of groundfish on the eastern Bering Sea (EBS) shelf. The first index provides a simple measure of the average North-South displacement of major fish and invertebrate taxa from their respective centers of gravity (e.g., Woillez et al. (2009)) based on EBS bottom trawl surveys for 1982–2022. Annual centers of gravity for each taxon were computed as the CPUE-weighted mean latitude across 285 standard survey stations that were sampled each year and an additional 58 stations sampled in all but one survey year. Each station (N=343) was weighted by the approximate area it represents. Initially, I selected 46 taxa (see Table 1 of Mueter and Litzow (2008)). Taxa that were not caught at any of the selected stations in one or more years were not included, resulting in a total of 39 taxa. In addition to quantifying N-S shifts, I computed CPUE and area-weighted averages of depth to quantify changes in depth distribution. Because much of the variability in distribution is likely to be related to temperature variability, I removed linear relationships between changes in distribution and temperature by regressing distributional shifts on annual mean bottom temperatures. Residuals from these regressions are provided as an index of temperature-adjusted shifts in distribution.

**Status and trends:** Both the latitudinal and depth distribution of the demersal community on the EBS shelf show strong directional trends over the last four decades, indicating significant distributional shifts to the north and into shallower waters (Figure 100). The distribution shifted slightly to the south and deeper in recent cold years (2006–2013) and shifted back to the north and shallower from 2014 to 2016. The distribution shifted slightly south in 2017, but remained near its northern maximum through 2019 before shifting south again in 2021. The mean latitude did not change between 2021 and 2022, but species on average shifted into slightly deeper waters. Strong shifts in distribution remain evident even after adjusting for linear temperature effects, although the residual trend appears to be leveling off since the early to mid-2000s (Figure 100).

The center of gravity of most individual species shifted to the northwest along the shelf or to the northeast onto the shelf in 2016, the warmest survey year (Figure 101). Cooler temperatures in 2017 appeared to result in an immediate and substantial southeastward shift, in contrast to a more moderate response to similar cooling in 2006. Following the return to higher bottom temperatures in 2018 and 2019, the overall center of gravity shifted slightly to the northwest, but in 2021 shifted back to the southeast followed by a moderate shift to the west (deeper) in 2022. However, northern Bering Sea (NBS) surveys since 2017 suggest that much of the biomass of fishes in recent years occurred in the NBS. The latitudinal gradient in the density of all major fish and invertebrate taxa combined declined from south to north in 2010 but increased from south to north in 2019, with much higher estimated densities near Bering Strait than off the Alaska Peninsula (Figure 102). This trend reversed again in 2021 and 2022, with mean densities near Bering Strait declining from >400 kg/ha in 2019 to <200 kg/ha in 2022. These patterns were primarily driven by changes in the distribution of pollock, Pacific cod, and some flatfishes (Figure 102, see also Stevenson and Lauth (2012); Thorson et al. (2019)).

**Factors influencing observed trends:** Many populations shift their distribution in response to temperature variability. Such shifts may be the most obvious response of animal populations to global warming (Parmesan and Yohe, 2003). However, distributional shifts of demersal populations in the Bering Sea are not a simple linear response to temperature variability (Mueter and Litzow (2008); Figure 100). The reasons for strong residual shifts in distribution that are not related to temperature changes remain unclear but could be related to density-dependent responses (Spencer, 2008) in combination with internal community dynamics (Mueter and Litzow, 2008). Unlike groundfish in the North Sea, which shift to deeper waters in response to warming (Dulvy et al., 2008), the Bering Sea groundfish community shifted to shallower waters during warm periods (Figure 100) because of the retreat of the cold pool from the middle shelf that allows subarctic species to expand from the outer shelf into shallower shelf regions.

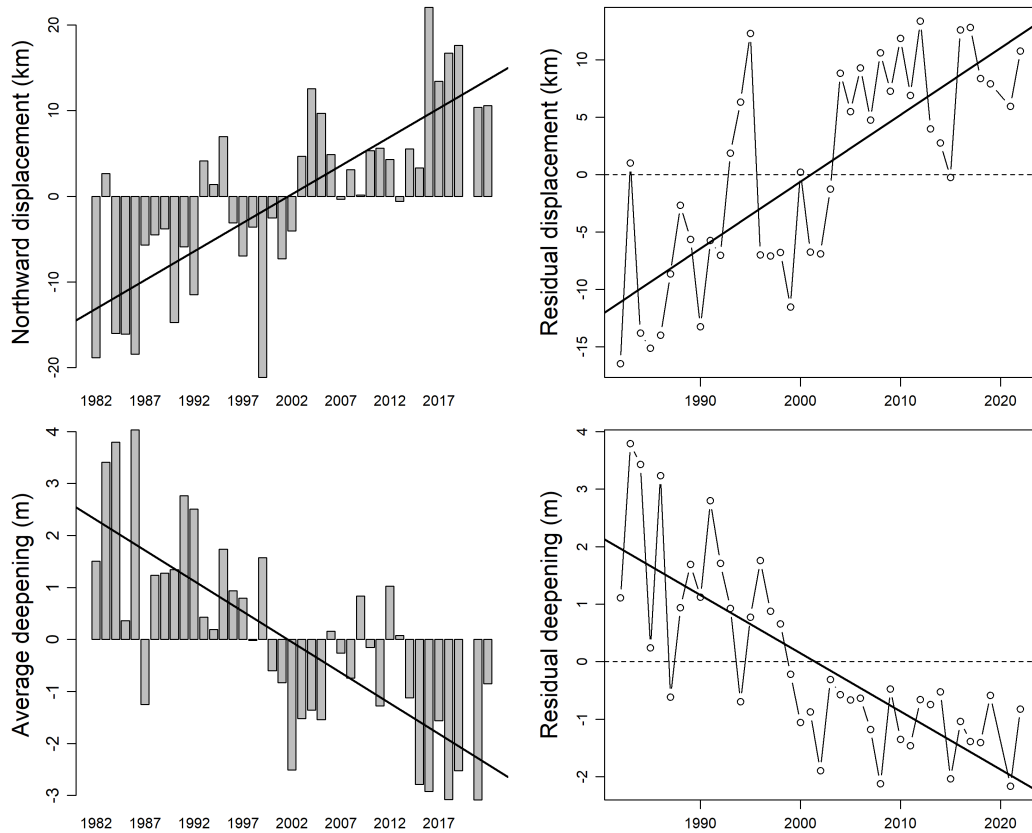


Figure 100: Left: Distributional shifts in latitude (average northward displacement in km from species-specific mean latitudes) and shifts in depth distribution (average vertical displacement in m from species-specific mean depth, positive indices indicate deeper distribution). Right: Residual displacement from species-specific mean latitude (top) and species-specific mean depth (bottom) after adjusting the indices on the left for linear effects of mean annual bottom temperature on distribution. Residuals were obtained by linear regression of the displacement indices on annual average temperature (Northward displacement:  $R^2=0.22$ ,  $t=4.24$ ,  $p<0.001$ ; Deepening:  $R^2=0.25$ ,  $t=-4.35$ ,  $p<0.001$ ). Solid trend lines denote linear regressions over time (Northward displacement:  $R^2=0.57$ ,  $t=5.82$ ,  $p<0.001$ ; Residual northward displacement:  $R^2=0.57$ ,  $t=5.04$ ,  $p<0.001$ ; Deepening:  $R^2=0.55$ ,  $t=-6.25$ ,  $p<0.001$ ; Residual deepening:  $R^2=0.59$ ,  $t=-7.42$ ,  $p<0.001$ ).

**Implications:** Changes in distribution have important implications for the entire demersal community, for other populations dependent on these communities, the fishing industry, and for stock assessments. The demersal community is affected because distributional shifts change the relative spatial overlap of different species, thereby affecting trophic interactions among species (Hunsicker et al., 2013; Spencer et al., 2016) and, ultimately, the relative abundances of different species (Uchiyama et al., 2020). Upper trophic level predators, for example fur seals and seabirds on the Pribilof Islands and at other fixed locations, are affected because the distribution and hence availability of their prey changes. Fisheries are directly affected by changes in the distribution of commercial species, which alters the economics of harvesting because fishing success within established fishing grounds may decline and travel distances to new fishing grounds may increase (Haynie and Pfeiffer, 2013). Finally, stock assessments are affected by shifts outside the standard survey area, such as the substantial redistribution of Pacific cod into the NBS in 2018 and the apparent redistribution of much of the overall biomass in the Bering Sea to the NBS shelf in 2019. This was followed in 2021 by substantial declines in mean density at most latitudes with the largest overall declines in the NBS (Figure 102).

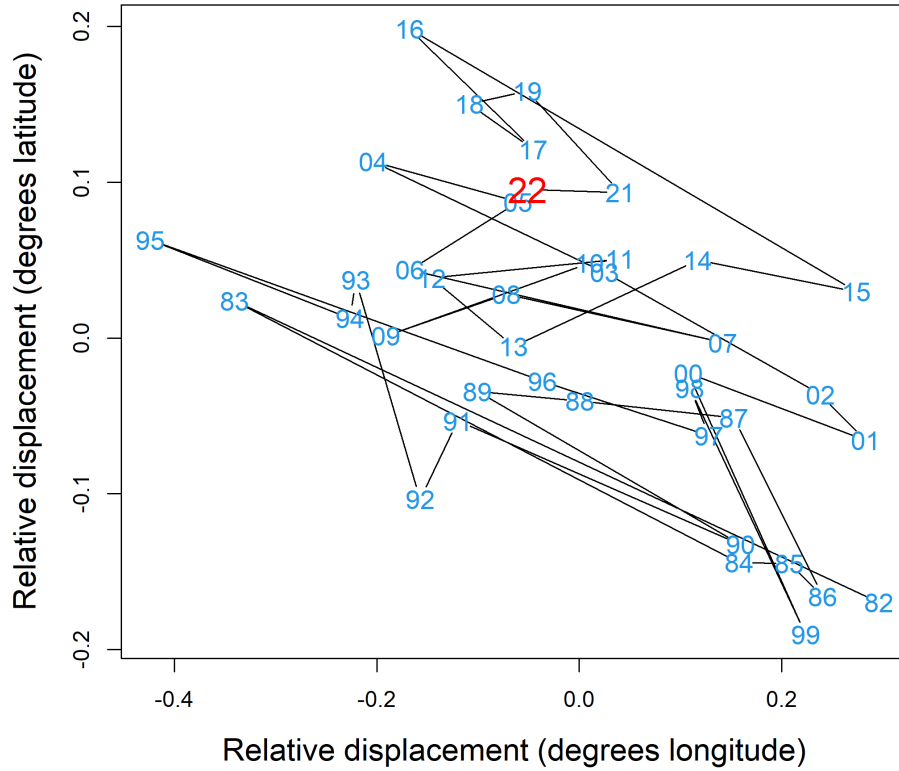


Figure 101: Average North-South and East-West displacement across 39 taxa on the eastern Bering Sea shelf relative to species-specific centers of distribution.

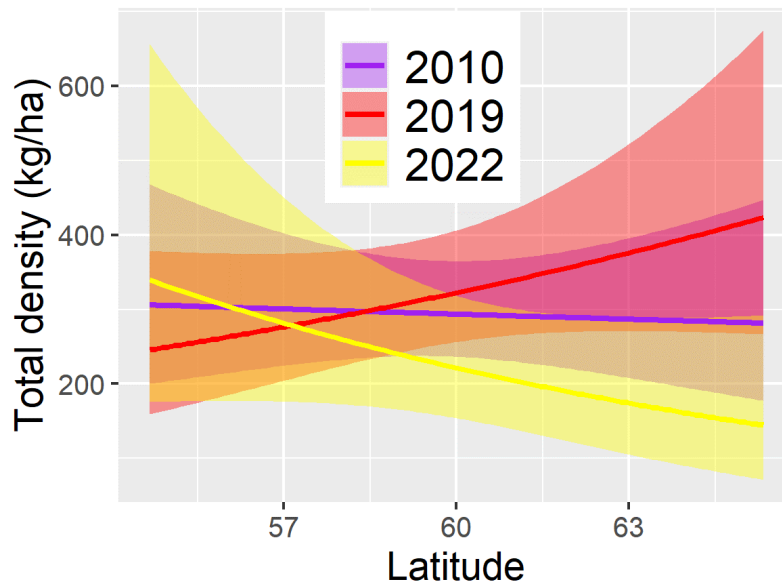


Figure 102: Estimated latitudinal trends in average macrofaunal density for all fish and invertebrate taxa combined from the Alaska Peninsula in the south to the Bering Strait in the North. Estimates are based on generalized additive models of  $\log(\text{catch-per-unit-effort})$  as a function of latitude and depth by year with an exponential spatial autocorrelation structure with 80% confidence bands.

## Mean Lifespan of the Fish Community

Contributed by George A. Whitehouse<sup>1</sup> and Geoffrey M. Lang<sup>2</sup>

<sup>1</sup>Cooperative Institute for Climate, Ocean, and Ecosystem Studies (CICOES), University of Washington, Seattle WA

<sup>2</sup>Resource Ecology and Fisheries Management Division, Alaska Fisheries Science Center, National Marine Fisheries Service, NOAA

Contact: andy.whitehouse@noaa.gov

**Last updated: October 2022**

**Description of indicator:** The mean lifespan of the community is a proxy for the turnover rate of species and communities and reflects the resistance of the community to perturbations (Shin et al., 2010). The indicator for mean lifespan of the groundfish community is modeled after the method for mean lifespan presented in Shin et al. (2010). Lifespan estimates of groundfish species regularly encountered during the NMFS/AFSC annual summer bottom-trawl survey of the eastern Bering Sea were retrieved from the AFSC Life History Database<sup>25</sup>. The groundfish community mean lifespan is weighted by biomass indices calculated from the bottom-trawl survey catch data.

This indicator specifically applies to the portion of the demersal groundfish community that is efficiently sampled by the trawling gear used by NMFS during this survey at the standard survey sample stations (for survey details see Lauth et al. (2019)). Species that are infrequently encountered or not efficiently caught by the bottom-trawling gear are excluded from this indicator (e.g., sharks, grenadiers, myctophids, pelagic smelts). The survey index used here is the same as that used for fish and invertebrate biomass indices on the report card (Figure 2).

Walleye pollock is a biomass dominant species in the eastern Bering Sea and may drive the value of community indicators. Therefore this indicator is presented as two time series, one that includes and one that excludes walleye pollock.

### Status and trends:

*With pollock included:* The mean lifespan of the eastern Bering Sea demersal fish community in 2022 is 29.6 years, down from 30.5 years in 2021 which was the second highest over the time series (Figure 103, circles). Mean groundfish lifespan has generally been stable over the time series with only a small amount of year-to-year variation, and shows no indication of a long-term trend.

*Without pollock included:* The mean lifespan of the eastern Bering Sea groundfish community without walleye pollock in 2022 is 27.4 years, down from 30.3 years in 2021. Over the time series, the patterns and trends are similar between the two series with the values being slightly lower for the series without pollock (Figure 103, triangles). The exception to this pattern was 1985 when the mean lifespan was 32.8 with pollock included and 34.3 without pollock.

**Factors influencing observed trends:** Fishing can affect the mean lifespan of the groundfish community by preferentially targeting larger, older fishes, leading to decreased abundance of longer-lived species and increased abundance of shorter-lived species (Pauly et al., 1998). Interannual variation in mean lifespan can be influenced by the spatial distribution of species and the differential selectivity of species and age classes to the trawling gear used in the survey. Strong recruitment events or periods of weak recruitment could also influence the mean community lifespan by altering the relative abundance of age classes and species. For example, the low value observed in 1993 reflects a year of peak biomass index for capelin, a shorter-lived species. The peak mean lifespan for both series in 1985 was in part elevated by high biomass indices for long-lived species, such as sablefish. The lifespan of pollock is slightly higher than the mean groundfish lifespan without pollock. When pollock are removed from this indicator, there is a small decrease in value but the same overall trend is followed.

<sup>25</sup><https://access.afsc.noaa.gov/reem/LHWeb/Index.php>

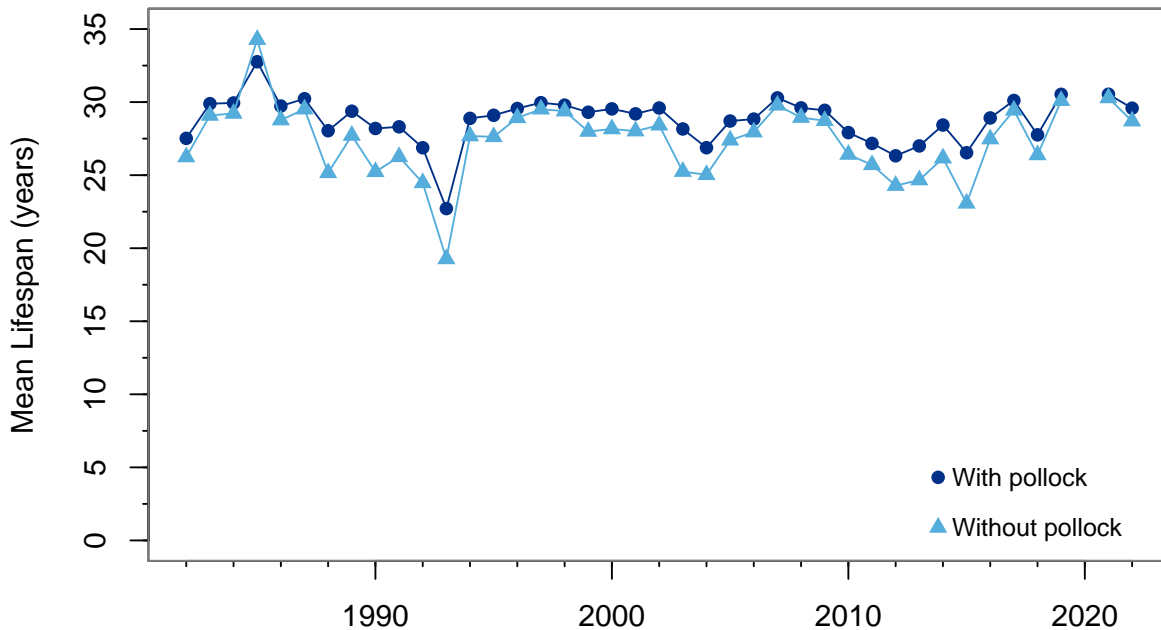


Figure 103: The mean lifespan of the eastern Bering Sea demersal fish community, weighted by biomass indices calculated from the NMFS/AFSC annual summer bottom-trawl survey. The circles are the series with pollock included and the triangles are the series without pollock included.

**Implications:** The groundfish mean lifespan has been stable over the time series of the summer bottom-trawl survey. There is no indication longer-lived species have decreased in relative abundance or are otherwise being replaced by shorter lived-species. Species that are short-lived are generally smaller and more sensitive to environmental variation than larger, longer-lived species (Winemiller, 2005). Longer-lived species help to dampen the effects of environmental variability, allowing populations to persist through periods of unfavorable conditions and to take advantage when favorable conditions return (Berkeley et al., 2004; Hsieh et al., 2006).

## Mean Length of the Fish Community

Contributed by George A. Whitehouse<sup>1</sup> and Geoffrey M. Lang<sup>2</sup>

<sup>1</sup>Cooperative Institute for Climate, Ocean, and Ecosystem Studies (CICOES), University of Washington, Seattle WA

<sup>2</sup>Resource Ecology and Fisheries Management Division, Alaska Fisheries Science Center, National Marine Fisheries Service, NOAA

Contact: andy.whitehouse@noaa.gov

**Last updated: October 2022**

**Description of indicator:** The mean length of the groundfish community tracks fluctuations in the size of groundfish over time. This size-based indicator is sensitive to the effects of commercial fisheries because larger predatory fish are often targeted by fisheries and their selective removal would reduce mean size (Shin et al., 2005). This indicator is also sensitive to shifting community composition of species with different mean sizes. Fish lengths are routinely recorded during the EBS bottom trawl survey, which has occurred each year from 1982 to 2022, except in 2020. Mean lengths are calculated for groundfish species (or functional groups of multiple species; e.g., eelpouts) from the length measurements collected during the trawl survey. The mean length for the groundfish community is calculated with the species mean lengths, weighted by biomass indices (Shin et al., 2010) calculated from the bottom-trawl survey catch data.

This indicator specifically applies to the portion of the demersal groundfish community that is efficiently sampled with the trawling gear used by NMFS during the summer bottom-trawl survey of the EBS at the standard survey sample stations (for survey details see Lauth et al. (2019)). Species that are infrequently encountered or not efficiently caught by the bottom-trawling gear are excluded from this indicator (e.g., sharks, grenadiers, myctophids, pelagic smelts). The survey index used here is the same as that used for fish and invertebrate biomass indices on the report card (Figure 2).

Species (or functional groups) infrequently sampled for lengths (less than five times over the time series) are excluded from this indicator (e.g., capelin, eulachon, greenlings). Twenty-two species are included in this indicator. Eleven species had their lengths sampled in all 40 years of the time series. Another eleven species were sampled between 11 and 37 times over the time series. In those years where lengths were not sampled for a species, we replaced it with a long-term mean for that species.

Walleye pollock is a biomass dominant species in the eastern Bering Sea and may drive the value of community indicators. Therefore this indicator is presented as two time series, one that includes and one that excludes walleye pollock.

**Status and trends:**

*With pollock included:* The mean length of the eastern Bering Sea groundfish community in 2022 is 36.2 cm, just up from 35.7 cm in 2021, and has remained above the long-term mean of 32.5 cm since 2014 (Figure 104, circles).

*Without pollock included:* The mean length of eastern Bering Sea groundfish without pollock is 33.2 cm in 2022, down from 34.5 cm in 2021 (Figure 104, triangles). This series trended upward from 2012 to 2018, but has declined each survey year since. However, it has remained above the long-term mean of 29.5 cm since 2016.

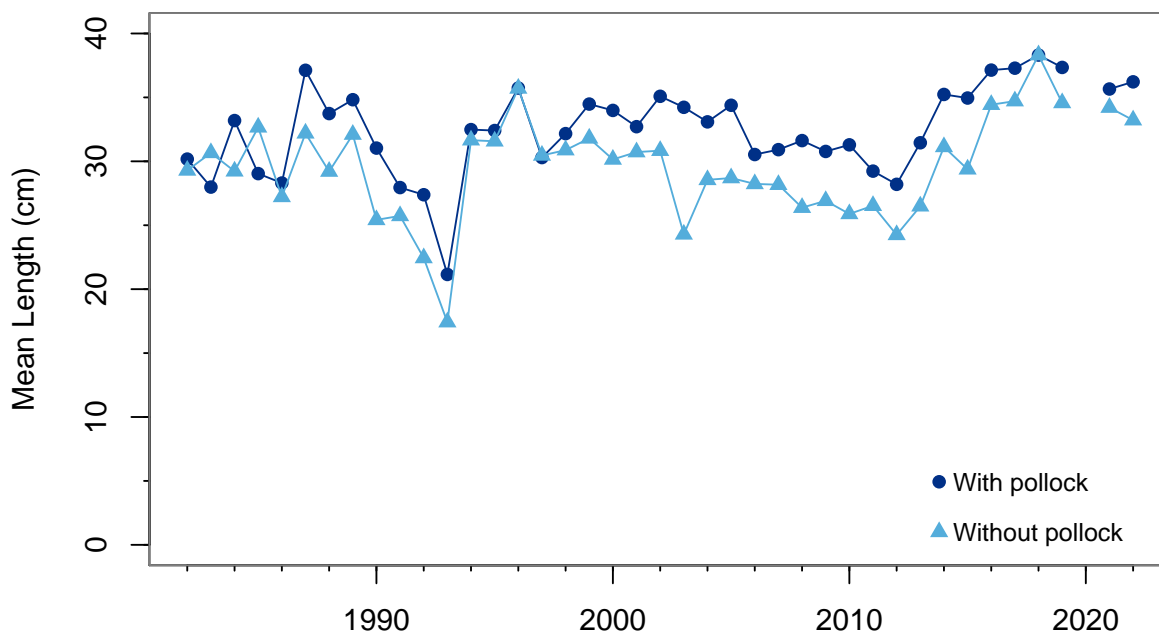


Figure 104: Mean length of the groundfish community sampled during the NMFS/AFSC annual summer bottom-trawl survey of the eastern Bering Sea (1982–2022). The groundfish community mean length is weighted by the relative biomass of the sampled species. The circles are the mean length with pollock included and the triangles are the series without pollock.

**Factors influencing observed trends:** This indicator is specific to the fishes that are routinely caught and sampled during the NMFS summer bottom-trawl survey. The estimated mean length can be biased if specific species-size classes are sampled more or less than others, and is sensitive to spatial variation in the size distribution of species. Changes in fisheries management or fishing effort could also affect the mean length of the groundfish community. Modifications to fishing gear, fishing effort, and targeted species could affect the mean length of the groundfish community if different size classes and species are subject to changing levels of fishing mortality. The mean length of groundfish could also be influenced by fluctuations in recruitment, where a large cohort of small forage species could reduce the mean length of the community. Environmental factors could also influence fish growth and mean length by affecting the availability and quality of food or by direct temperature effects on growth rate.

Walleye pollock is a biomass dominant component of this ecosystem and year-to-year fluctuations in their mean size and biomass have a noticeable effect on this indicator. In 1993, their biomass index was above average but their mean size was the fifth lowest of the time series. Additionally, 1993 was a pronounced peak in the biomass index of capelin. This reduced the proportional contribution of other species to the total groundfish biomass index, thus reducing the indicator value (i.e., mean length) in 1993. Years where this indicator attained its highest values (1987, 2016–2022) generally correspond to years of above-average mean size and/or biomass index for pollock, except 2018 and 2021 where pollock mean size was average but their biomass index was below average.

The series without pollock mirrored the overall trends in the series with pollock included, but was generally lower. This was because the mean length of pollock was generally a few cm greater than the mean length of the rest of the groundfish community. Exceptions occurred in 1983, 1985, and 2018 when the mean length of pollock was less than the mean of the rest of the groundfish community. In these three instances, the indicator value was higher for the series without pollock.

**Implications:** The mean length of the groundfish community in the eastern Bering Sea has been stable over the bottom-trawl time series (1982–2022) with some interannual variation. The collective stability of the combined biomass of relatively larger groundfish species has helped to maintain this indicator at its recent high values. Previous dips in this indicator were in part attributable to spikes in abundance of smaller forage species (e.g., capelin) as opposed to a sustained shift in community composition or reductions in species mean length.

## Stability of Groundfish Biomass

Contributed by George A. Whitehouse

Cooperative Institute for Climate, Ocean, and Ecosystem Studies (CICOES), University of Washington, Seattle WA

Contact: andy.whitehouse@noaa.gov

**Last updated: October 2022**

**Description of indicator:** The stability of the groundfish community total biomass is measured with the inverse biomass coefficient of variation (1 divided by the coefficient of variation of total groundfish biomass ( $1/CV[B]$ )). This indicator provides a measure of the stability of the ecosystem and its resistance to perturbations. The variability of total community biomass is thought to be sensitive to fishing and is expected to increase with increasing fishing pressure (Blanchard and Boucher, 2001). This metric is calculated following the methods presented in Shin et al. (2010). The CV is the standard deviation of the groundfish biomass index over the previous 10 years divided by the mean over the same time span. The biomass index for groundfish species was calculated from the catch of the NMFS/AFSC annual summer bottom-trawl survey of the eastern Bering Sea (EBS). Since 10 years of data are required to calculate this metric, the indicator values start in 1991, the tenth year in the trawl survey time series (1982–2022). This metric is presented as an inverse, so as the CV increases the value of this indicator decreases, and if the CV decreases the value of this indicator increases.

This indicator specifically applies to the portion of the demersal groundfish community that is efficiently sampled by the trawling gear used by NMFS during the annual summer survey at the standard survey sample stations (for survey details see Lauth et al. (2019)). Species that are infrequently encountered or not efficiently caught by the bottom-trawling gear are excluded from this indicator (e.g., sharks, grenadiers, myctophids, pelagic smelts). The survey index used here is the same as that used for fish and invertebrate biomass indices on the report card (Figure 2).

Walleye pollock is a biomass dominant species in the eastern Bering Sea and may drive the value of this community indicator. Therefore this indicator is presented as two time series, one that includes and one that excludes walleye pollock.

### Status and trends:

*With pollock included:* The state of this indicator in 2022 is 6.178, which is nearly equal to its value of 6.176 in 2021 (Figure 105, circles). The previous high of 7.90 was observed in 1992, which was followed by a steady decrease to a low of 3.84 in 2002. Since then it gradually increased to a value of 5.84 in 2018 before sharply increasing to a new high in 2019. This indicator is currently above the long-term mean of 5.2.

*Without pollock included:* This indicator had a modest increase from 7.05 in 2021 to 7.20 in 2022 (Figure 105, triangles). This indicator dropped sharply from 7.49 in 1992 to 3.41 in 1993, and remained below four until 2003, where the value increased to 5.44. The indicator remained relatively stable until 2010, when the indicator began a steady upward trend to the series high value in 2019.

**Factors influencing observed trends:** Fishing is expected to influence this metric as fisheries can selectively target and remove larger, long-lived species affecting population age structure (Berkeley et al., 2004; Hsieh et al., 2006). Larger, longer-lived species can become less abundant and be replaced by smaller shorter-lived species (Pauly et al., 1998). Larger, longer-lived individuals help populations to endure prolonged periods of unfavorable environmental conditions and can take advantage of favorable conditions when they return (Berkeley et al., 2004). A truncated age-structure could lead to higher population variability (CV) due to increased sensitivity to environmental dynamics (Hsieh et al., 2006). Interannual variation in this metric could also be influenced by interannual variation in species abundance in the trawl survey catch, patchy spatial distribution for some species, or species distribution shifts (Stevenson and Lauth, 2019; Thorson, 2019b). This metric, as calculated here with trawl-survey data, reflects the stability of the portion of the groundfish community that is represented in the catch data of the annual summer bottom-trawl survey.

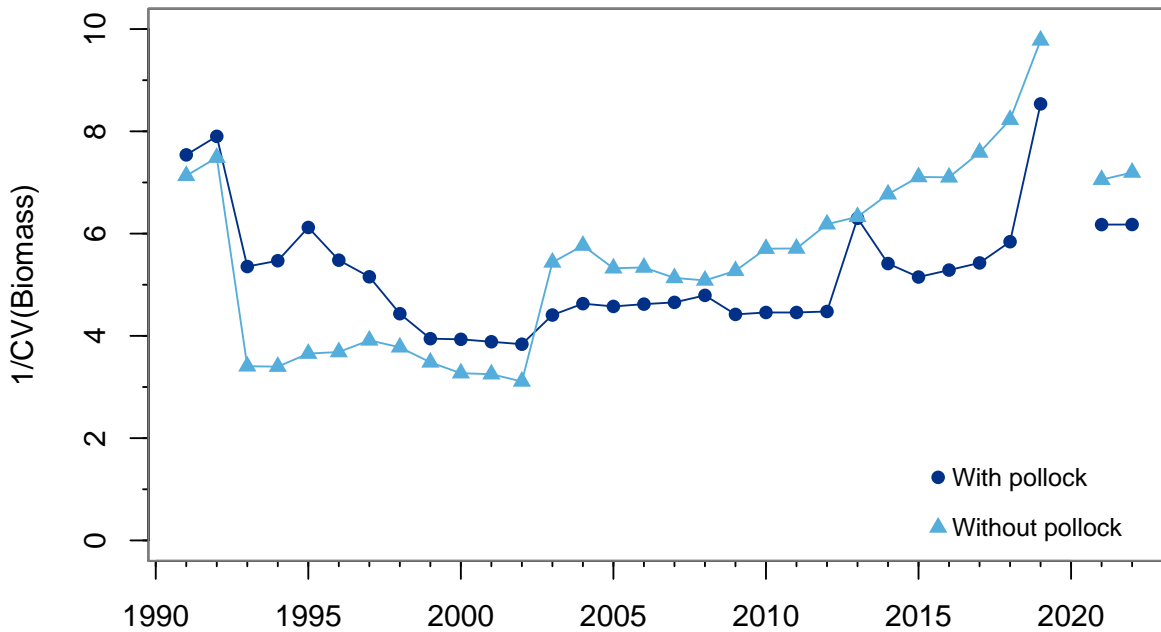


Figure 105: The stability of groundfish biomass in the eastern Bering Sea represented with the inverse biomass coefficient of variation of total groundfish biomass ( $1/CV[B]$ ). Ten years of data are required to calculate this metric, so this time series begins in 1991 after the tenth year of the NMFS/AFSC annual summer bottom-trawl survey. The circles are the series with pollock included in the index, and the triangles are the same series but with pollock excluded.

Both sharp increases or decreases in species index values can increase variability and reduce the indicator value.

The high values for this indicator in 2019 and at the start of the time series are indicative of stable groundfish biomass with a relatively low CV during the previous ten years. The CVs for both time series (with and without pollock) in 2019 were the lowest over their respective time series resulting in their highest indicator values. The sharp drop in total biomass in 2021, particularly for pollock, increased the CV resulting in lower indicator values in 2021. Previously, both series dropped sharply from 1992 to 1993. This was because the index for capelin in 1993 was anomalously high which increased variability and reduced the indicator value. In 2003, both series increased, which was in part due to the high capelin value in 1993 no longer being a part of the most recent 10 years.

In 2009, the series without pollock began a steady increase towards its high value in 2019. The series with pollock included has a more modest positive trend over the same span, with high values in 2013 and 2019. Pollock is a biomass dominant species in the eastern Bering Sea and interannual fluctuations in their biomass are sufficient to increase variability for the total groundfish community and thus, reduce the indicator value. The series without pollock is more sensitive to fluctuations of other species, such as capelin. The sharp increase in the capelin index in 1993 kept this series lower than the series with pollock included from 1993–2002.

**Implications:** The measure  $1/CV[B]$  indicates that the eastern Bering Sea groundfish community has been generally stable over the time period examined here, particularly since 2003. While the drop in biomass from 2019 to 2021 increased the CV and reduced both indicators (with and without pollock), both series remain above their long-term means in 2022 and indicate a maintenance of community biomass stability.

# Emerging Stressors

## Ocean Acidification

Contributed by Darren Pilcher<sup>1,2</sup>, Jessica Cross<sup>2</sup>, Esther Kennedy<sup>3</sup>, Elizabeth Siddon<sup>4</sup>, and W. Christopher Long<sup>5</sup>

<sup>1</sup>Cooperative Institute for Climate, Ocean, and Ecosystem Studies (CICOES), University of Washington, Seattle WA

<sup>2</sup>NOAA – Pacific Marine Environmental Laboratory [PMEL]

<sup>3</sup>University of California, Davis

<sup>4</sup>NOAA Fisheries, Alaska Fisheries Science Center, Auke Bay Laboratories, Juneau, AK

<sup>5</sup>NOAA Fisheries, Alaska Fisheries Science Center, Kodiak Laboratory, Kodiak, AK

Contact: darren.pilcher@noaa.gov

**Last updated: October 2022**

**Description of indicator:** The oceanic uptake of anthropogenic CO<sub>2</sub> is decreasing ocean pH and carbonate saturation states in a process known as ocean acidification (OA). The cold, carbon rich waters of the Bering Sea are already naturally more corrosive than other regions of the global ocean, making this region more vulnerable to rapid changes in ocean chemistry. The projected areal expansion and shallowing of these waters with continued absorption of anthropogenic CO<sub>2</sub> from the atmosphere poses a direct threat to marine calcifiers and an indirect threat to other species through trophic interactions. These OA risks demonstrate a clear need to track and forecast the spatial extent of acidified waters in the Bering Sea.

Here, we present updated carbonate chemistry output from the Bering Sea ROMS model (Bering10K; Pilcher et al. (2019)), which has been expanded from its previous 2003–2021 time frame to now span 1970–September 4, 2022. We show spatial plots for Bering Sea bottom water pH, including both the conditions in 2022 (Figure 106, left) as well as the 2022 detrended anomaly (Figure 106, right). The detrended anomaly removes the impact of ocean acidification (otherwise a slow, consistent process) and highlights the role of natural processes, which generate most of the interannual variability in the carbon system. It is calculated as the residual after removing the linear trend over the entire 1970–2022 hindcast, similar to removing the global warming trend from a long term temperature time series. This year, we were also able to collect pH measurements on-board the BASIS survey, allowing for a direct model-data comparison (Figure 106, left). We focus on bottom waters and the late summer time frame because this is where and when we expect the most acidic waters to develop, due to the combination of ocean acidification pressures and natural seasonal biological respiration. This is also when temperatures are close to their highest and are thus most likely to have synergistic negative effect on crabs (Swiney et al., 2017). This model output is used to develop indices for both pH and the aragonite saturation state ( $\Omega_{\text{arag}}$ ) using threshold values of biological significance (Figures 107 and 108). The growth and survival of red king crab and tanner crab are negatively affected at  $\text{pH} \leq 7.8$  (Long et al., 2013), and bivalve larvae are negatively affected at  $\Omega_{\text{arag}} < 1$  (Waldbusser et al., 2015). The goal of this index time series, along with the spatial anomaly plot, is to provide a quick assessment of the summer water pH and  $\Omega_{\text{arag}}$  conditions compared to previous years.

**Status and trends:** Modeled bottom water pH and  $\Omega_{\text{arag}}$  were slightly lower than the detrended shelf average conditions over most of the outer and middle shelf, with pH values generally near or less than 7.8 (Figure 106, left). In contrast to the lower values suggested by the model, preliminary data collected on the BASIS survey identified large portions of the middle shelf domain with  $\text{pH} > 7.8$ , though confirmed some regions of  $\text{pH} < 7.8$ . This comparison will help guide future efforts to identify any model deficiencies that may have generated this model-data mismatch, though preliminary work suggests that a coccolithophore bloom (which is not included in the model) may be partly responsible (see Nielsen et al., p. 73). Modeled inner shelf waters maintained much higher pH values, and were overall slightly higher than usual. An exception is visible in the northern inner shelf near Bering Strait, where modeled inner shelf waters were much lower

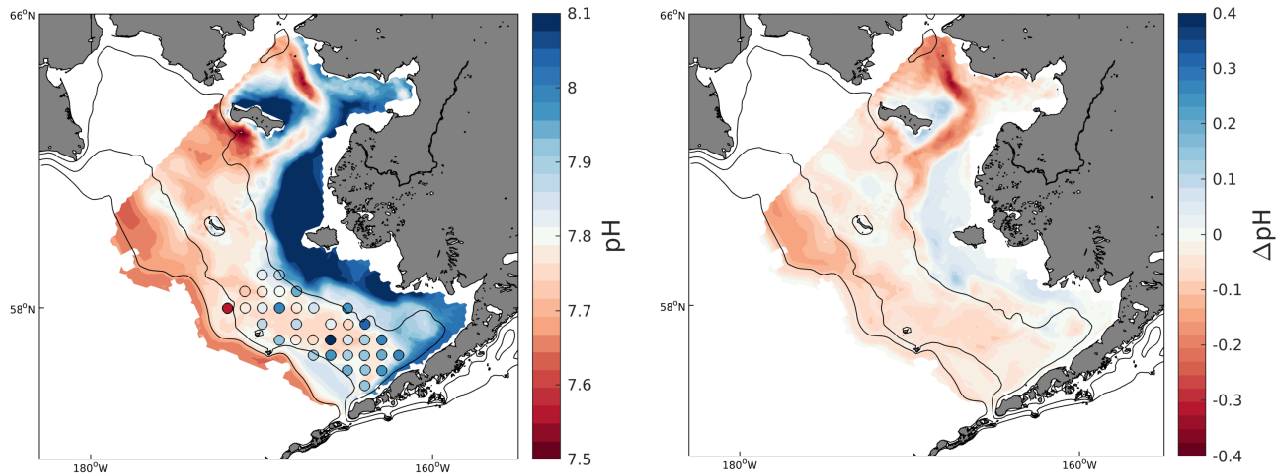


Figure 106: Model spatial maps of Jul-Sep averaged bottom water pH for (left) 2022 hindcast and (right) the 2022 (updated through Sep 04) detrended anomaly. The circles in the left panel represent the preliminary\* data collected on-board the fall BASIS survey, plotted on the same colorbar as the model output. Contour lines denote the 50m, 100m, and 200m isobaths. Regions that are outside of the eastern Bering Sea management region are omitted. Impacts of ocean acidification on fisheries are understood to be a combination of the temporal duration, biogeochemical intensity, and spatial extent. This visualization shows both the intensity and extent of acidified conditions over the eastern Bering Sea shelf. \*Data have not yet undergone quality assurance and control at the time of this writing.

in pH than average, leading to some localized regions of  $\text{pH} < 7.8$ . Notably, the outer shelf negative pH anomaly - a persistent anomaly in the model since 2018 - was still present, but has slightly weakened since 2021 (Figure 106, right).

**Factors influencing observed trends:** Relatively lower pH and  $\Omega_{\text{arag}}$  conditions this year are consistent with a return to average or slightly cooler modeled bottom water temperatures. The model consistently associates colder temperature years with lower pH and  $\Omega_{\text{arag}}$  due to both direct effects on solubility and indirect effects via increased fall productivity and ocean carbon uptake.

**Implications:** Based on the sensitivity of red king crab to pH, previous work suggests that OA may have significant negative impacts to the red king crab fishery (Seung et al., 2015; Punt et al., 2016). However, these effects are not expected to emerge at present, as other environmental variables (e.g., temperature) are better predictors of red king crab variability. Modeled pH and  $\Omega_{\text{arag}}$  water conditions in Bristol Bay for 2022 are near or slightly below the detrended average conditions and the shallower inner shelf waters that serve as habitat for juvenile red king crab are relatively well buffered. Although large portions of the outer and middle shelf contain model pH values less than 7.8, these waters are relatively more acidic at baseline. Furthermore, the preliminary BASIS survey data does not suggest as widespread of  $\text{pH} < 7.8$  conditions on the middle shelf, particularly in the southeastern portion. At this time, there is no evidence that OA can be linked to recent declines in surveyed snow crab and red king crab populations.

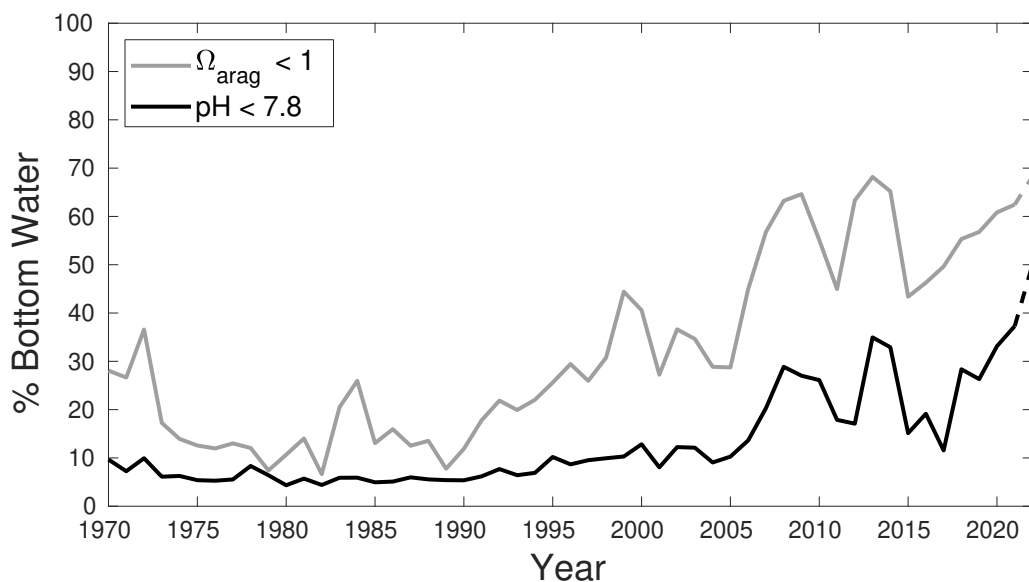


Figure 107: Model time series of the Jul-Sep pH index (black line) and  $\Omega_{\text{arag}}$  undersaturation index (grey line). Each index is calculated as the percent of spatial area of the eastern Bering Sea region (see Figure 106) where bottom waters have a Jul-Sep average below the denoted value. The dashed portion at the end represents the incomplete 2022 value, which is run up through Sep 4. Impacts of ocean acidification on fisheries are understood to be a combination of the temporal duration, biogeochemical intensity, and spatial extent. This visualization shows the percent area (spatial extent) of the shelf that is exposed to potentially harmful biogeochemical conditions.

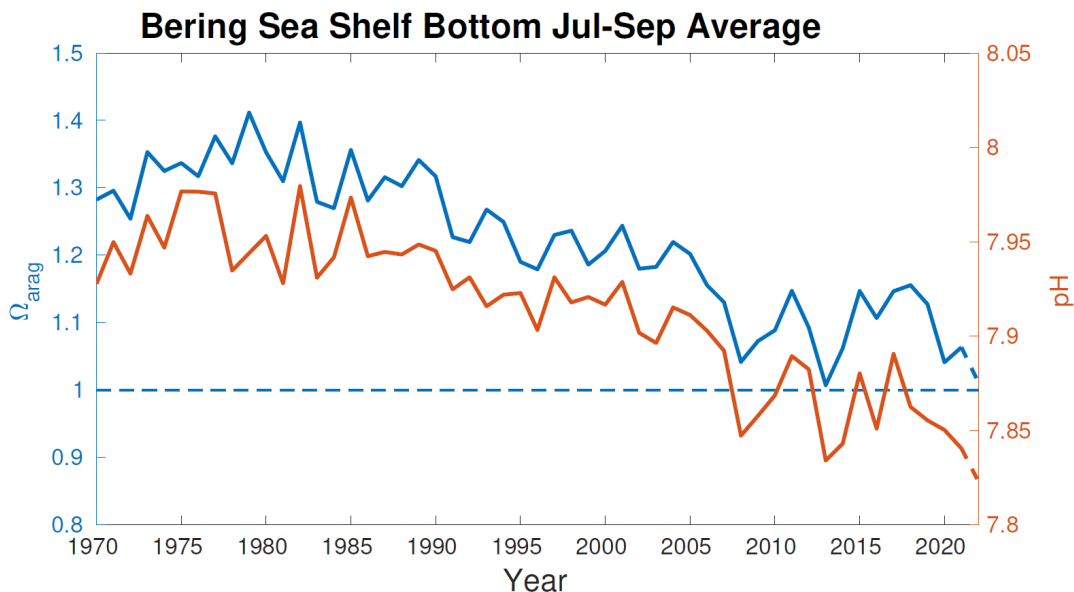


Figure 108: Model timeseries of the annualized Jul-Sep average bottom water  $\Omega_{\text{arag}}$  (left vertical axis, blue) and pH (right vertical axis, red). The dashed portion at the end represents the incomplete 2022 value, which is run up through Sep 4. Impacts of ocean acidification on fisheries are understood to be a combination of the temporal duration, biogeochemical intensity, and spatial extent. Visualizing the net shelf-wide average, rather than scaling these variables spatially (see Figure 107), helps show the intensity of aggregate conditions. However, it is important to consider this figure in context with Figures 106 and 107, as a shelf-wide average may disguise some areas of resilience (e.g., cool colors, Figure 106).

## Harmful Algal Blooms

Contributed by Thomas Farrugia<sup>1</sup>, Natalie Rouse<sup>2</sup>, Emma Pate<sup>3</sup>, Veronica Padula<sup>4</sup>, Hanna Hellen<sup>4</sup>, Opik Ahkinga<sup>5</sup>, Kathleen Easley<sup>6</sup>, Louisa Castrodale<sup>6</sup>

<sup>1</sup> Alaska Ocean Observing System, Anchorage, AK

<sup>2</sup> Alaska Veterinary Pathology Services, Eagle River, AK

<sup>3</sup> Norton Sound Health Corporation, Nome, AK

<sup>4</sup> Aleut Community of St. Paul, St. Paul Island, AK

<sup>5</sup> Little Diomedede, AK

<sup>6</sup> AK Department of Health and Social Services, Anchorage, AK

Contact: farrugia@aos.org

Last updated: September 2022

**Description of indicator:** Alaska's most well-known and toxic harmful algal blooms (HABs) are caused by *Alexandrium* spp. and *Pseudo-nitzschia* spp. *Alexandrium* produces saxitoxin (STX) which can cause paralytic shellfish poisoning (PSP) and has been responsible for five deaths and over 100 cases of PSP in Alaska since 1993<sup>26</sup>. Analyses of paralytic shellfish toxins are commonly reported as of toxin/100 g of tissue, where the FDA regulatory limit is 80/100g. Toxin levels between 80–1000/100 g are considered to potentially cause non-fatal symptoms, whereas levels above 1000/100g (~12x regulatory limit) are considered potentially fatal.

*Pseudo-nitzschia* produces domoic acid which can cause amnesic shellfish poisoning and inflict permanent brain damage. Domoic acid (DA) has been detected in 13 marine mammal species and has the potential to impact the health of marine mammals and birds in Alaska. No human health impacts of DA have been reported in Alaska, although both acute and chronic amnesic shellfish poisoning has been reported in several states, including Washington and Oregon.

The State of Alaska tests all commercial shellfish harvests. However, there is no state-run shellfish testing program for recreational and subsistence shellfish harvests. Regional programs, run by Tribal, agency, and university entities, have expanded over the past five years to provide test results to inform harvesters and researchers, and to reduce human health risk (Figure 109). All of these entities are partners in the Alaska Harmful Algal Bloom Network which was formed in 2017 to provide a statewide approach to HAB awareness, research, monitoring, and response in Alaska. More information on methods can be found on the Alaska HAB Network website<sup>27</sup> or through the sampling partners listed above.

### Status and trends:

*Alaska Region:* Results from shellfish and phytoplankton monitoring showed an overall lower presence of harmful algal blooms (HABs) throughout all regions of Alaska in 2022 compared to 2021, 2020, and 2019. However, bivalve shellfish from areas that are well known for having PSP levels above the regulatory limit, including Southeast Alaska and Unalaska, continued to have samples that tested above the regulatory limit (particularly from March to September), albeit less frequently than since 2019. Over the last few years, the dinoflagellate *Dinophysis* (which may cause Diarrhetic Shellfish Poisoning, DSP) has become more common and abundant in water samples, and 2022 continued that trend.

We are seeing a geographic expansion of areas that are being sampled for phytoplankton species, so the decrease in the number of HABs detected may be more related to generally cooler water temperatures, especially in the Gulf of Alaska. A detailed survey of HABs from the northern Bering Sea to the western Beaufort Sea was conducted. This is the first-ever extensive survey of HABs in this region.

<sup>26</sup>State of Alaska. Epidemiology Bulletin. 2022. Available at: [http://www.epi.alaska.gov/bulletins/docs/b2022\\_05.pdf](http://www.epi.alaska.gov/bulletins/docs/b2022_05.pdf)

<sup>27</sup><https://ahab.aos.org>

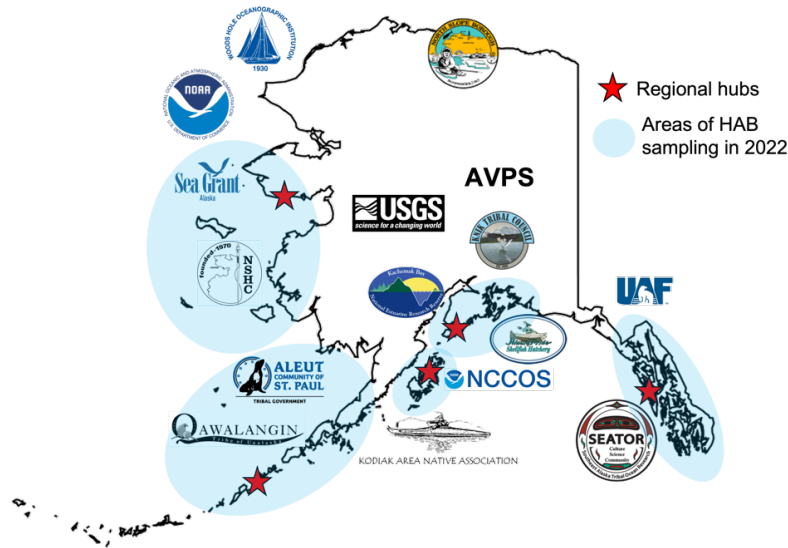


Figure 109: Map of 2022 sampling areas and partners conducted by partners of the Alaska Harmful Algal Bloom Network (AHAB). Opportunistic sampling of marine mammal tissue and other marine species occurs statewide and is not shown here.

The Alaska Department of Environmental Conservation tests bivalve shellfish harvested from classified shellfish growing areas meant for the commercial market for marine biotoxins including paralytic shellfish toxin (PST, tested by mouse bioassay and post-column oxidation) in all bivalve shellfish and domoic acid specifically in razor clams. The Environmental Health Laboratory (EHL) also does testing for research, tribal, and subsistence use. The EHL is the sole laboratory in the state of Alaska certified by the FDA to conduct regulatory tests for commercial bivalve shellfish. As of September 2022, the EHL has analyzed 371 commercial samples (DA: 0, PST: 371) and 723 non-commercial samples (DA: 537, PST: 186).

The sole commercial razor clam fishery in Alaska did not operate in 2022 as a result of the COVID-19 pandemic, and no regulatory tests for DA in razor clams were conducted.

The Alaska Department of Health, Section of Epidemiology (SOE), continues to partner with the AHAB network. Nurse consultants join in on the monthly meetings and collaborate with stakeholders so they can be made aware of reportable illness such as Paralytic shellfish Poisoning (PSP). In April 2022, an Epidemiology Bulletin describing cases was released<sup>28</sup>.

More information about PSP and other shellfish poisoning can be found on the SOE website<sup>29</sup>.

*Pribilof Islands:* The Aleut Community of St Paul ECO (Ecosystem Conservation Office) started sampling for HAB species around St. Paul Island in 2022. Tribal staff have brought and set up HAB sampling equipment to the island and started conducting phytoplankton tows from the docks on St. Paul. So far, samplers have identified over a dozen phytoplankton species in their samples, including HAB species such as *Alexandrium* sp., *Dinophysis* sp., and *Chaetoceros* sp. The ECO plans to continue sampling for HABs through next summer to capture a full year of phytoplankton samples along with environmental variables. Winter sampling may be less frequent due to the sampling dock becoming unavailable for the winter months.

*Northern Bering Sea:* Norton Sound Health Corporation (NSHC) staff continue high-paced communications with partners for the developing Norton Sound Tribal Harmful Algal Bloom Program (NSTHAB). To date, NSHC staff have traveled to Savoonga, Elim, and Gambell to inform these communities of the NSTHAB

<sup>28</sup>[http://www.epi.alaska.gov/bulletins/docs/b2022\\_05.pdf](http://www.epi.alaska.gov/bulletins/docs/b2022_05.pdf)

<sup>29</sup><https://health.alaska.gov/dph/Epi/id/Pages/dod/psp/default.aspx>

Program and include input from regional Tribes and environmental resources in the planning process. Regional samplers are working on collecting water samples and traditional food samples for toxin testing at all locations within the NSTHAB.

Water samples were collected regularly in 2022 in and near Nome, AK for microscopy to identify phytoplankton target species of *Alexandrium*, *Dynophysis*, and *Pseudo-nitzschia*. Identification is in the process of review through NOAA QA/QC to confirm results. The water at Cape Nome Port was sampled to complete microscopy in the UAF Science Lab. Sampling has also taken place off the Port of Nome two miles offshore based on weather and availability of the Harbormaster boat and driver.

The Native Village of Diomed developed a two-year BIA Tribal Resilience Program proposal for funds to continue monitoring crab, harmful algal blooms, ocean acidification, toxins, and crab distribution in 2021. During the first year of the project, staff identified *Dynophysis*, *Pseudo-nitzschia*, and *Alexandrium* species from collected net tow samples in April 2022. Samples were analyzed in Diomed and also confirmed by partners at NOAA NCCOS lab in Charleston SC with scanning electron microscopy. Crab tissue samples are currently being analyzed for toxicity using receptor binding assay at the NOAA NCCOS lab in Charleston.

Alaska Veterinary Pathology Services (AVPS) and University of Alaska Anchorage spearheaded a behavioral log as part of the ECOHAB project where any unusual (and potentially HABs exposure-related) wildlife behaviors could be recorded. Twenty samples were collected for saxitoxin and domoic acid for testing at WARRN West, pending shipment this fall.

Through the ECOHAB project “Harmful algal bloom toxins in Arctic food webs”, community samplers and researchers are collecting samples throughout the food web to test for HAB toxins. For more information about this project, see Lefebvre et al., p. 170.

**Factors influencing observed trends:** HABs are likely to increase in intensity and geographic distribution in Alaska waters with warming water temperatures. Observations in Southeast and Southcentral Alaska suggest *Alexandrium* spp. blooms occur at temperatures above 10°C and salinities above 20 (Vandersea et al., 2018; Tobin et al., 2019; Harley et al., 2020). As waters warm throughout Alaska, blooms may increase in frequency and geographic extent.

**Implications:** HABs pose a risk to human health when present in wildlife species that people consume, including shellfish, birds, and marine mammals. Research across the state is attempting to improve understanding of the presence and circulation of HABs in the food web. HAB toxins have been detected in stranded and harvested marine mammals from all regions of Alaska in past years (Lefebvre et al., 2016). A multi-disciplinary statewide study funded by NOAA’s ECOHAB program is underway and encompasses ship-based sediment samples, water samples, zooplankton samples, multiple species of fish, bivalves, and the continuation of sampling subsistence-harvested and dead, stranded marine mammals.

## ECOHAB: Harmful Algal Bloom (HAB) Toxins in Arctic Food Webs

Contributed by Kathi Lefebvre<sup>1</sup>, Don Anderson<sup>2</sup>, Gay Sheffield<sup>3</sup>, Evangeline Fachon<sup>2</sup>, Patrick Charapata<sup>1</sup>, Robert Pickart<sup>2</sup>, Emily Bowers<sup>1</sup>

<sup>1</sup>Environmental and Fisheries Science, Northwest Fisheries Science Center, National Marine Fisheries Service, NOAA, Seattle, WA

<sup>2</sup>Woods Hole Oceanographic Institution, Woods Hole, MA

<sup>3</sup>University of Alaska Fairbanks, Alaska Sea Grant, Nome, AK

Contact: kathi.lefebvre@noaa.gov

Last updated: September 2022

**Description of indicator:** *Alexandrium* and *Pseudo-nitzschia* are two common harmful algal bloom (HAB) species in Alaskan waters that produce neurotoxic compounds such as saxitoxin (STX; generated by *Alexandrium* species; causes Paralytic Shellfish Poisoning PSP) and domoic acid (DA; generated by *Pseudo-nitzschia* species; causes Amnesic Shellfish Poisoning ASP). Monitoring the presence and abundance of HAB cell (i.e., *Alexandrium* and *Pseudo-nitzschia*) densities and toxin (STX and DA) prevalence in marine food webs are useful indicators of ecosystem health and potential threats to wildlife and human health. There is clear evidence that HAB toxins are present in Arctic and Subarctic food webs (Figure 110). The risks of these toxins include human illness and death associated with seafood consumption as well as health impacts to marine wildlife at multiple trophic levels. Many commercially valuable shellfish and finfish are impacted by these toxins, as well as marine mammals, invertebrates, seabirds, and filter-feeding fishes that are harvested for subsistence purposes and consumed by Alaska's coastal communities.



Figure 110: Algal toxins detected in stranded and harvested marine mammals confirm widespread prevalence of HABs throughout the food web in all regions of Alaska (Lefebvre et al., 2016).

**Status and trends:** As the climate has warmed over the past few decades, the Pacific sector of the Arctic Ocean has warmed with dramatic consequences. The quality, quantity, and duration of sea ice has decreased markedly due to earlier melting and a delayed freeze-up (Frey et al., 2014). The input of Pacific water northwards through the Bering Strait has increased, warmed, and freshened (Woodgate et al., 2012). Warmer air temperatures are peaking earlier in the season and have led to increased summer ocean warming (Pickart et al., 2013). Stronger summertime northeasterly winds have led to upwelling-favorable conditions along the western Alaskan coast (Pickart et al., 2011). Combined, these physical changes have made conditions more favorable for HAB species, particularly the dinoflagellate *Alexandrium catenella* and diatoms in the genus *Pseudo-nitzschia* (Anderson et al., 2012).

Recent studies reveal increasing toxin prevalence in food webs (Hendrix et al., 2021) and the potential for increased *Alexandrium* cyst germination in certain cyst-dense areas, such as the seafloor in the northeastern Chukchi Sea, which are directly linked to warmer ocean bottom temperatures (Anderson et al., 2021). Saxitoxin doses were estimated during an anomalously warm year (2019) in the Arctic revealing that walrus were exposed to toxin concentrations at levels known to impact human health during shellfish poisoning events, as well as rodents in controlled laboratory studies (Lefebvre et al., 2022). In August of 2022, dangerously high abundances of *Alexandrium* were observed in the Kotzebue Sound area with surface cell densities  $>30,000$  Cells  $L^{-1}$  indicative of an intense HAB event (Figure 111 top). Clams sampled during the *Alexandrium* bloom exhibited STX concentrations near the seafood regulatory limit (Figure 111 bottom). The unclear nature of how HABs are formed over different spatial and temporal ranges in Alaska is an ongoing research objective.

**Factors influencing observed trends:** Increasing HAB events and toxin prevalence is linked to warming ocean temperatures throughout the water column (both surface and bottom) and increased sunlight associated with the loss of sea-ice cover. Powerful storms<sup>30</sup> re-suspend cysts into the water column and sustain ongoing blooms or inoculate new HAB events.

**Implications:** The impacts of increased biotoxin exposure include increased risks to ecosystem, wildlife, and public health in Northern Arctic regions. As ocean temperatures continue to rise, algal growth and cyst germination rates of toxic *Alexandrium* will continue to increase. Intense *Alexandrium* blooms and clams with potentially dangerous toxin levels were observed this past summer during an extensive HAB sampling effort conducted aboard the R/V Norseman II from July 17<sup>th</sup> through September 6<sup>th</sup>, 2022. These findings indicate that HAB events are intensifying in Alaskan waters and there is a clear need to monitor HAB densities and toxin concentrations throughout the food web. Impacts also include food security concerns to Arctic coastal peoples as well as conservation concerns for many species of marine resources, including several marine mammals currently listed under the Endangered Species Act (ESA). Arctic coastal people sampling efforts are being developed, but consistent funding is needed to sustain temporal and spatial monitoring coverage of HAB activity in the Alaskan ecosystem.

Alaskan Community Sampling:

In addition to research cruises, HAB sampling is performed by local communities. Seawater sampling (weekly) from the beach to monitor for *Alexandrium* and *Pseudo-nitzschia* continued at Nome into fall 2021 and stopped for the winter with the November arrival of sea ice. Weekly sampling resumed in early July 2022 at a new site off of the Cape Nome pier. Seawater samples were also collected at Diomed during September–October 2021 and March–May 2022. In response to the 2022 HAB event discovered by the Norseman II cruise in August in the Bering Strait region, additional nearshore seawater samples were collected during late August from the Point Spencer and Woolley Lagoon areas as well as along the north shore of the Seward Peninsula. Lastly, fecal samples from two dead stranded walrus and a harvested subadult spotted seal were collected during the same time period near Shishmaref. These samples will be analyzed to further elucidate the severity of HABs and toxin presence in the region.

---

<sup>30</sup><https://alaskapublic.org/2022/09/17/powerful-storm-slams-western-alaska/>

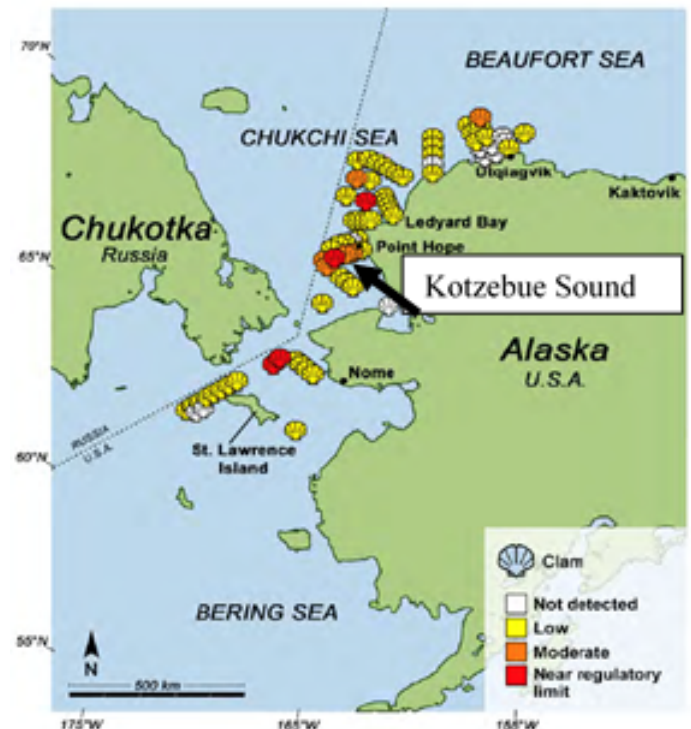
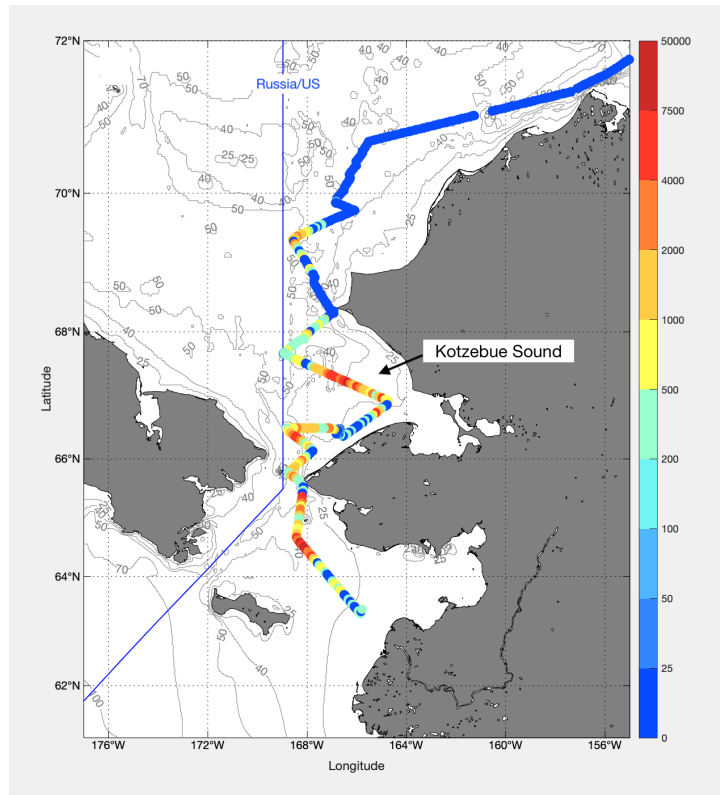


Figure 111: Top: *Alexandrium* cell densities (Cells L<sup>-1</sup>) at different stations (circles) sampled August 9–14, 2022 during the HABs Leg 1 cruise (unpubl. data from D. Anderson). Bottom: Paralytic shellfish toxins (Saxitoxin equivalents [STX equiv./100 g shellfish]) concentrations of clams sampled during the same period as the HAB event (unpubl. data from K. Lefebvre). Kotzebue Sound (arrow) had (A) surface cell densities at dangerous levels (>30,000 Cells L<sup>-1</sup>) and (B) clams had high STX concentrations (“Near Regulatory Limit” [Seafood Safety Regulatory Limit = 80 STX equiv./100 g shellfish]).

#### Future Steps:

Ongoing research projects include the continuous monitoring of *Alexandrium* and *Pseudo-nitzschia* within Alaskan waters and their biotoxins among marine trophic levels. Innovative technology such as the Imaging FlowCytobot (IFCB) allows continuous 24/7 underway sampling during extended research cruises (> 1 month). The IFCB can identify *Alexandrium* and *Pseudo-nitzschia* cells and provide cell densities using machine learning based algorithms. This proved crucial in alerting communities during the 2022 HAB event (Figure 111) and will be used during future cruises. Currently, the impacts of toxin exposure to the Arctic marine ecosystem during HABs are unknown. Thus, cruises will continue to collect samples from organisms throughout different components of the food web (phytoplankton, zooplankton, invertebrates, fish, and marine mammals) to develop toxin trophic transfer models that will estimate biotoxin exposure to commercially important marine resources and Native Alaskan food resources during HABs of different intensities. Data are available from 2019–2022 and various analyses relating to HAB species abundances and trophic transfer models are underway. Clearly, continuous HAB monitoring efforts need to be implemented to ensure future ecosystem and Native Alaskan community health.

# Maintaining Diversity: Discards and Non-Target Catch

## Time Trends in Groundfish Discards

Contributed by Anna Abelman

Resource Ecology and Fisheries Management Division, AFSC, NMFS, NOAA

Alaska Fisheries Information Network, Pacific States Marine Fisheries Commission

Contact: [anna.abelman@noaa.gov](mailto:anna.abelman@noaa.gov)

Last updated: September 2022

**Description of indicator:** Estimates of groundfish discards for 1993–2002 are sourced from NMFS Alaska Region’s blend data, while estimates for 2003 and later come from the Alaska Region’s Catch Accounting System. These sources, which are based on observer data in combination with industry landing and production reports, provide the best available estimates of groundfish discards in the North Pacific. Discard rates as shown in Figure 112 below are calculated as the weight of groundfish discards divided by the total (i.e., retained and discarded) catch weight for the relevant area gear-target sector. Where rates are described below for species or species groups, they represent the total discarded weight of the species/species group divided by the total catch weight of the species/species group for the relevant area-gear-target sector. These estimates include only catch of FMP-managed groundfish species within the FMP groundfish fisheries. Discards of groundfish in the halibut fishery and discards of forage fish and species managed under prohibited species catch limits, such as halibut, are not included.

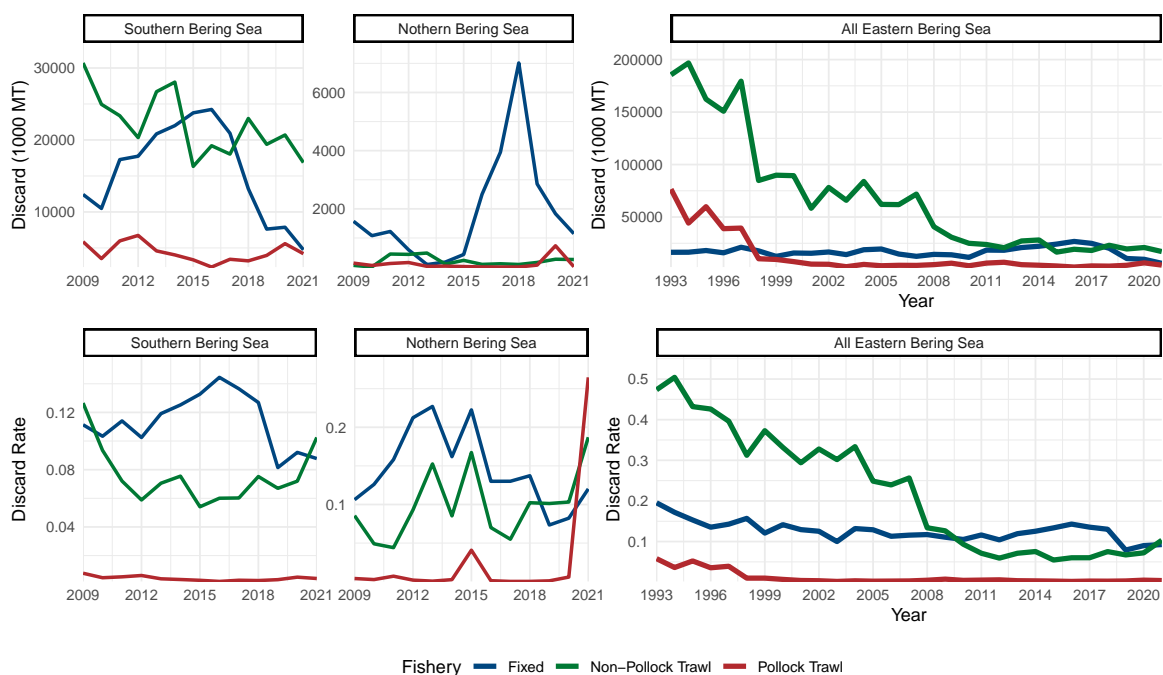


Figure 112: Total biomass and percent of total catch biomass of FMP groundfish discarded in the fixed gear, pollock trawl, and non-pollock trawl sectors for the eastern Bering Sea region, 1993–2021; and for northern (NBS) and southern (SBS) subregions, 2009–2021. Discard rates are calculated as total discard weight of FMP groundfish divided by total retained and discarded weight of FMP groundfish for the sector (includes only catch counted against federal TACs).

**Status and trends:** Since 1993, discard rates of groundfish in federally-managed Alaskan groundfish fisheries have generally declined in the trawl pollock and non-pollock trawl fisheries in the eastern Bering Sea (EBS) (Figure 112). Annual discard rates in the EBS pollock trawl sector declined from 10% to about 1% in 1999 and have since then remained below this level. The large increase in discard rate in 2021 is likely due to an overall decrease in total catch in NBS for pollock trawl sector. Rates in the non-pollock trawl sector have declined from a high of 50% in 1994 and have remained at 10% or lower since 2010. Discard rates and volumes in the fixed gear (hook-and-line and pot) sector trended upward from 2010 to 2016, reaching the highest annual discard biomass (26.7K metric tons) over the entire time series before declining from 2017 to 2021. Fixed gear discards in the northern Bering Sea trended upward from 2016 to 2018 as some vessels targeting Pacific cod moved their fishing activity northward, but these increases were offset by declines in discard biomass in the southern subregion. Through week 35 of 2022, discard biomass for non-pollock trawl and fixed sectors is trending higher relative to the 2017–2021 period, while trawl pollock gear discards are trending lower to date (Figure 113).

**Factors influencing observed trends:** Fishery discards may occur for economic or regulatory reasons. Economic discards include discarding of lower value and unmarketable fish, while regulatory discards are those required by regulation (e.g., upon reaching an allowable catch limit for a species). Minimizing discards is recognized as an ecological, economic, and moral imperative in various multilateral initiatives and in National Standard 9 of the Magnuson-Stevens Fishery Conservation and Management Act (Alverson et al., 1994; FAO, 1995; Karp et al., 2011). In the North Pacific groundfish fisheries, mechanisms to reduce discards include:

- Limited access privilege programs (LAPPs), which allocate catch quotas and may reduce economic discards by slowing down the pace of fishing
- In-season closure of fisheries once target or bycatch species quotas are attained
- Minimum retention and utilization standards for certain fisheries
- Maximum retainable amounts (MRAs), which allow for limited retention of species harvested incidentally in directed fisheries.

In the eastern Bering Sea, management and conservation measures aimed at reducing bycatch have contributed to an overall decline in groundfish discards since the early 1990s (NPFMC, 2016, 2017). Pollock roe stripping, wherein harvesters discard all but the highest value pollock product, was prohibited in 1991 (56 Federal Register 492). Throughout the 1990s, declines in total catch and discard of non-pollock groundfish in the pollock fishery coincided with the phasing out of bottom trawl gear in favor of pelagic gear, which allows for cleaner pollock catches (Graham et al., 2007). Full retention requirements for pollock and Pacific cod were implemented in 1998 for federally-permitted vessels fishing for groundfish (62 Federal Register 63880). Between 1997 and 1998 annual discard rates for cod fell from 13% to 1% in the non-pollock trawl sector and from 50% to 3% in the trawl pollock sector; pollock discards also declined significantly across both trawl gear sectors. In the trawl pollock fishery, discards of pollock have remained at nominal levels since passage of the American Fisheries Act, which established a sector-based LAPP and implemented more comprehensive observer requirements for the fishery in 2000. As of March 2020, the regulations 50 CFR 679.20(j) and 50 CFR 679.7(a)(5) were implemented to require operators of catcher vessels using hook-and-line, pot, or jig gear (fixed gear) to fully retain rockfish landings in the BSAI or GOA. These regulations also limit the amount of rockfish that can enter into the market with the overall purpose of limiting total catch of rockfish.

Low retention rates in the non-AFA trawl catcher processor (head and gut) fleet prompted Amendments 79 and 80 to the BSAI Groundfish FMP in 2008 (NPFMC, 2016). Amendment 79 established a Groundfish Retention Standard (GRS) Program with minimum retention and utilization requirements for vessels at least 125 feet LOA; industry-internal monitoring of retention rates has since replaced the program. Amendment 80 expanded the GRS program to all vessels in the fleet and established a cooperative-based LAPP with fixed allocations of certain non pollock groundfish species. In combination with the GRS program, these allocations are intended to remove the economic incentive to discard less valuable species caught incidentally

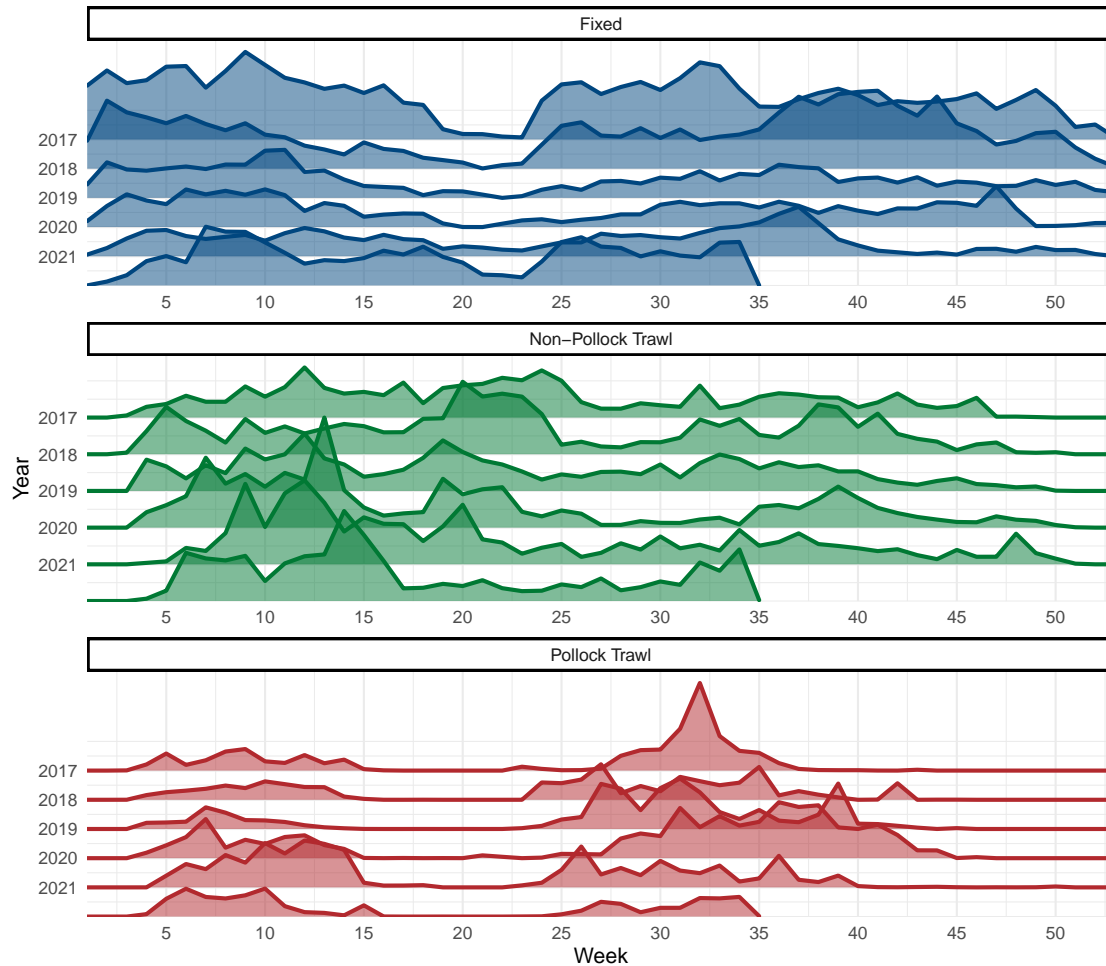


Figure 113: Total biomass of FMP groundfish discarded in the eastern Bering Sea region by sector and week, 2017–2022 (data for 2022 is shown through week 35). Plotted heights are not comparable across sectors.

in the multi-species fishery. In 2013, NMFS revised MRAs for groundfish caught in the BSAI Arrowtooth flounder fishery, including an increase from 0 to 20 percent for pollock, cod, and flatfish (78 Federal Register 29248). Groundfish discard rates in the trawl flatfish fishery fell from 23% to 12% between 2007 and 2008 and have continued on a gradual decline since then.

Since 2003 across all Bering Sea sectors combined, discard rates for species groups historically managed together as the “other groundfish” assemblage (skate, sculpin, shark, squid, and octopus) have ranged from 65% to 80%, with skates representing the majority of discards by weight. In the fixed gear sector other groundfish typically account for at least 70% of total groundfish discards annually. Fluctuations in discard volumes and rates for these species may be driven by changes in market conditions and in fishing behavior within the directed fisheries in which these species are incidentally caught. For example, low octopus catch from 2007–2010 may be attributable to lower processor demand for food-grade octopus and decreases in cod pot-fishing effort stemming from declines in cod prices (Conners et al., 2016).

**Implications:** Fishery bycatch adds to the total human impact on biomass without providing a benefit to the Nation and as such is perceived as “contrary to responsible stewardship and sustainable utilization of marine resources” (Kelleher, 2005). Bycatch may constrain the utilization of target species and increases the uncertainty around total fishing-related mortality, making it more difficult to assess stocks, define overfishing levels, and monitor fisheries for overfishing (Alverson et al., 1994; Clucas, 1997; Karp et al., 2011). Although ecosystem effects of discards are not fully understood, discards of whole fish and offal have the potential to alter energy flow within ecosystems and have been observed to result in changes to habitat (e.g., oxygen depletion in the benthic environment) and community structure (e.g., increases in scavenger populations) (Queirolo et al., 1995; Alverson et al., 1994; Catchpole et al., 2006; Zador and Fitzgerald, 2008). Monitoring discards and discard rates provides a means of assessing the efficacy of measures intended to reduce discards and increase groundfish retention and utilization.

## Time Trends in Non-Target Species Catch

Contributed by George A. Whitehouse<sup>1</sup> and Sarah Gaichas<sup>2</sup>

<sup>1</sup>Cooperative Institute for Climate, Ocean, and Ecosystem Studies (CICOES), University of Washington, Seattle WA

<sup>2</sup>Ecosystem Assessment Program, Northeast Fisheries Science Center, National Marine Fisheries Service, NOAA, Woods Hole MA

Contact: andy.whitehouse@noaa.gov

**Last updated: August 2022**

**Description of indicator:** We monitor the catch of non-target species in groundfish fisheries in the Eastern Bering Sea (EBS). In previous years we included the catch of “other” species, “non-specified” species, and forage fish in this contribution. However, stock assessments have now been developed or are under development for all groups in the “other species” category (sculpins, unidentified sharks, salmon sharks, dogfish, sleeper sharks, skates, octopus, squid), some of the species in the “non-specified” group (giant grenadier, other grenadiers), and forage fish (e.g., capelin, eulachon, Pacific sand lance, etc.), therefore we no longer include trends for these species/groups here<sup>31</sup>. Invertebrate species associated with habitat areas of particular concern, previously known as HAPC biota (seapens/whips, sponges, anemones, corals, and tunicates) are now referred to as structural epifauna. Starting with the 2013 Ecosystem Status Report, the three categories of non-target species we continue to track here are:

1. Scyphozoan jellyfish
2. Structural epifauna (seapens/whips, sponges, anemones, corals, tunicates)
3. Assorted invertebrates (bivalves, brittle stars, hermit crabs, miscellaneous crabs, sea stars, marine worms, snails, sea urchins, sand dollars, sea cucumbers, and other miscellaneous invertebrates).

Total catch of non-target species is estimated from observer species composition samples taken at sea during fishing operations, scaled up to reflect the total catch by both observed and unobserved hauls and vessels operating in all FMP areas. Catch since 2003 has been estimated using the Alaska Region’s Catch Accounting System (Cahalan et al., 2014). This sampling and estimation process does result in uncertainty in catches, which is greater when observer coverage is lower and for species encountered rarely in the catch.

For this contribution the catch of non-target species/groups from the Bering Sea includes the reporting areas 508, 509, 512, 513, 514, 516, 517, 521, 523, 524, and 530<sup>32</sup>.

<sup>31</sup>See AFSC stock assessment website at <https://www.fisheries.noaa.gov/alaska/population-assessments/north-pacific-groundfish-stock-assessments-and-fishery-evaluation>

<sup>32</sup><https://www.fisheries.noaa.gov/alaska/sustainable-fisheries/alaska-fisheries-figures-maps-boundaries-regulatory-areas-and-zones>

**Status and trends:** The catch of jellyfish more than doubled from 2020 to 2021 (Figure 114, top). Previous high catches of jellyfish occurred in 2011, 2014, and 2018 and were each followed by a sharp decrease in jellyfish catch the following year. Jellyfish are primarily caught in the pollock fishery.

The catch of structural epifauna has trended downward from 2015 to 2021, its second lowest catch over the time period examined (Figure 114, middle). Benthic urochordate caught in non-pelagic trawls were the dominant component of the structural epifauna catch in 2012 and 2015–2021. In 2013 and 2014, anemones caught in the Pacific cod fishery were the dominant part of the structural epifauna catch. Sponge were the dominant component of the structural epifauna catch in 2011 and were primarily caught in non-pelagic trawls.

Sea stars comprise more than 85% of the assorted invertebrate catch in all years (Figure 114, bottom) and are primarily caught in flatfish fisheries. The catch of assorted invertebrates generally trended upward from 2011 to 2015, then declined from 2015 to 2021.

**Factors influencing observed trends:** The catch of non-target species may change if fisheries change, if ecosystems change, or both. Because non-target species catch is unregulated and unintended, if there have been no large-scale changes in fishery management in a particular ecosystem, then large-scale signals in the non-target catch may indicate ecosystem changes. Catch trends may be driven by changes in biomass or changes in distribution (overlap with the fishery) or both. Fluctuations in the abundance of jellyfish in the EBS are influenced by a suite of biophysical factors affecting the survival, reproduction, and growth of jellyfish including temperature, sea-ice phenology, wind-mixing, ocean currents, and prey abundance (Brodeur et al., 2008). The lack of a clear trend in the catch of scyphozoan jellyfish may reflect interannual variation in jellyfish biomass or changes in the overlap with fisheries.

**Implications:** The catch of structural epifauna species and assorted invertebrates is very low compared with the catch of target species. Structural epifauna species may have become less available to the EBS fisheries or the fisheries avoided them more effectively. Abundant jellyfish may have a negative impact on fishes as they compete with planktivorous fishes for prey resources (Purcell and Arai, 2001), and additionally, jellyfish may prey upon the early life history stages (eggs and larvae) of fishes (Purcell and Arai, 2001; Robinson et al., 2014).

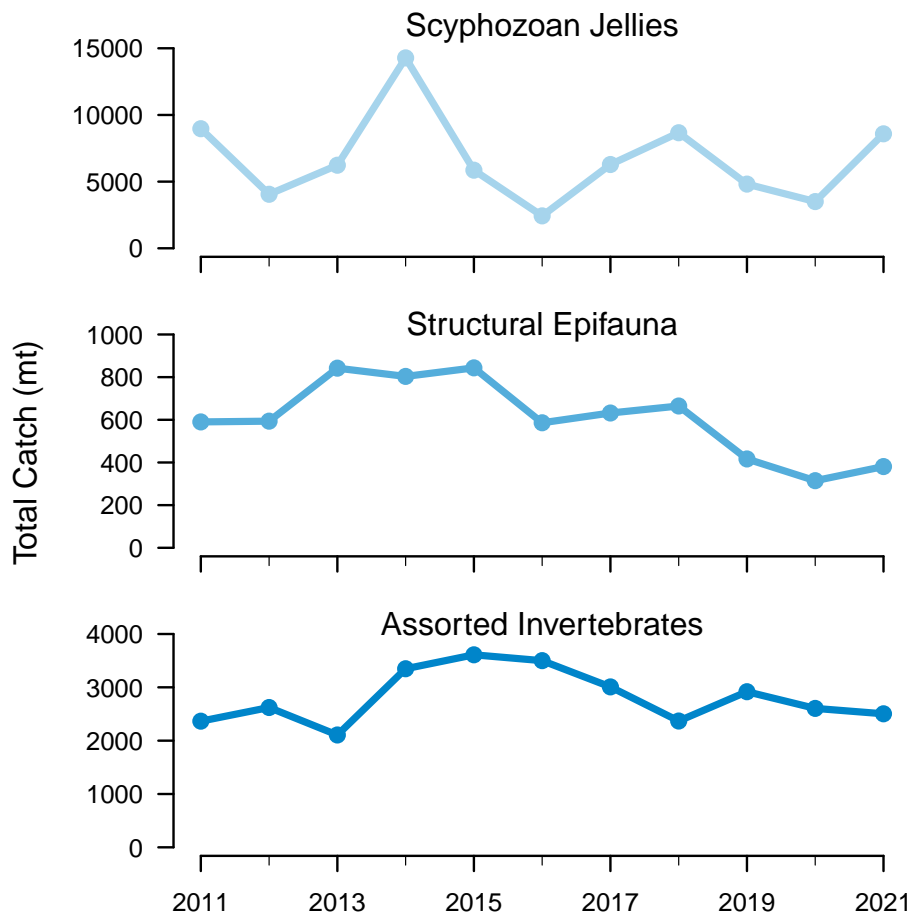


Figure 114: Total catch of non-target species (tons) in EBS groundfish fisheries (2011–2021). **Please note the different y-axis scales** between the species groups.

# Seabird Bycatch Estimates for Groundfish and Halibut Fisheries in the Eastern Bering Sea, 2012–2021

Contributed by Cathy Tide and Anne Marie Eich

Sustainable Fisheries Division, Alaska Regional Office, National Marine Fisheries Service, NOAA

Contact: [Cathy.Tide@noaa.gov](mailto:Cathy.Tide@noaa.gov)

**Last updated: August 2022**

**Description of indicator:** This report provides estimates of the number of seabirds caught as bycatch in commercial groundfish fisheries operating in waters off of Alaska in the eastern Bering Sea for the years 2012 through 2021 and halibut fisheries for the years 2013 through 2021. Data collection on the Pacific halibut longline fishery began in 2013 with the restructured North Pacific Observer Program. Estimates of seabird bycatch from earlier years using different methods are not included here. Fishing gear types represented are demersal longline, pot, pelagic trawl, and non-pelagic trawl. These numbers do not apply to jig, gillnet, seine, or troll fisheries<sup>33</sup>.

Estimates are based on three sources of information: (1) data provided by NMFS-certified fishery observers deployed to vessels and floating or shoreside processing plants, (2) video review of electronically monitored (EM) fixed gear vessels, and (3) industry reports of catch and production. Observer deployment plans are reviewed and updated annually in the Annual Deployment Plan<sup>34</sup>. The NMFS Alaska Regional Office Catch Accounting System (CAS) produces the estimates (Cahalan et al., 2010, 2014). The main purpose of the CAS is to provide near real-time delivery of accurate groundfish and prohibited species catch and bycatch information for inseason management decisions. The CAS also estimates non-target species (such as invertebrates) and seabird bycatch in the groundfish fisheries. The CAS produces estimates based on these three current data sets, which may have changed over time.

This report delineates and separately discusses estimates of seabird bycatch in the southeastern Bering Sea and the northern Bering Sea. Estimates of seabird bycatch from the southeastern Bering Sea include the reporting areas 508, 509, 512, 513, 514, 516, 517, 521, and 524 (estimates for 514 and 524 only include data south of 60°N). Estimates from the northern Bering Sea include areas north of 60°N and south of 65°N in reporting areas 514 and 524<sup>35</sup>. Estimates of seabird bycatch north of 65°N are not included in this report. In previous versions of this report, bycatch estimates in the southeastern Bering Sea, northern Bering Sea, and waters north of 65°N were all included as the eastern Bering Sea summaries.

## Status and trends:

### *Southeastern Bering Sea*

The numbers of seabirds estimated to be caught incidentally in the southeastern Bering Sea fisheries in 2021 (1,892 birds) decreased from 2020 (2,486 birds) by 24%, and was below the 2012–2020 average of 3,959 birds by 52% (Table 2, Figure 115). Northern fulmars, shearwaters, and gulls were the most common species or species groups caught incidentally in the southeastern Bering Sea fisheries in 2021 that could be identified. In 2021, the number of northern fulmars decreased by 46% and the number of shearwaters increased by 179%, compared to 2020. The estimated number of northern fulmars and shearwaters in 2021 were below the 2012–2020 average of 2,354 and 861 birds by 59% and 21%, respectively. In 2021, the number of gulls decreased by 37% compared to 2020 and was below the 2012–2020 average of 470 birds by 77%.

---

<sup>33</sup>This report does not include estimates of seabird bycatch in fisheries using gillnet, seine, troll, or jig gear because NOAA Fisheries does not have independent observer data from these fisheries. These estimates also do not apply to State of Alaska-managed salmon, herring, shellfish (including crab), or dive fisheries.

<sup>34</sup>The 2021 plan is available at: [https://www.fisheries.noaa.gov/tags/north-pacific-observer-program?title=annual%20deployment&field\\_species\\_vocab\\_target\\_id=&sort\\_by=created](https://www.fisheries.noaa.gov/tags/north-pacific-observer-program?title=annual%20deployment&field_species_vocab_target_id=&sort_by=created)

<sup>35</sup><https://www.fisheries.noaa.gov/alaska/commercial-fishing/alaska-fisheries-figures-maps-boundaries-regulatory-areas-and-zones>

Table 2: **Estimated** seabird bycatch in southeastern Bering Sea groundfish and halibut fisheries for all gear types, 2012 through 2021 (halibut fisheries 2013 through 2021). Note that these numbers represent extrapolations from observed bycatch, not direct observations. See text for estimation methods.

Species Group	2012	2013	2014	2015	2016	2017	2018	2019	2020	2021
Unidentified Albatross	0	0	12	0	0	0	0	0	0	0
Short-tailed Albatross	0	0	11	0	0	0	0	0	11	0
Laysan Albatross	36	8	13	12	12	18	148	13	7	23
Black-footed Albatross	0	<1	6	0	0	0	0	0	0	0
Northern Fulmar	2,602	2,729	663	2,299	4,438	2,756	1,933	1,980	1,790	964
Shearwaters	462	196	115	340	2,903	878	146	2,469	243	677
Storm Petrels	0	0	0	0	0	0	0	0	0	3
Gull	804	406	562	907	557	320	364	141	167	106
Kittiwake	5	3	4	12	0	22	37	16	21	13
Murre	6	3	47	0	52	10	0	0	6	1
Puffin	0	0	0	0	7	0	0	0	0	0
Auklets	7	4	67	18	1	25	0	0	0	0
Other Alcid	0	0	0	0	0	0	6	6	0	0
Cormorant	0	0	0	3	0	0	0	0	0	0
Other	0	0	0	0	0	63	0	0	7	0
Unidentified	299	267	73	144	257	230	52	135	232	105
Grand Total	4,222	3,616	1,573	3,737	8,228	4,323	2,686	4,760	2,486	1,892

Table 3: **Estimated** seabird bycatch in northern Bering Sea groundfish and halibut fisheries for all gear types, 2012 through 2021 (halibut fisheries 2013 through 2021). Note that these numbers represent extrapolations from observed bycatch, not direct observations. See text for estimation methods.

Species Group	2012	2013	2014	2015	2016	2017	2018	2019	2020	2021
Unidentified Albatross	0	0	<1	0	0	0	0	0	0	0
Short-tailed Albatross	0	0	<1	0	0	0	0	0	<1	0
Laysan Albatross	<1	1	<1	2	0	10	27	0	1	10
Black-footed Albatross	0	0	2	<1	0	0	0	0	0	0
Northern Fulmar	153	4	13	34	615	760	875	672	302	40
Shearwaters	8	0	<1	18	257	104	398	661	128	254
Storm Petrels	0	0	0	0	0	0	0	0	0	0
Gull	4	4	14	20	20	51	140	15	5	45
Kittiwake	<1	0	<1	0	5	0	0	2	3	0
Murre	<1	0	0	0	0	0	0	0	<1	7
Puffin	0	0	0	0	3	0	0	0	0	0
Auklets	<1	0	0	0	0	0	0	0	0	0
Other Alcid	0	0	0	0	0	0	0	0	0	0
Cormorant	0	0	0	0	0	0	0	0	0	0
Other	0	0	0	0	0	0	0	0	<1	0
Unidentified	<1	1	<1	0	25	22	25	50	133	60
Grand Total	165	11	29	73	925	948	1,465	1,399	571	415

### *Northern Bering Sea*

The numbers of seabirds estimated to be caught incidentally in the northern Bering Sea fisheries in 2021 (415 birds) decreased from 2020 (571 birds) by 27%, and was below the 2012–2020 average of 621 birds by 33% (Table 3, Figure 115). Northern fulmars, shearwaters, and gulls were the most common species or species groups caught incidentally in the northern Bering Sea fisheries in 2021 that could be identified. In 2021, the number of northern fulmars decreased by 87% and the number of shearwaters increased by 98%, compared to 2020. The estimated number of northern fulmars in 2021 was below the 2012–2020 average of 381 by 90%. In 2021, the number of shearwaters increased by 98% compared to 2020 and was above the 2012–2020 average of 175 birds by 45%. In 2021, the number of gulls increased by 800% compared to 2020 and was above the 2012–2020 average of 30 birds by 50%.

Pacific cod fisheries using demersal longline are responsible for the majority of seabird bycatch in the eastern Bering Sea. The average annual seabird bycatch across all fisheries in the eastern Bering Sea for 2012 through 2020 was 4,580 birds per year (Table 2, Table 3). The 2021 estimated seabird bycatch in the eastern Bering Sea (2,000 birds) was below the 2012–2020 average by 50% (4,016 birds per year; NMFS, unpublished data). Figure 116 shows the spatial distribution of observed seabird bycatch from 2016–2021 from the Pacific cod hook and line fisheries overlaid onto heat maps depicting fishing effort for the fishery.

Focusing solely on the bycatch of albatross (unidentified, short-tailed, Laysan, and black-footed) in the SEBS and NBS, an average of 39 albatross were taken per year from 2012–2021 (Table 2, Table 3, Figure 117). No black-footed or short-tailed albatross were reported as taken in the SEBS or NBS in 2021. The number of Laysan albatross taken in the SEBS in 2021 (23 birds) was similar to the 2012–2020 average of 30 birds. The number of Laysan albatross taken in the NBS in 2021 (10 birds) was similar compared to the 2012–2020 average of 5 birds. Two takes of short-tailed albatross were observed in the groundfish fisheries in 2020<sup>36</sup>. Both takes occurred in the EBS and from vessels fishing in the BSAI demersal longline fishery. These two short-tailed albatross takes count towards the incidental take statement in the 2021 USFWS biological opinion (USFWS, 2021) on the groundfish fisheries, which anticipated the take of no more than six short-tailed albatross in a 2-year period in the BSAI and GOA FMP areas (by demersal longline or trawl).

<sup>36</sup><https://www.fisheries.noaa.gov/bulletin/ib-20-76-noaa-fisheries-reports-take-short-tailed-albatross-bsai>; <https://www.fisheries.noaa.gov/bulletin/ib-20-80-noaa-fisheries-reports-take-second-short-tailed-albatross-bsai>

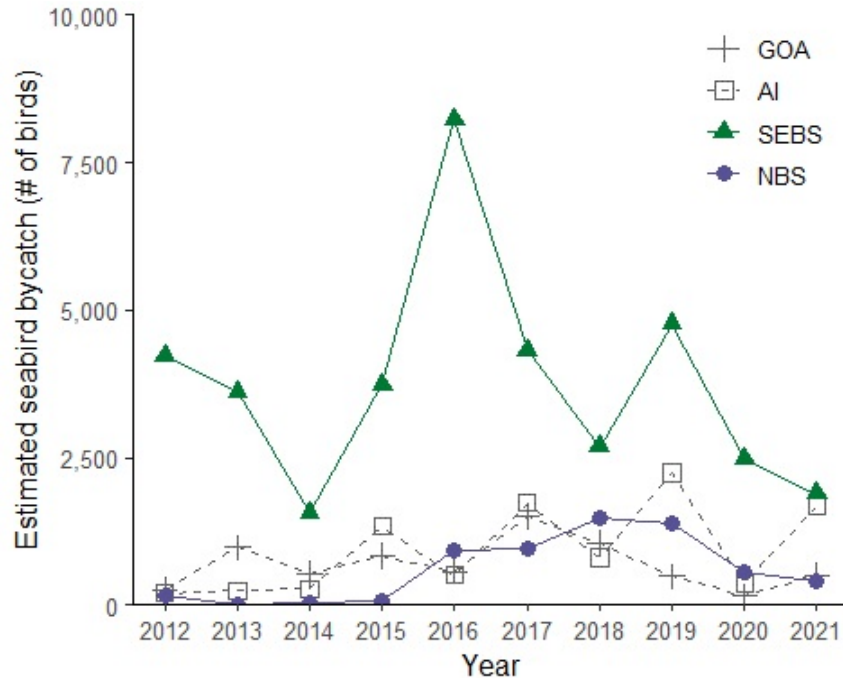


Figure 115: Total estimated seabird bycatch in Gulf of Alaska (GOA), Aleutian Islands (AI), southeastern Bering Sea (SEBS), and northern Bering Sea (NBS) groundfish and halibut fisheries, all gear types combined, 2012 through 2021 (halibut fisheries 2013 through 2021).

In addition to the endangered short-tailed albatross, two species of eider are also listed under the U.S. Endangered Species Act. These are the threatened spectacled eider and the threatened Alaska-breeding population of Steller’s eider. Two other populations of Steller’s eider occur in waters off Alaska but only the Alaska-breeding population is listed under the U.S. Endangered Species Act. Prior to 2019, there had been no reported takes of either the spectacled eider or the Alaska-breeding population of Steller’s eider by vessels operating in federal fisheries off Alaska. However, in October of 2019, twenty-two spectacled eider fatally collided with a demersal longline vessel in the NBS (NMFS did not receive a report on this take until 2020)<sup>37</sup>. Then in March of 2020, a Steller’s eider collided with another demersal longline vessel in the EBS<sup>38</sup>. These vessels were not fishing at the time of the bird strike mortality events. Since these birds were not taken by fishing gear, they are not included in the bycatch estimates provided in this report.

Because of the take of threatened spectacled and Steller’s eider, NMFS reinitiated formal consultation under section 7 of the ESA with USFWS to ensure that the BSAI and GOA groundfish fisheries are not likely to jeopardize the continued existence of the spectacled eider or adversely modify their designated critical habitat. In March of 2021, the USFWS finalized their 2021 Biological Opinion (USFWS, 2021), which anticipated the take of up to 25 spectacled eider every 4 years and up to 3 Steller’s eider from the Alaska-breeding population every 4 years in the BSAI and GOA FMP areas (either by demersal longline or trawl).

There have been zero takes of short-tailed albatross, Steller’s eider, or spectacled eider in the groundfish fisheries or the commercial Pacific halibut fisheries off Alaska in 2021. Seabird avoidance and mitigation measures remain in place; this includes the use of streamer lines as prescribed at 50 CFR 679.24(e).

**Factors influencing observed trends:** There are many factors that may influence annual variation in bycatch rates, including seabird distribution, population trends, prey supply, and fisheries activities.

<sup>37</sup><https://www.fisheries.noaa.gov/bulletin/ib-20-26-nmfs-reports-vessel-strike-mortality-event-22-spectacle-d-eiders-bering-sea>

<sup>38</sup><https://www.fisheries.noaa.gov/bulletin/ib-20-32-nmfs-reports-vessel-strike-mortality-alaska-breeding-population-stellers>

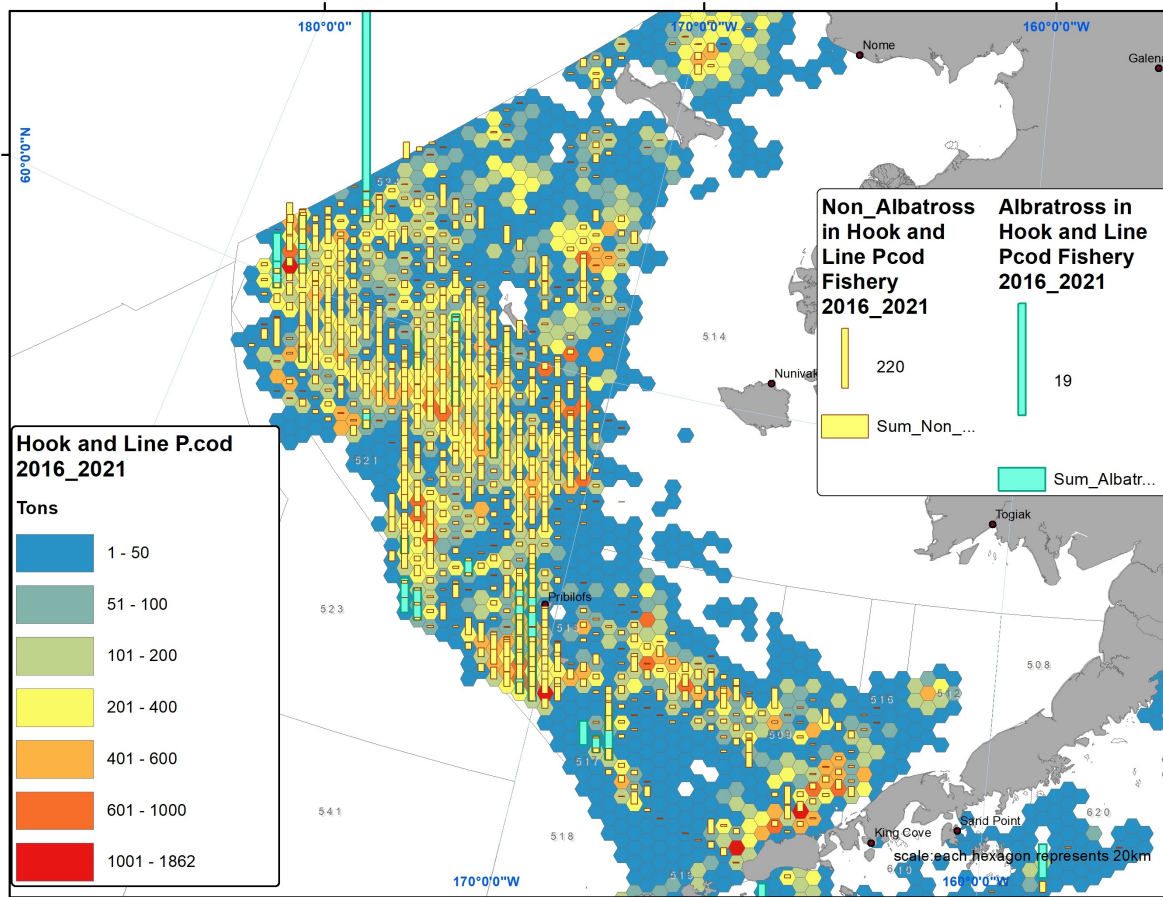


Figure 116: Spatial distribution of observed seabird bycatch from 2016–2021 from the Pacific cod hook and line fisheries. Colored vertical bars indicate the sum of incidental takes at a location grouped at 20km resolution. Incidental takes are separated between takes of albatross and takes of non-albatross seabirds. Map includes locations of incidental takes of seabirds overlaid on heat maps depicting fishing effort. Note the difference in scale of observed takes of seabirds.

A reduction in seabird bycatch in the groundfish and halibut fisheries off Alaska in the SEBS and NBS occurred in 2021 compared to 2020. As with many other things in 2020, the COVID-19 pandemic disrupted normal fishing operations throughout federal fisheries. In Alaska, such disruptions included lost fishing days due to closures and stand-downs (primarily at the beginning of the pandemic) and reduced market prices for fish as restaurants and other buyers were not operating at normal levels and thus were not purchasing as much fish product. The number of fishing trips in 2020 (13,493) was the lowest over the 2012–2020 time-period and down from a high of 19,246 trips in 2016 (NMFS Alaska Region, unpublished data). Less fishing effort would reduce the opportunities for interactions with seabirds and less seabird bycatch. The COVID-19 pandemic continued to disrupt normal fishing operations in 2021. Even fewer trips (12,873) were taken in 2021 (NMFS Alaska Region, unpublished data).

It is worth noting that standard observer sampling methods on trawl vessels do not account for additional mortalities from net entanglements, cable strikes, and other sources. Thus, the trawl estimates may be downward biased.

Dietrich and Fitzgerald (2010) found in an analysis of 35,270 longline sets from 2004 to 2007 that the most predominant species, northern fulmar, only occurred in 2.5% of all sets. Albatross, a focal species for conservation efforts, occurred in less than 0.1% of sets. Thus, while annual seabird bycatch estimates

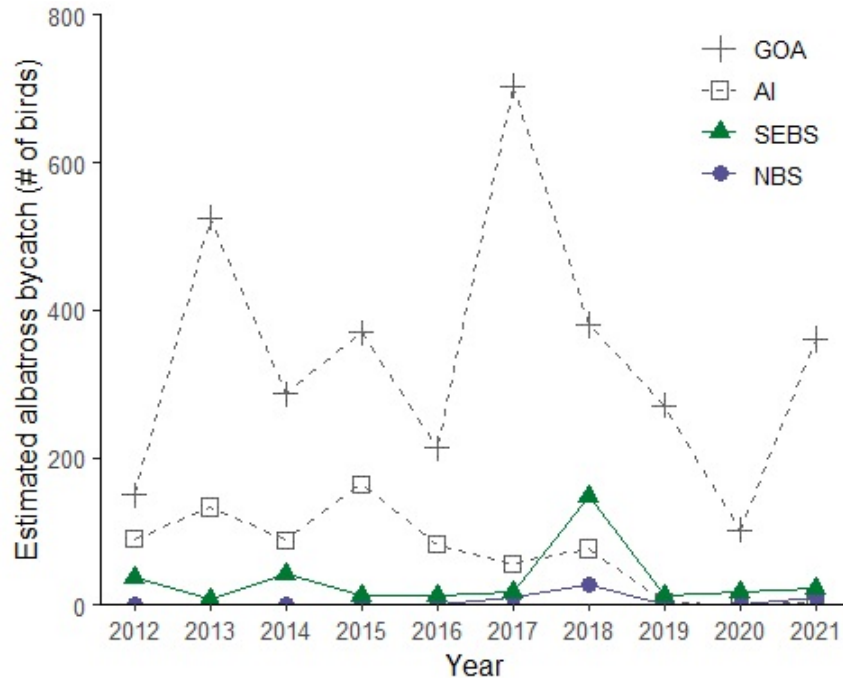


Figure 117: Total estimated albatross bycatch in Gulf of Alaska (GOA), Aleutian Islands (AI), southeastern Bering Sea (SEBS), and northern Bering Sea (NBS) groundfish and halibut fisheries, all gear types combined, 2012 through 2021 (halibut fisheries 2013 through 2021).

number in the 1,000's, given the vast size of the fishery, actual takes of seabird remains relatively uncommon (Tide and Eich, 2022).

**Implications:** Estimated seabird bycatch in the eastern Bering Sea federal fisheries off of Alaska in 2021 decreased from 2020, and was below the 2012–2020 average estimates for the SEBS and NBS.

The first reported interactions between fishing vessels in the SEBS and NBS groundfish fisheries in 2020 with threatened spectacled eider may be a direct result of ecological change in the EBS. Even though no takes of ESA-listed seabirds occurred in any federal fisheries off Alaska in 2021, recent changes in ocean temperatures in the BSAI and the resulting ecological response of commercially valuable fish species, mainly Pacific cod, has led to an increase in the amount of fishing vessel traffic in areas near spectacled eider designated critical habitat. NMFS has observed a corresponding northward shift in fishing vessel activity and an increased harvest of Pacific cod, primarily in the northern areas of regulatory zones 514 and 524 from 2016 through 2020. In NMFS (2020) (the NMFS analysis completed for the 2021 Biological Opinion, USFWS (2021)), the authors note that compared to the number of fishing vessels present in the northern areas of the Bering Sea in 2015 (the baseline for that analysis), 2016 through 2019 show a substantial increase in the number of vessels, especially north of 61°N (as described in Section 7.9.2 of NMFS (2020)). How this fleet response to new ecological conditions will affect other species of seabirds remains to be seen.

However, it can be difficult to determine how seabird bycatch estimates and trends in some fisheries are linked to changes in ecosystem components because seabird mitigation gear is used in the longline fleet. There does appear to be a link between poor ocean conditions and the peak bycatch years, on a species-group basis. Fishermen have noted in some years that the birds appear starved and attack baited longline gear more aggressively. This probably indicates changes in food availability rather than distinct changes in how well the fleet employs mitigation gear. A focused investigation of this aspect of seabird bycatch is needed and could inform management of poor ocean conditions if seabird bycatch rates (reported in real time) were substantially higher than average.

# Maintaining and Restoring Fish Habitats

## Fishing Effects to Essential Fish Habitat

Contributed by Molly Zaleski<sup>1</sup>, Scott Smeltz<sup>2</sup>, and Sarah Rheinsmith<sup>3</sup>

<sup>1</sup>Habitat Conservation Division, Alaska Regional Office, National Marine Fisheries Service, NOAA

<sup>2</sup>Alaska Pacific University, Anchorage, AK

<sup>3</sup>North Pacific Fishery Management Council, Anchorage, AK

Contact: molly.zaleski@noaa.gov

**Last updated: August 2022**

**Description of indicator:** Fishing gear can impact essential fish habitat (EFH) used by a fish or crab species for the processes of spawning, breeding, feeding, or growth to maturity. This indicator uses output from the Fishing Effects (FE) model to estimate the area of geological and biological features disturbed utilizing spatially-explicit VMS data. A time series for this indicator begins in 2003 when widespread VMS data became available.

**Status and trends:** The species and species complex time series data and FE maps are currently under review by stock assessment authors and experts as part of EFH component 2, “Fishing activities that may adversely affect EFH”, for the 2022 EFH 5-Year Review. The review process is part of an MSA requirement for Fishery Management Councils to describe and identify EFH for Fishery Management Plan species. It began with the 2005 EFH Environmental Impact Statement (NMFS, 2005) and then the first 5-Year Review was in 2010. The last FE model review was during the 2017 EFH 5-Year Review. For the 2022 Review, an updated model was published in 2019 (Smeltz et al., 2019) and model updates were presented to the North Pacific Fishery Management Council (NPFMC) Scientific and Statistical Committee (SSC) during the February 2022 NPFMC meeting. Stock author review of species or species complex results were presented to the Crab Plan Team and Joint Groundfish Plan Team meetings in September 2022, and the SSC during the October 2022 NPFMC meeting. During this review and analysis process, the most recent FE model output data is from December 2020 (see Siddon (2021)). Following the 2022 EFH 5-Year Review, updated Fishing Effects information will be available for future ESRs.

## Habitat Conservation Area Maps

For information on Habitat Conservation Areas in the eastern Bering Sea, please see: <https://www.fisheries.noaa.gov/resource/tool-app/habitat-conservation-area-maps>

# Sustainability (for consumptive and non-consumptive uses)

## Fish Stock Sustainability Index – Bering Sea and Aleutian Islands

Contributed by George A. Whitehouse

Cooperative Institute for Climate, Ocean, and Ecosystem Studies (CICOES), University of Washington, Seattle, WA

Contact: andy.whitehouse@noaa.gov

Last updated: July 2022

**Description of indicator:** The Fish Stock Sustainability Index (FSSI) is a performance measure for the sustainability of fish stocks selected for their importance to commercial and recreational fisheries<sup>39</sup>. The FSSI will increase as overfishing is ended and stocks rebuild to the level that provides maximum sustainable yield. The FSSI is calculated by awarding points for each stock based on the following rules:

1. Stock has known status determinations:
  - (a) overfishing level is defined = 0.5
  - (b) overfished biomass level is defined = 0.5
2. Fishing mortality rate is below the “overfishing” level defined for the stock = 1.0
3. Biomass is above the “overfished” level defined for the stock = 1.0
4. Biomass is at or above 80% of the biomass that produces maximum sustainable yield ( $B_{MSY}$ ) = 1.0 (this point is in addition to the point awarded for being above the “overfished” level)

The maximum score for each stock is 4.

In the Alaska Region, there are 35 FSSI stocks and an overall FSSI of 140 would be achieved if every stock scored the maximum value, 4. Over time, the number of stocks included in the FSSI has changed as stocks have been added and removed from Fishery Management Plans (FMPs). To keep FSSI scores for Alaska comparable across years we report the FSSI as a percentage of the maximum possible score (i.e., 100%).

The list of stocks included in the FSSI was revised in 2020 to focus on stocks of heightened commercial and recreational importance<sup>40</sup>. In the BSAI, the Pribilof Islands blue king crab, Saint Matthew Island blue king crab, Pribilof Islands red king crab, and the black-spotted/rougheye rockfish stocks were removed from the FSSI and added to the group of non-FSSI stocks. The BSAI stock of Kamchatka flounder, the AI Pacific cod stock, and the Bogoslof stock of walleye pollock were added to the BSAI FSSI. These changes resulted in a net reduction from 22 to 21 FSSI stocks in the BSAI. With few exceptions, groundfish species (or species complex) in the BSAI are managed as single stocks and not separately for the Bering Sea and Aleutian Islands. As such, the FSSI scores are reported for the BSAI as a whole.

Additionally, there are 26 non-FSSI stocks in Alaska, three ecosystem component species complexes, and Pacific halibut which are managed under an international agreement. Two of the non-FSSI crab stocks are overfished but are not subject to overfishing. The Pribilof Islands blue king crab stock is in year eight of a rebuilding plan, and the Saint Matthews Island blue king crab stock is in year two of a 26-year rebuilding plan. None of the other non-FSSI stocks are known to be subject to overfishing, are overfished, or are approaching an overfished condition. For more information on non-FSSI stocks see the Status of U.S. Fisheries webpage (<https://www.fisheries.noaa.gov/national/population-assessments/status-us-fisheries>).

<sup>39</sup><https://www.fisheries.noaa.gov/national/population-assessments/fishery-stock-status-updates>

<sup>40</sup><https://www.fisheries.noaa.gov/national/population-assessments/status-us-fisheries#fish-stock-sustainability-index>

Table 4: Summary of status for the 21 FSSI stocks in the BSAI, updated through June 2022.

BSAI FSSI (21 stocks)	Yes	No	<i>Unknown</i>	<i>Undefined</i>	N/A
Overfishing	0	21	0	0	0
Overfished	1	18	2	0	0
Approaching Overfished Condition	0	18	2	0	1

**Status and trends:** The overall Alaska FSSI generally trended upwards from 80% in 2006 to a high of 94% in 2018 (Figure 118) and has since trended downward to 88.2% in 2022.

As of June 30, 2021, no BSAI groundfish stock or stock complex is subject to overfishing, is known to be overfished, or known to be approaching an overfished condition (Table 4). The BSAI groundfish FSSI score is 59 out of a maximum possible 64. The AI Pacific cod stock and the walleye pollock Bogoslof stock both have FSSI scores of 1.5 due to not having known overfished status or known biomass relative to their overfished levels or to  $B_{MSY}$ . All other BSAI groundfish FSSI stocks received the maximum possible score of four points.

The BSAI king and tanner crab FSSI is 17 out of a possible 20. One point was deducted for the Bristol Bay red king crab stock’s biomass decreasing to below the  $B/B_{MSY}$  threshold and two points were deducted for Bering Sea snow crab becoming overfished and their biomass dropping to 17% of  $B_{MSY}$ .

The overall BSAI FSSI score is 76 out of a maximum possible score of 84 (Table 5). The BSAI FSSI trended upward from 74% in 2006 to a peak of 95.5% in 2019 but has since declined to 90.5% (Figure 119).

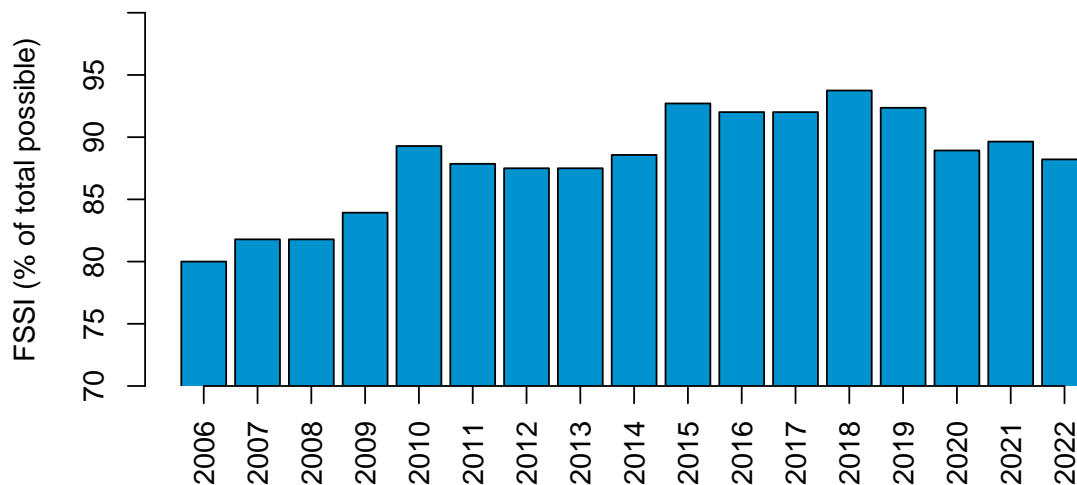


Figure 118: The trend in overall Alaska FSSI from 2006 through 2022 as a percentage of the maximum possible FSSI. The maximum possible FSSI was 140 from 2006 to 2014, 144 from 2015 to 2019, and 140 since 2020. All scores are reported through the second quarter (June) of each year, and are retrieved from the Status of U.S. Fisheries website: <https://www.fisheries.noaa.gov/national/population-assessments/fishery-stock-status-updates>.

**Factors influencing observed trends:** The overall trend in Alaska FSSI has been positive over much of the duration examined here (2006–2022). The decline in the Alaska total FSSI and in BSAI from 2021 to 2022 reflect the points lost for Bering Sea snow crab becoming overfished and their decreased biomass.

**Implications:** The majority of Alaska groundfish and crab fisheries appear to be sustainably managed. None of the FSSI groundfish stocks in the BSAI are subject to overfishing or known to be overfished. Only snow crab is currently overfished.

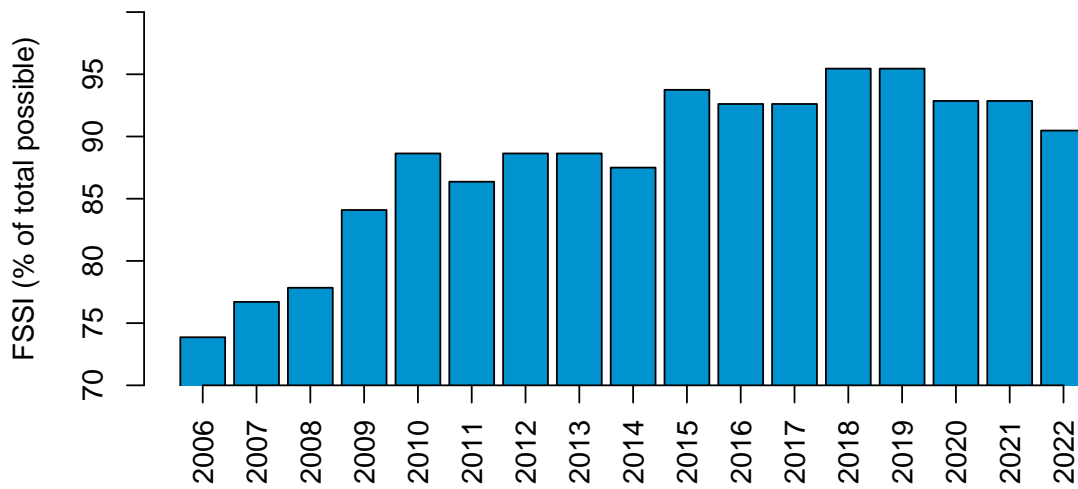


Figure 119: The trend in BSAI FSSI from 2006 through 2022 as a percentage of the maximum possible FSSI. All scores are reported through the second quarter (June) of each year, and are retrieved from the Status of U.S. Fisheries website: <https://www.fisheries.noaa.gov/national/population-assessments/fishery-stock-status-updates>.

Table 5: BSAI FSSI stocks under NPFMC jurisdiction updated through June 2022 adapted from the NOAA Fishery Stock Status Updates webpage: <https://www.fisheries.noaa.gov/national/population-assessments/fishery-stock-status-updates>. \*See FSSI and Non-FSSI Stock Status Table on the Fishery Stock Status Updates webpage for definition of stocks, stock complexes, and notes on rebuilding.

Stock	Overfishing	Overfished	Approaching	Progress	B/Bmsy	FSSI Score
Golden king crab - Aleutian Islands*	No	No	No	NA	1.289/1.15	4
Red king crab - Bristol Bay	No	No	No	NA	0.59	3
Red king crab - Norton Sound	No	No	No	NA	1.07	4
Snow crab - Bering Sea*	No	Yes	NA	NA	0.17	2
Southern Tanner crab - Bering Sea	No	No	No	NA	0.96	4
BSAI Alaska plaice	No	No	No	NA	1.58	4
BSAI Atka mackerel	No	No	No	NA	1.12	4
BSAI Arrowtooth Flounder	No	No	No	NA	2.57	4
BSAI Kamchatka flounder	No	No	No	NA	1.53	4
BSAI Flathead Sole Complex*	No	No	No	NA	2.08	4
BSAI Rock Sole Complex*	No	No	No	NA	1.67	4
BSAI Skate Complex*	No	No	No	NA	2.28	4
BSAI Greenland halibut	No	No	No	NA	1.7	4
BSAI Northern rockfish	No	No	No	NA	2.1	4
BS Pacific cod	No	No	No	NA	1.06	4
AI Pacific cod	No	Unknown	Unknown	NA	not estimated	1.5
BSAI Pacific Ocean perch	No	No	No	NA	1.58	4
Walleye pollock - Aleutian Islands	No	No	No	NA	1.39	4
Walleye pollock - Bogoslof	No	Unknown	Unknown	NA	not estimated	1.5
Walleye pollock - Eastern Bering Sea	No	No	No	NA	1.31	4
BSAI Yellowfin sole	No	No	No	NA	1.90	4

## Total Annual Surplus Production of Commercial Groundfish Stocks

Contributed by Franz Mueter

University of Alaska Fairbanks, 17101 Point Lena Loop Road, Juneau, AK 99801

Contact: fmueter@alaska.edu

Last updated: August 2022

**Description of indicator:** Total annual surplus production (ASP) of 14 groundfish stocks on the eastern Bering Sea (EBS) shelf from 1978–2019 was estimated by summing annual production across major commercial stocks for which assessment data were available over this time period from NOAA Fisheries (2021) (Table 6). Annual surplus production in year  $t$  can be estimated as the change in total adult biomass across species from year  $t$  ( $B_t$ ) to year  $t+1$  ( $B_{t+1}$ ) plus total catches in year  $t$  ( $C_t$ ):

$$ASP_t = \Delta B_t + C_t = B_{t+1} - B_t + C_t$$

All estimates of B and C are based on the most recent stock assessments. An index of total exploitation rate within each region was obtained by dividing the total catch across the major commercial species by the estimated combined biomass at the beginning of the year:

$$u_t = C_t / B_t$$

Table 6: Species included in computing annual surplus production in the BSAI management area. Data retrieved from NOAA Fisheries on August 12, 2022 ([www.st.nmfs.noaa.gov/stocksmart](http://www.st.nmfs.noaa.gov/stocksmart)).

---

<i>Stock (BSAI unless otherwise indicated)</i>
EBS walleye pollock ( <i>Gadus chalcogrammus</i> )
AI walleye pollock ( <i>Gadus chalcogrammus</i> )
EBS Pacific cod ( <i>Gadus macrocephalus</i> )
Yellowfin sole ( <i>Limanda aspera</i> )
Arrowtooth flounder ( <i>Atheresthes stomias</i> )
Greenland turbot ( <i>Reinhardtius hippoglossoides</i> )
Flathead sole ( <i>Hippoglossoides elassodon</i> )
Northern rock sole ( <i>Lepidopsetta polyxystra</i> )
Alaska plaice ( <i>Pleuronectes quadrituberculatus</i> )
Pacific Ocean Perch ( <i>Sebastes alutus</i> )
Northern rockfish ( <i>Sebastes polyspinus</i> )
Rougeye/Blackspotted rockfish ( <i>Sebastes aleutianus</i> , <i>Sebastes melanostictus</i> )
Alaska skate ( <i>Bathyraja parmifera</i> )
Atka mackerel ( <i>Pleurogrammus monopterygius</i> )

---

**Status and trends:** The resulting indices suggest high variability in production in the eastern Bering Sea with periods of below- and above-average surplus production (Figure 120). ASP was lowest in the late 1980s, mid-1990s, from 2004–2007, and in 2017. Total exploitation rates (catch/mature biomass) for the combined species ranged from 6–13% (Figure 120). Overall exploitation rates were highest early in the time series and when biomass declined to low levels following periods of low surplus production in the late 1980s and mid-2000s. Trends in annual surplus production in the eastern Bering Sea are largely driven by variability in Walleye pollock (Figure 121). Therefore, ASP for the Bering Sea was also computed after excluding Walleye pollock (Figure 122). The results suggest highly variable aggregate surplus production of all non-pollock species ranging from a high of more than 1.4 million tons in 1980, due to strong recruitment of a number of species, to a low of less than 200,000 t in the late 1990s. Annual non-pollock surplus production has fluctuated but has remained relatively stable on average since the mid-1980s.

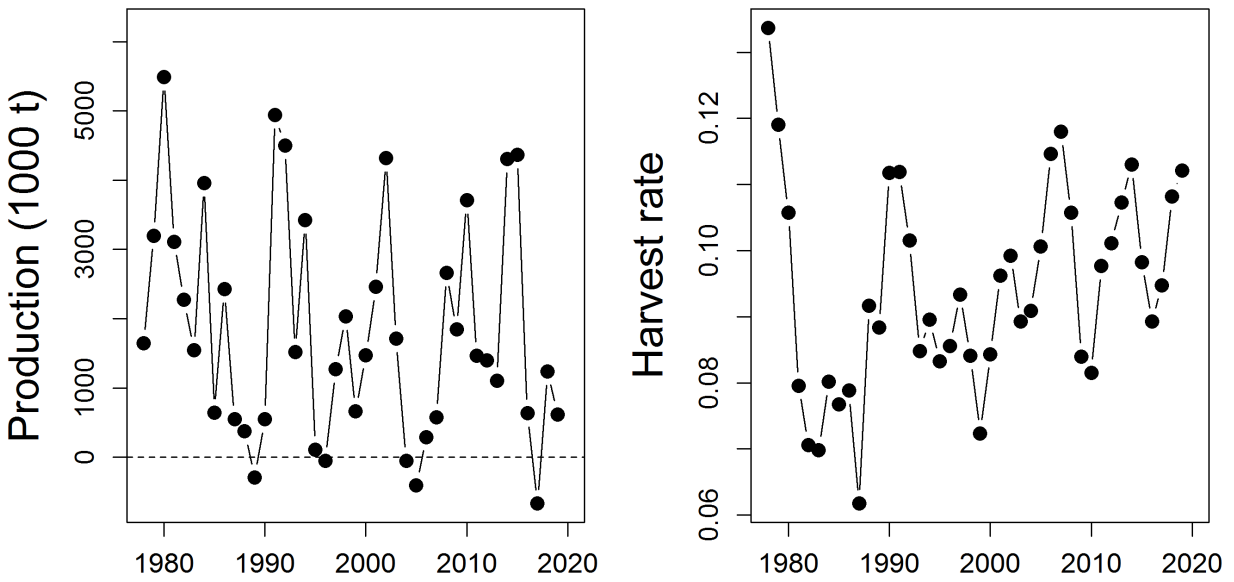


Figure 120: Total annual surplus production (change in biomass plus catch) across major groundfish stocks in the Bering Sea/Aleutian Islands (left) and total harvest rate (total catch/beginning-of-year biomass, each summed across the major stocks in Table 6).

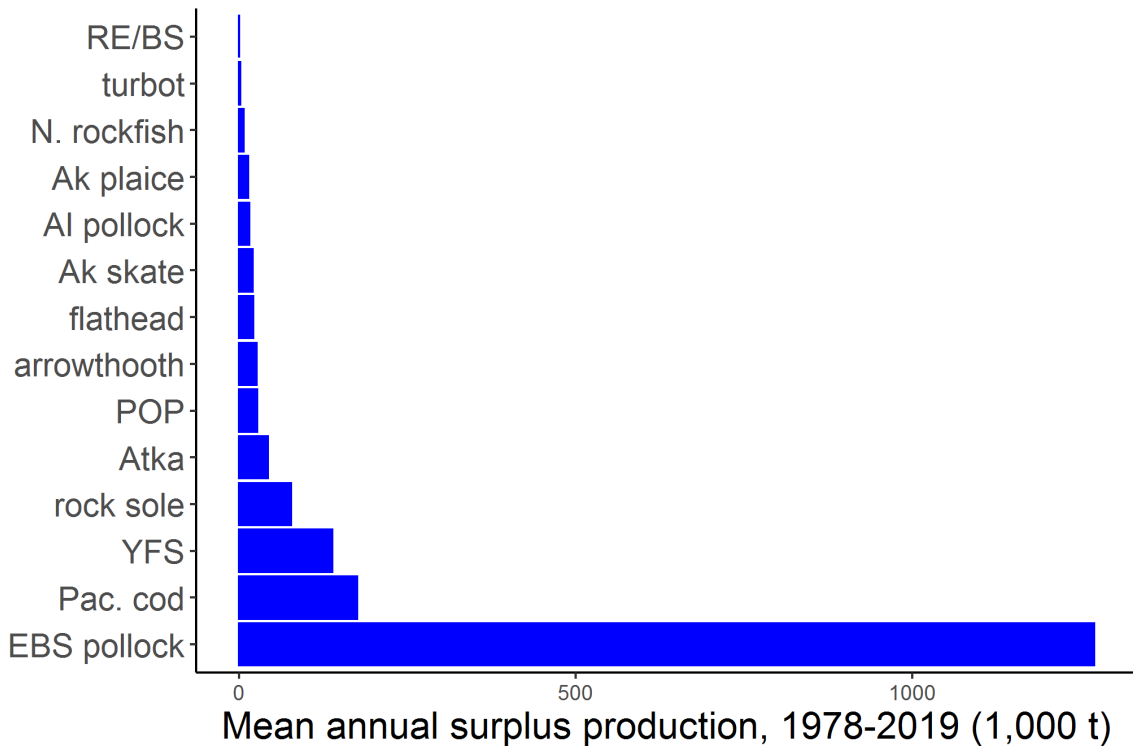


Figure 121: Contributions of each stock to mean annual surplus production.

**Factors influencing observed trends:** Surplus production has been relatively low in recent years, reflecting a decreasing trend in total groundfish biomass, while catches have remained stable near the 2 million ton cap. The observed biomass declines were largely due to decreases in Walleye pollock and Pacific cod. Changes in biomass of these species, in particular Walleye pollock, are linked to variations in recruitment and growth driven in part by ocean temperature and sea-ice variability (Hunt et al., 2011; Oke et al., 2022). Thus current low levels of surplus production are likely a consequence of the recent marine heat wave, similar to the response that followed warm conditions in the early 2000s. Exploitation rates are primarily determined by management and are constrained by an overall system-level cap on catches, reflecting a relatively precautionary management regime with rates that have averaged about 9.4% of the total combined biomass of the species in Table 6.

**Implications:** Annual surplus production is an estimate of the sum of new growth and recruitment minus deaths from natural mortality (i.e., mortality from all non-fishery sources) during a given year. It is highest during periods of increasing total biomass and lowest during periods of decreasing biomass (e.g., 2004–2007 and in recent years). In the absence of a long-term trend in total biomass, ASP is equal to the long-term average catch. Monitoring surplus production provides insights into the overall productivity of the system and a decreasing trend or prolonged periods of low or negative surplus production in an exploited system can indicate reduced system productivity.

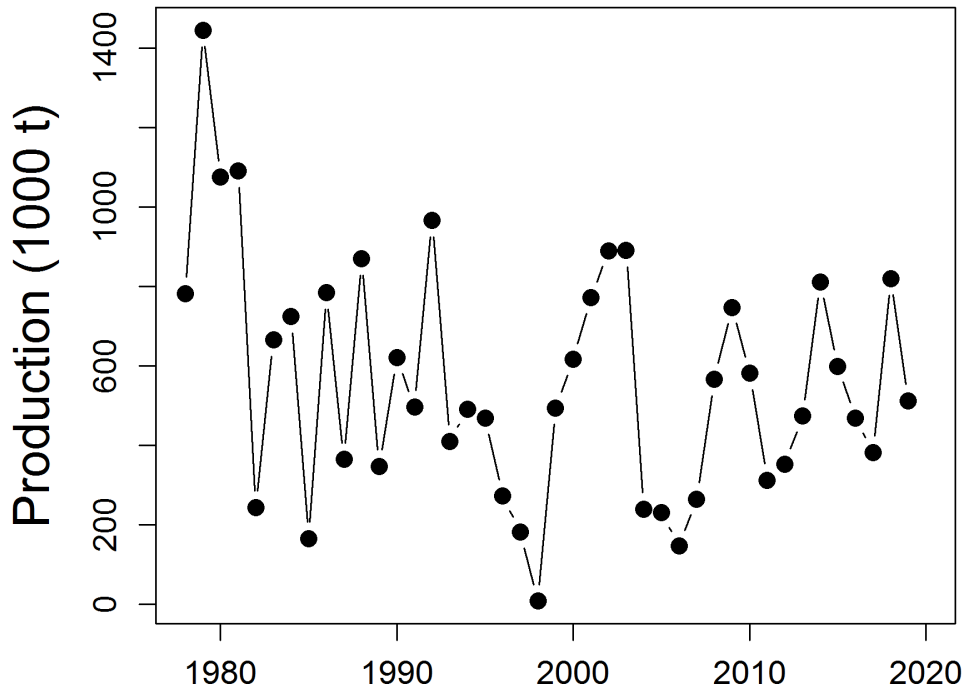


Figure 122: Total annual surplus production (change in biomass plus catch) across the major commercial stocks in Table 6, *excluding Walleye pollock*.

# References

- Aagaard, K., T. J. Weingartner, S. L. Danielson, R. A. Woodgate, G. C. Johnson, and T. E. Whitledge. 2006. Some controls on flow and salinity in Bering Strait. *Geophysical Research Letters* **33**.
- ADFG. 2013. Chinook salmon stock assessment and research plan, 2013. Report.
- Alverson, D. L., M. H. Freeberg, S. A. Murawski, and J. Pope. 1994. A global assessment of fisheries bycatch and discards (Vol. 339). Food Agriculture Organization.
- Anderson, D. M., T. J. Alpermann, A. D. Cembella, Y. Collos, E. Masseret, and M. Montresor. 2012. The globally distributed genus *Alexandrium*: multifaceted roles in marine ecosystems and impacts on human health. *Harmful algae* **14**:10–35.
- Anderson, D. M., E. Fachon, R. S. Pickart, P. Lin, A. D. Fischer, M. L. Richlen, V. Uva, M. L. Brosnahan, L. McRaven, and F. Bahr. 2021. Evidence for massive and recurrent toxic blooms of *Alexandrium catenella* in the Alaskan Arctic. *Proceedings of the National Academy of Sciences* **118**.
- Andrews III, A. G., M. Cook, E. Siddon, and A. Dimond. 2019. Prey Quality Provides a Leading Indicator of Energetic Content for Age-0 Walleye Pollock. Stock Assessment and Fishery Evaluation Report, North Pacific Fishery Management Council, 605 W 4th Ave, Suite 306, Anchorage, AK 99501.
- Andrews III, A. G., W. W. Strasburger, E. V. Farley Jr, J. M. Murphy, and K. O. Coyle. 2016. Effects of warm and cold climate conditions on capelin (*Mallotus villosus*) and Pacific herring (*Clupea pallasii*) in the eastern Bering Sea. *Deep Sea Research Part II: Topical Studies in Oceanography* **134**:235–246.
- Aydin, K., and F. Mueter. 2007. The Bering Sea - a dynamic food web perspective. *Deep Sea Research Part II: Topical Studies in Oceanography* **54**:2501–2525.
- Baduini, C., K. Hyrenbach, K. Coyle, A. Pinchuk, V. Mendenhall, and G. Hunt. 2001. Mass mortality of short-tailed shearwaters in the southeastern Bering Sea during summer 1997. *Fisheries Oceanography* **10**:117–130.
- Baier, C. T., and J. M. Napp. 2003. Climate-induced variability in *Calanus marshallae* populations. *Journal of Plankton Research* **25**:771–782.
- Baker, M. R. 2021. Contrast of warm and cold phases in the Bering Sea to understand spatial distributions of Arctic and sub-Arctic gadids. *Polar Biology* pages 1–23 .
- Balch, W., H. R. Gordon, B. Bowler, D. Drapeau, and E. Booth. 2005. Calcium carbonate measurements in the surface global ocean based on Moderate-Resolution Imaging Spectroradiometer data. *Journal of Geophysical Research: Oceans* **110** (C7).
- Barbeaux, S., L. Barnett, J. Connor, J. Nielson, S. K. Shotwell, E. Siddon, and I. Spies. 2022. Assessment of the Pacific Cod Stock in the Eastern Bering Sea. Report, North Pacific Fishery Management Council, Anchorage, AK.
- Barbeaux, S. J., K. Holsman, and S. Zador. 2020. Marine heatwave stress test of ecosystem-based fisheries management in the Gulf of Alaska Pacific Cod Fishery. *Frontiers in Marine Science* **7**:703.

- Batten, S. D., G. T. Ruggerone, and I. Ortiz. 2018. Pink salmon induce a trophic cascade in plankton populations in the southern Bering Sea and around the Aleutian Islands. *Fisheries Oceanography* **27**:548–559.
- Beamish, R. J., and C. Mahnken. 2001. A critical size and period hypothesis to explain natural regulation of salmon abundance and the linkage to climate and climate change. *Progress in Oceanography* **49**:423–437.
- Berkeley, S. A., M. A. Hixon, R. J. Larson, and M. S. Love. 2004. Fisheries sustainability via protection of age structure and spatial distribution of fish populations. *Fisheries* **29**:23–32.
- Blackwell, B. G., M. L. Brown, and D. W. Willis. 2000. Relative weight ( $W_r$ ) status and current use in fisheries assessment and management. *Reviews in Fisheries Science* **8**:1–44.
- Blanchard, F., and J. Boucher. 2001. Temporal variability of total biomass in harvested communities of demersal fishes. *Fisheries Research* **49**:283–293.
- Boldt, J. 2007. Ecosystem Considerations for 2008. Stock Assessment and Fishery Evaluation Report for the Groundfish Resources of the Bering Sea/Aleutian Islands and Gulf of Alaska. North Pacific Fishery Management Council, 605 W. 4th Ave., Suite 306, Anchorage, AK 99501.
- Boldt, J. L., and L. J. Haldorson. 2004. Size and condition of wild and hatchery pink salmon juveniles in Prince William Sound, Alaska. *Transactions of the American Fisheries Society* **133**:173–184.
- Bolin, J. A., D. S. Schoeman, K. J. Evans, S. F. Cummins, and K. L. Scales. 2021. Achieving sustainable and climate-resilient fisheries requires marine ecosystem forecasts to include fish condition. *Fish and Fisheries* **22**:1067–1084.
- Bond, N. A., M. F. Cronin, H. Freeland, and N. Mantua. 2015. Causes and impacts of the 2014 warm anomaly in the NE Pacific. *Geophysical Research Letters* **42**:3414–3420.
- Brannian, L. K., K. A. Rowell, and F. Funk. 1993. Forecast of the Pacific herring biomass in Togiak District, Bristol Bay, 1993. Alaska Department of Fish and Game, Division of Commercial Fisheries Management and Development, Regional Information Report 2D93-42, Anchorage .
- Brenner, R. E., S. J. Donnellan, and A. R. Munro. 2022. Run forecasts and harvest projections for 2022 Alaska salmon fisheries and review of the 2021 season. Alaska Department of Fish and Game, Special Publication No. 22-11. Anchorage, AK.
- Brodeur, R., C. Mills, J. Overland, G. Walters, and J. Schumacher. 1999. Recent increase in jellyfish biomass in the Bering Sea: Possible links to climate change. *Fisheries Oceanography* **8**:286–306.
- Brodeur, R. D., M. B. Decker, L. Ciannelli, J. E. Purcell, N. A. Bond, P. J. Stabeno, E. Acuna, and G. L. Hunt. 2008. Rise and fall of jellyfish in the eastern Bering Sea in relation to climate regime shifts. *Progress in Oceanography* **77**:103–111.
- Brodeur, R. D., R. L. Emmett, J. P. Fisher, E. Casillas, D. J. Teel, and T. W. Miller. 2004. Juvenile salmonid distribution, growth, condition, origin, and environmental and species associations in the Northern California Current. *Fishery Bulletin* **102**:25–46.
- Brodeur, R. D., H. Sugisaki, and G. L. Hunt. 2002. Increases in jellyfish biomass in the Bering Sea: implications for the ecosystem. *Marine Ecology Progress Series* **233**:89–103.
- Broerse, A., T. Tyrrell, J. Young, A. Poulton, A. Merico, W. Balch, and P. Miller. 2003. The cause of bright waters in the Bering Sea in winter. *Continental Shelf Research* **23**:1579–1596.
- Cahalan, J., J. Gasper, and J. Mondragon. 2014. Catch sampling and estimation in the Federal groundfish fisheries off Alaska, 2015 edition. Report, U.S. Dep. Commer., NOAA Tech. Memo. NMFS-AFSC-286, 46 p.

- Cahalan, J., J. Mondragon, and J. Gasper. 2010. Catch sampling and estimation in the Federal groundfish fisheries off Alaska. Report, U.S. Dep. Commer., NOAA Tech. Memo. NMFS-AFSC-205, 42 p.
- Catchpole, T., C. Frid, and T. Gray. 2006. Resolving the discard problem - A case study of the English *Nephrops* fishery. *Marine Policy* **30**:821–831.
- Cheng, W., A. J. Hermann, A. B. Hollowed, K. K. Holsman, K. A. Kearney, D. J. Pilcher, C. A. Stock, and K. Y. Aydin. 2021. Eastern Bering Sea shelf environmental and lower trophic level responses to climate forcing: Results of dynamical downscaling from CMIP6. *Deep Sea Research Part II: Topical Studies in Oceanography* **193**:104975.
- Ciannelli, L., R. Drodeur, and T. Buckley. 1998. Development and application of a bioenergetics model for juvenile walleye pollock. *Journal of Fish Biology* **52**:879–898.
- Cieciel, K., E. V. Farley Jr, and L. B. Eisner. 2009. Jellyfish and juvenile salmon associations with oceanographic characteristics during warm and cool years in the eastern Bering Sea. *North Pacific Anadromous Fish Commission Bulletin* **5**:209–224.
- Clucas, I. 1997. A study of the options for utilization of bycatch and discards from marine capture fisheries. *FAO fisheries circular* **928**:1–59.
- Coiley-Kenner, P., T. Krieg, M. Chythlook, and G. Jennings. 2003. Wild resource harvests and uses by residents of Manokotak, Togiak, and Twin Hills, 1999/2000. Alaska Department of Fish and Game Division of Subsistence Technical Paper **No. 275**.
- Connors, M. E., K. Y. Aydin, and C. L. Conrath. 2016. Assessment of the octopus stock complex in the Bering Sea and Aleutian Islands. Report, North Pacific Fishery Management Council.
- Cooper, D. W., and T. K. Wilderbuer. 2020. OSCURS wind forcing. Stock Assessment and Fishery Evaluation Report, North Pacific Fishery Management Council, 605 W 4th Ave, Suite 306, Anchorage, AK 99501.
- Courtney, M. B., M. D. Evans, J. F. Strøm, A. H. Rikardsen, and A. C. Seitz. 2019. Behavior and thermal environment of Chinook salmon *Oncorhynchus tshawytscha* in the North Pacific Ocean, elucidated from pop-up satellite archival tags. *Environmental Biology of Fishes* **102**:1039–1055.
- Coyle, K., and G. Gibson. 2017. Calanus on the Bering Sea shelf: probable cause for population declines during warm years. *Journal of Plankton Research* **39**:257–270.
- Coyle, K. O., L. Eisner, F. J. Mueter, A. Pinchuk, M. Janout, K. Cieciel, E. Farley, and A. Andrews. 2011. Climate change in the southeastern Bering Sea: impacts on pollock stocks and implications for the Oscillating Control Hypothesis. *Fisheries Oceanography* **20**:139–156.
- Coyle, K. O., and A. Pinchuk. 2002. The abundance and distribution of euphausiids and zero-age pollock on the inner shelf of the southeast Bering Sea near the Inner Front in 1997–1999. *Deep Sea Research Part II: Topical Studies in Oceanography* **49**:6009–6030.
- Danielson, S., O. Ahkinga, C. Ashjian, E. Basyuk, L. Cooper, L. Eisner, E. Farley, K. Iken, J. Grebmeier, and L. Juranek. 2020. Manifestation and consequences of warming and altered heat fluxes over the Bering and Chukchi Sea continental shelves. *Deep Sea Research Part II: Topical Studies in Oceanography* **177**:104781.
- De Robertis, A., D. R. McKelvey, and P. H. Ressler. 2010. Development and application of an empirical multifrequency method for backscatter classification. *Canadian Journal of Fisheries and Aquatic Sciences* **67**:1459–1474.
- Dietrich, K. S., and S. M. Fitzgerald. 2010. Analysis of 2004–2007 vessel-specific seabird bycatch data in Alaska demersal longline fisheries. Alaska Fisheries Science Center, Resource Ecology and Fisheries Management Division.

- Dorn, M. W., and S. G. Zador. 2020. A risk table to address concerns external to stock assessments when developing fisheries harvest recommendations. *Ecosystem Health and Sustainability* **6**:1813634.
- Duffy-Anderson, J. T., P. Stabeno, A. G. Andrews III, K. Cieciel, A. Deary, E. Farley, C. Fugate, C. Harpold, R. Heintz, and D. Kimmel. 2019. Responses of the northern Bering Sea and southeastern Bering Sea pelagic ecosystems following record-breaking low winter sea-ice. *Geophysical Research Letters* **46**:9833–9842.
- Duffy-Anderson, J. T., P. J. Stabeno, E. C. Siddon, A. G. Andrews, D. W. Cooper, L. B. Eisner, E. V. Farley, C. E. Harpold, R. A. Heintz, and D. G. Kimmel. 2017. Return of warm conditions in the southeastern Bering Sea: Phytoplankton-Fish. *PloS one* **12**:e0178955.
- Dulvy, N., S. Rogers, S. Jennings, V. Stelzenmuller, D. Dye, and H. Skjoldal. 2008. Climate change and deepening of the North Sea fish assemblage: a biotic indicator of warming seas. *Journal of Applied Ecology* **45**:1029–1039.
- Edullantes, B. 2019. ggplottimeseries: Visualisation of Decomposed Time Series with ggplot2. R package version **0.1.0**.
- Eisner, L. B., J. M. Napp, K. L. Mier, A. I. Pinchuk, and A. G. Andrews III. 2014. Climate-mediated changes in zooplankton community structure for the eastern Bering Sea. *Deep Sea Research Part II: Topical Studies in Oceanography* **109**:157–171.
- Eisner, L. B., A. I. Pinchuk, D. G. Kimmel, K. L. Mier, C. E. Harpold, and E. C. Siddon. 2018. Seasonal, interannual, and spatial patterns of community composition over the eastern Bering Sea shelf in cold years. Part I: zooplankton. *ICES Journal of Marine Science* **75**:72–86.
- Eisner, L. B., E. C. Siddon, and W. W. Strasburger. 2015. Spatial and temporal changes in assemblage structure of zooplankton and pelagic fish in the eastern Bering Sea across varying climate conditions. *Izv TINRO* **181**:141–160.
- Eisner, L. B., E. M. Yasumiishi, A. G. Andrews III, and C. A. O’Leary. 2020. Large copepods as leading indicators of walleye pollock recruitment in the southeastern Bering Sea: Sample-Based and spatio-temporal model (VAST) results. *Fisheries Research* **232**:105720.
- Elison, T., P. Salomone, T. Sands, G. Buck, K. Sechrist, and D. Koster. 2018. 2017 Bristol Bay area annual management report. Report, Alaska Department of Fish and Game, Fishery Management Report No. 18-11.
- Fall, J., C. Brown, N. Braem, L. Hutchinson-Scarborough, D. Koster, T. Krieg, and A. Brenner. 2012. Subsistence harvests and uses in three Bering Sea communities, 2008: Akutan, Emmonak, and Togiak. ADFG Division of Subsistence, Technical Paper **No. 371**.
- FAO. 1995. Code of Conduct for Responsible Fisheries. Food and Agriculture Organization, Rome.
- Farley, E., J. Moss, and R. Beamish. 2007. A Review of the critical size, critical period hypothesis for juvenile Pacific salmon. *North Pacific Anadromous Fish Commission Bulletin* **4**:311–317.
- Farley, E. V., and J. H. Moss. 2009. Growth rate potential of juvenile chum salmon on the eastern Bering Sea shelf: an assessment of salmon carrying capacity. *North Pacific Anadromous Fish Commission Bulletin* **5**:265–277.
- Farley, E. V., A. Starovoytov, S. Naydenko, R. Heintz, M. Trudel, C. Guthrie, L. Eisner, and J. R. Guyon. 2011. Implications of a warming eastern Bering Sea for Bristol Bay sockeye salmon. *ICES Journal of Marine Science* **68**:1138–1146.
- Farley Jr, E. V., J. M. Murphy, K. Cieciel, E. M. Yasumiishi, K. Dunmall, T. Sformo, and P. Rand. 2020. Response of Pink salmon to climate warming in the northern Bering Sea. *Deep Sea Research Part II: Topical Studies in Oceanography* **177**:104830.

- Fetterer, F., K. Knowles, W. N. Meier, M. Savoie, and A. K. Windnagel. 2017. Sea Ice Index, Version 3. Regional Daily Data. Report, Boulder, Colorado USA. NSIDC: National Snow and Ice Data Center.
- Frey, K. E., J. A. Maslanik, J. C. Kinney, and W. Maslowski. 2014. Recent variability in sea ice cover, age, and thickness in the Pacific Arctic region, pages 31–63 . Springer.
- Froese, R. 2006. Cube law, condition factor and weight–length relationships: history, meta-analysis and recommendations. *Journal of Applied Ichthyology* **22**:241–253.
- Funk, F., L. K. Brannian, and K. A. Rowell. 1992. Age Structured Assessment of the Togiak Herring Stock, 1978-1992, and Preliminary Forecast of Abundance for 1993. Report, Alaska Department of Fish and Game, Division of Commercial Fisheries.
- Funk, F., and K. A. Rowell. 1995. Population model suggests new threshold for managing Alaska’s Togiak Fishery for Pacific herring in Bristol Bay. *Alaska Fishery Research Bulletin* **2**:125–136.
- Glover, D. M., W. J. Jenkins, and S. C. Doney. 2011. Modeling methods for marine science. Cambridge University Press.
- Goethel, D., C. Rodgveller, K. Echave, S. K. Shotwell, K. Siwicke, D. Hanselman, P. Malecha, M. Cheng, M. Williams, K. Omori, and C. Lunsford. 2022. Assessment of the Sablefish Stock in Alaska. Report, North Pacific Fishery Management Council, Anchorage, AK.
- Gordon, H. R., G. C. Boynton, W. M. Balch, S. B. Groom, D. S. Harbour, and T. J. Smyth. 2001. Retrieval of coccolithophore calcite concentration from SeaWiFS imagery. *Geophysical Research Letters* **28**:1587–1590.
- Graham, C. J., T. M. Sutton, M. D. Adkison, M. V. McPhee, and P. J. Richards. 2019. Evaluation of growth, survival, and recruitment of Chinook salmon in southeast Alaska rivers. *Transactions of the American Fisheries Society* **148**:243–259.
- Graham, N., R. S. Ferro, W. A. Karp, and P. MacMullen. 2007. Fishing practice, gear design, and the ecosystem approach—three case studies demonstrating the effect of management strategy on gear selectivity and discards. *ICES Journal of Marine Science* **64**:744–750.
- Grebmeier, J. M., L. W. Cooper, H. M. Feder, and B. I. Sirenko. 2006. Ecosystem dynamics of the Pacific-influenced Northern Bering and Chukchi Seas in the Amerasian Arctic. *Progress in Oceanography* **71**:331–361.
- Grüss, A., J. Gao, J. T. Thorson, C. N. Rooper, G. Thompson, J. L. Boldt, and R. Lauth. 2020. Estimating synchronous changes in condition and density in eastern Bering Sea fishes. *Marine Ecology Progress Series* **635**:169–185.
- Grüss, A., J. T. Thorson, C. C. Stawitz, J. C. Reum, S. K. Rohan, and C. L. Barnes. 2021. Synthesis of interannual variability in spatial demographic processes supports the strong influence of cold-pool extent on eastern Bering Sea walleye pollock (*Gadus chalcogrammus*). *Progress in Oceanography* **194**:102569.
- Hare, S. R., N. J. Mantua, and R. C. Francis. 1999. Inverse production regimes: Alaska and west coast Pacific salmon. *Fisheries* **24**:6–14.
- Harley, J. R., K. Lanphier, E. G. Kennedy, T. A. Leighfield, A. Bidlack, M. O. Gribble, and C. Whitehead. 2020. The Southeast Alaska Tribal Ocean Research (SEATOR) Partnership: Addressing Data Gaps in Harmful Algal Bloom Monitoring and Shellfish Safety in Southeast Alaska. *Toxins* **12**:407.
- Harris, R. P., P. H. Wiebe, J. Lenz, H. R. Skjoldal, and M. Huntley. 2000. ICES Zooplankton Methodology Manual. Amsterdam, The Netherlands.
- Hauser, M., F. Engelbrecht, and E. Fischer. 2021. Transient Global Warming Levels for CMIP5 and CMIP6 (v0. 2.0)[Data Set]. Zenodo .

- Haynie, A. C., and L. Pfeiffer. 2013. Climatic and economic drivers of the Bering Sea walleye pollock (*Theragra chalcogramma*) fishery: implications for the future. *Canadian Journal of Fisheries and Aquatic Sciences* **70**:841–853.
- Heintz, R. A., E. C. Siddon, E. V. Farley Jr, and J. M. Napp. 2013. Correlation between recruitment and fall condition of age-0 pollock (*Theragra chalcogramma*) from the eastern Bering Sea under varying climate conditions. *Deep Sea Research Part II: Topical Studies in Oceanography* **94**:150–156.
- Hendrix, A. M., K. A. Lefebvre, L. Quakenbush, A. Bryan, R. Stimmelmayer, G. Sheffield, G. Wisswaesser, M. L. Willis, E. K. Bowers, and P. Kendrick. 2021. Ice seals as sentinels for algal toxin presence in the Pacific Arctic and subarctic marine ecosystems. *Marine Mammal Science* .
- Hermann, A. J., K. Kearney, W. Cheng, D. Pilcher, K. Aydin, K. K. Holsman, and A. B. Hollowed. 2021. Coupled modes of projected regional change in the Bering Sea from a dynamically downscaling model under CMIP6 forcing. *Deep Sea Research Part II: Topical Studies in Oceanography* **194**:104974.
- Hilborn, R., T. P. Quinn, D. E. Schindler, and D. E. Rogers. 2003. Biocomplexity and fisheries sustainability. *Proceedings of the National Academy of Sciences of the United States of America* **100**:6564–6568.
- Hollowed, A. B., K. K. Holsman, A. C. Haynie, A. J. Hermann, A. E. Punt, K. Aydin, J. N. Ianelli, S. Kasperski, W. Cheng, and A. Faig. 2020. Integrated modeling to evaluate climate change impacts on coupled social-ecological systems in Alaska. *Frontiers in Marine Science* **6**:775.
- Holsman, K. K., and K. Aydin. 2015. Comparative methods for evaluating climate change impacts on the foraging ecology of Alaskan groundfish. *Marine Ecology Progress Series* **521**:217–235.
- Holsman, K. K., K. Aydin, J. Sullivan, T. Hurst, and G. H. Kruse. 2019. Climate effects and bottom-up controls on growth and size-at-age of Pacific halibut (*Hippoglossus stenolepis*) in Alaska (USA). *Fisheries Oceanography* **28**:345–358.
- Holsman, K. K., J. Ianelli, K. Aydin, A. E. Punt, and E. A. Moffitt. 2016. A comparison of fisheries biological reference points estimated from temperature-specific multi-species and single-species climate-enhanced stock assessment models. *Deep Sea Research Part II: Topical Studies in Oceanography* **134**:360–378.
- Honkalehto, T., A. McCarthy, and N. Lauffenburger. 2018. Results of the acoustic-trawl survey of walleye pollock (*Gadus chalcogrammus*) on the U.S. Bering Sea shelf in June - August 2016 (DY1608). Report.
- Howard, K. G., S. Garcia, J. Murphy, and T. Dann. 2019. Juvenile Chinook salmon abundance index and survey feasibility assessment in the northern Bering Sea, 2014–2016. Report, Alaska Department of Fish and Game, Fishery Data Series No. 19-04, Anchorage.
- Howard, K. G., S. Garcia, J. Murphy, and T. Dann. 2020. Northeastern Bering Sea juvenile Chinook salmon survey, 2017 and Yukon River adult run forecasts, 2018–2020. Report, Alaska Department of Fish and Game, Fishery Data Series No. 20-08, Anchorage.
- Hsieh, C.-H., C. S. Reiss, J. R. Hunter, J. R. Beddington, R. M. May, and G. Sugihara. 2006. Fishing elevates variability in the abundance of exploited species. *Nature* **443**:859–862.
- Hunsicker, M. E., L. Ciannelli, K. M. Bailey, S. Zador, and L. C. Stige. 2013. Climate and Demography Dictate the Strength of Predator-Prey Overlap in a Subarctic Marine Ecosystem. *PLoS ONE* **8**:e66025.
- Hunt, G. L., P. H. Ressler, G. A. Gibson, A. De Robertis, K. Aydin, M. F. Sigler, I. Ortiz, E. J. Lessard, B. C. Williams, and A. Pinchuk. 2016. Euphausiids in the eastern Bering Sea: A synthesis of recent studies of euphausiid production, consumption and population control. *Deep Sea Research Part II: Topical Studies in Oceanography* **134**:204–222.
- Hunt, G. L., P. Stabeno, G. Walters, E. Sinclair, R. D. Brodeur, J. M. Napp, and N. A. Bond. 2002. Climate change and control of the southeastern Bering Sea pelagic ecosystem. *Deep-Sea Research Part II-Topical Studies in Oceanography* **49**:5821–5853.

- Hunt, G. L., E. M. Yasumiishi, L. B. Eisner, P. J. Stabeno, and M. B. Decker. 2020. Climate warming and the loss of sea ice: the impact of sea-ice variability on the southeastern Bering Sea pelagic ecosystem. *ICES Journal of Marine Science* .
- Hunt, J., George L., K. O. Coyle, L. B. Eisner, E. V. Farley, R. A. Heintz, F. Mueter, J. M. Napp, J. E. Overland, P. H. Ressler, S. Salo, and P. J. Stabeno. 2011. Climate impacts on eastern Bering Sea foodwebs: a synthesis of new data and an assessment of the Oscillating Control Hypothesis. *ICES Journal of Marine Science* **68**:1230–1243.
- Huntington, H. P., S. L. Danielson, F. K. Wiese, M. Baker, P. Boveng, J. J. Citta, A. De Robertis, D. Dickson, E. Farley, and J. C. George. 2020. Evidence suggests potential transformation of the Pacific Arctic ecosystem is underway. *Nature Climate Change* **10**:342–348.
- Ianelli, J., B. Fissel, K. Holsman, A. De Robertis, T. Honkalehto, S. Kotwicki, C. Monnahan, E. Siddon, and J. Thorson. 2020. Assessment of the Walleye Pollock Stock in the Eastern Bering Sea. Report, North Pacific Fishery Management Council, 1007 W 3rd Ave, Suite 400, Anchorage, AK 99501.
- Ianelli, J., B. Fissel, S. Stienessen, T. Honkalehto, E. Siddon, and C. Allen-Akselrud. 2021. Assessment of the walleye pollock stock in the Eastern Bering Sea. In *Stock Assessment and Fishery Evaluation Report for the Groundfish Resources of the Bering Sea/Aleutian Islands*. Report, North Pacific Fishery Management Council, Anchorage, AK.
- Ianelli, J., K. K. Holsman, A. E. Punt, and K. Aydin. 2016. Multi-model inference for incorporating trophic and climate uncertainty into stock assessments. *Deep Sea Research Part II: Topical Studies in Oceanography* **134**:379–389.
- Ianelli, J., S. Stienessen, T. Honkalehto, E. Siddon, and C. Allen-Akselrud. 2022. Assessment of the Walleye Pollock Stock in the Eastern Bering Sea. Report, North Pacific Fishery Management Council, Anchorage, AK.
- Iida, T., K. Mizobata, and S.-I. Saitoh. 2012. Interannual variability of coccolithophore *Emiliania huxleyi* blooms in response to changes in water column stability in the eastern Bering Sea. *Continental Shelf Research* **34**:7–17.
- IPCC. 2021. Summary for Policymakers. In: *Climate Change 2021: The Physical Science Basis. Contribution of Working Group I to the Sixth Assessment Report of the Intergovernmental Panel on Climate Change*. Cambridge University Press, Cambridge, United Kingdom and New York, NY, USA.
- IPCC. 2022. *Climate Change 2022: Impacts, Adaptation and Vulnerability. Contribution of Working Group II to the Sixth Assessment Report of the Intergovernmental Panel on Climate Change*. Cambridge University Press, Cambridge University Press, Cambridge, UK and New York, NY, USA.
- Jones, B., P. Crane, C. Larson, and M. Cunningham. 2021. Traditional Ecological Knowledge and Harvest Assessment of Dolly Varden and Other Nonsalmon Fish Utilized by Residents of the Togiak National Wildlife Refuge. Report, Alaska Department of Fish and Game, Division of Subsistence, Technical Paper No. 482, Anchorage, AK.
- Jones, T., L. M. Divine, H. Renner, S. Knowles, K. A. Lefebvre, H. K. Burgess, C. Wright, and J. K. Parrish. 2019. Unusual mortality of Tufted puffins (*Fraterecula cirrhata*) in the eastern Bering Sea. *PLoS one* **14**:e0216532.
- Jurado-Molina, J., P. A. Livingston, and J. N. Ianelli. 2005. Incorporating predation interactions in a statistical catch-at-age model for a predator-prey system in the eastern Bering Sea. *Canadian Journal of Fisheries and Aquatic Sciences* **62**:1865–1873.
- Kalnay, E., M. Kananitcu, R. Kistler, W. Collins, and D. Deaven. 1996. The NCEP/NCAR 40-year reanalysis project. *Bulletin of the American Meteorological Society* **77**:437–471.

- Karp, W. A., L. L. Desfosse, and S. G. Brooke. 2011. US National bycatch report. Report, U.S. Dep. Commer., NOAA Tech. Memo., NMFS-F/SPO-117E, 508 p.
- Kearney, K., A. Hermann, W. Cheng, I. Ortiz, and K. Aydin. 2020. A coupled pelagic–benthic–sympagic biogeochemical model for the Bering Sea: documentation and validation of the BESTNPZ model (v2019.08.23) within a high-resolution regional ocean model. *Geoscientific Model Development* **13** (2).
- Kelleher, K. 2005. Discards in the world’s marine fisheries: an update. Report 9251052891, Food Agriculture Org., Vol. 470.
- Kimmel, D. G., L. B. Eisner, M. T. Wilson, and J. T. Duffy-Anderson. 2018. Copepod dynamics across warm and cold periods in the eastern Bering Sea: Implications for walleye pollock (*Gadus chalcogrammus*) and the Oscillating Control Hypothesis. *Fisheries Oceanography* **27**:143–158.
- Kotwicki, S., and R. R. Lauth. 2013. Detecting temporal trends and environmentally-driven changes in the spatial distribution of bottom fishes and crabs on the eastern Bering Sea shelf. *Deep Sea Research Part II: Topical Studies in Oceanography* **94**:231–243.
- KRITFC. 2022. Kuskokwim River Salmon Situation Report. Report, Kuskokwim River Inter-Tribal Fish Commission. [https://static1.squarespace.com/static/5afdc3d5e74940913f78773d/t/6359792089ec3e15693c80dd/1666808118921/Salmon+Sit+Report+2022\\_10-03-22\\_FINAL.pdf](https://static1.squarespace.com/static/5afdc3d5e74940913f78773d/t/6359792089ec3e15693c80dd/1666808118921/Salmon+Sit+Report+2022_10-03-22_FINAL.pdf)
- Ladd, C., L. Eisner, S. Salo, C. Mordy, and M. Iglesias-Rodriguez. 2018. Spatial and Temporal Variability of Coccolithophore Blooms in the Eastern Bering Sea. *Journal of Geophysical Research: Oceans* **123**:9119–9136.
- Ladd, C., and P. J. Stabeno. 2012. Stratification on the Eastern Bering Sea shelf revisited. *Deep Sea Research Part II: Topical Studies in Oceanography* **65**:72–83.
- Lauth, R. R., E. J. Dawson, and J. Conner. 2019. Results of the 2017 eastern and northern Bering Sea continental shelf bottom trawl survey of groundfish and invertebrate fauna. Report.
- Lebida, R. C., and D. C. Whitmore. 1985. Bering Sea herring aerial survey manual. Report, Alaska Department of Fish and Game, Division of Commercial Fisheries, Bristol Bay Data Report No. 85-2, Anchorage, AK.
- Lefebvre, K. A., E. Fachon, E. K. Bowers, D. G. Kimmel, J. A. Snyder, R. Stimmelmayer, J. M. Grebmeier, S. Kibler, D. R. Hardison, and D. M. Anderson. 2022. Paralytic shellfish toxins in Alaskan Arctic food webs during the anomalously warm ocean conditions of 2019 and estimated toxin doses to Pacific walrus and bowhead whales. *Harmful Algae* **114**:102205.
- Lefebvre, K. A., L. Quakenbush, E. Frame, K. B. Huntington, G. Sheffield, R. Stimmelmayer, A. Bryan, P. Kendrick, H. Ziel, and T. Goldstein. 2016. Prevalence of algal toxins in Alaskan marine mammals foraging in a changing arctic and subarctic environment. *Harmful Algae* **55**:13–24.
- Lewis, B., W. S. Grant, R. E. Brenner, and T. Hamazaki. 2015. Changes in size and age of Chinook salmon *Oncorhynchus tshawytscha* returning to Alaska. *PloS one* **10**:e0130184.
- Liller, Z. 2021. Adult Salmon Run Failures Throughout the Arctic-Yukon-Kuskokwim Region. Stock Assessment and Fishery Evaluation Report, North Pacific Fishery Management Council, 1007 West Third Ave., Anchorage, AK.
- Litzow, M. A., M. E. Hunsicker, N. A. Bond, B. J. Burke, C. J. Cunningham, J. L. Gosselin, E. L. Norton, E. J. Ward, and S. G. Zador. 2020a. The changing physical and ecological meanings of North Pacific Ocean climate indices. *Proceedings of the National Academy of Sciences* **117**:7665–7671.
- Litzow, M. A., M. J. Malick, N. A. Bond, C. J. Cunningham, J. L. Gosselin, and E. J. Ward. 2020b. Quantifying a Novel Climate Through Changes in PDO-Climate and PDO-Salmon Relationships. *Geophysical Research Letters* **47**:e2020GL087972.

- Livingston, P. A., K. Aydin, T. W. Buckley, G. M. Lang, M.-S. Yang, and B. S. Miller. 2017. Quantifying food web interactions in the North Pacific—a data-based approach. *Environmental Biology of Fishes* **100**:443–470.
- Long, W. C., K. M. Swiney, C. Harris, H. N. Page, and R. J. Foy. 2013. Effects of ocean acidification on juvenile red king crab (*Paralithodes camtschaticus*) and Tanner crab (*Chionoecetes bairdi*) growth, condition, calcification, and survival. *PLoS one* **8**:e60959.
- Lovvorn, J. R., C. L. Baduini, and G. L. Hunt. 2001. Modeling underwater visual and filter feeding by planktivorous shearwaters in unusual sea conditions. *Ecology* **82**:2342–2356.
- Mantua, N. J., S. R. Hare, Y. Zhang, J. M. Wallace, and R. C. Francis. 1997. A Pacific Interdecadal Climate Oscillation with Impacts on Salmon Production. *Bulletin of the American Meteorological Society* **78**:1069–1079.
- Martinson, E. C., H. H. Stokes, and D. L. Scarnecchia. 2012. Use of juvenile salmon growth and temperature change indices to predict groundfish post age-0 yr class strengths in the Gulf of Alaska and eastern Bering Sea. *Fisheries Oceanography* **21**:307–319.
- Matson, P. G., L. Washburn, E. A. Fields, C. Gotschalk, T. M. Ladd, D. A. Siegel, Z. S. Welch, and M. D. Iglesias-Rodriguez. 2019. Formation, development, and propagation of a rare coastal coccolithophore bloom. *Journal of Geophysical Research: Oceans* **124**:3298–3316.
- Mayzaud, P., S. Falk-Petersen, M. Noyon, A. Wold, and M. Boutoute. 2016. Lipid composition of the three co-existing *Calanus* species in the Arctic: impact of season, location and environment. *Polar Biology* **39**:1819–1839.
- McCarthy, A., T. Honkalehto, N. Lauffenburger, and A. De Robertis. 2020. Results of the acoustic-trawl survey of walleye pollock (*Gadus chalcogrammus*) on the US Bering Sea Shelf in June-August 2018 (DY1807).
- Mueter, F. J., and M. A. Litzow. 2008. Sea ice retreat alters the biogeography of the Bering Sea continental shelf. *Ecological Applications* **18**:309–320.
- Murphy, J., S. Garcia, J. Dimond, J. Moss, F. Sewall, W. Strasburger, E. Lee, T. Dann, E. Labunski, T. Zeller, A. Gray, C. Waters, D. Jallen, D. Nicolls, R. Conlon, K. Ciciel, K. Howard, B. Harris, N. Wolf, and E. Farley. 2021. Northern Bering Sea surface trawl and ecosystem survey cruise report, 2019. Report, U.S. Dep. Commer., NOAA Tech. Memo. NMFS-AFSC-423, 124 p.
- Murphy, J. M., K. G. Howard, J. C. Gann, K. C. Ciciel, W. D. Templin, and C. M. Guthrie. 2017. Juvenile Chinook Salmon abundance in the northern Bering Sea: Implications for future returns and fisheries in the Yukon River. *Deep-Sea Research Part II-Topical Studies in Oceanography* **135**:156–167.
- Napp, J. M., and G. L. Hunt. 2001. Anomalous conditions in the south-eastern Bering Sea 1997: linkages among climate, weather, ocean, and Biology. *Fisheries Oceanography* **10**:61–68.
- NASA. 2019. NASA Goddard Space Flight Center, O.E.L., Ocean Biology Processing Group. Report, Greenbelt, MD, USA.
- NMFS. 2005. Final Environmental Impact Statement for Essential Fish Habitat Identification and Conservation in Alaska: Volume I. Report, National Marine Fisheries Service, Alaska Region, 1124 p. <https://repository.library.noaa.gov/view/noaa/17391>.
- NMFS. 2020. Programmatic biological assessment on the effects of the fishery management plans for the Gulf of Alaska and Bering Sea/Aleutian Islands groundfish fisheries and the State of Alaska parallel groundfish fisheries on the endangered short-tailed albatross (*Phoebastria albatrus*), the threatened Alaska-breeding population of Steller’s eider (*Polysticta stelleri*), and the threatened spectacled eider (*Somateria fischeri*). Report, Juneau, Alaska, 97 p.

- NPFMC. 2016. Bering Sea/Aleutian Islands Groundfish Fishery Management Plan Amendment Action Summaries. Report, North Pacific Fishery Management Council, 605 W 4th Ave Suite 306, Anchorage, Alaska 99501.
- NPFMC. 2017. Fishery Management Plan for Groundfish of the Bering Sea and Aleutian Islands Management Area. Report, North Pacific Fishery Management Council, 605 W 4th Ave Suite 306, Anchorage, Alaska 99501.
- Oke, K., C. Cunningham, P. Westley, M. Baskett, S. Carlson, J. Clark, A. Hendry, V. Karatayev, N. Kendall, and J. Kibele. 2020. Recent declines in salmon body size impact ecosystems and fisheries. *Nature communications* **11**:1–13.
- Oke, K. B., F. Mueter, and M. A. Litzow. 2022. Warming leads to opposite patterns in weight-at-age for young versus old age classes of Bering Sea walleye pollock. *Canadian Journal of Fisheries and Aquatic Sciences* **79**:1655–1666.
- Olson, M. B., and S. L. Strom. 2002. Phytoplankton growth, microzooplankton herbivory and community structure in the southeast Bering Sea: insight into the formation and temporal persistence of an *Emiliana huxleyi* bloom. *Deep Sea Research Part II: Topical Studies in Oceanography* **49**:5969–5990.
- ONeill, B. C., E. Kriegler, K. Riahi, K. L. Ebi, S. Hallegatte, T. R. Carter, R. Mathur, and D. P. van Vuuren. 2014. A new scenario framework for climate change research: the concept of shared socioeconomic pathways. *Climatic Change* **122**:387–400.
- Ortiz, I., F. Weise, and A. Greig. 2012. Marine regions boundary data for the Bering Sea shelf and slope. UCAR/NCAR—Earth Observing Laboratory/Computing, Data, and Software Facility. Dataset. doi **10**:D6DF6P6C.
- Parnesan, C., and G. Yohe. 2003. A globally coherent fingerprint of climate change impacts across natural systems. *Nature* **421**:37–42.
- Paul, A., and J. Paul. 1999. Interannual and regional variations in body length, weight and energy content of age-0 Pacific herring from Prince William Sound, Alaska. *Journal of fish biology* **54**:996–1001.
- Pauly, D., V. Christensen, J. Dalsgaard, R. Froese, and F. Torres. 1998. Fishing down marine food webs. *Science* **279**:860–863.
- Pease, C. H. 1980. Eastern Bering sea ice processes. *Monthly Weather Review* **108**:2015–2023.
- Petitgas, P. 1993. Geostatistics for fish stock assessments: a review and an acoustic application. *ICES Journal of Marine Science: Journal du Conseil* **50**:285–298.
- Pickart, R., G. Moore, T. Weingartner, S. Danielson, and K. Frey. 2013. Physical Drivers of the Chukchi, Beaufort, and Northern Bering Seas. *Developing a Conceptual Model of the Arctic Marine Ecosystem* **2**.
- Pickart, R. S., M. A. Spall, G. W. Moore, T. J. Weingartner, R. A. Woodgate, K. Aagaard, and K. Shimada. 2011. Upwelling in the Alaskan Beaufort Sea: Atmospheric forcing and local versus non-local response. *Progress in Oceanography* **88**:78–100.
- Pierson, J. J., H. Batchelder, W. Saumweber, A. Leising, and J. Runge. 2013. The impact of increasing temperatures on dormancy duration in *Calanus finmarchicus*. *Journal of plankton research* **35**:504–512.
- Pilcher, D. J., D. M. Naiman, J. N. Cross, A. J. Hermann, S. A. Siedlecki, G. A. Gibson, and J. T. Mathis. 2019. Modeled effect of coastal biogeochemical processes, climate variability, and ocean acidification on aragonite saturation state in the Bering Sea. *Frontiers in Marine Science* **5**:508.
- Pinger, C., L. Copeman, M. Stowell, B. Cormack, C. Fugate, and M. Rogers. 2022. Rapid measurement of total lipids in zooplankton using the sulfo-phospho-vanillin reaction. *Analytical Methods* **14**:2665–2672.

- Platt, T., C. Fuentes-Yaco, and K. T. Frank. 2003. Marine ecology: spring algal bloom and larval fish survival. *Nature* **423**:398–399.
- Punt, A. E., R. J. Foy, M. G. Dalton, W. C. Long, and K. M. Swiney. 2016. Effects of long-term exposure to ocean acidification conditions on future southern Tanner crab (*Chionoecetes bairdi*) fisheries management. *ICES Journal of Marine Science* **73**:849–864.
- Purcell, J. E., and M. N. Arai. 2001. Interactions of pelagic cnidarians and ctenophores with fish: a review. *Hydrobiologia* **451**:27–44.
- Queirolo, L. E., L. Fritz, P. Livingston, M. Loefflad, D. Colpo, and Y. DeReynier. 1995. Bycatch, utilization, and discards in the commercial groundfish fisheries of the Gulf of Alaska, eastern Bering Sea, and Aleutian Islands. NOAA Tech. Memo. NMFS-AFSC **58**:148.
- Ressler, P., A. De Robertis, and S. Kotwicki. 2014. The spatial distribution of euphausiids and walleye pollock in the eastern Bering Sea does not imply top-down control by predation. *Marine Ecology Progress Series* **503**:111–122.
- Ressler, P. H., A. De Robertis, J. D. Warren, J. N. Smith, and S. Kotwicki. 2012. Developing an acoustic survey of euphausiids to understand trophic interactions in the Bering Sea ecosystem. *Deep Sea Research Part II: Topical Studies in Oceanography* **65–70**:184–195.
- Richardson, A., A. Walne, A. John, T. Jonas, J. Lindley, D. Sims, D. Stevens, and M. Witt. 2006. Using continuous plankton recorder data. *Progress in Oceanography* **68**:27–74.
- Robinson, K. L., J. J. Ruzicka, M. B. Decker, R. Brodeur, F. Hernandez, J. Quiñones, E. Acha, S. Uye, H. Mianzan, and W. Graham. 2014. Jellyfish, forage fish, and the world's major fisheries. *Oceanography* **27**:104–115.
- Rodgveller, C. J. 2019. The utility of length, age, liver condition, and body condition for predicting maturity and fecundity of female sablefish. *Fisheries Research* **216**:18–28.
- Rogers, L. A., and D. E. Schindler. 2011. Scale and the detection of climatic influences on the productivity of salmon populations. *Global Change Biology* **17**:2546–2558.
- Rooper, C. N., M. F. Sigler, P. Goddard, P. Malecha, R. Towler, K. Williams, R. Wilborn, and M. Zimmermann. 2016. Validation and improvement of species distribution models for structure-forming invertebrates in the eastern Bering Sea with an independent survey. *Marine Ecology Progress Series* **551**:117–130.
- Ruggerone, G. T., B. A. Agler, B. M. Connors, E. V. Farley Jr, J. R. Irvine, L. I. Wilson, and E. M. Yasumiishi. 2016. Pink and sockeye salmon interactions at sea and their influence on forecast error of Bristol Bay sockeye salmon. *North Pacific Anadromous Fish Commission Bulletin* **6**:349–361.
- Ruggerone, G. T., and J. L. Nielsen. 2004. Evidence for competitive dominance of pink salmon (*Oncorhynchus gorbuscha*) over other salmonids in the North Pacific Ocean. *Reviews in Fish Biology and Fisheries* **14**:371–390.
- Schindler, D., C. Krueger, P. Bisson, M. Bradford, B. Clark, J. Conitz, K. Howard, M. Jones, J. Murphy, and K. Myers. 2013. Arctic-Yukon-Kuskokwim Chinook salmon research action plan: Evidence of decline of Chinook salmon populations and recommendations for future research. Prepared for the AYK Sustainable Salmon Initiative (Anchorage, AK) **70**.
- Schindler, D. E., R. Hilborn, B. Chasco, C. P. Boatright, T. P. Quinn, L. A. Rogers, and M. S. Webster. 2010. Population diversity and the portfolio effect in an exploited species. *Nature* **465**:609–613.
- Schindler, D. E., P. R. Leavitt, S. P. Johnson, and C. S. Brock. 2006. A 500-year context for the recent surge in sockeye salmon (*Oncorhynchus nerka*) abundance in the Alagnak River, Alaska. *Canadian Journal of Fisheries and Aquatic Sciences* **63**:1439–1444.

- Seung, C. K., M. G. Dalton, A. E. Punt, D. Poljak, and R. Foy. 2015. Economic impacts of changes in an Alaska crab fishery from ocean acidification. *Climate Change Economics* **6**:1550017.
- Shin, Y.-J., M.-J. Rochet, S. Jennings, J. G. Field, and H. Gislason. 2005. Using size-based indicators to evaluate the ecosystem effects of fishing. *ICES Journal of marine Science* **62**:384–396.
- Shin, Y.-J., L. J. Shannon, A. Bundy, M. Coll, K. Aydin, N. Bez, J. L. Blanchard, M. d. F. Borges, I. Diallo, and E. Diaz. 2010. Using indicators for evaluating, comparing, and communicating the ecological status of exploited marine ecosystems. Part 2. Setting the scene. *ICES Journal of Marine Science* **67**:692–716.
- Siddon, E. 2021. Ecosystem Status Report 2021: Eastern Bering Sea. Report, North Pacific Fishery Management Council, 1007 West Third, Suite 400, Anchorage, Alaska 99501.
- Siddon, E., J. Ianelli, and S. Dressel. 2020. Incidental catch of herring in groundfish fisheries increased in 2020. Stock Assessment and Fishery Evaluation Report, North Pacific Fishery Management Council, 1007 West Third Ave, Suite 400, Anchorage, AK 99501.
- Siddon, E. C., R. A. Heintz, and F. J. Mueter. 2013. Conceptual model of energy allocation in walleye pollock (*Theragra chalcogramma*) from age-0 to age-1 in the southeastern Bering Sea. *Deep Sea Research Part II: Topical Studies in Oceanography* **94**:140–149.
- Sigler, M. F., P. J. Stabeno, L. B. Eisner, J. M. Napp, and F. J. Mueter. 2014. Spring and fall phytoplankton blooms in a productive subarctic ecosystem, the eastern Bering Sea, during 1995–2011. *Deep Sea Research Part II: Topical Studies in Oceanography* **109**:71–83.
- Simonsen, K. A., P. H. Ressler, C. N. Rooper, and S. G. Zador. 2016. Spatio-temporal distribution of euphausiids: an important component to understanding ecosystem processes in the Gulf of Alaska and eastern Bering Sea. *ICES Journal of Marine Science: Journal du Conseil* page fsv272 .
- Smeltz, T. S., B. P. Harris, J. V. Olson, and S. A. Sethi. 2019. A seascape-scale habitat model to support management of fishing impacts on benthic ecosystems. *Canadian Journal of Fisheries and Aquatic Sciences* **76**:1836–1844.
- Smith, J. N., P. H. Ressler, and J. D. Warren. 2013. A distorted wave Born approximation target strength model for Bering Sea euphausiids. *ICES Journal of Marine Science: Journal du Conseil* **70** (1):204–214.
- Smith, S. L. 1991. Growth, development and distribution of the euphausiids *Thysanoessa raschi* (M. Sars) and *Thysanoessa inermis* (Krøyer) in the southeastern Bering Sea. *Polar Research* **10**:461–478.
- Spear, A., and A. G. Andrews III. 2021. Vertical Distribution of Age-0 Pollock in the Southeastern Bering Sea. In Ecosystem Status Report 2021: Eastern Bering Sea. Report, North Pacific Fishery Management Council, 1007 W 3rd Ave, Suite 400, Anchorage, AK 99501.
- Spencer, P. D. 2008. Density-independent and density-dependent factors affecting temporal changes in spatial distributions of eastern Bering Sea flatfish. *Fisheries Oceanography* **17**:396–410.
- Spencer, P. D., K. K. Holsman, S. Zador, N. A. Bond, F. J. Mueter, A. B. Hollowed, and J. N. Ianelli. 2016. Modelling spatially dependent predation mortality of eastern Bering Sea walleye pollock, and its implications for stock dynamics under future climate scenarios. *ICES Journal of Marine Science* **73**:1330–1342.
- Springer, A. M., C. P. McRoy, and M. V. Flint. 1996. The Bering Sea Green Belt: Shelf-edge processes and ecosystem production. *Fisheries Oceanography* **5**:205–223.
- Springer, A. M., and G. B. van Vliet. 2014. Climate change, pink salmon, and the nexus between bottom-up and top-down forcing in the subarctic Pacific Ocean and Bering Sea. *Proceedings of the National Academy of Sciences* **111**:E1880–E1888.

- Stabeno, P., S. Danielson, D. Kachel, N. Kachel, and C. Mordy. 2016. Currents and transport on the eastern Bering Sea shelf: An integration of over 20 years of data. *Deep Sea Research Part II: Topical Studies in Oceanography* **134**:13–29.
- Stabeno, P., and G. L. Hunt. 2002. Overview of the inner front and southeast Bering Sea Carrying Capacity Programs. *Deep Sea Research II* **49**:6157–6168.
- Stabeno, P. J., and S. W. Bell. 2019. Extreme conditions in the Bering Sea (2017–2018): record-breaking low sea-ice extent. *Geophysical Research Letters* **46**:8952–8959.
- Stabeno, P. J., J. Farley, E. V., N. B. Kachel, S. Moore, C. W. Mordy, J. M. Napp, J. E. Overland, A. I. Pinchuk, and M. F. Sigler. 2012. A comparison of the physics of the northern and southern shelves of the eastern Bering Sea and some implications for the ecosystem. *Deep-Sea Research Part II-Topical Studies in Oceanography* **65-70**:14–30.
- Stevenson, D., and G. Hoff. 2009. Species identification confidence in the eastern Bering Sea shelf survey (1982 - 2008). Report, NOAA NMFS-AFSC, 7600 Sand Point Way NE, Seattle, WA 98115, AFSC Processed Report 2009-04, 46 p.
- Stevenson, D., K. Weinberg, and R. Lauth. 2016. Estimating confidence in trawl efficiency and catch quantification for the eastern Bering Sea shelf survey. Report, U.S. Dep. Commer., NOAA Tech. Memo., NMFS-AFSC-335, 51 p.
- Stevenson, D. E., and R. R. Lauth. 2012. Latitudinal trends and temporal shifts in the catch composition of bottom trawls conducted on the eastern Bering Sea shelf. *Deep-Sea Research Part II-Topical Studies in Oceanography* **65-70**:251–259.
- Stevenson, D. E., and R. R. Lauth. 2019. Bottom trawl surveys in the northern Bering Sea indicate recent shifts in the distribution of marine species. *Polar Biology* **42**:407–421.
- Stockwell, D. A., T. E. Whitledge, S. I. Zeeman, K. O. Coyle, J. M. Napp, R. D. Brodeur, A. I. Pinchuk, and G. L. Hunt. 2001. Anomalous conditions in the south-eastern Bering Sea, 1997: nutrients, phytoplankton and zooplankton. *Fisheries Oceanography* **10**:99–116.
- Stram, D. L., and J. N. Ianelli. 2015. Evaluating the efficacy of salmon bycatch measures using fishery-dependent data. *ICES Journal of Marine Science* **72**:1173–1180.
- Swiney, K. M., W. C. Long, and R. J. Foy. 2017. Decreased pH and increased temperatures affect young-of-the-year red king crab (*Paralithodes camtschaticus*). *ICES Journal of Marine Science* **74**:1191–1200.
- Team, R. C. 2020. R: A language and environment for statistical computing. R Foundation for Statistical Computing. <http://www.R-project.org/>, Vienna, Austria.
- Thorson, J., M. Fosshem, F. Mueter, E. Olsen, R. Lauth, R. Primicerio, B. Husson, J. Marsh, A. Dolgov, and S. Zador. 2019. Comparison of near-bottom fish densities show rapid community and population shifts in Bering and Barents Seas. *Arctic Report Card* .
- Thorson, J. T. 2019a. Guidance for decisions using the Vector Autoregressive Spatio-Temporal (VAST) package in stock, ecosystem, habitat and climate assessments. *Fisheries Research* **210**:143–161.
- Thorson, J. T. 2019b. Measuring the impact of oceanographic indices on species distribution shifts: The spatially varying effect of cold-pool extent in the eastern Bering Sea. *Limnology and Oceanography* **64**:2632–2645.
- Thorson, J. T., L. Ciannelli, and M. A. Litzow. 2020. Defining indices of ecosystem variability using biological samples of fish communities: A generalization of empirical orthogonal functions. *Progress in Oceanography* **181**:102244.

- Thorson, J. T., and K. Kristensen. 2016. Implementing a generic method for bias correction in statistical models using random effects, with spatial and population dynamics examples. *Fisheries Research* **175**:66–74.
- Thorson, J. T., A. O. Shelton, E. J. Ward, and H. J. Skaug. 2015. Geostatistical delta-generalized linear mixed models improve precision for estimated abundance indices for West Coast groundfishes. *ICES Journal of Marine Science* **72**:1297–1310.
- Tide, C., and A. Eich. 2022. Seabird bycatch estimates for Alaska Groundfish Fisheries: 2021. Report, U.S. Department of Commerce NOAA Technical Memorandum NMFS-F/AKR-XX, 46 p.
- Tobin, E. D., C. L. Wallace, C. Crumpton, G. Johnson, and G. L. Eckert. 2019. Environmental drivers of paralytic shellfish toxin producing *Alexandrium catenella* blooms in a fjord system of northern Southeast Alaska. *Harmful algae* **88**:101659.
- Tojo, N., G. H. Kruse, and F. C. Funk. 2007. Migration dynamics of Pacific herring (*Clupea pallasii*) and response to spring environmental variability in the southeastern Bering Sea. *Deep Sea Research Part II: Topical Studies in Oceanography* **54**:2832–2848.
- Uchiyama, T., F. J. Mueter, and G. H. Kruse. 2020. Multispecies biomass dynamics models reveal effects of ocean temperature on predation of juvenile pollock in the eastern Bering Sea. *Fisheries Oceanography* **29**:10–22.
- USFWS. 2021. Biological Opinion on the Proposed Modification of the EPA General Permit AKG524000 for Offshore Seafood Processors in Alaska and on the NMFS Groundfish Fishery for the Gulf of Alaska, Bering Sea, and Aleutians Islands. Anchorage, AK. Report, 80 p.
- Vandersea, M. W., S. R. Kibler, P. A. Tester, K. Holderied, D. E. Hondolero, K. Powell, S. Baird, A. Doroff, D. Dugan, and R. W. Litaker. 2018. Environmental factors influencing the distribution and abundance of *Alexandrium catenella* in Kachemak bay and lower cook inlet, Alaska. *Harmful algae* **77**:81–92.
- von Biela, V. R., L. Bowen, S. D. McCormick, M. P. Carey, D. S. Donnelly, S. Waters, A. M. Regish, S. M. Laske, R. J. Brown, and S. Larson. 2020. Evidence of prevalent heat stress in Yukon River Chinook salmon. *Canadian Journal of Fisheries and Aquatic Sciences* **77**:1878–1892.
- Waga, H., H. Eicken, T. Hirawake, and Y. Fukamachi. 2021. Variability in spring phytoplankton blooms associated with ice retreat timing in the Pacific Arctic from 2003–2019. *Plos one* **16**:e0261418.
- Waldbusser, G. G., B. Hales, C. J. Langdon, B. A. Haley, P. Schrader, E. L. Brunner, M. W. Gray, C. A. Miller, and I. Gimenez. 2015. Saturation-state sensitivity of marine bivalve larvae to ocean acidification. *Nature Climate Change* **5**:273–280.
- Watson, J. 2020. Marine heatwaves in the Eastern Bering Sea. Stock Assessment and Fishery Evaluation Report, North Pacific Fishery Management Council, 605 W 4th Ave, Suite 306, Anchorage, AK 99501.
- Wespestad, V., and D. Gunderson. 1991. Climatic induced variation in Eastern Bering Sea herring recruitment. Report, Proceedings of the International Herring Symposium, Anchorage, AK. Alaska Sea Grant.
- Wilderbuer, T. K. 2017. Eastern Bering Sea Winter Spawning Flatfish Recruitment and Wind Forcing. Stock Assessment and Fishery Evaluation Report, North Pacific Fishery Management Council, 605 W 4th Ave, Suite 306, Anchorage, AK 99501.
- Williams, E. H., and T. J. Quinn. 2000. Pacific herring, *Clupea pallasii*, recruitment in the Bering Sea and north-east Pacific Ocean, I: relationships among different populations. *Fisheries Oceanography* **9**:285–299.
- Winemiller, K. O. 2005. Life history strategies, population regulation, and implications for fisheries management. *Canadian Journal of Fisheries and Aquatic Sciences* **62**:872–885.
- Wuillez, M., J. Rivoirard, and P. Petitgas. 2009. Notes on survey-based spatial indicators for monitoring fish populations. *Aquatic Living Resources* **22**:155–164.

- Woodgate, R. A., T. J. Weingartner, and R. Lindsay. 2012. Observed increases in Bering Strait oceanic fluxes from the Pacific to the Arctic from 2001 to 2011 and their impacts on the Arctic Ocean water column. *Geophysical Research Letters* **39**.
- Wuenschel, M. J., W. D. McElroy, K. Oliveira, and R. S. McBride. 2019. Measuring fish condition: an evaluation of new and old metrics for three species with contrasting life histories. *Canadian Journal of Fisheries and Aquatic Sciences* **76**:886–903.
- Yasumiishi, E. M., K. Cieciel, A. G. Andrews, J. Murphy, and J. A. Dimond. 2020. Climate-related changes in the biomass and distribution of small pelagic fishes in the eastern Bering Sea during late summer, 2002–2018. *Deep Sea Research Part II: Topical Studies in Oceanography* **181**:104907.
- Zador, S. G., and S. Fitzgerald. 2008. Seabird attraction to trawler discards. Report, Alaska Fisheries Science Center, NOAA, NMFS, 7600 Sand Point Way NE, Seattle WA 98115.

# Appendix

## High resolution climate change projections for the Eastern Bering Sea

Contributed by Kirstin K. Holsman<sup>1</sup>, Albert Hermann<sup>2,3</sup>, Wei Cheng<sup>2,3</sup>, Kelly Kearney<sup>2</sup>, Darren Pilcher<sup>2</sup>, Kerim Aydin<sup>1</sup>, Ivonne Ortiz<sup>2</sup>

<sup>1</sup>Alaska Fisheries Science Center, NOAA, 7600 Sand Point Way N.E., Bld. 4, Seattle, Washington 98115

<sup>2</sup>Cooperative Institute for Climate, Ocean and Ecosystem Studies, University of Washington, Seattle, WA. 98195

<sup>3</sup>Pacific Marine Environmental Laboratory, Seattle, WA 98115 Contact: kirstin.holsman@noaa.gov

**Last updated: November 2022**

**Description of indicator:** We report trends in modeled bottom temperature and sea surface temperature from a 30-layer Bering Sea regional oceanographic model at 10km horizontal resolution which has incorporated lower trophic level biology (Kearney et al., 2020) and marine carbonate chemistry (Pilcher et al., 2019). See the Bering 10K dataset documentation for more information and technical details<sup>41</sup>. We present the Alaska NOAA Integrated Ecosystem Assessment<sup>42</sup> program annual hindcast and two carbon mitigation scenarios projected as part of the Alaska Climate Integrated Modeling (ACLIM) project<sup>43</sup>. In this, a high carbon mitigation scenario (ssp126) and a low carbon mitigation scenario (ssp585; O'Neill et al. (2014)) and three global Earth System Models (ESMs; 'cesm', 'gfdl', and 'miroc') were selected from the Coupled Model Intercomparison Project (CMIP6)<sup>44</sup> and used to force the regional model. See Hermann et al. (2021); Cheng et al. (2021); Kearney et al. (2020); Pilcher et al. (2019) for details about the regional model projections and Hollowed et al. (2020) for details about the ACLIM project and forcing (climate scenario and ESM) selection.

In support of ACLIM, a number of different biophysical index timeseries were calculated based on the Bering10K simulations and provide the primary means of linking the physical and lower trophic level dynamics to the ACLIM suite of upper trophic level and socioeconomic models; see Hollowed et al. (2020) for further details. The timeseries reported here are derived from the area-weighted strata averages for Summer (months Jul-Sep) and Winter (Jan-Feb) for the Northern Bering Sea (NEBS; strata 70, 81, 82, 90 of the eastern Bering Sea shelf bottom trawl survey) and Southern Bering Sea (SEBS; strata 10, 20, 31, 32, 50, 20, 41, 42, 43, 61, 62). The timeseries were bias-corrected to hindcast simulations using historical forcing (during 1980–2013) from each ESM. More detail on this approach is available by request.

The climate simulations presented here are dynamically downscaled from a selection of the historical and shared socioeconomic pathway simulations from the sixth phase of the CMIP6. Names reflect the parent global model simulation (miroc = MIROC ES2L, cesm = CESM2, gfdl = GFDL ESM4) and emis-

<sup>41</sup>[https://zenodo.org/record/4586950/files/Bering10K\\_dataset\\_documentation.pdf](https://zenodo.org/record/4586950/files/Bering10K_dataset_documentation.pdf)

<sup>42</sup><https://www.integratedecosystemassessment.noaa.gov/>

<sup>43</sup><https://www.fisheries.noaa.gov/alaska/ecosystems/alaska-climate-integrated-modeling-project>

<sup>44</sup><https://www.wcrp-climate.org/wgcm-cmip/wgcm-cmip6>

sions scenario via Shared Socioeconomic Pathways (SSPs) (ssp126 = SSP1-2.6, ssp585 = SSP5-8.5, historical=Historical). Scenario ssp126 represents a high carbon mitigation (low greenhouse gas emissions) scenario; ssp585 represents the low carbon mitigation scenario. More information on the SSPs and their use in climate projections is available in O'Neill et al. (2014).

To determine mean temperatures associated with standardized levels of global warming for each scenario and ESM, we used CMIP6 Global Warming Levels from Hauser et al. (2021) and available at [https://github.com/mathause/cmip\\_warming\\_levels](https://github.com/mathause/cmip_warming_levels).

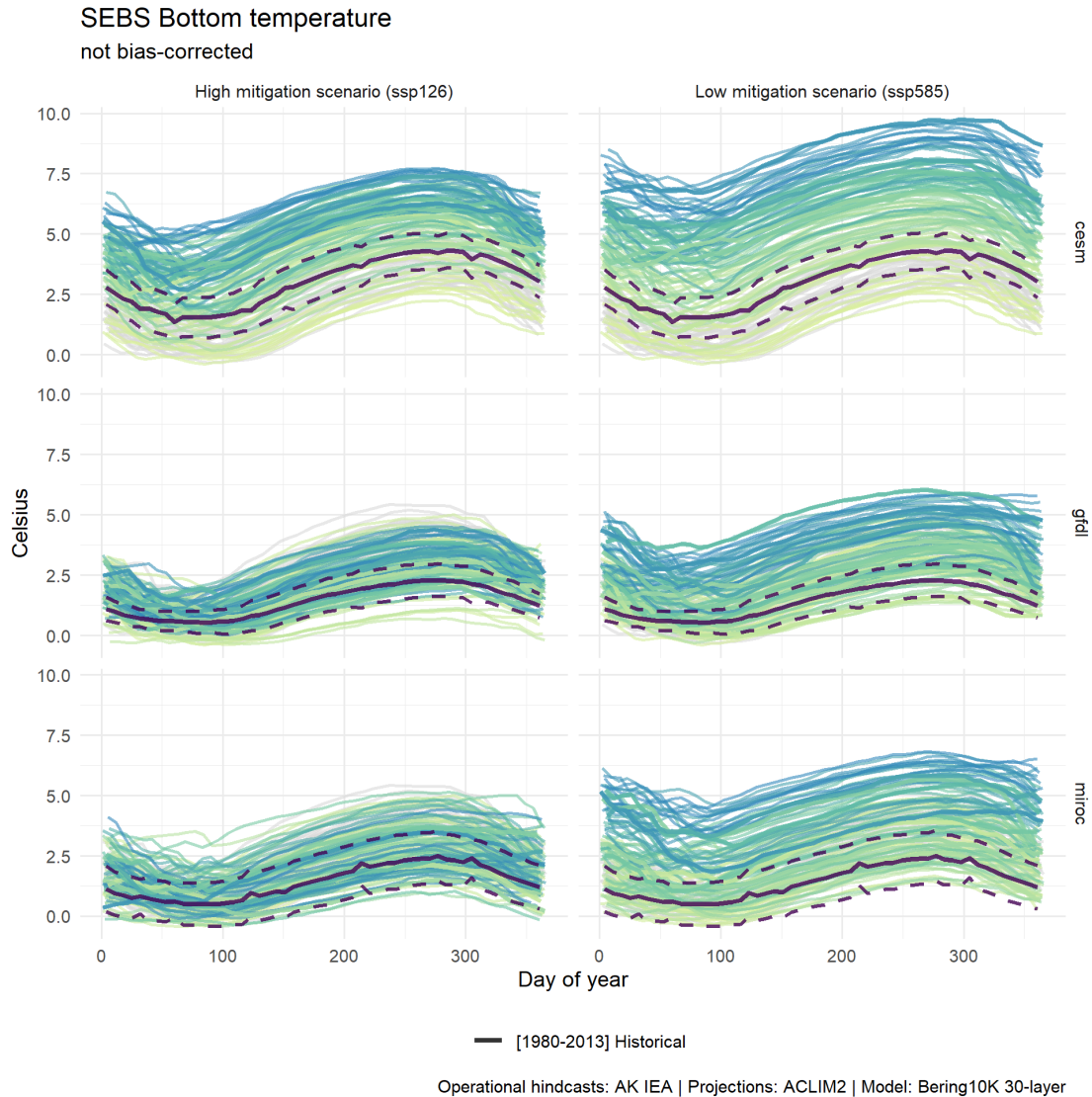


Figure 123: Southern Bering Sea (SEBS) bottom water temperature ( $^{\circ}\text{C}$ ) projected under two climate scenarios; high carbon mitigation via Shared Socioeconomic Pathways (ssp126, left column); low carbon mitigation (ssp585, right column). Rows reflect the parent global model simulation (miroc = MIROC ES2L, cesm = CESM2, gfdl = GFDL ESM4) dynamically downscaled to a high resolution regional model (Bering10K K20P19 30 layer ROMSNPZ model). Average modeled climatology from the reference period (1980–2013) of the historical run for each ESM is shown as the solid blue line; dashed lines represent  $\pm 1$  standard deviation of the mean; colors of each line correspond to year from present day (light green) to 2100 (darker teal).

**Status and trends:** Summer bottom temperatures in both the SEBS and the NEBS are projected to increase over time, with higher rates of warming associated with low carbon mitigation scenarios relative to high carbon mitigation scenarios (ssp585 vs ssp126; 4 and 5). Three Earth Systems Models (ESMs) are presented to reflect the spread in projections across ensemble members. There is general agreement in all three models (ESMs) with respect to trends in warming associated with alternative climate scenarios. For the SEBS, estimates of end of century warming relative to recent historical bottom temperatures [(2080–2100)-(1980–2013)] range from +0.04 to +2.51°C for high carbon mitigation (ssp126) scenarios and +2.05 to +4.17°C for low carbon mitigation (ssp585) scenarios (ranges represent  $\pm 1$  standard deviation [SD]; Figure 4).

For the NEBS, estimates of end of century warming of bottom temperatures [(2080–2100)-(1980–2013)] range from +0.07 to +3.01°C for high carbon mitigation (ssp126) scenarios and +2.82 to +6.58°C for low carbon mitigation (ssp585) scenarios (Figure 5). In low mitigation scenarios, bottom temperatures for the SEBS and NEBS by the mid-century (2050–2060) are projected to consistently exceed the upper range of historical modeled temperatures from the Bering Sea. For reference, average historical (1980–2013) bottom temperatures are 3.2°C (SD=0.76) and 2.65°C (SD=0.98) for the SEBS and NEBS, respectively.

While SSTs are generally warmer than BTs, projected warming trends in SST over the next century are similar to those of BT and have higher agreement for all three models under low carbon mitigation scenarios (ssp585). Under low carbon mitigation scenarios (ssp585), estimates of end of century warming of SST range from +3.05 to +5.09°C for the SEBS, and are roughly 2–3 times higher than warming projected under high carbon mitigation scenarios where average temperatures between years 2080 and 2100 are projected to be +0.65 to +3.02°C higher than historical mean temperatures (1980–2013). Similarly, NEBS estimates of end of century warming of SST [(2080–2100)-(1980–2013)] range from +0.72 to +3.88°C for high carbon mitigation (ssp126) scenarios and +4.03 to +6.69°C for low carbon mitigation (ssp585) scenarios (Figure 5). Mean historical (1980–2013) average SSTs are 9.7°C ( $\pm 0.8$ ) and 8.34°C ( $\pm 1.01$ ) for the SEBS and NEBS, respectively.

Global Warming Levels (GWL) are standardized indices used to describe changes in average global surface temperature over the next century relative to a pre-industrial baseline for global average temperatures (1850–1900). As a point of reference, in the most recent 6<sup>th</sup> assessment report the IPCC found that 2019 GWL was +1.08°C (IPCC, 2021). GWLs of +3 and +4°C over pre-industrial temperatures are associated with significant warming of SSTs and BTs in both the NEBS and SEBS (Figure 6). In contrast, under GWL of +1.5°C, SST and BT in the next century in both regions is only slightly warmer than contemporary temperatures and year-to-year variation in temperatures is within the near-present range of climate variability (2010–2021). GWL of +3 and +4°C are also associated with the occurrence of a number of extreme heat events where annual bottom temperatures exceed 10°C (filled points in Figure 6).

There are sub-regional (NEBS vs. SEBS) differences in projections of warming across seasons and future climate scenarios (Figures 123 and 124). We selected a cool ('gfdl'), middle-of-the-road ('cesm'), and warm running ('miroc') earth systems model (ESM) from a set of more than 35 models used by the IPCC to project climate change impacts. In general there is agreement in warming trends among the three ESM members for all seasons in the SEBS, especially under low carbon mitigation (high greenhouse gas emissions; ssp585) scenarios (Figure 123; note however, the magnitude of warming varies with ESM such that cesm > miroc > gfdl). Importantly, in the NEBS under high mitigation scenarios (ssp126) two of three models project little warming in winter months, while one model, 'cesm', projects moderate winter warming. This indicates possible continued cold winter conditions and sea ice formation in the NEBS associated with high carbon mitigation measures. In contrast, under low carbon mitigation (ssp585) scenarios, all three models project warming in winter months (i.e., reduced sea ice) as well as substantial warming in spring, summer, and fall BT (Figure 124). These findings suggest that delayed and low levels of carbon mitigation are associated with continued rapid sea ice decline (and probable complete loss of sea ice) in the Bering Sea over the next century.

**Factors influencing observed trends:** For more information about climate change impacts, risks, adaptation, and mitigation see the Intergovernmental Panel on Climate Change (IPCC) 6<sup>th</sup> Assessment Report<sup>45</sup> and [www.climate.gov](http://www.climate.gov).

Carbon dioxide (CO<sub>2</sub>) is a naturally occurring greenhouse gas (GHG) that along with other GHGs acts to absorb and re-emit infrared energy (heat) from solar radiation, warming the earth’s surface (i.e., the ‘greenhouse effect’). Naturally occurring CO<sub>2</sub> (ocean off-gassing, volcanoes, etc.) is offset by carbon sinks (e.g., photosynthesis of plants on land and in the ocean) which have acted to keep CO<sub>2</sub> relatively stable for more than 800,000 years at or below 300 parts per million (ppm). However, scientific observations and models have shown that atmospheric CO<sub>2</sub> concentrations have been rising steadily over the past century due to anthropogenic (human) activities, primarily the burning of fossil fuels for energy and other uses. Rates of anthropogenic CO<sub>2</sub> release into the atmosphere exceed natural carbon sinks and have resulted in a rapid accumulation of atmospheric CO<sub>2</sub>. The IPCC 6<sup>th</sup> Assessment Report states that “observed increases in well-mixed greenhouse gas (GHG) concentrations since around 1750 are unequivocally caused by human activities” and that the “land and ocean have taken up a near-constant proportion (globally about 56% per year) of CO<sub>2</sub> emissions from human activities over the past six decades, with regional differences (high confidence)” (IPCC, 2021).

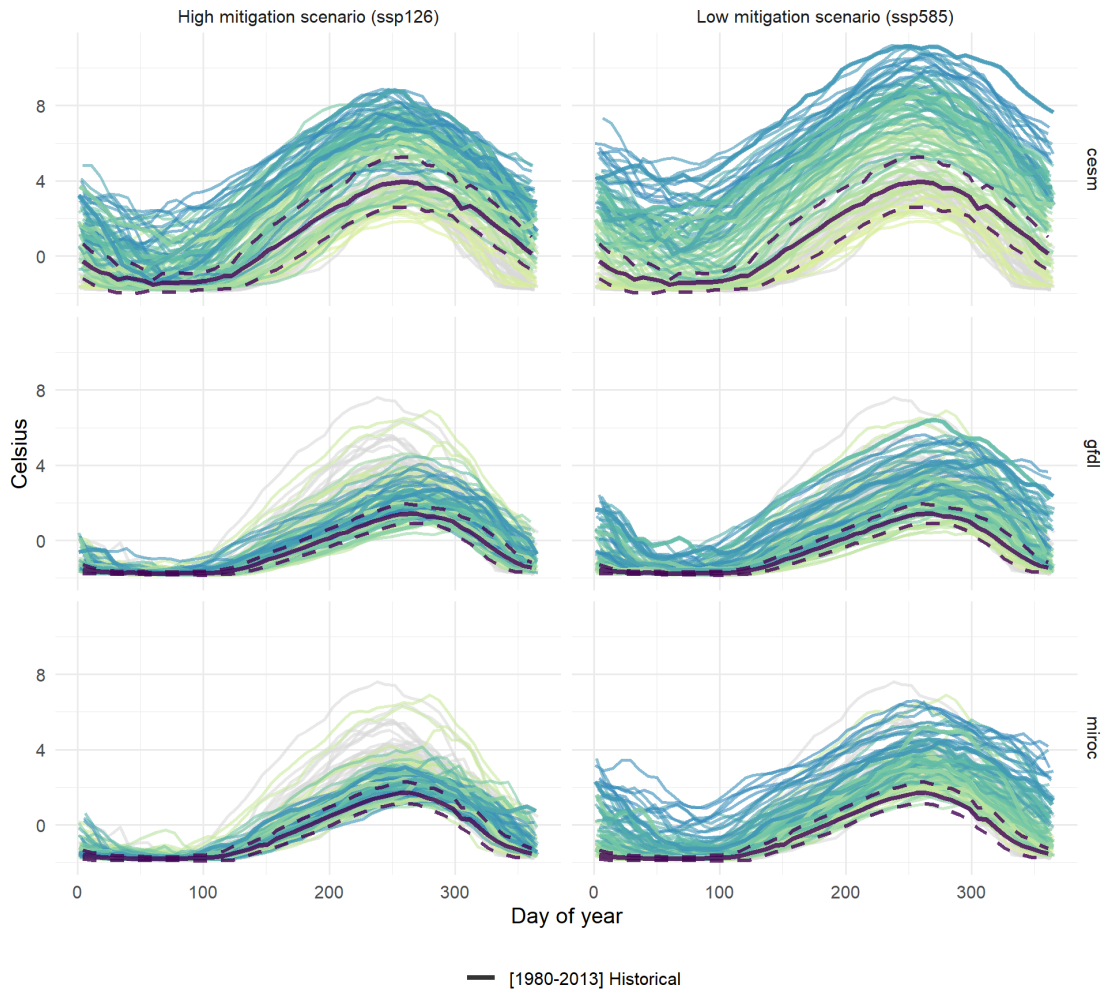
Current atmospheric CO<sub>2</sub> levels of 410 ppm (IPCC, 2021) have not been experienced for at least 2 million years, and the rate of increase in CO<sub>2</sub> over the last century is unprecedented in the last 800,000 years (based on multiple lines of evidence including Antarctic ice core data and isotopes; IPCC (2021)). There is a near-linear relationship between cumulative CO<sub>2</sub> emissions and increases in global surface temperature (IPCC, 2021), and changes in atmospheric CO<sub>2</sub> and associated warming have direct impacts on ocean processes and chemistry. In the most recent assessment report, the IPCC (2021) states “better integration of paleo-oceanographic data with modelling along with higher-resolution analyses of transient changes have improved understanding of long-term ocean processes... This paleo context supports the assessment that ongoing increase in ocean heat content (OHC) represents a long-term commitment, essentially irreversible on human time scales (high confidence)”. This “paleo context” has also helped illuminate the complex role of oceans in the regulation of the global climate and atmospheric CO<sub>2</sub> during previous glacial–interglacial warming intervals. Presently, absorption of atmospheric heat by the world’s oceans increases water temperature, warming the water column from surface waters to depth and raising the “ocean heat content”. Absorption of atmospheric CO<sub>2</sub> alters the chemistry of the ocean, increasing acidity and lowering the pH. In addition, atmospheric warming alters physical and chemical processes (e.g., precipitation, wind patterns, sea level, ocean circulation, and sea ice thickness and extent) in ways that further change the ocean and atmospheric processes, i.e., the climate of a given region. Accordingly, the IPCC (2021) states “it is virtually certain that the global upper ocean (0–700m) has warmed since the 1970s and extremely likely that human influence is the main driver. It is virtually certain that human-caused CO<sub>2</sub> emissions are the main driver of current global acidification of the surface open ocean”.

The near linear relationship between cumulative CO<sub>2</sub> emissions and increases in global surface temperature (IPCC, 2021) has enabled scientists to evaluate future climate conditions under alternative CO<sub>2</sub> and GHG emissions scenarios, known as Shared Socioeconomic Pathways (SSPs; O’Neill et al. (2014)). These allow for projections of changes in climate and ocean temperature and chemistry under Global Warming Levels (GWLs). Patterns of warming reported in this contribution reflect global changes in atmospheric carbon, climate conditions, and oceanic conditions from Earth Systems Models, but are refined through a regional lens via a the high resolution Bering10K ROMSNPZ ocean model that is able to replicate fine scale oceanographic processes (e.g., distinct biophysical zones across the EBS shelf and changes in seasonal sea ice on the EBS) that act to amplify or attenuate larger scale climate change effects.

---

<sup>45</sup>[www.ipcc.ch/assessment-report/ar6/](http://www.ipcc.ch/assessment-report/ar6/)

NEBS Bottom temperature  
not bias-corrected



Operational hindcasts: AK IEA | Projections: ACLIM2 | Model: Bering10K 30-layer

Figure 124: Northern Bering Sea (NEBS) bottom water temperature ( $^{\circ}\text{C}$ ) projected under two climate scenarios; high carbon mitigation via Shared Socioeconomic Pathways (ssp126, left column); low carbon mitigation (ssp585, right column). Rows reflect the parent global model simulation (miroc = MIROC ES2L, cesm = CESM2, gfdl = GFDL ESM4) dynamically downscaled to a high resolution regional model (Bering10K K20P19 30 layer ROMSNPZ model). Average modeled climatology from the reference period (1980–2013) of the historical run for each ESM is show as the solid blue line; dashed lines represent  $\pm 1$  standard deviation of the mean.

**Implications:** Historically, cooler conditions in the Bering sea are associated with higher production of prey, fish, and fisheries catch while warming temperatures and marine heatwaves have been associated with changes to food-web dynamics, species redistribution, and ecosystem structure and processes (Huntington et al., 2020). Projected ocean warming from global models is associated with declines in marine fish biomass, benthic biomass, and fisheries catch potential (IPCC, 2022). Evaluations of projected temperature effects in Bering sea ecosystems and fisheries under high emission scenarios (ssp585) are still underway but include modeled declines in winter sea ice and summer cold pool extent associated with increased warming. Increased warming in EBS projections is also associated with emergent declines in modeled fall euphausiid and large copepod biomass (Hermann et al., 2021), shifts in spring bloom timing to earlier (30–60 d) and slightly larger phytoplankton and zooplankton blooms (relative to hindcasts), and declines in the magnitude of fall total phytoplankton and large zooplankton blooms (Cheng et al., 2021).

## History of the ESRs

Since 1995, staff at the Alaska Fisheries Science Center have prepared a separate Ecosystem Status (formerly Considerations) Report within the annual Stock Assessment and Fishery Evaluation (SAFE) report. Each new Ecosystem Status Report provides updates and new information to supplement the original report. The original 1995 report presented a compendium of general information on the Gulf of Alaska, Bering Sea, and Aleutian Island ecosystems as well as a general discussion of ecosystem-based management. The 1996 edition provided additional information on biological features of the North Pacific, and highlighted the effects of bycatch and discards on the ecosystem. The 1997 edition provided a review of ecosystem-based management literature and ongoing ecosystem research, and provided supplemental information on seabirds and marine mammals. The 1998 edition provided information on the precautionary approach, essential fish habitat, effects of fishing gear on habitat, El Niño, local knowledge, and other ecosystem information. The 1999 edition again gave updates on new trends in ecosystem-based management, essential fish habitat, research on effects of fishing gear on seafloor habitat, marine protected areas, seabirds and marine mammals, oceanographic changes in 1997/98, and local knowledge.

In 1999, a proposal came forward to enhance the Ecosystem Status Report by including more information on indicators of ecosystem status and trends and more ecosystem-based management performance measures. The purpose of this enhancement was to accomplish several goals:

1. Track ecosystem-based management efforts and their efficacy
2. Track changes in the ecosystem that are not easily incorporated into single-species assessments
3. Bring results from ecosystem research efforts to the attention of stock assessment scientists and fishery managers
4. Provide a stronger link between ecosystem research and fishery management
5. Provide an assessment of the past, present, and future role of climate and humans in influencing ecosystem status and trends

Each year since 1999, the Ecosystem Status Reports have included some new contributions and will continue to evolve as new information becomes available. Evaluation of the meaning of observed changes should be in the context of how each indicator relates to a particular ecosystem component. For example, particular oceanographic conditions, such as bottom temperature increases, might be favorable to some species but not for others. Evaluations should follow an analysis framework such as that provided in the draft Programmatic Groundfish Fishery Environmental Impact Statement that links indicators to particular effects on ecosystem components.

In 2002, stock assessment scientists began using indicators contained in this report to systematically assess ecosystem factors such as climate, predators, prey, and habitat that might affect a particular stock. Information regarding a particular fishery's catch, bycatch, and temporal/spatial distribution can be used to assess possible impacts of that fishery on the ecosystem. Indicators of concern can be highlighted within each assessment and can be used by the Groundfish Plan Teams and the Council to justify modification of allowable biological catch (ABC) recommendations or time/space allocations of catch.

We initiated a regional approach to the ESR in 2010 and presented a new ecosystem assessment for the eastern Bering Sea. In 2011, we followed the same approach and presented a new assessment for the Aleutian Islands based on a similar format to that of the eastern Bering Sea. In 2012, we provided a preliminary ecosystem assessment on the Arctic. Our intent was to provide an overview of general Arctic ecosystem information that may form the basis for more comprehensive future Arctic ecosystem assessments. In 2015, we presented a new Gulf of Alaska report card and assessment, which was further divided into Western and Eastern Gulf of Alaska report cards beginning in 2016. This was also the year that the previous Alaska-wide ESR was

split into four separate report, one for the Gulf of Alaska, Aleutian Islands, eastern Bering Sea, and the Arctic<sup>46</sup>.

The eastern Bering Sea and Aleutian Islands ecosystem assessments were based on additional refinements contributed by Ecosystem Synthesis Teams. For these assessments, the teams focused on a subset of broad, community-level indicators to determine the current state and likely future trends of ecosystem productivity in the EBS and ecosystem variability in the Aleutian Islands. The teams also selected indicators that reflect trends in non-fishery apex predators and maintaining a sustainable species mix in the harvest as well as changes to catch diversity and variability. Indicators for the Gulf of Alaska report card and assessment were also selected by a team of experts, via an online survey first, then refined in an in-person workshop.

Originally, contributors to the Ecosystem Status Reports were asked to provide a description of their contributed indicator, summarize the historical trends and current status of the indicator, and identify potential factors causing those trends. Beginning in 2009, contributors were also asked to describe why the indicator is important to groundfish fishery management and implications of indicator trends. In particular, contributors were asked to briefly address implications or impacts of the observed trends on the ecosystem or ecosystem components, what the trends mean and why are they important, and how the information can be used to inform groundfish management decisions. Answers to these types of questions will help provide a “heads-up” for developing management responses and research priorities. In 2018, a risk table framework was developed for individual stock assessments as a means of documenting concerns external to the stock assessment model, but relevant to setting the Acceptable Biological Catch (ABC) value. These concerns could be categorized as those reflecting the assessment model, the population dynamics of the stock, and environmental and ecosystem concerns—including those based on information from Ecosystem Status Reports. In the past, concerns used to justify an ABC below the maximum calculated by the assessment model were documented in an ad hoc manner in the stock assessment report or in the minutes of the groundfish Plan Teams or Scientific and Statistical Committee reviews. With the risk table, formal consideration of concerns—including ecosystem—are documented and ranked, and the stock assessment author presents a recommendation for the maximum ABC or a value lower. Five risk tables were completed in 2018 as a test case. After review, the Council requested risk tables to be included in all stock assessments in 2019.

*In Briefs* were started in 2018 for the Eastern Bering Sea, 2019 for the Gulf of Alaska, and 2020 for the Aleutian Islands. These more public-friendly succinct versions of the full ESRs are now planned to be produced in tandem with the ESRs.

In 2019, risk tables were completed for all full assessments. Ecosystem scientists collaborated with stock assessment scientists to use the Ecosystem Status Reports to help inform the ecosystem concerns in the risk tables.

Ecosystem and Socioeconomic Profiles (ESPs) were initiated in 2017 (Sablefish) and ESR editors began working closely with ESP teams in 2019 (starting with GOA walleye pollock). These complimentary annual status reports inform groundfish management and alignment in research that feeds these reports increases efficiency and collaboration between ecosystem and stock assessment scientists.

This report represents much of the first three steps in Alaska’s IEA: defining ecosystem goals, developing indicators, and assessing the ecosystems (Figure 125). The primary stakeholders in this case are the North Pacific Fishery Management Council. Research and development of risk analyses and management strategies is ongoing and will be referenced or included as possible.

It was requested that contributors to the Ecosystem Status Reports provide actual time series data or make them available electronically. The Ecosystem Status Reports and data for many of the time series presented within are available online at: <http://access.afsc.noaa.gov/reem/ecoweb/>. These reports and data are also available through the NOAA-wide IEA website at: <https://www.integratedecosystemassessment.noaa.gov/regions/alaska>.

Past reports and all groundfish stock assessments are available at: <https://www.fisheries.noaa.gov/ala>

---

<sup>46</sup>The Arctic report is under development

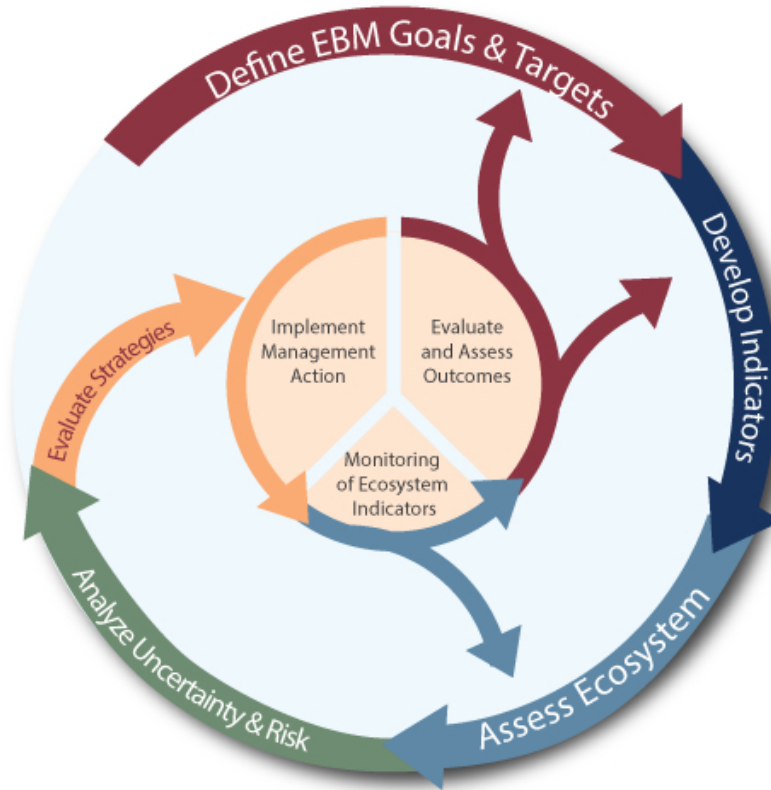


Figure 125: The IEA (integrated ecosystem assessment) process.

ska/population-assessments/north-pacific-groundfish-stock-assessment-and-fishery-evaluation.

If you wish to obtain a copy of an Ecosystem Considerations Report version prior to 2000, please contact the Council office at: 1-907-271-2809.

## Responses to SSC comments from December 2021 and October 2022

### December 2021 SSC Final Report to the NPFMC C-3 BSAI and C-4 GOA Ecosystem Status Reports

*The SSC received presentations by Elizabeth Siddon (NOAA-AFSC), Bridget Ferriss (NOAA-AFSC), and Ivonne Ortiz (UW-CICOES) on the Ecosystem Status Reports (ESRs) for the eastern Bering Sea, Gulf of Alaska, and the Aleutian Islands. The presentations were informative and highlighted the great strides that the authors and editors of the ESRs have made in producing documents that are insightful and of benefit to the management of federal fisheries off Alaska. The SSC appreciates the consistent high quality of the ESRs and their presentations. There was no public testimony.*

Thank you. We want to acknowledge the effort and thank all those involved in collecting, analyzing, interpreting, and communicating the observations included in these reports.

### General Comments applicable to all three ESRs

*The general summaries and integrated sections on the physical environment and seabirds (GOA, EBS, AI), and Regional Highlights (AI) were information-dense and provided excellent syntheses of the individual reports. The SSC appreciates the efforts that went into these components of the reports. The Noteworthy Topics sections continue to highlight observations and issues that demand attention. The excision of the Executive Summary reduced redundancy and streamlined the summary portion of the ESR. The Report Card remains very useful.*

Thank you. We appreciate the SSC's feedback. We will continue to revise how information is presented through the ESRs in response to your feedback and to optimize the utility and effectiveness of the ESRs

*The SSC supports a holistic review of how economic and social science information is communicated and applied to Council decision-informing analytic products in 2022 (See Economic SAFE Section of this SSC report, and October 2021 SSC Minutes). The SSC requests that the review be transparent and inclusive, consistent with its suggestion for such a review during the October 2021 meeting. The SSC looks forward to the planned synthesis products for the Fishing and Human Dimensions section. In anticipation of this holistic review, some human dimensions indicators were not included in the 2021 report to better align the focus of the ESRs on informing next year's ABC determinations.*

The response below was provided by NOAA's Alaska Fisheries Science Center Economics and Social Science Research Program.

“The AFSC Economics and Social Science Research Program (ESSRP) devised a framework<sup>47</sup> to help explain the economic and social information it provides in various annual reports to the NPFMC (see Figure 126). This framework has guided ESSRP's annual provision of social and economic information into NPFMC harvest specifications processes since 2021. There are several socio-economic documents produced annually by ESSRP and the placement of future social and economic indicators across these outlets will be guided by the decision the document is intended to inform (e.g., ABC/TAC/general management), the geographic and time scales of the indicator, and whether the indicator is intended to inform stock health. A SocioEconomic Aspects in Stock Assessments Workshop (SEASAW), specifically for the North Pacific, as suggested by the SSC in October 2021 is likely of interest to many, but the goals of that type of workshop are confounded by the NPFMC motion from October 2018<sup>48</sup>, which states that socio-economic factors are to be considered during TAC setting but should not be incorporated into ABC recommendations. In light of this, ESSRP will not produce synthesized products for a “Fishing and Human Dimensions” section of the ESR, but will continue to provide syntheses and analyses of the economic condition of groundfish and crab fisheries in their respective economic SAFE reports as well as social conditions for communities highly engaged in FMP groundfish and FMP crab fisheries in the Annual Community Engagement and Participation Overview (ACEPO). These documents offer the appropriate length and context to address these critical socio-economic issues. ESSRP

<sup>47</sup>[https://meetings.npfmc.org/CommentReview/DownloadFile?p=7a902abf-29ba-4c62-8b7e-4930eb80800b.pdf&fileName=PRESENTATION\\_ESSRP\\_GPT20210921.pdf](https://meetings.npfmc.org/CommentReview/DownloadFile?p=7a902abf-29ba-4c62-8b7e-4930eb80800b.pdf&fileName=PRESENTATION_ESSRP_GPT20210921.pdf)

<sup>48</sup><https://meetings.npfmc.org/CommentReview/DownloadFile?p=c93128f5-9fb8-42be-92bf-9b4c5daec17e.pdf&fileName=C2%20COUNCIL%20MOTION%20SocioEconomic.pdf>

seeks to avoid duplicative effort by recreating this information in the ESR or potentially providing unusable information at the Large Marine Ecosystem (LME) scale. Stock-specific economic indicators are currently provided for economic context within the stock assessment itself via the Economic Performance Report (EPR) for several stocks (including EBS pollock), or are included as an appendix. Economic and social metrics that have a direct impact on stock health (and thus ABC recommendation) could potentially be included in an ESP, except for the prohibition on doing so according to the NPFMC October 2018 motion. Therefore, relatively few social and economic metrics are included in the ESR and ESPs. However, extensive social and economic information are provided at appropriate scales in the Economic SAFE and ACEPO reports as well as available on the web via AKFIN's Human Dimensions of Fisheries Data Explorer<sup>49</sup>."

*The "Purpose of the ESR" section (p.4) in each report indicates that the SSC is the primary audience (for setting ABCs/OFLs) but also the AP and Council. The SSC has frequently discussed the numerous ecosystem-related documents that are produced through the Council process and some excellent infographics have been developed to indicate how and when they are used and how they differ (e.g., through the Climate Change Task Force, BS FEP). While the SSC/AP/Council are the main audiences for the report, many industry and community stakeholders use the ESRs as well as the "In Briefs". **The SSC suggests including such a flow chart/infographic in this section of the ESR to visualize the process.***

An infographic has been added to the "Purpose of the Ecosystem Status Reports" section (see p. 4, Figure 1). This figure depicts the current flow of ecosystem information in the ESRs that supports Ecosystem-Based Fisheries Management through Alaska's annual harvest specification process. The 'honeycomb' on the right shows examples of ecosystem indicators that are provided to Ecosystem Status Reports (ESRs) at the Large Marine Ecosystem (LME) scale and/or to Ecosystem and Socio-economic Profiles (ESPs) at the species-based level.

*"In Briefs" are planned for the EBS, GOA, and AI and a second outreach video is being developed - summarizing the ESR products and process. The authors have settled on a strategy that includes the annual production of "In Briefs". The authors noted there will be intermittent production of storymaps focused on specific ecosystem stories and no additional videos at this time. **The SSC is supportive of these continued efforts to disseminate ESR information to stakeholders and communities and appreciates the efforts to provide hard-copy products to remote communities where digital media may be difficult to download or otherwise access.** The SSC looks forward to hearing any feedback from end-users on how these products are used and valued. The SSC notes the ESR author participation at the recent Coastal Communities Forum in Unalaska/Dutch Harbor hosted by the Qawalangin Tribe as a potentially rich context for the two-way flow of information on ESR topics of relevance to local communities and is supportive of similar future outreach efforts whenever practicable.*

In December 2021, NOAA AFSC released a short video<sup>50</sup> describing how ecosystem scientists work collaboratively to develop Alaska's Ecosystem Status Reports.

The ESR authors greatly appreciate the support of the AFSC Communications team to help produce the "In Briefs". At this time, StoryMaps are not planned for the 2022 ESRs.

---

<sup>49</sup><https://reports.psmfc.org/akfin/f?p=501:2000>

<sup>50</sup>The video can be found here: <https://videos.fisheries.noaa.gov/detail/videos/alaska/video/6287018070001/alaska%E2%80%99s-ecosystem-status-report:-a-collaborative-approach?autoStart=true>

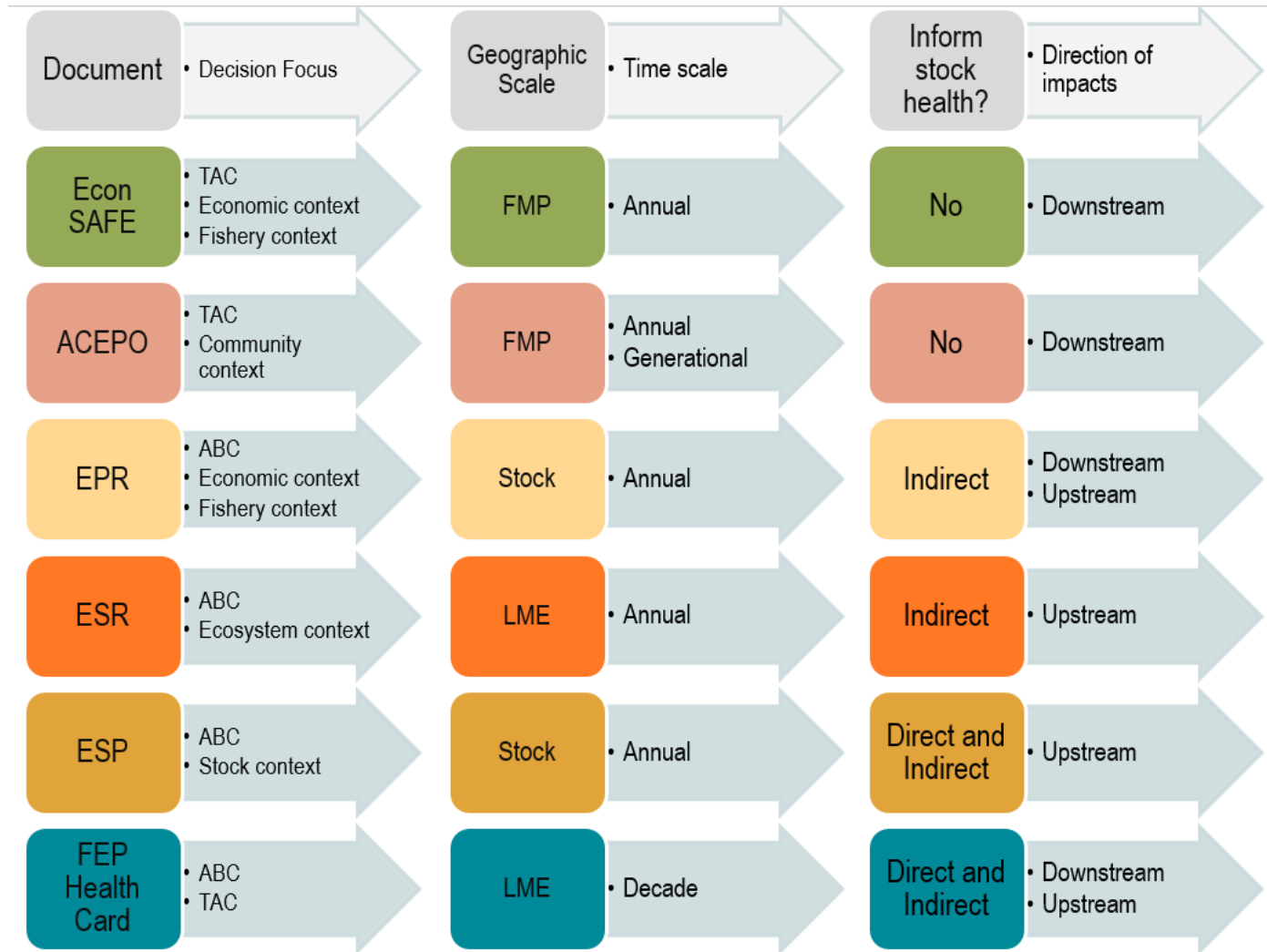


Figure 126: NOAA Alaska Fisheries Science Center's human dimensions indicators mapping. Impacts are assessed with respect to the health of a given stock(s) and are considered 'upstream' of the stocks when impacting environmental conditions and 'downstream' of the stocks when impacting social-economic outcomes of the fishery.

### **Harmful Algal Blooms**

Harmful Algal Blooms (HABs) were reported from all three regions (EBS, AI, GOA), as well as in the NBS and Chukchi Sea. Toxins were detected in shellfish (GOA, AI) and marine mammal flesh (NBS, Chukchi). No human fatalities were reported in 2021.

### **BSAI Ecosystem Status Reports**

#### **Bering Sea**

##### *Issues of Concern:*

(1) *The integration of information from many discipline-specific reports in both the Northern Bering Sea (NBS) and the eastern Bering Sea (EBS) in the overview section identified **multiple indications of warming in the EBS and declining productivity in the Bering Sea as a whole**. Whereas, the response of individual stocks to ocean warming was more mixed, with some stocks exhibiting declines in the availability of species for harvest (due to declining abundance or shifting spatial distributions) and/or changes in weight at length or age, while others showed more mixed responses.*

(2) *The extremely weak returns of Yukon River Chinook and chum salmon remain issues of concern. The SSC supports continued research on the potential causes of these weak runs. Hypotheses considered in the ESR include: (a) reduced ocean survival; (b) reduced stocks of lipid-rich large crustacean zooplankton in the NBS (see paragraph below on seabird die-offs in the NBS); (c) competition with, or even predation by, Asian pink salmon; and (d) recent changes in PSC of chum salmon. The factors responsible for the weak runs are areas of active research.*

Please see the ‘Noteworthy’ entitled “Factors Affecting 2022 Western Alaska Chinook Salmon Runs & Sub-sistence Harvest” on p. 24 of this Report for an update on this topic.

(3) *Continued seabird die-offs and reduced reproductive success in the NBS are of concern. The die-offs were a mix of planktivorous (e.g., shearwaters) and piscivorous species, as was the case for reproductive failures (e.g., both murre species, and puffins), indicating that the abundance of large, lipid-rich zooplankton and forage fish may be reduced. Since these zooplankton are also important prey of forage fish and pollock, these seabird die-offs may indicate that the NBS has a limited ability to support increasing abundances of commercially important fish species.*

Please see the ‘Integrated Seabird Information’ section on p. 142 of this Report for an update on this topic.

##### *Physical environment synthesis*

*In 2021, there was a decoupling of the winds in the northern Bering Sea (strong winds from the north) and the southeastern Bering Sea (moderate to strong winds from the south). As a result, there was widespread and thick sea ice in the northern Bering, and continued low sea-ice extent and thickness in the southeast. Over the southeastern shelf, the advancement of sea ice stalled at the end of January, resulting in a relatively small cold pool, similar in size to those occurring in the warm years of the early 2000s.*

*Indicators showing warming in the EBS included: St. Paul air temperatures show a strong positive trend over the past 40 years, freeze-up occurs later in the season (March versus December), sea-ice extent (October 15- December 15) is approximately 50% of its long-term mean, reduction in cold pool area and its southern boundary has shifted northwestward, and bottom temperatures were elevated in 2018 and 2019 (~2° C above long-term mean, compared to 0.5° C above the mean in 2021).*

*If the available weather models as a group are correct, late winter and early spring of 2022 will bring near-normal water temperatures to most of the Bering Sea and Aleutian Islands. Despite considerable inter-model variability, most, but not all, of the models project sea ice extending south of 60° N, and possibly to M2 in the EBS.*

Please see the ‘Physical Environment Synthesis’ section on p. 31 for an update on this section; the “Seasonal Projections from the National Multi-Model Ensemble (NMME)” subsection (p. 64) includes a review of the 2021 model projections.

##### *Reduced productivity*

*Indicators showing productivity declines throughout the Bering Sea since the beginning of the warm period in 2014 included: (1) declines in surface chlorophyll concentrations as measured by satellite, with below-average values since 2016, (southern and middle shelf) or since 2014 (NBS outer shelf), (2) for 2020, the Continuous Plankton Recorder showed that the diatom abundance anomaly was negative, and the mesozooplankton biomass and the size distribution of copepods were reduced, (3) the CPUE of benthic foragers measured during the bottom trawl survey (June–August) in 2021 was at the lowest level over the times series, more than one and a half standard deviations below mean 1982–2021 levels, (4) the biomass of crabs, including hermit, king, tanner and snow crab, are all below their long-term means, (5) the CPUE of all fish combined and major invertebrate taxa sampled in the 2021 NOAA bottom-trawl survey decreased in both the NBS and the EBS, with the southern portion at the lowest level since 2009, and (6) fish condition (length-weight or weight at age residuals) declined between 2019 and 2021 for benthic, pelagic and apex predators, though juvenile pollock condition has trended upward.*

*In the NBS, specifically, there is evidence of a decline in pelagic food availability since 2017. Piscivorous seabirds had below-average reproductive success, with black-legged kittiwakes experiencing complete failure at Hall Island. Murres and puffins had delayed nesting and/or reduced reproductive success. Least auklets, primarily zooplankton eaters, had average success. Arctic-Yukon-Kuskokwim Chinook and chum salmon had low returns in 2021. It has been suggested that these return failures may be due to low ocean survival, and a number of hypotheses have been suggested that might account for this poor ocean survival. **The SSC is very supportive of continued research and monitoring efforts to explore the various hypotheses the ESR authors presented that may explain the observed changes in the EBS/NBS including cumulative impacts of increased thermal exposure and metabolic demands, vertical mismatch/stratification in prey distribution in the water column, and functional redundancy within the ecosystem.***

Please see the ‘Ecosystem Assessment’ on p. 9.

*It is noteworthy that, in the face of COVID-19 cancellations of most NOAA Fisheries surveys in the eastern and northern Bering Sea in 2020, some data gaps were partially filled by state/university partners, tribal governments, and coastal community members who provided new and innovative contributions to inform the ESR team’s understanding of the ecosystem status. **The SSC suggests that going forward it will be important to build on lessons learned from these collaborations** and to examine how such collaborations, and the value of the information derived therefrom, may be strengthened and remain relevant and useful after regular NOAA survey efforts resume to pre-pandemic coverage. As an example, **the SSC suggested that local partners in Nome (e.g., Kawerak, Inc. or NSEDC) could be approached to see if they might help organize a local effort to monitor sea temperatures in the Norton Sound region.***

The ESR Team greatly appreciates the on-going collaborations and contributions from scientists and fishery managers at NOAA, other U.S. federal and state agencies, academic institutions, tribes, nonprofits, and other sources. We continually seek to engage in conversations and information-exchange with people connected to the EBS ecosystem

***The SSC suggests that the editors and authors consider the development of a single, “all-purpose”, combined map of the eastern and northern Bering Sea, combined, that would show an agreed upon set of zones, such as those used for the BSIERP map (Ortiz et al., 2012) with whatever modifications seem appropriate. This map would be in addition to the maps of the eastern Bering Sea and northern Bering Sea bottom trawl surveys and the slope survey. In the present EBS ESR, there were at least four different maps presented, each with a unique set of zones or divisions. These differences make integration of information across disciplines challenging.***

Thank you. This is an area of on-going improvement within the EBS ESR and with contributors. We appreciate the challenge it presents in integrating information, but strive to present ecologically relevant information that may be sampled at various spatial scales.

***BSAI Forage Fish***

***The SSC concurs with the BSAI GPT recommendation for a forage species workshop to discuss (1) surveying and population estimation of forage species, (2) importance of forage to different managed species (e.g., evaluate the suite of current food web models), (3) questions about how climate change may impact forage biomass and exploitation rates, (4) how best to report on changing populations, scientific knowledge about forage species, and the dependence of other species on them; including timing, frequency, and scope of the report, and (5) potential resulting management measures from shift in bycatch or spatial distribution of the forage base. The SSC also recommends that in light of the recent substantial increases in squid catch levels, this workshop focuses on identifying the threshold for placing squid back in the fishery.***

*The BSAI GPT recommended coordination between editors of the ESR and the forage report to reduce redundancy. While the SSC supports efforts to reduce redundancy, there was hesitancy to support the initial suggestion of considering a combined forage species report for Alaska due to the significant differences in stock structure, ecosystem role, and dynamics across the GOA, BS, and AI. The SSC recommends that this topic would be a good discussion topic for the proposed workshop.*

The ESR editors, the Forage Report editor, and others at NOAA's Alaska Fisheries Science Center convened a virtual "Forage Congress" with two half-day meetings on March 30 and April 6, 2022. This Forage Congress had four major objectives: (1) identify major forage taxa for each Large Marine Ecosystem; (2) inventory major research including surveys, process research, fishery-dependent collections, and analytic methods; (3) identify major scientific goals and knowledge gaps; and (4) provide specific recommendations to AFSC leadership regarding future research priorities (a NOAA Tech Memo is in development). This workshop helped to develop an understanding of AFSC's internal engagement in forage research and monitoring, to be able to better engage in the broader discussions described by the SSC in these comments.

## **October 2022 SSC Draft Report to the NPFMC C-1 BSAI Crab**

### **Ecosystem Status Report Preview**

*The SSC received remote presentations from Elizabeth Siddon (NOAA-AFSC), Ivonne Ortiz (NOAA-AFSC), and Bridget Ferriss (NOAA-AFSC). There was no public testimony. The SSC thanks the presenters for their efforts in providing excellent, targeted information related to crab stock assessments. In particular, the SSC greatly appreciates the presentation of slides with the "big picture" summary at the top, and then supporting information provided below in highly condensed form. The new format resulted in a smooth, clear, efficient presentation.*

Thank you. We appreciate the SSC's feedback. We will continue to strive to provide 'smooth, clear, efficient' presentations.

***In general, there were no new major environmental concerns reported to date in 2022. The major climate indices were in the normal range, with indications that the marine heatwaves were of less concern in the GOA and EBS but continued in the Aleutian Islands (AI).***

### *Eastern Bering Sea*

*The authors provided a highly condensed discussion of ecosystem aspects that have the potential to influence crab stocks in the EBS marine ecosystem. Although the Arctic Oscillation has been positive since spring 2021, 2021-2022 exhibited near-normal sea surface temperatures (SST). Marine heatwaves were infrequent and brief. Winds in winter 2022 were more northerly than the long-term average, with rapid sea-ice growth in November 2012 and rapid loss in April 2022. Sea ice was thinner than in 2021. The cold pool was average in extent when compared to other cool years.*

*For 2022, pH was relatively low over the outer and middle shelf of the EBS, and near the Bering Strait, decreasing at a rate comparable to the global oceans due to ocean acidification. **These conditions have been shown experimentally to negatively impact the growth and survival of red king crab and Tanner crab.***

*Prey resources for crab in the EBS marine ecosystem appear to have been near the long-term mean. Chlorophyll-*

*a biomass was near the long-term mean, as was bloom timing. A coccolithophore bloom was recorded, the implications of which may include longer trophic chains and reduced foraging success for visual predators. In spring 2022, copepods were more abundant than in 2021, especially small copepods. Visual inspection of collection vials suggested that Calanus spp. were low in lipids.*

*Competitors for benthic crab remained high or increased in 2022 (brittle/sea stars and other echinoderms, epibenthic fish), as did competitors for pelagic crab. Both pelagic (pollock and herring) and benthic predators of crab (Pacific cod and arrowtooth flounder) increased in 2022, and 2022 was the largest Bristol Bay sockeye run on record (>78 million). Pacific cod condition was average for the EBS survey area and was improved from the below-average condition in 2021.*

*Finally, the authors noted two issues of general concern in the EBS: 1) the continued failures of some salmon runs in western Alaska that impact a number of fisheries and communities, and 2) impacts from Typhoon Merbok. Typhoon Merbok circulated in western Alaska in September 2022 and caused considerable damage to coastal communities, especially hunting and fishing camps and subsistence harvests. The impacts on benthic and pelagic communities have not been investigated.*

***The SSC concluded that none of these physical or biological elements presented unusually problematic conditions for EBS crab stocks.***

## Description of the Report Card Indicators

**1. Bering Sea ice extent:** The Bering Sea ice year is defined as 1 August–31 July. Bering Sea ice extent data are from the National Snow and Ice Center's Sea Ice Index, version 3 (Fetterer et al., 2017), and use the Sea Ice Index definition of the Bering Sea, effectively south of the line from Cape Prince of Wales to East Cape, Russia (i.e., this index includes ice extent in both the western and eastern Bering Sea). The daily mean annual ice extent integrates the full ice season into a single value. *Implications:* Seasonal sea-ice coverage impacts, for example, the extent of the cold pool, bloom strength and timing, and bottom-up productivity.

*Contact: Rick Thoman  
rthoman@alaska.edu*

**2. Cold pool extent:** Area of the cold pool in the eastern Bering Sea (EBS) shelf bottom trawl survey area (including strata 82 and 90) from 1982–2021. The cold pool is defined as the area of the southeastern Bering Sea continental shelf with bottom temperature  $<2^{\circ}\text{C}$ , in square kilometers ( $\text{km}^2$ ). *Implications:* The cold pool has a strong influence on the thermal stratification and influences the spatial structure of the demersal community (Spencer, 2008; Kotwicky and Lauth, 2013; Thorson et al., 2020), trophic structure of the eastern Bering Sea food web (Mueter and Litzow, 2008; Spencer et al., 2016), and demographic processes of fish populations (Grüss et al., 2021).

*Contact: Sean Rohan and Lewis Barnett  
Sean.Rohan@noaa.gov and Lewis.Barnett@noaa.gov*

**3. Euphausiid biomass:** In the absence of direct measurements of secondary production in the eastern Bering Sea, we rely on estimates of biomass. We use an estimate of euphausiid biomass as determined by acoustic backscatter and midwater trawl data collected during biennial pollock surveys. *Implications:* Euphausiids form a key, large group of macrozooplankton that function as intermediaries in the trophic transfer from primary production to living marine resources (commercial fisheries and protected species). Understanding the mechanisms that control secondary production is an obvious goal toward building better ecosystem syntheses.

*Contact: Patrick Ressler  
Patrick.Ressler@noaa.gov*

**4. Pelagic forage fish:** This index represents the relative biomass of small fishes captured in the BASIS surface trawl (upper 25m) survey in the eastern Bering Sea during late summer. The aggregate biomass includes age-0 pollock, age-0 Pacific cod, herring, capelin, and all species of juvenile salmonids. Due to changes in survey station locations and timing across years, a Vector Autoregressive Spatio-Temporal model with day of year as a catchability covariate was used. *Implications:* When this index is higher (lower), it indicates there may be more (less) food available to upper trophic predators (e.g., fish, seabirds, and mammals).

*Contact: Ellen Yasumiishi  
Ellen.Yasumiishi@noaa.gov*

**5., 6., 7., 8. Description of the Fish and Invertebrate Biomass Indices:** We present four guilds to indicate the status and trends for fish and invertebrates in the eastern Bering Sea: motile epifauna, benthic foragers, pelagic foragers, and apex predators. Each is described in detail below. The full guild analysis involved aggregating all eastern Bering Sea species included in a food web model (Aydin and Mueter, 2007) into 18 guilds by trophic role, habitat, and physiological status (Table 7). For the four guilds included here, time trends of biomass are presented for 1982–2021. Foraging guild biomass is based on catch data

from the NMFS-AFSC annual summer bottom trawl survey of the EBS shelf (<200 m), modified by an Ecopath-estimated catchability coefficient that takes into account the minimum biomass required to support predator consumption (see Appendix 1 in (Boldt, 2007) for complete details). This survey index is specific to the standard bottom trawl survey area in the southeastern Bering Sea (does not include strata 82 and 90) and does not include the northern Bering Sea. New this year, foraging guild biomass is weighted by strata area (km<sup>2</sup>) which has resulted in a minor shift in the biomass values from reporting in previous years but the trends and patterns remain the same. Also, we no longer include species that lack time series and were previously represented by a constant biomass equal to the mid-1990s mass balance level estimated in (Aydin and Mueter, 2007).

*Contact: Kerim Aydin or George A. Whitehouse  
Kerim.Aydin@noaa.gov or Andy.Whitehouse@noaa.gov*

Table 7: Composition of foraging guilds in the eastern Bering Sea.

Motile Epifauna	Benthic Foragers	Pelagic Foragers	Apex Predators
Eelpouts	Yellowfin sole	W. pollock	P. cod
Octopuses	Flathead sole	P. herring	Arrowtooth
Tanner crab	N. rock sole	Atka mackerel	Kamchatka fl.
King crab	Alaska plaice	Misc. fish shallow	Greenland turbot
Snow crab	Dover sole	Salmon returning	P. halibut
Sea stars	Rex sole	Capelin	Alaska skate
Brittle stars	Misc. flatfish	Eulachon	Other skates
Other echinoderms	Greenlings	Sandlance	Sablefish
Snails	Other sculpins	Other pelagic smelts	Large sculpins
Hermit crabs		Other managed forage	
Misc. crabs		Scyphozoid jellies	

**5. Motile epifauna (fish and benthic invertebrates):** This guild includes both commercial and non-commercial crabs, sea stars, snails, octopuses, other mobile benthic invertebrates, and eelpouts. There are ten commercial crab stocks in the current Fishery Management Plan for Bering Sea/Aleutian Islands King and Tanner Crabs; we include seven on the eastern Bering Sea shelf: two red king crab *Paralithodes camtschaticus* (Bristol Bay, Pribilof Islands), two blue king crab *P. platypus* (Pribilof District and St. Matthew Island), one golden king crab *Lithodes aequispinus* (Pribilof Islands), and two Tanner crab stocks (southern Tanner crab *Chionoecetes bairdi* and snow crab *C. opilio*). The three dominant species comprising the eelpout group are marbled eelpout (*Lycodes raridens*), wattled eelpout (*L. plearis*), and shortfin eelpout (*L. brevipes*). The composition of seastars in shelf trawl catches is dominated by the purple-orange seastar (*Asterias amurensis*), which is found primarily in the inner/middle shelf regions, and the common mud star (*Ctenodiscus crispatus*), which is primarily an inhabitant of the outer shelf. *Implications:* Trends in the biomass of motile epifauna indicate benthic productivity and/or predation pressure, although individual species and/or taxa may reflect shorter or longer time scales of integrated impacts of bottom-up or top-down control.

**6. Benthic foragers (fish only):** The species which comprise the benthic foragers group are the Bering Sea shelf flatfish species, greenlings, and small sculpins. *Implications:* Trends in the biomass of benthic foragers indirectly indicate availability of infauna (i.e., prey of these species).

**7. Pelagic foragers (fish and Scyphozoid jellies only):** This guild includes adult and juvenile Walleye pollock (*Gadus chalcogrammus*), other forage fish such as Pacific herring (*Clupea pallasii*), Capelin (*Mallotus villosus*), Eulachon (*Thaleichthys pacificus*), and Sandlance, salmon, Atka mackerel (*Pleurogrammus monopterygius*), and Scyphozoid jellies. *Implications:* Trends in the biomass of pelagic foragers largely track Walleye pollock which is an important component of the Bering Sea ecosystem, both as forage and as a predator.

**8. Apex predators (shelf fish only):** This guild includes Pacific cod (*Gadus macrocephalus*), Arrowtooth flounder, Kamchatka flounder (*Atheresthes evermanni*), Pacific halibut (*Hippoglossus stenolepis*), Greenland

turbot (*Reinhardtius hippoglossoides*), Sablefish (*Anoplopoma fimbria*), Alaska skate, and large sculpins. *Implications:* Trends in the biomass of apex predators indicate relative predation pressure on zooplankton and juvenile fishes within the ecosystem.

**9. Multivariate seabird breeding index:** This index represents the dominant trend among 17 reproductive seabird data sets from the Pribilof Islands that include diving and surface-foraging seabirds. The trend of the leading principal component (PC1) explains 51% of the variance among the data sets and represents all seabird hatch timing and the reproductive success of murre and cormorants, defined as loadings  $>|0.2|$ . *Implications:* Above-average index values reflect high reproductive success and/or early breeding (assumed to be mediated through food supply) and indicate better than average recruitment of year classes that seabirds feed on (e.g., age-0 pollock), or better than average supply of forage fish that commercially-fished species feed on (e.g., capelin eaten by both seabirds and Pacific cod).

*Contact: Stephani Zador  
Stephani.Zador@noaa.gov*

**10. St. Paul Northern fur seal pup production:** Pup production on St. Paul Island was chosen as an index for pinnipeds on the eastern Bering Sea shelf because the foraging ranges of females that breed on this island are largely on the shelf, as opposed to St. George Island which, to a greater extent, overlap with deep waters of the Basin and slope. Bogoslof Island females forage almost exclusively in pelagic habitats of the Basin and Bering Canyon and, as such, would not reflect foraging conditions on the shelf. *Implications:* Pup production reflects foraging conditions over the eastern Bering Sea shelf with above-average values indicating good foraging conditions.

*Contact: Rod Towell  
Rod.Towell@noaa.gov*

## Methods Description for the Report Card Plots

For each plot, the mean (green dashed line) and  $\pm 1$  standard deviation (SD; green solid lines) are shown as calculated for the entire time series. Time periods for which the time series was outside of this  $\pm 1$  SD range are shown in yellow (for high values) and blue (for low values).

The shaded green window shows the most recent 5 years prior to the date of the current report. The symbols on the right side of the graph are all calculated from data inside this 5-year moving window (maximum of 5 data points). The first symbol represents the “2016–2020 Mean” as follows: ‘+ or -’ if the recent mean is outside of the  $\pm 1$  SD long-term range, ‘.’ if the recent mean is within this long-term range, or ‘x’ if there are fewer than 2 data points in the moving window. The symbol choice does not take into account statistical significance of the difference between the recent mean and long-term range. The second symbol represents the “2016–2020 Trend” as follows: if the magnitude of the linear slope of the recent trend is greater than 1 SD/time window (a linear trend of  $>1$  SD in 5 years), then a directional arrow is shown in the direction of the trend (up or down), if the change is  $<1$  SD in 5 years, then a double horizontal arrow is shown, or ‘x’ if there are fewer than 3 data points in the moving window. Again, the statistical significance of the recent trend is not taken into account in the plotting.

The intention of the figure is to flag ecosystem features and the magnitude of fluctuations within a generalized “fisheries management” time frame (i.e., trends that, if continued linearly, would go from the mean to  $\pm 1$  SD from the mean within 5 years or less) for further consideration, rather than serving as a full statistical analysis of recent patterns.